

5-19-2020

## Cell Surface Regulatory Immune Targets in Anaplastic Thyroid Cancer

Sanjukta Chakraborty  
*New York Medical College*

Follow this and additional works at: [https://touro scholar.touro.edu/nymc\\_students\\_theses](https://touro scholar.touro.edu/nymc_students_theses)



Part of the [Medical Microbiology Commons](#)

---

### Recommended Citation

Chakraborty, Sanjukta, "Cell Surface Regulatory Immune Targets in Anaplastic Thyroid Cancer" (2020). *NYMC Student Theses and Dissertations*. 42.  
[https://touro scholar.touro.edu/nymc\\_students\\_theses/42](https://touro scholar.touro.edu/nymc_students_theses/42)

This Doctoral Dissertation - Open Access is brought to you for free and open access by the Students at Touro Scholar. It has been accepted for inclusion in NYMC Student Theses and Dissertations by an authorized administrator of Touro Scholar. For more information, please contact [touro.scholar@touro.edu](mailto:touro.scholar@touro.edu).

CELL SURFACE REGULATORY IMMUNE TARGETS IN  
ANAPLASTIC THYROID CANCER

Sanjukta Chakraborty

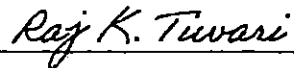
A Doctoral Dissertation in the Department of Microbiology and Immunology

Submitted to the Faculty of the  
Graduate School of Basic Medical Sciences  
In Partial Fulfillment of the Requirements for the  
Degree of Doctor of Philosophy in  
Microbiology and Immunology  
At  
New York Medical College  
Valhalla, NY 10595

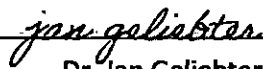
2020

# Cell surface regulatory immune targets in Anaplastic Thyroid Cancer

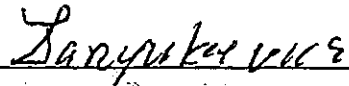
Sanjukta Chakraborty



Dr. Raj K Tiwari



Dr. Jan Geliebter



Dr. Zbigniew Darzynkiewicz



Dr. Paul Arnaboldi



Dr. Marina K Holz



Dr. Augustine Moscatello



Date of approval

© Copyright Sanjukta Chakraborty 2020  
All Rights Reserved

## ACKNOWLEDGEMENTS

Firstly, I would like to express my sincere gratitude to my mentor and graduate program director, Dr. Raj Tiwari for taking me under his wings for my dissertation research. His continuous support, patience, motivation, and immense knowledge have always helped me to gain valuable insight on different aspects of my research. Dr. Tiwari has given me the most incredible work experience in his laboratory over the past few years. His faith in me and relentless guidance inspired and motivated me to set the right goals and achieve them in a timely manner. Our discussions have not only helped me shape my scientific approach but have also given me unique perspective on broader issues of life. He has always been extremely supportive of my ideas, good or bad and made sure that I followed the good ones through. Under his mentorship, I have grown into a more independent, confident and perseverant individual. I could not have imagined having a better advisor and mentor for my Ph.D. studies.

Besides my advisor, I would like to thank my dissertation committee members. Dr. Jan Geliebter has always been instrumental in shaping my thoughts since the days of my coursework. His passion, enthusiasm and energy are contagious and helped me push through my ups and downs in last four years. I would like to thank Dr. Paul Arnaboldi for his thorough evaluation of my work and for asking all the right questions at the right time. I am very fortunate to have him in my committee. I would like to thank Dr. Zbigniew Darzynkiewicz for accepting the responsibility of guiding me. I am honored to have gotten the opportunity to learn from him. I thank Dr. Marina Holz for her guidance and encouragement which have equipped me to face the future with enthusiasm and positive spirit. I also thank Dr. Augustine Moscatello for widening my clinical research outlook. I want to thank all of them for letting my defense be an enjoyable moment, and for their brilliant comments and suggestions. Without all their help, it wouldn't have been possible for me to be where I am today.

This work would not have been possible without the technical assistance of Dr. Humayun Islam and Olena Ardacheva at Westchester Medical Center pathology and the late Anne Sollas at NYMC histopathology core facility. I thank Dr. Dana Mordue and my friend Dr. Corey Galylets for their patient and persistent help with microscopy. Thanks to Dr. Radha Iyer for helping me with the qRT PCR assay. I am grateful to Dr. Jiangwei Li and Dr. Dorota Halicka at the cytometry core, for helping me design and perform some of the most tedious flow cytometry experiments.

I would like to thank the office administrative staff Colin Ahyoung for making the students' life much simpler and supporting us every possible way, Tonta Galbriath for being an amazing person and constantly encouraging us. I thank Elba Rosario, and past administrator Linda Zimblar for their support. I deeply thank all the faculty members in the department of microbiology and immunology who are instrumental in creating a nurturing research environment and incredible collaboration between the laboratories.

My experience at NYMC would not have been the same without my amazing fellow lab mates. My past lab mates Dr. Neha Y. Tuli and Dr. Rachana R. Maniyar welcomed me in the laboratory

with open arms and gradually we became close friends. I thank my present lab members Dr. Sarnath Singh and Dr. Ghada Ben Rahoma for their caring hearts. I sincerely thank Tara Jarboe and Michelle Carnazza for the stimulating discussions, scientific and otherwise and for making me feel home away from home. I thank Sina Dadafarin for teaching me CRISPRi and for helping me with the experiments. I would also like to thank some of my first friends at NYMC, Hannah Mulhall, Christina D'arco and Dr. Cen Li for their unceasing emotional support throughout this journey.

I would like to take this opportunity to thank the previous dean of the graduate school of basic medical sciences, Dr. Francis Belloni, who gave me the opportunity to undertake my doctoral training, supporting me all along. My sincere gratitude goes to the graduate school office staff, Valerie Romeo-Messana, Barbara Lewis, Barbara Gleason and Marie Gomez for their continuous administrative support. I thank Ms. Elizabeth Ward for helping me out with visa related issues.

I would like to thank my university professors back in India, Dr. Banabihari Jana, Dr. Anilava Kaviraj and Dr. Samiran Chakrabarti for their confidence in me and helping me in the graduate school application process.

Lastly, I would like to thank my family, especially my husband Sayantan Das without whom, none of these would have been possible. He helped me discover myself and taught me how to chase the dreams that kept me awake. I thank him for helping me overcome the adversities of life with a smile on my face, to be adventurous, and to always focus on positivity. I would like to thank my eight-year-old son Syamantak Das who has supported me every possible way during this time. At the age of 5, sitting at my desk on multiple occasions while I did my experiments, he always had a smile on his face and never forgot to tell me how proud he was. I would like to thank my parents and parents in law (back home in India) and my sister in law who were my driving force all along. I would like to thank them all for their unconditional love and support throughout the years of my life.

## TABLE OF CONTENTS

TITLE.....	i
Approval.....	ii
Copyright Page.....	iii
Acknowledgements.....	iv
Table of contents. ....	vi
List of tables.....	xii
List of figures.....	xiii
Abbreviations.....	xvi
Abstract.....	xxii
<b>CHAPTER 1: INTRODUCTION: .....</b>	<b>1</b>
<b>THYROID GLAND.....</b>	<b>1</b>
<i>Functional anatomy.....</i>	<i>1</i>
<i>Homeostatic control of TH secretion and its function .....</i>	<i>6</i>
<b>THYROID CANCER .....</b>	<b>9</b>
<i>Epidemiology .....</i>	<i>9</i>
<i>Patient-related and environmental risk factors .....</i>	<i>10</i>
<i>Histological subtypes of TC.....</i>	<i>12</i>
<i>Molecular carcinogenesis in TC .....</i>	<i>19</i>

<i>MAPK signaling pathway</i> .....	27
<i>PI3K–AKT signalling pathway</i> .....	30
<i>NF-κB Signaling Pathway</i> .....	30
<b>THERAPEUTIC OPTIONS IN THYROID CANCER</b> .....	<b>33</b>
<i>Diagnosis:</i> .....	33
<i>Surgery:</i> .....	33
<i>Radioiodine ablation therapy (RAIT):</i> .....	34
<i>Kinase inhibitors:</i> .....	36
<b>IMMUNE LANDSCAPE IN ANAPLASTIC THYROID CANCER</b> .....	<b>41</b>
<i>Genetic lesions and immune microenvironment: a close relationship</i> .....	41
<i>Immune surveillance in thyroid cancer</i> .....	42
<b>IMMUNE CHECKPOINT MOLECULES IN CANCER</b> .....	<b>45</b>
<i>T cell co-signaling molecules</i> .....	50
<i>Potential of immunotherapy in ATC</i> .....	56
<b>HYPOTHESIS AND OVERVIEW OF SPECIFIC AIMS</b> .....	<b>59</b>
<b>AIM 1:</b> EXPRESSION OF IMMUNOMODULATORY MOLECULES AT TRANSCRIPT AND PROTEIN LEVELS IN THYROID CANCER CELL LINES AND PATIENT TISSUES.....	59
<b>AIM 2A:</b> EXAMINE THE MODULATION OF IMMUNE CHECKPOINT MOLECULE HVEM BY INFLAMMATORY COMPONENTS IN ANAPLASTIC THYROID CANCER .....	60
<b>AIM 2B:</b> EXAMINE POSSIBLE TUMOR INTRINSIC FUNCTION OF HVEM IN ANAPLASTIC THYROID CANCER .....	60
<b>AIM 3:</b> EXAMINE THE FEASIBILITY OF A COMBINATORIAL THERAPEUTIC APPROACH WITH MEK INHIBITOR AND ANTAGONISTIC ANTIBODIES IN ATC .....	60

<b>CHAPTER 2: MATERIALS AND METHODS.....</b>	<b>61</b>
CELL CULTURE:.....	61
RNA EXTRACTION AND QUANTITATIVE PCR:.....	61
WESTERN BLOT: .....	64
FLOW CYTOMETRY: .....	67
IMMUNOHISTOCHEMISTRY: .....	68
IL-8, TNF $\alpha$ , IFN $\gamma$ AND RHLIGHT TREATMENT: .....	70
FRACTIONATION OF NUCLEAR AND CYTOPLASMIC EXTRACTS FROM THYROID CANCER CELLS.....	71
ENZYME-LINKED IMMUNOSORBENT ASSAY (ELISA): .....	71
HVEM KNOCKDOWN BY CRISPRi: .....	72
<i>Generation of CRISPRi plasmid: .....</i>	<i>72</i>
<i>Generation of lentiviral particles and viral transduction: .....</i>	<i>73</i>
COLONY FORMATION ASSAY:.....	76
TRANS WELL INVASION ASSAY:.....	76
GENERATION OF PLX4032 RESISTANT T238 AND SW1736: .....	77
XTT ASSAY: .....	77
CELL CYCLE ANALYSES: .....	78
BRAFi AND MEKi TREATMENT: .....	78
<b>CHAPTER3: RESULTS .....</b>	<b>80</b>
<b>SPECIFIC AIM 1: EXPRESSION OF IMMUNOMODULATORY MOLECULES AT TRANSCRIPT AND PROTEIN LEVELS IN</b>	
<b>THYROID CANCER CELL LINES AND PATIENT TISSUES .....</b>	<b>80</b>

1a. <i>in vitro</i> screening for the expression of twenty-five immunomodulatory molecules in four ATC, three PTC and one FTC cell lines at transcript level compared to normal thyroid epithelial cell line .....	80
1b. Evaluation of the expression of the immunomodulatory molecules at protein level by western blot and immunofluorescence .....	85
1d. Evaluation of the expression of immunomodulatory molecules of interest in thyroid cancer tissues by immunohistochemistry .....	94
Summary.....	101
Conclusion:.....	101
<b>SPECIFIC AIM 2A: EXAMINE THE MODULATION OF HVEM BY INFLAMMATORY COMPONENTS IN ANAPLASTIC THYROID CANCER .....</b>	<b>102</b>
2ai) <i>Analysis of immune infiltrate composition in thyroid cancer patient tissues by immunohistochemistry .....</i>	<i>103</i>
2aii) <i>Analysis of cytokine milieu in thyroid cancer patient tissues by immunohistochemistry .....</i>	<i>113</i>
2aiii) <i>Analysis of the effect of inflammatory cytokines TNF<math>\alpha</math>, IL-8 and IFN<math>\gamma</math> on expression of tumor cell – HVEM.....</i>	<i>119</i>
2aiv) <i>Examine the implications of HVEM/LIGHT interaction in anaplastic thyroid cancer .....</i>	<i>138</i>
<b>SPECIFIC AIM 2B: EXAMINE POSSIBLE TUMOR INTRINSIC FUNCTION OF HVEM IN ANAPLASTIC THYROID CANCER .....</b>	<b>143</b>
2bi) <i>Knockdown HVEM in ATC cell line by CRISPRi .....</i>	<i>144</i>

2bii) <i>Assess the tumorigenicity profile by colony formation assay and invasion assay ...</i>	147
.....	
<i>Summary</i> .....	151
<i>Conclusion</i> .....	152
<b>SPECIFIC AIM 3: EXAMINE THE FEASIBILITY OF A COMBINATORIAL THERAPEUTIC APPROACH WITH MEK</b>	
<b>INHIBITOR AND ANTAGONISTIC ANTIBODIES IN ATC .....</b>	<b>153</b>
<i>3a. Evaluation of the effect of vemurafenib on the expression of immunomodulatory molecules in thyroid cancer cell lines .....</i>	<i>154</i>
<i>3b. Evaluation of the expression profile of the immunomodulatory molecules in vemurafenib-resistant ATC cell lines.....</i>	<i>167</i>
<i>3c. Evaluation of the combined effect of MEKi and BRAFV600E inhibitor on expression of these molecules in thyroid cancer cells .....</i>	<i>175</i>
<i>Summary</i> .....	<i>179</i>
<i>Conclusion</i> .....	<i>179</i>
<b>OVERALL SUMMARY .....</b>	<b>180</b>
<b>CHAPTER 4: DISCUSSION: .....</b>	<b>184</b>
<b>ATC IS REFRACTORY TO CURRENT CONVENTIONAL THERAPEUTIC MODALITIES.....</b>	<b>184</b>
<i>Diagnosis of ATC: A difficult clinical challenge .....</i>	<i>184</i>
<i>Limited surgical options for ATC patients.....</i>	<i>185</i>
<i>Radioiodine ablation therapy (RAIT) and EBRT: Limited potential with grim outcome in ATC.....</i>	<i>186</i>
<i>Chemotherapy in ATC: Debilitating side effects .....</i>	<i>186</i>

<i>Small molecule inhibitors: Big problem of resistance.....</i>	<i>187</i>
<i>Immune contexture in ATC: scope of immunotherapy .....</i>	<i>188</i>
<b>IMMUNE MODULATORY MOLECULES IN ATC: AN UNEXPLORED REALM .....</b>	<b>189</b>
<i>Immune Related Adverse Effects (irAE): The unprecedented consequences.....</i>	<i>190</i>
<i>Second generation of immune checkpoint molecules in ATC:.....</i>	<i>191</i>
<b>INFLAMMATION AND IMMUNE CHECKPOINT MOLECULES: A COMPLEX INTERPLAY .....</b>	<b>195</b>
<b>HVEM: POTENTIAL INVOLVEMENT IN SUPPORTING TUMORIGENESIS IN ATC.....</b>	<b>199</b>
<b>TARGETING HVEM/BTLA/CD160/LIGHT AXIS AND GENETIC LESIONS IN ATC: A CASE FOR</b>	
<b>COMBINATORIAL APPROACH .....</b>	<b>201</b>
<i>The rational combinatorial approach:.....</i>	<i>204</i>
<b>CHAPTER 5: APPENDIX .....</b>	<b>207</b>
<b>PRESENTATIONS RESULTING FROM THIS THESIS .....</b>	<b>207</b>
<b>BIBLIOGRAPHY .....</b>	<b>208</b>

## **List of tables**

Table 1. List of primers used for qRT PCR

Table 2. List of antibodies used in western blots

Table 3. List of antibodies used in flow cytometry

Table 4. List of antibodies used in immunohistochemistry

Table 5. Primer sequences for sgRNA cassette targeting HVEM promoter

## **List of figures**

Figure 1. Gross anatomical features of thyroid gland

Figure 2. Biosynthesis of triiodothyronine (T3) and thyroxine (T4) from thyroglobulin.

Figure 3. Hypothalamic-pituitary-thyroid axis.

Figure 4. Different histological variants of PTC. (A)

Figure 5. Various histological patterns of ATC. (a)

Figure 6. Histological subtypes of cancer with most prevalent genetic lesions

Figure 7. MAPK signaling pathway.

Figure 9. Mechanistic overview of targeted therapeutic agents in ATC.

Figure 8. The immune synapses between T cell, DCs and tumor cell

Figure 10. Immunomodulatory molecules in T cell activation.

Figure 11. Map of dCas9-KRAB-GFP plasmid

Figure 12. Expression of co-stimulatory molecules in thyroid cancer cell lines.

Figure 13. Expression of immune-checkpoint molecules in thyroid cancer cell lines.

Figure 14. Expression of immunomodulatory proteins in thyroid cancer cell lines.

Figure 15. Sub-cellular localization of HVEM and BTLA in thyroid cancer cell lines.

Figure 16. Constitutive expression of cell surface immunomodulatory molecules by anaplastic thyroid cancer cell lines.

Figure 17. Constitutive surface expression of immunomodulatory molecules in ATC cell lines

Figure 18. Percentage of cells positive for expression of immunomodulatory molecules

Figure 19. Expression of HVEM in follicular cells of ATC and PTC.

Figure 20. Expression of BTLA in follicular cells of ATC and PTC

Figure 21. Expression of CD160 in follicular cells of ATC and PTC

Figure 22. Expression of HVEM, BTLA and CD160 in follicular cells of ATC and PTC

Figure 23. Tumor infiltrating CD3 and CD8 lymphocytes in ATC

Figure 24. Tumor infiltrating CD3 and CD8 lymphocytes in PTC

Figure 25. CD3 and CD8 lymphocytes infiltration in normal thyroid tissue

Figure 26. Infiltration of FoxP3+ lymphocytes in normal thyroid tissue

Figure 27. Tumor infiltrating FoxP3+ lymphocytes in ATC and PTC

Figure 28. Tumor infiltrating CD4+ lymphocytes in ATC, PTC and normal thyroid tissue

Figure 29. T cell infiltration in ATC, PTC and normal thyroid tissues

Figure 30. Expression of IDO1 in ATC and PTC. ATC (A-D); PTC (E-H); normal (I)

Figure 31. Expression of IL17 in ATC and PTC. ATC (A-D); PTC (E-H); normal (I)

Figure 32. Expression of IL10 in ATC and PTC. ATC (A-D); PTC (E-G); normal (H)

Figure 33. IL-8 and TNF $\alpha$  mediated regulation of HVEM transcription in 8505C

Figure 34. IL-8 and TNF $\alpha$  mediated regulation of surface HVEM in T238 and HTh74

Figure 35. IL-8 and TNF $\alpha$  mediated regulation of surface HVEM in 8505C and SW1736

Figure 36. IL-8 and TNF $\alpha$  mediated regulation of surface HVEM in normal thyroid epithelial cell line Nthy-ori-3-1

Figure 37. Soluble HVEM in conditioned media from ATC cell lines

Figure 38. Soluble HVEM in conditioned media from Nthy-ori-3-1

Figure 39. IL-8 and TNF $\alpha$  mediated regulation of ADAM17 in ATC cell lines

Figure 40. IFN $\gamma$  sensitivity of HTh74 and SW1736

Figure 41. IFN $\gamma$  inducible gene expression of HVEM, BTLA, CD160, and PD-L1 in ATC cell lines

Figure 42. IFN $\gamma$  inducible gene expression of HVEM, BTLA, CD160, and PD-L1 in ATC cell lines

Figure 43. IFN $\gamma$  inducible surface expression of HVEM in ATC cell line HTh74

Figure 44. Activation of stress related MAPK on rhLIGHT treatment in ATC cell lines

Figure 45. Relative expression of stress related MAPKs, pI $\kappa$ B and ADAM17 upon LIGHT treatment

Figure 46. Nuclear translocation of NF $\kappa$ B on rhLIGHT treatment in 8505C and Nthy-ori-3-1.

Figure 47. CRISPRi mediated stable knockdown of HVEM in 8505C

Figure 48. Colony formation assay in HVEM<sup>KD</sup> 8505C

Figure 49. Matrigel invasion assay with HVEM<sup>KD</sup> 8505C

Figure 50. Representative image of cell cycle synchronization in SW1736

Figure 51. Effect of PLX4032 on expression of immunomodulatory molecules in ATC

Figure 52. Effect of PLX4032 on expression of immunomodulatory molecules in FTC and PTC

Figure 53. PLX4032-mediated modulation of HVEM, BTLA, CD160, TIM3 and LGALS9B

Figure 54. Expression of HVEM in thyroid cancer cell lines after PLX4032 treatment

Figure 55. Expression of BTLA in thyroid cancer cell lines after PLX4032 treatment

Figure 56. Expression of CD160 in thyroid cancer cell lines after PLX4032 treatment

Figure 57. Expression of TIM3 in thyroid cancer cell lines after PLX4032 treatment

Figure 58. PLX4032-mediated modulation of the expression of immunomodulatory molecules in thyroid cancer cell lines

Figure 59. Induction of PLX4032 resistance in ATC cell lines

Figure 60. Activation of compensatory pathways in PLX4032 resistant ATC cell lines leading to hyperactivation of ERK

Figure 61. PLX4032 resistant ATC cell lines are characterized by hyperactivated MEK and ERK at higher concentrations of PLX4032

Figure 62. Higher expression of immunomodulatory molecules in vemurafenib (PLX4032) resistant ATC cell lines

Figure 63. Higher surface expression of HVEM, BTLA and CD160 in Vemurafenib (PLX4032) resistant ATC cell lines

Figure 64. Differential effect of BRAFV600E and MEK inhibitors on surface expression of HVEM in PLX4032-sensitive and PLX4032-resistant T238 and SW1736

Figure 65. Persistent expression of HVEM upon combination treatment with PLX4032 and trametinib.

Figure 66. HVEM/BTLA/CD160/LIGHT Signaling in T cells and antigen presenting cells

Figure 67. STAT3 (A) and NF $\kappa$ B (B) binding sites in HVEM promoter

Figure 68. ADAM17 mediated ectodomain shedding in HVEM

Figure 69. Rationale for targeting HVEM/BTLA axis with small molecule inhibitors of the MAPK pathway in anaplastic thyroid cancer.

## **Abbreviations**

4-1-BB	Tumor Necrosis Factor Receptor Superfamily Member 9
AJCC	American Joint Committee on Cancer
AKT	Protein Kinase B
ALK	Anaplastic Lymphoma Kinase
APC	Antigen Presenting Cell
ATA	American Thyroid Association
ATC	Anaplastic Thyroid Cancer
ATCC	American Type Culture Collection
B-Raf	v-Raf murine sarcoma viral oncogene homolog B1
BRAFV600Ei	BRAFV600E Inhibitor
BTLA	B and T Lymphocyte Attenuator
CCH	C-Cell Hyperplasia
CD	Cluster of Differentiation
CDKN2A	Cyclin Dependent Kinase Inhibitor 2A
CSFBS	Charcoal Stripped Fetal Bovine Serum
CTLA4	Cytotoxic T Lymphocyte Associated Protein 4
CTNB1	Beta catenin
CXCR4	C-X-C Motif Chemokine Receptor 4
D1	Type 1 Deiodinase
DC	Dendritic Cell
DEPTOR	DEP domain-containing mTOR-interacting protein
DFS	Disease Free Survival
DIT	Diiodo tyrosine
DMSO	Dimethyl Sulfoxide
DNA	Deoxyribonucleic Acid
DR3	Death Receptor 3
EBRT	External Beam Radiation Therapy

EGFR	Epidermal Growth Factor Receptor
EIF1AX	Eukaryotic Initiation Factor 1AX
eIF4E	Eukaryotic Initiation Factor 4E
EMT	Epithelial to Mesenchymal Transition
ERK1/2	Mitogen activated protein kinase kinase
FA	Follicular Adenoma
FACS	Fluorescence-activated cell sorting
FcγR	Fc Gamma Receptor
FDA	Food and Drug Administration
FNA	Fine Needle Aspiration
FNAC	Fine Needle Aspiration and Cytology
FoxP3	Forkhead Box P3
FTC	Follicular Thyroid Cancer
GAB	GRB2 - associated binder
GAPDH	Glyceraldehyde 3-phosphate dehydrogenase
GITR	Glucocorticoid-Induced TNFR Family Related
GITRL	Glucocorticoid-Induced TNFR Family Ligand
GM-CSF	Granulocyte Macrophage Colony Stimulating Factor
GRB2	Growth factor receptor-bound protein 2
GTP	Guanosine-5'-triphosphate
HAVCR1	Hepatitis A Virus Cell Receptor 1
HCC	Hürthle Cell Carcinoma
HCl	Hydrogen Chloride
HDL	High Density Lipoprotein
HLA	Human Leukocyte Antigen
HPF	High Power Field
HPT	Hypothalamic Pituitary Thyroid axis
HRP	Horse Radish Peroxidase
HVEM	Herpes Virus Entry Mediator

ICOS	Inducible T-cell Costimulator
ICOSL	Inducible T-cell Costimulator Ligand
IDH1	Isocitrate Dehydrogenase 1
IDO1	Indoleamine 2,3-Dioxygenase 1
IgSF	Immunoglobulin Super Family
I $\kappa$ B	Inhibitor of $\kappa$ B
IKK	Inhibitor of kappa kinase
IL	Interleukin
irAE	Immune Related Adverse Effect
IRS	Insulin Receptor Substrate
ITC	Insular Thyroid Carcinoma
LAG3	Lymphocyte activation gene 3
LAIR1	Leukocyte Associated Immunoglobulin Like Receptor 1
LBD	Ligand Binding Domain
LIGHT	homologous to Lymphotoxin, exhibits Inducible expression and competes with HSV Glycoprotein D for binding to Herpesvirus entry mediator, a receptor expressed on T lymphocytes
MAPK	Mitogen Activated Protein Kinase
MCT8	Mono Carboxylate Transporter 8
MDSC	Myeloid Derived Suppressor Cell
MEK1/2	Mitogen activated protein kinase kinase
MEKi	MEK inhibitor
MEN	Multiple Endocrine Neoplasia
MFI	Mean Fluorescence Intensity
MHC	Major Histocompatibility Complex
MIS	Mitochondrial Insertion Signal
MIT	Mono Iodo Tyrosine
mLST8	MTOR associated protein, LST8 homolog
MRI	Magnetic Resonance Imaging

mRNA	Messenger Ribonucleic Acid
MTC	Medullary Thyroid Cancer
mTORC	Mammalian Target of Rapamycin
NES	Nuclear Export Signal
NF1	Neurofibromatosis type 1
NFkB	Nuclear Factor k-Light chain enhancer of activated B cells
NGS	Next Generation Sequencing
NIS	Sodium Iodide Symporter
NLS	Nuclear Localization Signal
NMTC	Nonmedullary Thyroid Cancer
p-AKT	Phosphorylated Protein Kinase B
PAX8	Paired box 8
PBF	PTTG1 Binding Factor
PBS	Phosphate Buffered Saline
PD1	Programmed Cell Death Protein 1
PDGFR	Platelet Derived Growth Factor Receptor
PK1	3-phosphoinositide-dependent kinase 1
PDL1	Programmed Death Ligand 1
PDTC	Poorly Differentiated Thyroid Cancer
PI3K	Phosphoinositide 3-kinase
PIP3	Phosphatidyl Inositol 3,4,5 triphosphate
PLC $\gamma$	Phospholipase C $\gamma$
PPAR $\gamma$	Peroxisome Proliferator Activated Receptor $\gamma$
PTC	Papillary Thyroid Cancer
PTEN	Phosphatase and Tensin Homolog
PTM	Post Translational Modifications
PTTG1	Pituitary Tumor Transforming Gene 1
RAF	Rapidly Accelerated Fibrosarcoma
RAIT	Radioiodine Ablation Therapy

RAPTOR	Regulatory Associated Protein of mTOR
RAR $\beta$	Retinoic Acid Receptor $\beta$
RAS	Rat Sarcoma
RB	Retinoblastoma
RET	Rearranged during Transfection
RIPA	Radioimmunoprecipitation assay
RLN	Recurrent Laryngeal Nerve
RNA	Ribonucleic Acid
RNAseq	RNA sequencing
RPMI	Roswell Park Memorial Institute
RTK	Receptor Tyrosine Kinase
RT-PCR	Reverse Transcriptase Polymerase Chain Reaction
S6K	S6 Kinase
SDS	Sodium Dodecyl Sulphate
SEER	Surveillance Epidemiology and End Results
SEM	Standard Error of Mean
SNV	Single Nucleotide Variant
SOS	Son of Sevenless
STAT	Signal Transducer and Activator of Transcription
STI	Solid Trabecular or Insular
TAM	Tumor Associated Macrophage
TBG	Thyroxine Binding Globulin
TBPA	Thyroxine Binding Pre-Albumin
TBS	Tris buffered saline
TBST	Tris buffered saline - tween
TC	Thyroid Cancer
TCR	T cell receptor
Teff	T effector cell
TERT	Telomerase reverse transcriptase

Tg	Thyroglobulin
TGFβ	Transforming Growth Factor Beta
TH	Thyroid Homone
THD	TNF Homology Domain
TIGIT	T-cell Immunoreceptor with Ig and ITIM domains
TIGIT	T Cell Immunoreceptor With Ig And ITIM Domains
TIL	Tumor Infiltrating Lymphocyte
TIM	T-cell immunoglobulin and mucin domain
TIMP3	Tissue Inhibitor of Metalloprotease 3
TNF	Tumor Necrosis Factor
TNFR	Tumor Necrosis Factor Receptor
TNFRSF	Tumor Necrosis Factor Receptor Super Family
TNFSF	Tumor Necrosis Factor Super Family
TNM	Tumor, Node and Metastasis
TP53	Tumor Protein P53
TPO	Thyroid Peroxidase
TR	Thyroid Receptor
TRE	Thyroid hormone Response Element
Treg	T regulatory cell
TRH	TSH Releasing Hormone
TSH	Thyroid Stimulating Hormone
TTF1	Thyroid Transcription Factor 1
VEGF	Vascular Endothelial Growth Factor
v-Raf	Virus induced Rapidly accelerated Fibrosarcoma
WBS	Whole Bosy Scintigraphy
WDTC	Well Differentiated Thyroid Cancer

## **ABSTRACT**

Thyroid cancer incidence is increasing at an alarming rate almost trebling every decade. 52,070 new cases of thyroid cancer (14,260 in men and 37,810 in women) were diagnosed in 2019 with an estimated death toll of 2170. Although most thyroid tumors are treatable and has good prognosis, anaplastic thyroid cancer (ATC) is extremely aggressive with a grim poor prognosis of 6-9 months post diagnosis. ATC is completely refractory to mainstream therapies.

In our study, immunohistochemical analyses of ATC tissues confirmed a T cell inflamed “hot” tumor immune microenvironment (TIME) as evidenced by presence of CD3<sup>+</sup> and CD8<sup>+</sup> T cells. This kind of tumors are amenable to immune checkpoint blockade (ICB) therapy. This therapeutic avenue is unexplored in ATC. In this study, we explored the feasibility of a combination therapy of small molecule inhibitor and ICB in ATC.

We used an *in vitro* model system representative of papillary (TPC-1, K1, BCPAP), anaplastic (8505C, T238, SW1736, HTh74), follicular (CGTH-W-1) thyroid cancer and Nthy-ori-3-1 as normal thyroid follicular cell. The cells were screened for expression of 29 immune-checkpoint molecules by qRT PCR. We noted a higher expression of HVEM, BTLA, CD160 in ATC cell lines compared to the rest. Expression level of HVEM was more than 30-fold higher in ATC compared to the other cell lines on average. immunocytochemistry, western blot and flow cytometry analyses confirmed expression of these proteins in ATC. Additionally, HVEM had highest surface expression in ATC. HVEM is a member of TNFRSF which acts as a bidirectional switch by interacting with BTLA, CD160 and LIGHT in a *cis* or *trans* manner. Given

the T cell inflamed hot TIME in ATC, expression of HVEM on tumor cells was suggestive of a possibility of complex crosstalk of HVEM with inflammatory cytokines. Increased transcription and solubilization of HVEM were observed in ATC cell lines in response to pro-inflammatory cytokines IL-8 and TNF $\alpha$ . Our study also indicates that HVEM is inducible by IFN $\gamma$  as evidenced by more than 5-fold increase in HVEM transcription in response to the cytokine. Our study reports for the first time, a tumor intrinsic stress induced MAPK signaling transduced by HVEM upon interaction with soluble LIGHT. Induction of pJNK and p-c-Jun was indicative of increased proliferative potential of these cells triggered by this interaction. HVEM/LIGHT interaction also triggered nuclear translocation of NF $\kappa$ B in ATC. Silencing HVEM in 8505C by CRISPRi highly dampened proliferative and invasive potential of the cells signifying possible tumor intrinsic function of HVEM in ATC.

BRAFV600E is a common mutation in ATC which is largely responsible for remodeling of TIME and is a prominent candidate for targeted therapy. Unfortunately, emergence of resistance is extremely common. BRAFV600E inhibitor PLX4032 resistant ATC cell lines were generated in this study, and their immune phenotypes were profiled. PLX4032 resistant cells had activation of alternate signaling molecules rescuing BRAFV600E inhibition and had dramatically higher expression of HVEM, BTLA and CD160 compared to the sensitive phenotype. The surface expression of HVEM persisted in resistant cells after combination therapy with PLX4032 and trametinib.

Altogether, our studies provide evidence for T cell inflamed TIME in ATC along with expression of immune checkpoint proteins HVEM, BTLA and CD160 in ATC. We also discovered active tumor intrinsic signaling transduced by HVEM/LIGHT interaction in ATC and the persistent

expression of these immune checkpoint molecules in case of BRAFV600Ei resistant ATC. We propose that a combination of small molecule inhibitor targeting downstream effectors of MAPK pathway and antagonistic antibodies targeting HVEM/BTLA axis might provide a viable therapeutic avenue for ATC patients.

## CHAPTER 1: INTRODUCTION:

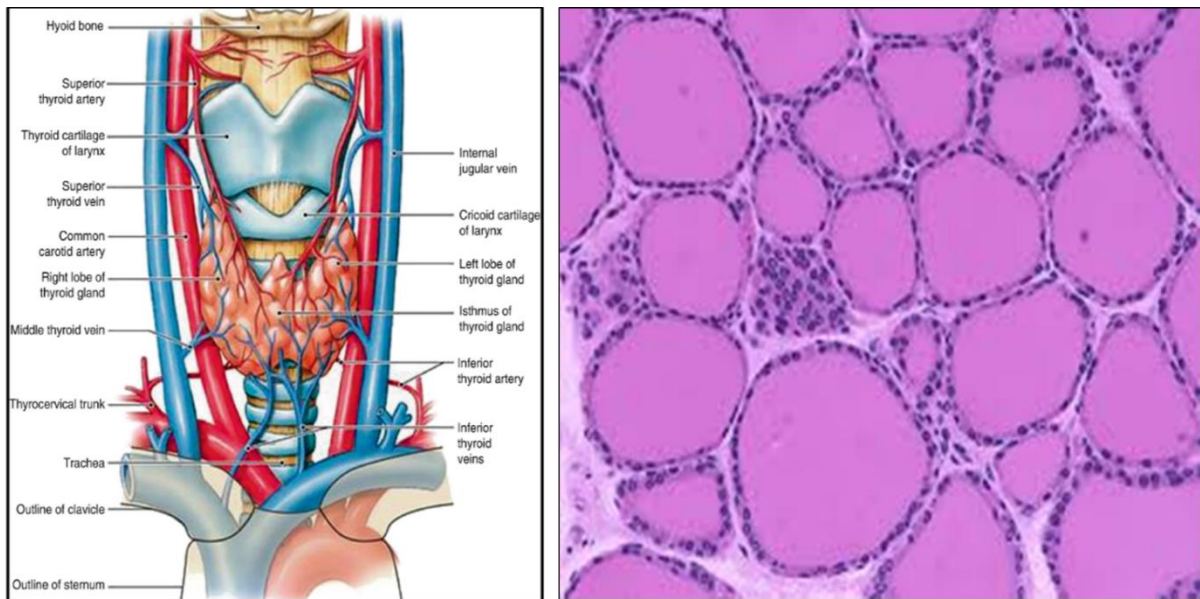
### Thyroid gland

#### *Functional anatomy*

The thyroid gland is a bilobular endocrine gland located anteriorly in the neck between C5 and T1 vertebrae deep in the platysma, sternothyroid and sternohyoid muscles. It is the first endocrine gland to develop in humans and the largest. The gland weighs approximately 15-20 grams. It is a soft reddish parenchymal organ with two lobes connected by the isthmus (Fig 1). Each lobe is about 4 cm in length, 2 cm in width and about 2-3 cm in thickness. The gland is highly vascular with a blood supply rate of 5ml/g/min. It is enclosed in layers of the deep cervical fascia and covered anteriorly by the strap muscles and laterally by sternocleidomastoid muscle. The capsule is firmly adherent to the gland, developing protrusions into the thyroid, forming multiple septae and dividing the gland into lobes and lobules (Benvenega et al., 2018). Each lobule contains a cluster of follicles which are the structural and functional units of the gland. Each follicle is surrounded by a layer of thin connective tissue stroma enriched with fenestrated capillaries and lymphatics. There are about three million follicles in adult human thyroid gland. Follicles are lined with epithelial cells which may be cuboidal, columnar or squamous in appearance depending on their state of activity. In active follicles, the cells are usually cuboidal to low columnar in shape whereas in inactive state, they are squamous in appearance. The follicular cells are also known as thyrocytes. These follicular cells are anatomically polarized with a distinct basolateral and an apical surface; the former faces the extrafollicular space, while the latter faces the follicular lumen (Nilsson & Fagman, 2017). This polarity is highly significant, as iodine uptake occurs at the

basolateral face, whereas thyroid hormone (TH) secretion occurs at the apical face. The lumen of the follicle is filled with an acidophilic glycoprotein – thyroglobulin (Tg). Synthesis of TH requires iodine which is concentrated in the cytoplasm of the follicular cells via sodium iodide symporters (NIS) expressed at the basolateral surface of the follicular cells. Upon entering the follicular cells, iodide ions move apically where they are oxidized and incorporated into Tg forming monoiodotyrosine (MIT) and diiodotyrosine (DIT), depending on the number of iodine ions incorporated in Tg (Fig 2). This step requires thyroid peroxidase (TPO) and  $H_2O_2$ . Iodinated thyroglobulin is taken up by the follicular cells by micropinocytosis after which thyroglobulin ends up in the endosomes which later fuse with the prelysosomes inside the cells depending on their level of iodination. Highly iodinated molecules are fused with pre-lysosomes, where they are cleaved by lysosomal endopeptidases, such as cathepsins B, D, and L, thus releasing triiodothyronine or T3 and thyroxine or T4. The most important transporter known to be responsible for thyroid hormone transport is the SLC16A2 or monocarboxylate transporter 8 (MCT8), which mediates both uptake and efflux of TH and participates in the release of TH from the thyroid gland (D. P. Carvalho & Dupuy, 2017). Poorly iodinated Tg molecules are recycled and returned to the apical surface from where they once again enter the colloid. Thyroid gland has another type of cell, known as parafollicular cells or C cells. C-cells are scattered between follicles, primarily in the posterolateral region of the lobes, or are present beyond the basement membrane within the follicles, in close proximity with the thyrocytes (Nilsson & Fagman, 2017). These cells secrete the hormone calcitonin. C cells constitute about 0.1% of thyroid cells and are usually identified using

immunohistochemical staining for calcitonin. Calcitonin reduces blood calcium level (Hazard, 1977).



A.

B.

Figure 1. Gross anatomical features of thyroid gland in anterior view (A) and histological features (B). The thyroid gland is shaped like a butterfly (A) and overlies trachea. Thyroid follicles are of varying size with the hollow interior filled with an acidophilic glycoprotein colloid thyroglobulin (B). C cells are also visible scattered in between the follicles. Source: [http://medcell.med.yale.edu/histology/endocrine\\_systems\\_lab/thyroid.php](http://medcell.med.yale.edu/histology/endocrine_systems_lab/thyroid.php)

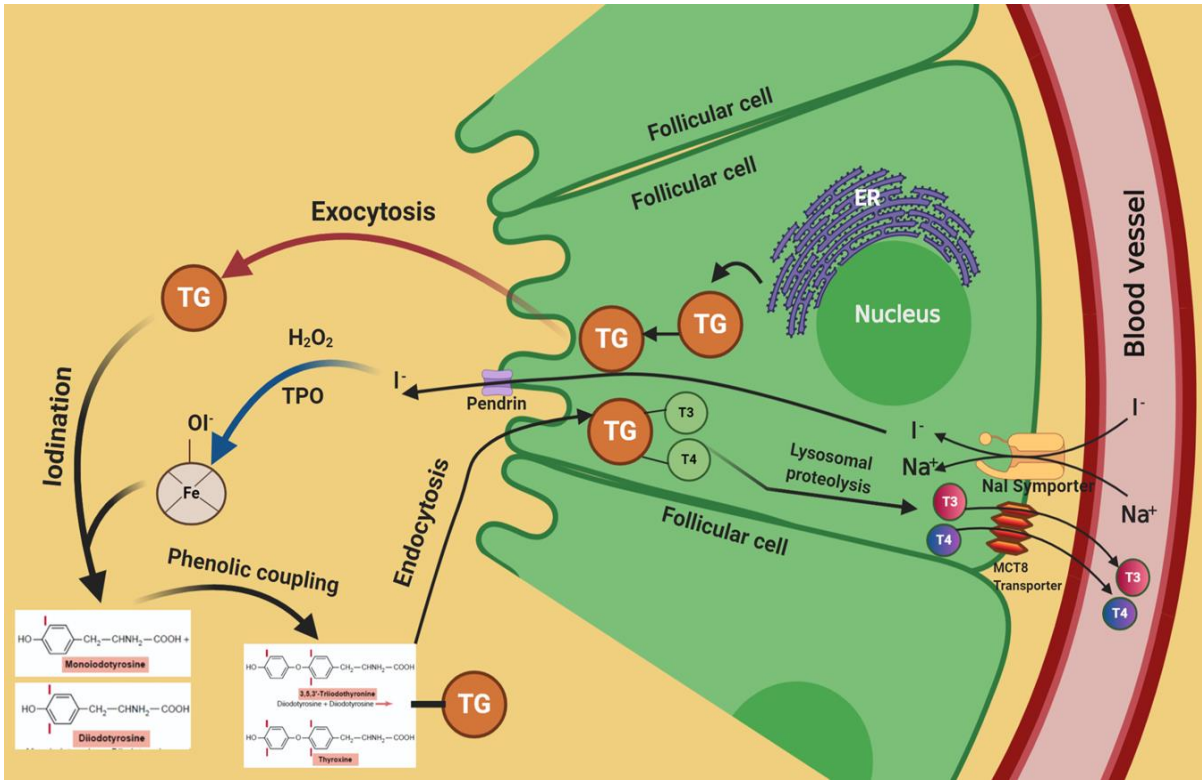


Figure 2. Biosynthesis of triiodothyronine (T3) and thyroxine (T4) from thyroglobulin.

### *Homeostatic control of TH secretion and its function*

TH play a pivotal role in regulation of differentiation, growth and cellular metabolism. TH biosynthesis is regulated by three major factors – the hypothalamic-pituitary-thyroid (HPT) axis, iodine availability and iodothyronine deiodinase activity. Serum concentrations of T4 and its biologically active form T3 are tightly regulated within a narrow range in the body by the ability of TH to control its own synthesis by a negative feedback at the hypothalamic TSH-releasing hormone (TRH) neuron and pituitary thyrotropes. TRH is a tripeptide (PyroGlu-His-Pro) synthesized in the paraventricular nucleus of hypothalamus and subsequently travels to the median eminence via axons. From there, it reaches anterior pituitary via the portal capillary plexus. Upon reaching, it binds to the TRH receptors expressed on the thyrotropes leading to release and synthesis of new TSH in the thyrotropes. Both TSH and TRH are under negative feedback regulation by TH (Hoermann et al., 2015). Several thyroid genes, including thyroglobulin (Tg), NIS, and TPO, are stimulated by TSH and promote the synthesis of TH (Fig 3). The activation and inactivation of TH are regulated by deiodinases in the circulation. Type 2 deiodinase (D2) act on the outer ring of T4 converting it to T3. Type 3 deiodinase (D3) deiodinates the inner ring of both T4 and T3, converting them into metabolically inert reverse T3 (rT3) and T2 respectively. Interestingly, type I deiodinase (D1) acts both on the inner and outer rings. D1 and D2 are the most abundant deiodinases in thyroid gland. The majority of thyroid hormone released, is in the form of T4 as the total serum T4 level is 40-fold higher than serum T3 level (90 vs. 2 nM) (Yen, 2001). Once in circulation, almost all the T3 and T4 are bound by various plasma transporter proteins, like thyroxine binding globulin (TBG), thyroxine binding pre-albumin (TBPA or transthyretin), high density lipoprotein (HDL) and albumin. All classes of lipoproteins can bind T4, T3, and rT3. Predominantly, thyroid

hormones interact with apoA, apoB100, apoC, and apoE, and this interaction is hindered by lipids (Bevenga & Robbins, 1996). Only 0.3% of T3 and 0.03% of T4 hormones are freely available in blood and are responsible for the biological activity. Upon entering the cells of the target organ, T3 binds to thyroid receptors (TR) which belongs to the family of nuclear receptors. There are two isoforms of TR, TR $\alpha$  and TR $\beta$  which are encoded by different genes located on chromosome 17 and 3 respectively. Each isoform has three variants (  $\alpha$ 1-3 and  $\beta$ 1-3) (Cheng et al., 2010). TR is a single polypeptide with a carboxyl terminal ligand binding domain (LBD) that interacts with co-regulators and mediate homo or hetero dimerization. TR contains a highly conserved central domain that interacts with the thyroid hormone response element (TRE). Almost every tissue of the body expresses TR but there are crucial post translational modifications (PTMs) suggesting a crucial interplay between the nuclear localization signal (NLS), nuclear export signal (NES) motifs and mitochondrial insertion signal (MIS) motifs that finally determines the localization of TR in the target tissue and partly accountable for the observed heterogeneity across different tissue types. Thyroid hormones have profound effects on diverse physiological processes including development, growth and oxidative metabolism. Many of these actions takes place co-operatively with other hormones – also known as permissive action where thyroid hormones modulate the responsiveness of a cell towards other hormone (Norris & Carr, 2013). Recently, non-genomic actions of thyroid hormones have been reported that have an extremely rapid onset ranging from minutes to hours (Hammes & Davis, 2015) (Cheng et al., 2010). These non-genomic actions can be initiated by T3, T4 or rT3 binding to truncated or non-truncated TR or integrin  $\alpha$ v $\beta$  on cell membrane, cytoplasm, and cytoskeleton (Bevenga et al., 2018).

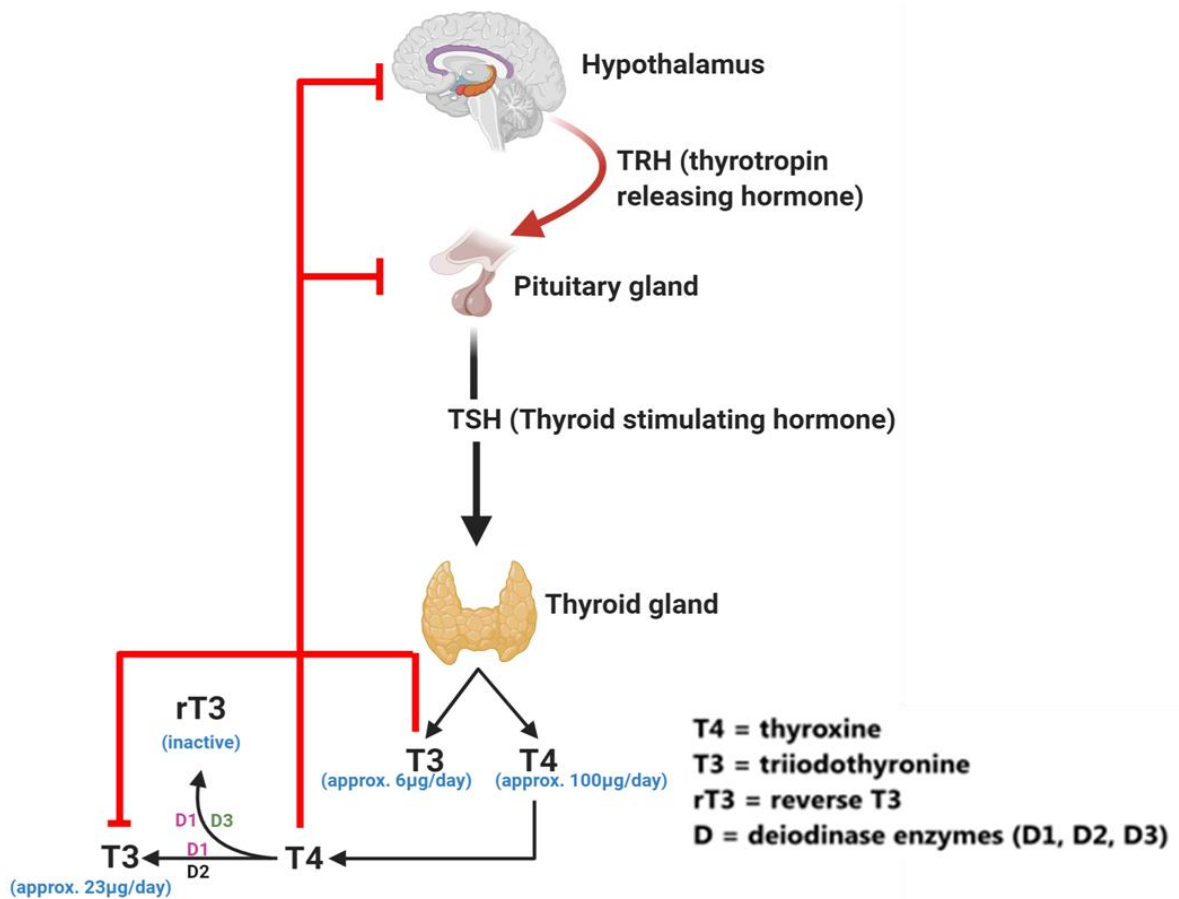


Figure 3. Hypothalamic-pituitary-thyroid axis. The hypothalamic neurons secrete TRH which is carried down to the adenohypophysis of the pituitary by the hypothalamic portal vein where it releases TSH. The released TSH reaches thyroid glands via blood stream and binds to TSHR and stimulates production of T3 and T4. Enhanced level of T3 triggers a negative feedback loop via TR $\beta$  inhibiting production of TSH and TRH.

## Thyroid cancer

### *Epidemiology*

Thyroid cancer (TC) is the most common endocrine malignancy with an alarming rate of increase over the last few decades (Aschebrook-Kilfoy et al., 2013; Davies et al., 2010; Davies & Welch, 2014). A Surveillance, Epidemiology, and End Results Program (SEER)-based study observed that from 1975 to 2009 there was a three-fold increase in incidence rates, from 4.9 to 14.3 per 100,000 individuals, primarily in small (<2cm) papillary carcinomas (Davies et al., 2010). 52,070 new cases of thyroid cancer (14,260 in men and 37,810 in women) were diagnosed in 2019 with an estimated death toll of 2170 (*Thyroid Cancer - Cancer Stat Facts*, 2019). Thyroid cancer can be divided into four histological subtypes, namely papillary thyroid cancer (PTC), follicular thyroid cancer (FTC), anaplastic thyroid cancer (ATC) and medullary thyroid cancer (MTC). PTC and FTC are known as well differentiated thyroid cancers (WDTC). PTC and FTC account for 75-80% and 10-15% of total TC cases, respectively. MTC arises from the parafollicular cells or the C cells and accounts for 5-10% TC cases. MTC can occur in sporadic (approximately 70-80%) or familial (approximately 20-30%) form. The familial form has been associated with multiple endocrine neoplasia (MEN) 2A, MEN 2B, or with the familial medullary thyroid carcinoma syndrome (Yadav et al., 2018). The inherited form of MTC often results from autosomal dominant mutations in “rearranged during translocation” (RET) proto-oncogene with an incomplete penetrance. This malignancy often presents itself as a multifocal disease with a high background of C cell hyperplasia (CCH) (Yadav et al., 2018). Calcitonin is still produced by the C cells of MTC and serum calcitonin level serves as a crucial biomarker in these patients (Etit et al., 2008). PTC is the most prevalent form of thyroid malignancy that accounts for 75-80% of the cases and is associated with very good prognosis.

ATC is the rarest and the most aggressive form of thyroid malignancy that makes up less than 3% of all the thyroid cancer cases, but is responsible for up to 40% mortality resulting from this malignancy (Reddi et al., 2015). The growing incidence of thyroid cancer has been partially attributed to overdiagnosis (Salvatore et al., 2016). It is debated that a combination of advanced diagnostic techniques such as fine-needle aspiration (FNA), ultrasonography (USG), computed tomography (CT), magnetic resonance imaging (MRI) and increased medical awareness are collectively responsible for increased detection of early stage sub-clinical small papillary lesions of 1-5 cm which might not necessarily be malignant in nature . There are a host of factors contributing to this phenomenon. *Jina et.al* mentioned that national and international factors, like limited access to healthcare, immigration patterns, differences in diagnostic procedures, and variability in cancer registries have to be analyzed thoroughly before we reach any conclusion about this increment in TC incidence (Kim et al., 2020). Possible exposure to various risk factors should also be considered as a contributing factor in this increase.

#### ***Patient-related and environmental risk factors***

##### *Exposure to ionizing radiation*

Exposure to radiation is the most well-established environmental risk factor for the development of TC. The thyroid gland is especially susceptible to the carcinogenic effects of radiation, particularly during childhood or adolescence. Repeated exposure to the radiation associated with advanced medical imaging system, like CT scans during childhood or adolescence can immensely impact the normal physiology of thyroid gland and push it towards malignant transformation (Mathews et al., 2013).

### *Familial influences*

A patient with family history of thyroid cancer or benign thyroid disease is at risk for developing thyroid cancer (Balasubramaniam et al., 1969; La Vecchia et al., 1995; Nosé, 2011). Familial thyroid cancer can be sub-divided into two groups based on their origin - parafollicular (C cell) origin, namely MTC, and of follicular cell origin, including differentiated thyroid cancer (PTC, FTC and Hurthle cell). Familial thyroid cancers of follicular origin are referred to as familial non-medullary thyroid cancers and they account for 3-9% of the familial thyroid cancer cases. These NMTCs can culminate into papillary, follicular, Hurthle cell and very rarely anaplastic thyroid cancer which might run in the same family. These variants are often considered to be extremely aggressive phenotypes by several studies, but the results are ambiguous (El Lakis et al., 2019).

### *Obesity*

Last three decades have witnessed a steep lifestyle change across the world leaning towards a sedentary type especially in developed countries. A meta-analysis of twenty-two prospective studies was performed for studying the association between TC incidence and body height and BMI. The study included 833,176 men and 1,260,871 women from different geographical location including USA, Canada, Sweden, Australia, Netherlands and China. Obesity was associated with incidences of total thyroid cancer and most major thyroid cancer subtypes, including anaplastic thyroid cancer (Kitahara et al., 2015). Interestingly, another large European prospective study (European Prospective Investigation in Cancer and Nutrition - EPIC) for the determination of the association between anthropometric factors and thyroid cancer incidences had similar findings, but only for women. In women, higher body weight, height, BMI, waist circumference and waist-to-hip ratio were associated with a

significantly higher risk of differentiated thyroid cancer. This pattern was not observed in men (Rinaldi et al., 2012).

#### *Smoking*

Cigarette smoking has been traditionally associated with cancer incidence. Interestingly, several studies noted an inverse relationship between current cigarette smoking and TC risk (Kitahara et al., 2012). This might be attributed to lower level of TSH in cigarette smokers compared to non-smokers which is well established as an etiologic factor in thyroid carcinogenesis (Cho et al., 2018).

#### *Genetic lesions*

Patients with mutation(s) in oncogenes or tumor suppressor genes are often pre-disposed to development of cancer in general. Mutation in specific oncogenes like RAS, BRAF, RET/PTC are often associated with high incidence of TC (Bible & Ryder, 2016).

#### *Histological subtypes of TC*

##### *Papillary thyroid cancer (PTC)*

Papillary thyroid cancer (PTC) constitutes about 80-85% of all TC cases (Zhu et al., 2015) and is prevalent in countries with iodine-excess diet such as China (Al-Salamah et al., 2002). It is usually detected between third and fifth decade of the life with a mean age of 40 (Iryani Abdullah et al., 2019). Fine needle aspiration and cytology (FNAC) is the method of choice for the diagnosis of PTC. This is a minimally invasive and rapid procedure that involves the use of a narrow-gauge needle to obtain a sample of the lesion for microscopic examination. The biopsy specimens are classified by their cytological appearance into benign, suspicious (or indeterminate), or malignant cells. As discussed before, overall frequency of TC is on the rise and PTC is the most significant one. Interestingly, a gender discrepancy is observed in PTC

with a female to male ratio of 3:1 (Yan et al., 2017). One plausible explanation of this observation is differential expression of sex hormone estrogen between men and women. Estrogen has been shown to be an important player for modulation of metastatic phenotype in thyroid cancer (Rajoria et al., 2011). Estrogen is known to be involved in a host of cellular processes such as growth, cell motility and organ functions. Consistent with this, different research groups have reported estrogen as a crucial player in the modulation of TC proliferation and migration (Lee et al., 2005; Manole et al., 2001) (Rajoria et al., 2010). Different variants of PTC include, classical (figure 4A), papillary microcarcinoma (Fig 4B), encapsulated (Fig 4C), diffuse sclerosing (Fig 4D), and tall cell (Fig 4E).

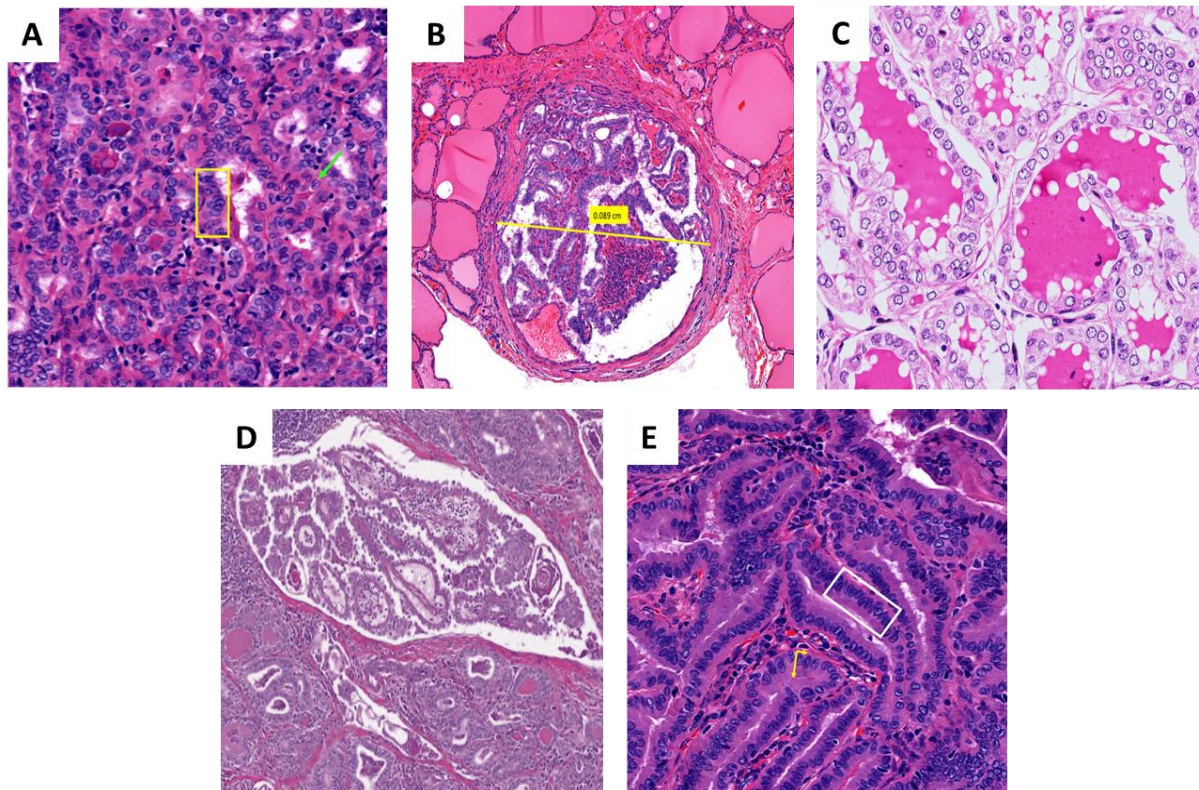


Figure 4. Different histological variants of PTC. (A) Classical variant: characterized by enlarged, overlapping nuclei (in yellow box), nuclear clearing and nuclear grooving (green arrow); (B) Papillary microcarcinoma: characterized by architectural and cellular features of PTC, but measuring <1cm in diameter; (C) Encapsular follicular variant: characterized by brightly stained colloid with frequent scalloping and retraction from the follicle; (D) Diffuse sclerosing variant: characterized by dense sclerosis, numerous micropapillary formations, frequent psammoma bodies; (E): Tall cell variant characterized by cellular height at least 2-3 times cell width (yellow arrows). Source: A-C and E From: <https://medicine.uiowa.edu/iowaprotocols/variants-papillary-thyroid-carcinoma-microcarcinoma-tall-cell-columnar-follicular> and D is from Rom J Morphol Embryol , 53 (4), 1007-12, 2012

### *Follicular thyroid cancer (FTC)*

Follicular thyroid cancer (FTC) accounts for approximately 10% of all thyroid cancer cases in iodine sufficient areas (Davies & Welch, 2014). FTC is more prevalent in women, especially in their post-menopausal phase of life (Davies & Welch, 2014). O'Neil et al. combined the invasive pattern and angioinvasion, and classified FTC into three groups: (i) minimally invasive (MI - capsule invasion only) FTC, (ii) encapsulated angioinvasive FTC and (iii) widely invasive (WI) FTC. Disease-free survival (DFS) rates at 40 months were 97%, 81% and 46%, respectively in these three groups (O'Neill et al., 2011). FTC is more aggressive than PTC and usually affects the older age group. As the name suggests, MI FTC has limited capsular and vascular invasion as opposed to WI FTC. Chances of recurrence is also lower in MI FTC compared to WI FTC. Lymph node metastasis is not common in FTC.

Differential diagnosis between FTC and follicular adenoma (FA) is not possible just by histopathologic assessment via FNA. Identification of subtype-specific genetic lesions help in the process of differential diagnosis. PAX8/PPAR $\gamma$  rearrangements, RAS mutations and TERT promoter mutations occur in both MI-FTC and WI-FTC (Foukakis et al., 2006; Wang et al., 2014). Additionally, some genetic aberrations, like loss of heterozygosity (LOH) for HGF, have been observed in MI-FTC only, but not in PTC (Trovato et al., 1999).

### *Poorly differentiated thyroid cancer (PDTC)*

Histological gradation of thyroid cancer subtypes is spread along a continuum, with WDTC at one end of the spectrum comprising of PTC and FTC, and undifferentiated TC comprising of ATC at the other end. While the former is easily manageable and almost always has an excellent prognosis, the latter is uniformly aggressive and almost always fatal. There is ample

evidence for the existence of an intermediate subtype between WDTC and ATC, in terms of both morphological characteristics and pathology. These tumors, classified as poorly differentiated thyroid carcinoma (PDTC), may aptly represent intermediate entities during the progression of WDTC to ATC. There are two different subtypes of PDTC – the insular thyroid carcinoma (ITC) and large cell poorly differentiated thyroid carcinoma. Macroscopic features of ITC include a solid, grayish-white tumor with multiple foci of necrosis. They tend to be larger in size (>4cm), often display an invasive margin, and can be either single or multinodular. The microscopic features include solid clusters ('nests') of tumor cells containing a variable number of small follicles, often sharply divided by invaginations or clefts. After a lot of ambiguity over the diagnosis criteria, the current algorithm has incorporated the Turin criteria and needs the presence of solid/trabecular or insular growth pattern (STI), hypercellularity, high nuclear/cytoplasmic ratio with convoluted nuclei, small necrotic foci and at least three mitoses/ 10 high power field (HPF) (Dettmer et al., 2019).

#### *Anaplastic thyroid cancer (ATC)*

Anaplastic thyroid cancer (ATC) is the one of the most aggressive malignancies in humans. Unlike WDTC, ATC cells lose all the characteristics of normal thyroid follicular cells such as iodine uptake, thyroglobulin synthesis and TSH dependence. It has extremely poor prognosis with average survival of 6-9 months post diagnosis. ATC is primarily a geriatric disease mostly affecting people in their sixth decade of life or beyond. ATC presents itself as a rapidly growing neck mass of approximately 3 cm to 20 cm in size followed by noticeable dysphagia, dysphonia and stridor (Nagaiah et al., 2011). 50% of the patients present with multiple distant metastases frequently to lungs, bone or brain (Hundahl et al., 1998). The American Joint

Committee on Cancer (AJCC) defines all cases of ATC as stage IV, and primary tumors are categorized as stage T4. Strictly intrathyroidal (T4a) tumors without lymph node involvement or distant metastases (N0 and M0, respectively) are designated as stage IVA. In stage IVB, the primary tumor exhibits gross extrathyroidal extensions (T4b; any N and M0). Patients with distant metastases (any T, any N, M1) are at stage IVC (Smallridge et al., 2012). Owing to the extremely aggressive nature, the tumor burden increases rapidly with tumor volume usually doubling in each week leading to eventual involvement of trachea which is discernible from appearance of hemoptysis. Involvement of cervical lymph nodes and recurrent laryngeal nerve (RLN) are also noted in 30-40% of the cases (NEL et al., 1985). Histopathological features of ATC vary from patient to patient and at the intratumoral level also. ATC is composed of a heterogeneous mixture of spindled, epithelioid and pleomorphic giant cells. The most commonly observed variant is the spindle cell pattern (approximately 50% of patients), followed by the pleomorphic giant cell pattern (approximately 30–40% of patients) and the squamoid pattern (less than 20% of patients) (Nikiforov et al., 2009) (Fig 5). Some common histological features include extreme invasiveness, extensive tumor necrosis, marked nuclear pleomorphism and high mitotic index. Neoplastic cells have pleomorphic nuclei that show highly irregular nuclear contours and coarse chromatin. Mitoses are typically abundant, with presence of atypical mitotic figures with a tripolar shape that consists of three radiating spokes from a center. This type of mitotic figure indicates aberrant mitosis and is a definitive sign of malignancy. Additionally, there is a complete lack of normal follicular structure with colloid in ATC and the cells form solid sheets with abundant necrotic centers (Nikiforov et al., 2009).

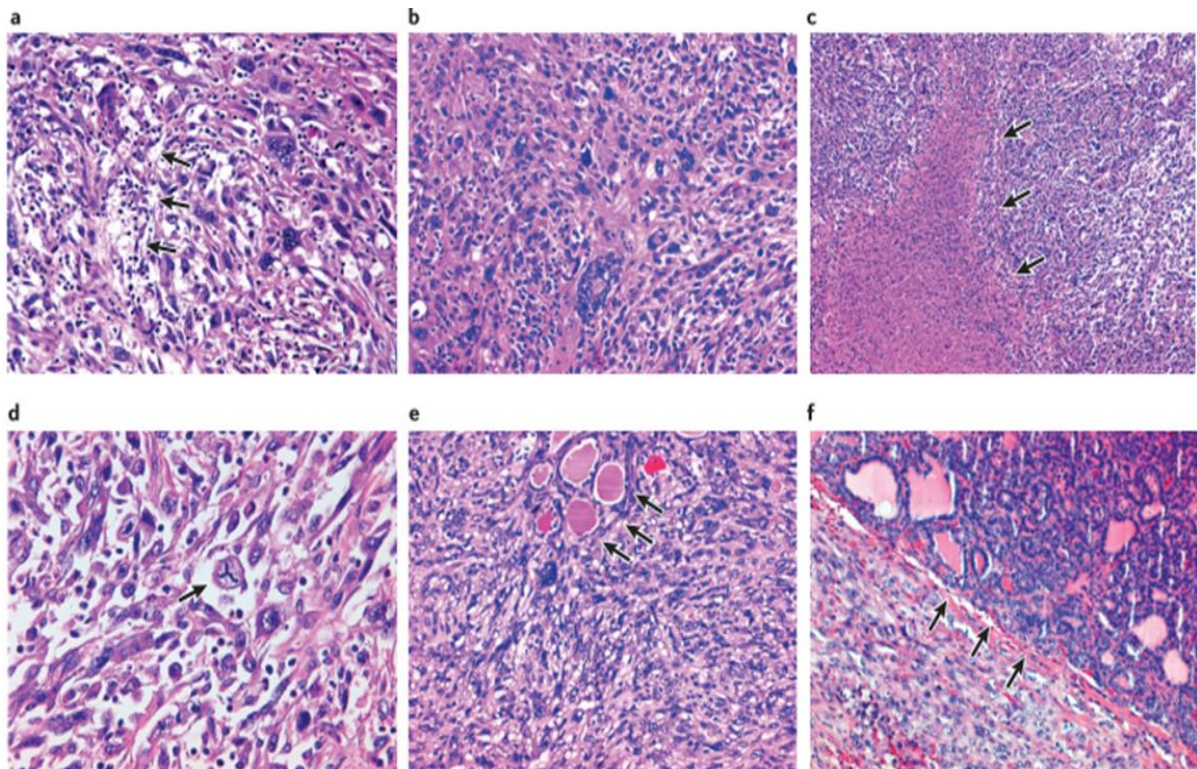


Figure 5. Various histological patterns of ATC. (a) Neoplastic cells with spindled and pleomorphic giant pattern. (b) Arrows indicate infiltrating lymphocytes; Giant cell pattern; (c) presence of extensive tumor necrosis indicated by arrows; (d) atypical mitotic figure with tripolar mitosis indicated by arrow; (e) entrapped non-neoplastic follicles indicated by arrows; (f) ATC with adjacent differentiated PTC indicated by arrows. Adopted from: Nat Rev Endocrinol, 13 (11), 644-660

### *Molecular carcinogenesis in TC*

Like any other malignancy, TC also results from a multistep process of carcinogenesis when the normal thyroid follicular cells experience single or multiple assault at the molecular level culminating into malignant transformation. While some of these mutations and aberrant signaling pathways are involved in the early stages of thyroid carcinogenesis, others are responsible for its progression. A plethora of genetic and epigenetic events contribute to the genesis and progression of TC at different stages.

### *Gene mutations*

There are numerous genetic alterations that culminate into thyroid carcinogenesis. One of the most prominent instances is the transverse point mutation T1799A in v-Raf murine sarcoma viral oncogene homolog B1 (BRAF) resulting in a valine-to-glutamic acid switch at codon 600, resulting in expression of BRAFV600E protein. This leads to a ligand independent constitutive activation of this serine threonine kinase (Cohen et al., 2003; Fakhruddin et al., n.d.; Fukushima et al., 2003; Kim et al., 2016; Kim et al., 2018). This mutation is an early event in thyroid carcinogenesis and is prevalent in almost 53% of PTC (Fukushima et al., 2003) and 20-25% of ATC. Previous studies have demonstrated that BRAFV600E is a poor prognostic factor in PTC which is often associated with aggressive pathological features, increased recurrence and loss of radioiodine avidity leading to treatment failure. There is a high prevalence of BRAF mutations in the aggressive tall-cell variant papillary thyroid carcinoma (55–100%), whereas a relatively low prevalence of only 7-14% has been reported in follicular variant papillary thyroid carcinoma (Nikiforova et al., 2003; Salvatore et al., 2004; Trovisco et al., 2005; Xing, 2013). Interestingly, in some cases of PTC, intra-tumoral heterogeneity in the BRAF status has been noted where the number of cells with WT BRAF supersedes the number

of cells with BRAFV600E (Guerra et al., 2012). This raises a dilemma of whether BRAFV600E lesion is a pre-requisite for PTC formation or BRAFV600E is followed by tumorigenesis (M. Xing, 2013). It might be possible, that once the tumorigenesis is triggered by BRAFV600E, there are secondary mutations that are selected for instead of BRAFV600E during tumor progression (M. Xing, 2012). The second common early mutation observed in PTC and ATC, is a point mutation in RAS. In its active state, RAS is bound to GTP. The intrinsic GTPase activity of RAS hydrolyzes GTP into GDP and RAS returns to its inactive form. Mutated RAS loses the intrinsic GTPase activity and stays in a constitutively active state. Among the three isoforms of RAS (HRAS, KRAS and NRAS), NRAS mutation is most commonly observed in thyroid malignancies mostly involving codons 12 and 61 (M. Xing, 2013). NRAS and HRAS mutations can be found in 8.5% and 3.5% of PTCs respectively but the frequency is higher in ATC that has some DTC component in the tumor. RAS mutation can trigger aberrant activation of the mitogen-activated protein kinase (MAPK) pathway or PI3K/AKT (protein kinase B) pathway. The major driving lesions in different histological subtypes of TC are summarized in figure 6. In case of thyroid malignancies, RAS mutation has been observed to trigger PI3K/AKT pathway as evidenced by preferential association of RAS mutation and AKT phosphorylation (Abubaker et al., 2008; Liu et al., 2008). Other crucial genes that are mutated in thyroid neoplasms include TERT,  $\beta$ -catenin (CTNNB1), TP53, isocitrate dehydrogenase 1 (IDH1), anaplastic lymphoma kinase (ALK), and epidermal growth factor receptor (EGFR). These mutations are associated with the aggressive variants - PDTC and ATC, which is suggestive of their role in the progression and aggressiveness of these subtypes.  $\beta$ -catenin (CTNNB1) is a very significant player in Wnt/  $\beta$ -catenin signaling which is one of the most fundamental pathways

involved in embryogenesis as well as a plethora of normal cellular processes and is under strict spatio-temporal regulation. Unfortunately, upregulation of this pathway is often observed to be associated with later stages of thyroid tumorigenesis, especially in the process of epithelial-mesenchymal transition (EMT). EMT is a process which has been historically associated with metastasis, but the etiological association between these two events are debated (Fischer et al., 2015; Welch & Hurst, 2019). Interestingly, ATC is often associated with overexpression of this protein which might partially explain the high metastatic potential of this disease. Next generation sequencing (NGS) studies from multiple centers have identified novel genes and driver mutations associated with ATC. A recent study by Jeon *et al* reported novel single nucleotide variants (SNVs) associated with ATC. Some of the novel ATC genes include PKHD1, NF2, ANKLE, BUB1, EIF1AX, CLTC, ERBBZIP, ERCC4, EZH2 (Jeon et al., 2016). TERT mutation is the most frequent one observed in ATC (73%) and at later stages of PTC. TERT encodes for the reverse transcriptase component of telomerase and is usually over expressed in most of the tumors. Commonly identified mutations include C228T and C250T. The role of TP53 mutation in ATC is well established in the process of carcinogenesis. Multiple loss of function - polymorphisms have been reported in this tumor suppressor gene. EIF1AX is a novel ATC related gene that encodes for X-linked eukaryotic translation initiation factor 1A. This gene mutation is closely associated with RAS mutation and is claimed to be crucial in transformation of FTC into ATC (Landa et al., 2016a) (Agrawal et al., 2014). Though ATC is historically known as a tumor with low mutational burden, recent findings confirm, presence of novel somatic mutations in ATC that partially changes the typical notion.

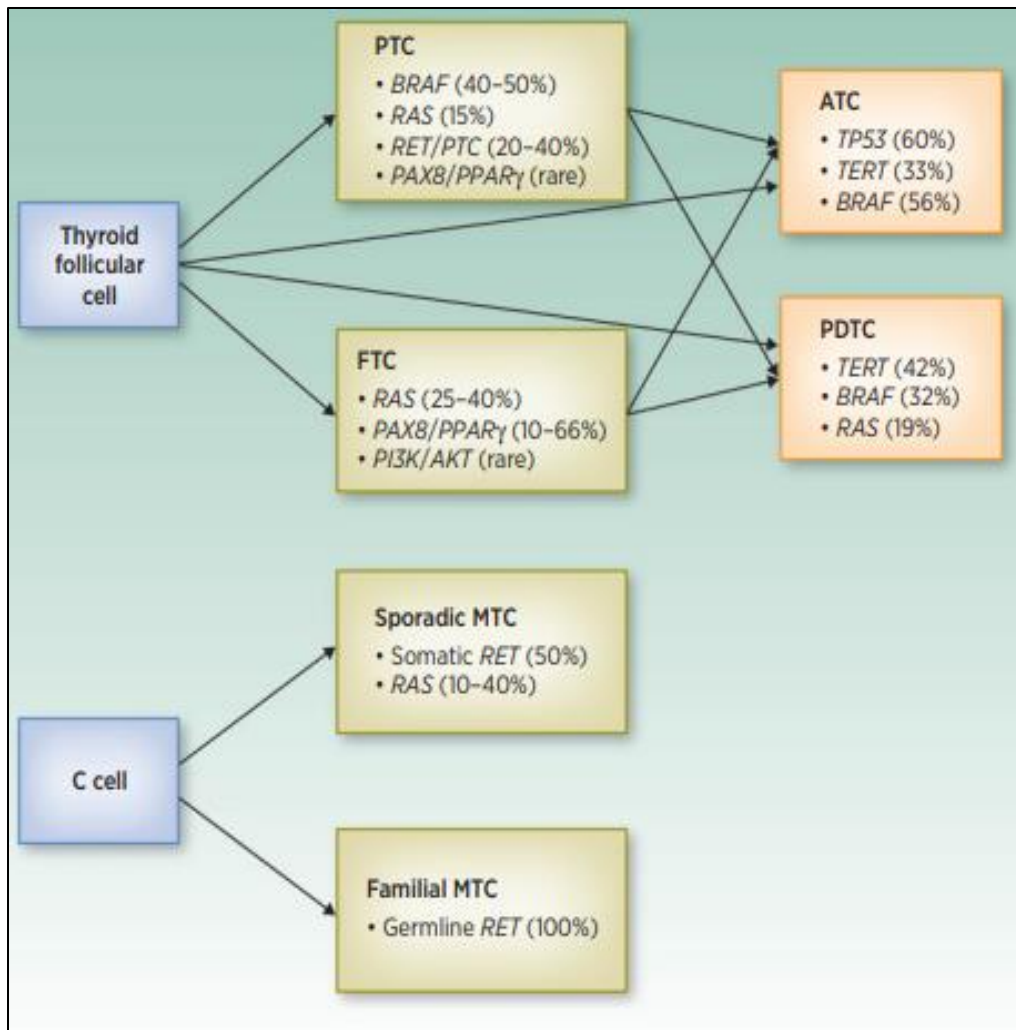


Figure 6. Histological subtypes of cancer with most prevalent genetic lesions (in percentage). Source: Clin Cancer Res; 22(20) October 15, 2016

### *Genomic instability*

Genomic instability has been closely associated with tumorigenesis. Increased mitotic rate in elderly patients with ATC or aggressive variants of PTC often results in aneuploidy eventually altering the copy number of genes. Copy number gain is commonly observed in genes of PI3K pathway, including pIK3CA, PDK-1, AKT1 and AKT2 (Abubaker et al., 2008; Liu et al., 2008). Interestingly, recent findings suggest that in Hürthle cell carcinoma (HCC), the genome is in near haploid state, which occurs early in the process of tumorigenesis and is stable throughout the entire course. This study also noted complex I mitochondrial DNA mutation occurring early in the disease process and maintained throughout the entire course. These observations point to the likelihood of these aberrations being a driver phenomenon, not simply markers (Ganly et al., 2018; Gopal et al., 2018). A recent study by Naveen *et al.* identified significant genomic amplifications in ATC. 70% of the patients' genome were polyploid and all of them were associated with multiple breakpoints mostly around the centromere with a median frequency of sixteen (Ravi et al., 2019). 80% of the cases had high level of genetic amplification which is defined by the authors as gain of more than three copies over the basal level. The amplified regions included genes like POP4, PLEKHF1, C19orf12, CCNE1, and URI1. POP4 encodes one of the protein subunits of small nucleolar ribonucleoprotein complexes: the endoribonuclease for mitochondrial RNA processing complex and the ribonuclease P complex. This protein is involved in processing of precursor RNA and aberrant expression of this protein might result in formation of alternatively spliced variants of a transcript with unknown function. CCNE1 codes for cyclin E1 which is the regulatory subunit of CDK2 and is required for G1/S transition in cell cycle. In non-thyroid malignancies such as bladder cancer, ovarian adenocarcinoma and triple negative breast

cancer (Zhao et al., 2019). An increase in copy number of this gene is often considered as a poor prognostic marker in cancer, but it is not conclusive (Zhao et al., 2018). Nevertheless, multicenter studies with large groups of patients have identified gain of copy number in CCNE1 in close to 30% of ATC cases (Zhao et al., 2018).

#### *Gene translocations*

The most frequent gene translocation observed in thyroid cancer is RET/PTC translocation. RET is a protooncogene encoding a receptor tyrosine kinase (RTK). RET/PTC rearrangement results from genetic recombination between the 3' tyrosine kinase portion of RET and the 5' portion of a partner gene resulting in oncogenic transformation in the thyroid. More than 10 types of RET–PTC translocation have been reported namely, RET/PTC1, RET/PTC3 etc. Each translocation usually involves one partner gene with RET. RET–PTC is a classical oncoprotein that activates both MAPK and PI3K–AKT pathways via recruitment of signaling adaptors to phosphorylated Y1062 on the intracellular domain of RET fusion protein (Hayashi et al., 2000). The second prominent recombinant oncogene in TC is the paired box 8 (PAX8)–peroxisome proliferator-activated receptor- $\gamma$  (PPARG) fusion gene (PAX8–PPARG). This rearrangement is extremely prevalent in both FA, FTC and follicular variant of PTC (Dwight et al., 2003; Eberhardt et al., 2010; Kroll et al., 2000). PAX8 is a thyroid-specific paired-box transcription factor involved in development of thyroid follicular cells and expression of thyroid-specific genes. PAX8 releases the hormones that are important for regulating growth, brain development, and metabolism. PAX8 and other transcription factors regulate expression of genes like TPO, NIS and TSH receptor that are involved in thyroid hormone biosynthesis. PPAR $\gamma$ , which is encoded by PPARG (located on chromosome 3p25), is a member of the

steroid nuclear-hormone - receptor superfamily that forms heterodimers with retinoid X receptor. It plays a crucial role in differentiation of adipocytes and facilitates insulin-regulated metabolic functions. During the chromosomal exchange, the 2q13-qter region is translocated to 3p25, resulting in an in-frame fusion between most of the coding sequence of PAX8 (on 2q13) and the entire translated reading-frame of PPAR $\gamma$  (on 3p25) (Eberhardt et al., 2010). Unfortunately, the PAX8-PPAR $\gamma$  fusion protein employs a dominant-negative effect on the wild-type tumor suppressor PPAR $\gamma$ . Novel chromosomal translocations have been reported with ALK. The breakpoint of ALK often occurs at intron 19, resulting in severance of the 3' end of exons 20-29 from 5' end sequences. This encompasses the promoter, regulatory elements and coding sequences corresponding to the extracellular and transmembrane domains of ALK. Several ALK fusion genes have been reported in thyroid cancer, including EML4-ALK (Ho Ji et al., 2015), TFG-ALK and STRN-ALK (Kelly et al., 2014). Ceritinib is an FDA approved drug for non-small cell lung cancer (NSCLC) which is under phase II/III clinical trial for ALK rearranged ATC (Godbert et al., 2015).

#### *Epigenetic factors*

Multiple studies have confirmed the role of epigenetic mediators in tumorigenesis. Genes that control epigenetic status of a cell are often found dysregulated in tumor initiating cells and their subclones often persist even after rigorous treatment. Aberrant gene methylation is often observed in thyroid cancer (M. M. Xing, 2007). Epigenetic regulation of genes relies on a fine balance between different proteins as there are number of normal cellular processes that are epigenetically controlled. Any type of discordant epigenetic event can disrupt this balance between different cellular processes leading to malignancy. Interestingly, some of

these epigenetic events are often associated with specific oncogenes. In PTC, BRAFV600E is often associated with promoter hypermethylation of a number of tumor suppressor genes, like TIMP3 (tissue inhibitor of metalloproteinases 3) and RAR $\beta$  (retinoic acid receptor beta) (Hu et al., 2006). In FTC and ATC, promoter methylation is commonly observed in the well-known tumor suppressor gene PTEN leading to its suppression. PTEN methylation is often accompanied with aberration in PI3K – AKT pathway in TC (Hou et al., 2008). Additionally, genes encoding components of SWI/SNF chromatin remodeling complex are often mutated in ATC. A study by Land *et al.* detected mutation in ARID1A, ARID1B, ARID2, ARID5B, SMARCB1, PBRM1, and ATRX in advanced TC. Their study confirmed missense mutation in ARID1A and a frameshift mutation in SMARCB1 in ATC at low frequency (Landa et al., 2016b). These proteins often form a functional complex and disruption of any one protein can render the whole complex dysfunctional. 24% of the ATC cases had mutations in different histone methyl transferases in this study (Landa et al., 2016b). Some of these mutations were exclusive for ATC.

Accumulation of all these genetic and epigenetic assaults finally culminate into dysregulation of normal cellular signaling pathways resulting in formation of a neoplastic cell with better survival skill, which eventually outgrows the healthy cells by clonal expansion and establishes the tumor. In ATC, the extremely aggressive phenotype results from a combination of some of these accumulated the genetic lesions over the time and the crosstalk between aberrant cellular signaling pathways. A better understanding of the tumor biology in the context of crosstalk between different signaling pathways and compensatory survival strategies is extremely crucial for identification of effective therapeutic targets in ATC.

*Clinically significant molecular pathways involved in thyroid carcinogenesis*

The development, progression, and metastasis of TC are closely associated with accumulation of multiple genetic alterations and progressive aberrations in multiple signaling pathways, accompanied by numerous secondary molecular alterations in the cell and tumor microenvironment, which could serve as a potential biomarker for diagnosis and prediction of prognosis. There are some classical proliferation and survival pathways known to play role in thyroid carcinogenesis and there are some novel pathways currently under consideration for development of targeted therapies for the aggressive and resistant variants of TC such as ATC.

*MAPK signaling pathway*

MAPK signaling pathway is instrumental in proliferation and survival strategies adopted by tumor cells. This pathway is extremely important in normal development also but is hyper-activated in disease states. This pathway couples extracellular stimuli to specific transcription program. This is an extremely ubiquitous pathway involved in not just cellular proliferation, but in cellular development, differentiation and apoptosis as well. This signaling cascade starts from a receptor tyrosine kinase (RTK) and the main effector molecule is RAS (Fig 7). Upon ligand binding, RAS is activated and changes in active GTP bound form to activate the Ser/Thr kinase RAF. RAF has three isoforms, ARAF, BRAF and CRAF. The proto-oncogene form of BRAF is on chromosome 7q24 and encodes a Ser/Thr kinase that transduces regulatory signals through the Ras–Raf–MEK–ERK cascade. As discussed before, several gain of function point mutations in BRAF (e.g. BRAFV600E) lead to ligand independent aberrant activation of ERK signaling which has a domino effect on myriad of cellular processes aiding in neoplastic transformation. This particular genetic lesion makes this protein a very attractive target for

development of small molecule inhibitors (Huang et al., n.d.; Hyman et al., 2015; Jia et al., 2018; Lin et al., 2014). Activated RAF phosphorylates and activates MEK (a tyrosine/threonine kinase) which finally phosphorylates ERK (extracellular signal-regulated kinase) in the activation loop. ERK has a negative feedback loop regulating the pathway. ERK1/2 mediates inhibitory phosphorylation on juxtamembrane domain of receptor tyrosine kinases (e.g. T669 phosphorylation of EGFR), that leads to negative feedback inhibition of the signaling cascade. The target specificity of active ERK is controlled by substrate availability, scaffolding, and subcellular localization. Scaffolding proteins tether MEK and ERK to specific substrates and subcellular compartments and are essential for ERK phosphorylation of the corresponding bound or local targets (Mendoza et al., 2011).

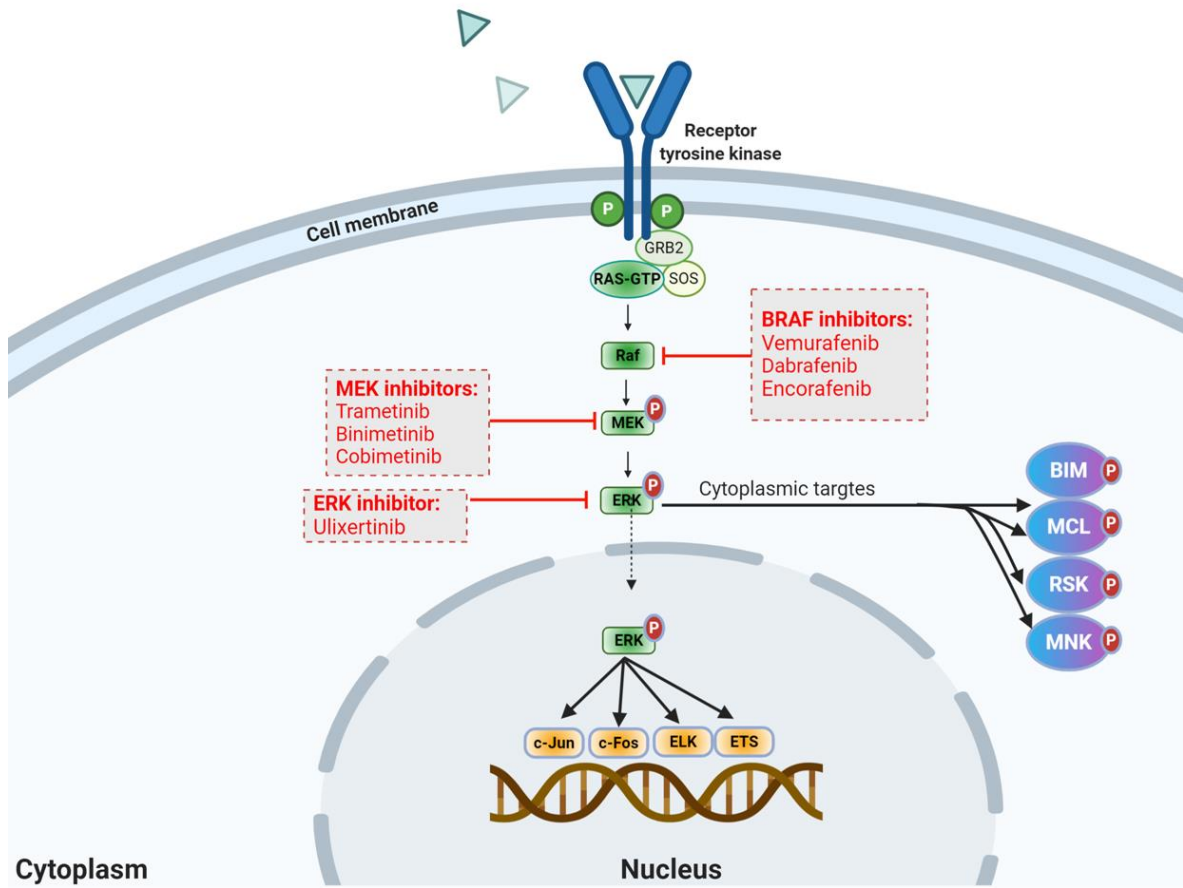


Figure 7. MAPK signaling pathway. Adapted from: Cancer Discov; 8(2); 140–2

### *PI3K–AKT signalling pathway*

PI3K/AKT pathway is an extremely crucial player in thyroid carcinogenesis. Early evidence for this hypothesis came from the association observed between Cowden's syndrome (caused by germline mutations of PTEN) and FA and FTC (Liaw et al., 1997). This is another key pathway regulating cellular metabolism, division and survival. PI3K (phosphatidylinositol 3-kinase) is a lipid kinase which is activated by growth factors either through direct receptor recruitment or via recruitment of docking proteins, like insulin receptor substrate (IRS) or GRB2-associated binder (GAB). PI3K produces PIP3 (phosphatidyl inositol 3,4,5 triphosphate), which in turn recruits protein kinase AKT to the cell membrane. There, AKT gets activated by 3-phosphoinositide-dependent kinase 1 (PDK1). This is not enough for activation of Akt. Phosphorylation of Akt at Ser473 by mTORC2 (mammalian target of rapamycin) stimulates full enzymatic activity. mTORC2. mTORC1 comprises of the Ser/Thr kinase mTOR, the regulatory-associated protein of mTOR (RAPTOR), mLST8 (mammalian lethal with Sec13 protein 8), proline-rich AKT1 substrate 1 (PRAS) and DEP domain-containing mTOR-interacting protein (DEPTOR). This complex phosphorylates eukaryotic initiation factor 4E (eIF4E)-binding protein (4E-BP) and S6K (p70 ribosomal S6 Kinase). These events modulate biogenesis of ribosomes and the translation of proteins involved in cell growth and division. Amino acid availability, overall cellular energy status, and oxygen levels modulate this pathway.

### *NF- $\kappa$ B Signaling Pathway*

The nuclear factor kappa-light-chain-enhancer of activated B cells (NF- $\kappa$ B) transcription factor pathway has been one of the crucial pathways that has been characterized as a “double-edged sword” due to its pivotal role in the promotion of inflammation and tumor

development, as well as in the regulation of the immune system against cancer. This is an extremely crucial signaling pathway regulating tumor cell proliferation, cellular survival, angiogenesis, invasion, metastasis and drug/radiation resistance. In mammals, the NF $\kappa$ B family includes p50 (NF $\kappa$ B1), p52 (NF $\kappa$ B2), RelA (p65), RelB, and cRel. NF $\kappa$ B can be activated by either canonical or alternative pathways. The central players of the canonical pathway are the p65 and p50 subunits, whereas in the alternative pathway the central transcriptionally active heterodimer is the p100/p52: RelB complex. Without stimulus, NF- $\kappa$ B is repressed by inhibitor of kappa B (I $\kappa$ B) proteins. Upon stimulation by members of tumor necrosis factor (TNF) superfamily, IL-1, and/or pathogen-associated molecular patterns (e.g. LPS), adaptor proteins like MyD88 and TRAF signal for the activation of inhibitor of kappa B kinase (I $\kappa$ BK or IKK), which phosphorylates either I $\kappa$ B (canonical pathway) or the p100 subunit of NF- $\kappa$ B (alternative pathway). In the canonical pathway, various stimuli induce phosphorylation of I $\kappa$ B $\alpha$ , leading to release of NF- $\kappa$ B from the inhibitory complex and triggers its nuclear translocation. The canonical NF- $\kappa$ B signaling facilitates vital tumor-promoting mechanisms like stimulation of cell proliferation and inhibition of apoptosis, EMT, angiogenesis, invasiveness, as well as metastasis. As a driver of such crucial mechanisms inducing and promulgating tumor growth, NF- $\kappa$ B was shown to be constitutively active in a broad range of cancers including aggressive form of PTCs. Studies have shown that NF- $\kappa$ B activation is positively associated with aggressive phenotypes, including extrathyroidal extension and lymph node metastasis in human PTCs (Pyo et al., 2013). Activation of NF- $\kappa$ B has been implicated in the case of MEK independent hyperactive BRAFV600E in PTCs (Bommarito et al., 2011) which in turn activates tissue inhibitor of metalloproteinases (TIMP-1) triggering an

autocrine loop finally upregulating AKT. More recent studies have revealed that NF- $\kappa$ B contributes to activation of anti-apoptotic signaling mechanisms in aggressive PTCs in a small GTPase – RAC1b dependent way (Faria et al., 2017). A recent study by Ken Shiraiwa revealed that activation of JAK/STAT3 pathway and NF- $\kappa$ B pathways are extremely crucial for maintenance of cancer stem cell populations in ATC, but not in normal thyroid (Shiraiwa et al., 2019). These findings suggest that NF- $\kappa$ B might play a pivotal role in the progression of PTCs towards a more aggressive phenotype and eventually to ATC.

All these genetic mutations and aberrant signaling pathways are triggered at different stages of the disease and play unique role in the process of tumorigenesis. This suggests a phase of initial tumor transformation followed by development of a cancer-prone niche where cells have heightened susceptibility to secondary or passenger mutations. With the progressive accumulation of deregulated signaling pathways and aberrant functional proteins (not only MAPK and PI3K-AKT, but also  $\beta$ -catenin, hTERT, TP53, and so on), the tumor cells eventually start shaping their microenvironment and promote selective recruitment of cells nurturing tumor progression. This results in gradual progression of the tumor towards a more clinically aggressive phenotype which is difficult to manage.

### Therapeutic options in thyroid cancer

The therapeutic approach towards thyroid cancer is shaped by a combination of accurate diagnostic procedures and proper characterization of the histology and assessment degree of extrathyroidal involvement.

#### *Diagnosis:*

Presence of palpable thyroid nodules are extremely common in the general populace with a ratio of 5:1 in women vs men. Use of ultrasound scanning increases the ratio to 50-70%. Long-term prognosis for DTC is excellent, with survival rates for adults being 92–98 % at 10-year follow-up. However, 5–20 % of patients develop local or regional recurrence requiring further treatment and 10–15 % of patients eventually develop distant metastases. The American Thyroid Association (ATA) provided detailed guidelines on the therapeutic approach of DTC (Haugen et al., 2016). Features of the nodules are major deciding factors for biopsy. While solid hypoechoic nodule or solid hypoechoic component of a partially cystic nodule with irregular margins, microcalcifications, altered length/width ratio, rim calcifications with small extrusive soft tissue component are mandated for needle aspiration biopsy, purely cystic nodules are excluded from this group.

#### *Surgery:*

The initial management of DTC and MTC almost always involves surgical resection. For tumors <4 cm and lacking aggressive features, like extrathyroidal extensions, angioinvasion, multifocality or distant invasion, hemithyroidectomy is recommended. The most important aim of primary surgery is to achieve complete macroscopic disease clearance. Extracapsular thyroidectomy with preservation of the recurrent laryngeal nerve and parathyroid glands is usually the standard. This helps achieve disease clearance and minimize the risk of future

thyroid bed recurrence. Need for further surgical intervention is dependent on involvement of other organs, like trachea or esophagus. Patients with non-metastatic PTC and FTC often respond well to surgical resection and hormone replacement therapy without the need for radioiodine ablation.

*Radioiodine ablation therapy (RAIT):*

In the current ATA guidelines, radioactive iodine (RAI) is not routinely recommended post - thyroidectomy for the low risk patients, but it is considered for intermediate and high-risk patients (Haugen et al., 2016). In low-risk patients, total thyroidectomy usually removes the remnant, thus postoperative RAI ablation does not affect the prognosis (Luster et al., 2008). Surgical resection followed by RAI is often advised for high risk tumors. The effectiveness of radioiodine therapy depends on the patient's serum TSH level. A TSH level of  $\geq 30$  mU/L usually increases NIS expression and thereby helps the follicular cells concentrate the radioiodine (Cooper et al., 2006). Realistically, it is difficult for the patients to achieve this concentration of TSH naturally either by prolonged withdrawal from levothyroxine or just waiting for at least three weeks post thyroidectomy. Additionally, this is associated with severe side effects which leads to patient non-cooperation. To circumvent this, recombinant TSH (rhTSH) is usually given before RAI ablation. The current approved regimen of rhTSH is two consecutive daily intramuscular injections of 0.9 mg. Second injection of rhTSH is followed by radioiodine therapy after 1 day and serum thyroglobulin testing in 3-4 days. Diagnostic whole-body scintigraphy (WBS) is performed, after 48-72 hrs. of RAI administration. Post-therapy WBS is performed 2–7 days following RAI administration. Though RAIT is a cornerstone in the routine adjuvant management in patients with high-risk

differentiated thyroid cancer (DTC), 5-15% of the patients with DTC and 50% of metastatic DTCs and almost all ATC patients are refractory to RAI (Haugen et al., 2016). Patients with RAI refractory phenotype has extremely poor prognosis. Specially in metastatic patients, 10 year survival plummets to 10% (Durante et al., 2006). Patients with advanced stage of DTC or MTC are often at risk of developing complications that change their quality of life. In these cases, a more aggressive approach involving localized or systemic therapy should be undertaken. Localized therapy is often the first choice for delaying the initiation of systemic therapy. Palliative external beam radiation therapy (EBRT) is often used in TC patients with painful bony metastases, as are bone-modulating drugs such as denosumab and zoledronic acid (Haugen et al., 2016). With better understanding of the molecular pathways involved in thyroid carcinogenesis, considerable effort has been put in understanding the regulation of NIS expression and the reason for its downregulation in metastatic thyroid cancers like aggressive PTCs or ATC. PI3K-AKT pathway activation leads to suppression of NIS glycosylation and its surface translocation. mTOR inhibitors can promote redifferentiation of thyroid cancer cells by upregulation of NIS mRNA and protein expression through increased transcription of thyroid transcription factor 1 (TTF1). Another crucial positive regulator of NIS expression is PTEN which is often suppressed in metastatic DTCs and ATC. TSH signals through the heterotrimeric G-protein complex and increases transcription of the NIS gene via activation of cAMP. Aberrant activation of the MAPK signaling pathway inhibits expression of phosphatidylinositol glycan anchor biosynthesis class U (PIGU) and NIS basolateral transport. Overexpression of pituitary tumor transforming gene 1 (PTTG1) and PTTG1 binding factor (PBF) results in decreased NIS levels in thyroid cancer. These observations suggested that

kinase inhibitors might hold some promise for induction of redifferentiation in the thyroid cancer cells and re-expression of NIS.

*Kinase inhibitors:*

Cellular dedifferentiation in thyroid cancers causes tumor progression with development of a more aggressive phenotype, metastasis, loss of iodide uptake, or unresponsiveness to RAI therapy, and correlates with the degree of MAPK activation. Tyrosine kinases are deeply involved in the MAPK signaling pathway through phosphorylation/dephosphorylation of several intracellular proteins, which underlies the rationale for the use of tyrosine kinase inhibitors (TKIs) in these cancers. Tyrosine kinase inhibitors are emerging as potentially effective option in advanced TC over last decade. Most agents that were tested in phase II and III trials were developed further for treatment of advanced radioiodine refractory (RAI-R) thyroid cancers. Major kinase inhibitors in clinical trials often target multiple tyrosine kinase receptors and referred to as multikinase inhibitors. They act on pathways responsible for angiogenesis, growth, invasiveness, and metastasis. Additionally, since none of these pathways are malignancy-specific, these inhibitors have been tried in different types of malignancies as well including MTC and ATC. Lenvatinib is a promising multikinase inhibitor targeted against VEGFR1, VEGFR2 and VEGFR3. An overall survival benefit was noted with the use of lenvatinib in patients > 65 years of age with radioiodine refractory (RAI-R) DTCs (Brose et al., 2017). In 2015, lenvatinib was approved for the treatment of ATC in Japan. A recent study by Hiroyuki *et al.* tested the efficacy of lenvatinib in 32 patients with stage IVC ATC. While the treated patients had a survival benefit of approximately 2months over the placebo group, two of the apparent responders acceded to massive necrosis and bleeding which

suggested the need for further dose adjustment (Iwasaki et al., 2019). Sorafenib is another multikinase inhibitor targeting RAF, VEGFR and PDGFRs. The combination of lenvatinib and sorafenib, are currently used for the treatment of RAI-R DTC, and two others, vandetanib (NCT01876784) and cabozantinib (NCT03690388), are under investigation in phase III trials for patients with progressive RAI-R DTCs and advanced RAI-R DTCs unresponsive to previous VEGFR therapy, respectively (Brose et al., 2019; Cabanillas et al., 2017; *Evaluation of Efficacy, Safety of Vandetanib in Patients With Differentiated Thyroid Cancer - Study Results - ClinicalTrials.gov*, n.d.). Pazopanib is an orally available multikinase inhibitor of VEGFR, platelet-derived growth factor (PDGF) receptor, KIT, fibroblast growth factor (FGF) receptor, and RAF which is approved for advanced renal cell carcinoma and advanced refractory soft-tissue sarcoma. This drug is being tested in pre-clinical studies in a combinatorial setting with topoisomerase I inhibitor topotecan in ATC (Di Desidero et al., 2019). This study showed that this specific combination has synergistic effect on ATC cell lines and the authors proposed a possible adaptation of this combination into future clinical trials for ATC patients. Interestingly, pazopanib was evaluated in a phase I clinical trial with MEK Inhibitor trametinib in advanced solid tumors and differentiated thyroid cancers (Kurzrock et al., 2019). Unfortunately, the trial did not meet the goal for the patients with follicular thyroid cancer, resulting in closing the trial for enrollment. This study did not recruit any ATC cases. Sorafenib is another orally active TKI that targets BRAF, VEGFR1, VEGFR2 and RET with proapoptotic and antiangiogenic effects *in vivo* (Kim et al., 2007). Though sorafenib has been approved for RAI-R DTC and PDTC, it had dismal impact in ATC patients with a median progression free overall survival time of 1.9 months (Savvides et al., 2013). Two other multikinase inhibitors

gefitinib and sunitinib have been evaluated in phase II clinical trials for advanced DTC and ATC but did not show promising results in either. A more targeted approach was taken for ATC with BRAFV600E inhibitor vemurafenib. Though the initial response was promising, a CT scan after 2 months of treatment initiation showed rapid progression of the disease along with metastasis to brain and esophagus. This not only indicated acquired resistance to vemurafenib, but reactivation of additional pathways leading to metastasis. In May 2018, United States Federal Drug Agency (FDA) approved the combination of dabrafenib and MEK inhibitor trametinib for the treatment of ATC with BRAF (B-Raf Proto-Oncogene, Serine/Threonine Kinase) mutation. Dabrafenib is an inhibitor of some mutated forms of BRAF kinases of V600E, V600K and V600D. Dabrafenib also inhibits wild type BRAF and CRAF kinases. A major side effect of long term dabrafenib treatment is cardiomyopathy and secondary congestive heart failure. This mandated constant evaluation of cardiac function prior to and during therapy in these patients. Other major side effects of dabrafenib include but not limited to uveitis, hyperpyrexia, and serious skin toxicity. Evaluation of BRAFV600E status is an absolute prerequisite before this treatment to avoid paradoxical contribution of the drug in activation of MAPK pathway in tumor cells with WT BRAF. Another targeted approach against ATC involves mTOR inhibitor everolimus. This strategy was evaluated in phase II clinical trials in 40 patients with locally advanced or metastatic, unresectable or iodine-refractory thyroid cancer among which 6% had ATC. 90% of the subjects had already undergone different treatment modalities before enrolling (Lim et al., 2013). The ATC patients had a PFS of only 10 weeks. A brief summary of targeted therapies against ATC is provided in figure 9.

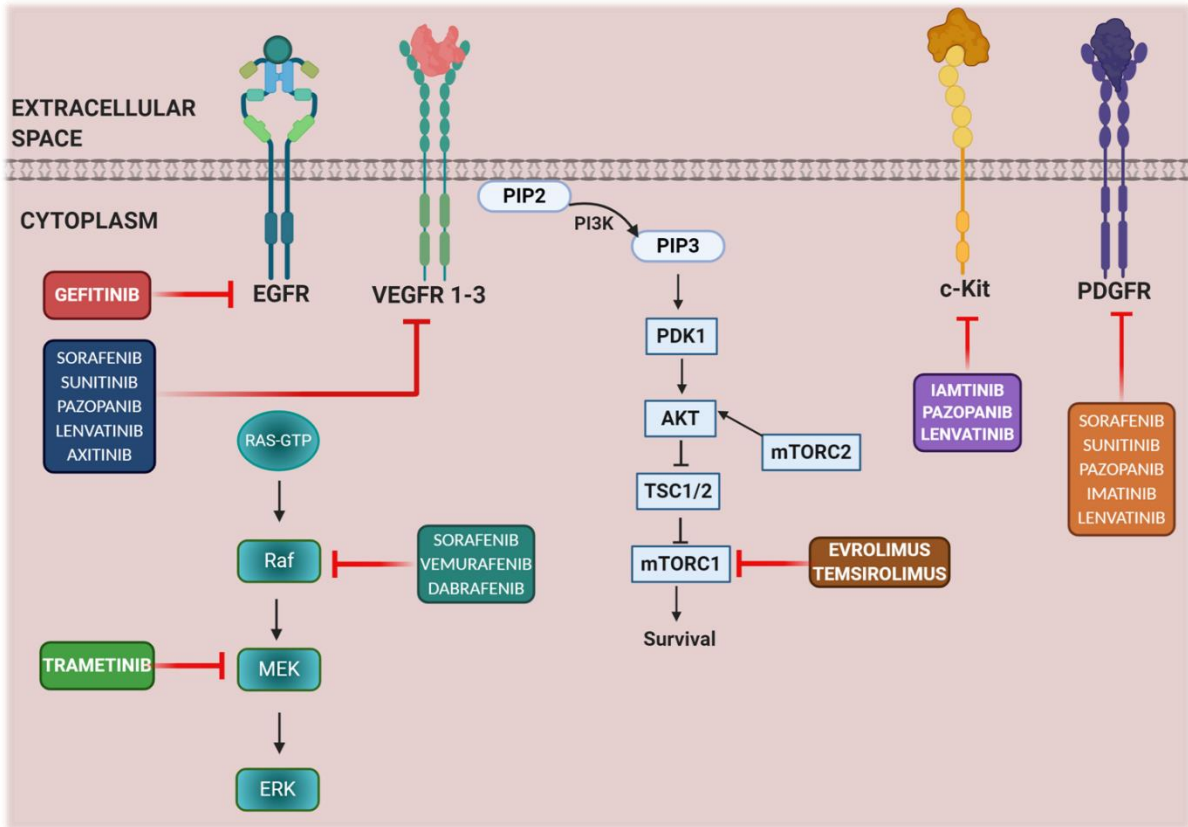


Figure 8. Mechanistic overview of targeted therapeutic agents in ATC.

Although TKIs have revolutionized the field of targeted therapies in aggressive PTCs, these treatments are often associated with severe side effects and have minimal effect on PDTs and ATCs. The undifferentiated nature confers unique refractory phenotype on ATC. This refractory phenotype is often associated with activation of compensatory pathways under the pressure of the drug which rescues the tumor. A multitude of such pathways have been reported in ATC. Recent pre-clinical study has shown that BRAF inhibition in 8505C cells leads to overexpression of c-Met which in turn results in reactivation of MAPK pathway and also PI3K/AKT pathway (Byeon et al., 2016). Other mechanisms of resistance against BRAFV600E inhibitors have also been suggested. RAF inhibitors can selectively express a truncated splice variant of BRAFV600E that lacks the RAS-binding domain and dimerizes constitutively, rendering it drug-resistant (Poulikakos et al., 2011). A recent report described as a possible mechanism of resistance to vemurafenib, via enhanced HER2/HER3 signaling pathway due to autocrine secretion of Neuregulin-1, observed in BRAF-mutant undifferentiated thyroid cancer cell lines post-vemurafenib treatment. Reactivation of MAPK pathway via CRAF activity has also been reported in PTCs during development of acquired resistance to vemurafenib (Hanly et al., 2016).

The crucial genetic lesions and complex crosstalk between the cellular pathways not only influence the tumor cell - phenotypes in ATC, but it helps the tumor cells shape their microenvironment which in turn favors the selection of more resilient cells. The complex

nature and significance of this interaction was underappreciated until recently. Oncogene driven expression of cytokines from the tumor cells play crucial role in dictating the nature of immune cells recruited in the tumor microenvironment (TME) and eventually shapes the tumor immune microenvironment (TIME) and anti-tumor immune response. This event is extremely crucial for an aggressive cancer like ATC, where a better understanding of this crosstalk is an absolute prerequisite for the development of alternative therapeutic approach.

#### Immune landscape in anaplastic thyroid cancer

##### *Genetic lesions and immune microenvironment: a close relationship*

The genetic lesion BRAFV600E, and transcription factor STAT3, which is frequently linked to aberrant oncogenic signaling, have been shown to drive expression of IL-6, IL-10 and VEGF, cytokines that encourage a tolerogenic monocyte-derived DC phenotype *in vitro* (Sumimoto et al., 2006), a phenomenon that could potentially modulate their antigen presentation efficiency and dampen anti-tumor T cell response *in vivo*. This process is facilitated by BRAFV600E mediated upregulation of WNT/ $\beta$ -catenin which induces ATF3, a transcriptional suppressor of the chemokine CCL4. A diminished amount of this cytokine is associated with polarization of dendritic cells (DCs) towards a tolerogenic phenotype which is incapable of optimal antigen presentation. Also, two reports have suggested immunosuppressive cytokine secretion by tumor cells harboring the KRAS<sup>G12D</sup> mutation. These studies have shown that cells with these mutations secrete granular macrophage colony stimulating factor (GM-CSF), which in turn recruits myeloid derived suppressor cells (MDSCs) and leads to poor prognosis

in mouse models of pancreatic adenocarcinoma (Pylayeva-Gupta et al., 2012). In this study, this mutation was associated with recruitment of Gr1+CD11b+ double-positive cells which represent a heterogeneous population composed of MDSCs, monocytes, and immature myeloid cells in mouse. At the molecular level, KRAS induces expression and secretion of the suppressive cytokines IL10 and TGF $\beta$ -1 by cancer cells in a MEK/ERK/AP-1 dependent way which promote Treg induction (Zdanov et al., 2016). A recent study by Julianna *et al.* has shown that tumor specific loss of P53 can re-orchestrate the immune microenvironment towards an immune suppressive type where CD8<sup>+</sup>T cell activity is diminished (Blagih et al., 2020). Interestingly, these are some of the high-ranking somatic mutations identified in ATCs by multiple studies. Activation of oncogenic pathways drives production of cytokines triggering recruitment of innate immune cells, namely macrophages. These macrophages in turn contribute to cancer progression by producing pro-inflammatory mediators such as IL-6, tumor necrosis factor (TNF) and interferon- $\gamma$  (IFN $\gamma$ ) and growth factors including epidermal growth factor (EGF) and WNTs which create a highly mutagenic microenvironment. These cytokines upregulate transcription factors promoting tumorigenesis. This complex cytokine milieu controls the immune surveillance in TC via recruitment of immune cells conducive to tumor progression. Conception of this pro-tumorigenic niche precludes the tumor cells from immune surveillance via recruitment of tolerogenic immune cells that secrete primarily immune suppressive cytokines dampening T cell response leading to immune escape.

#### *Immune surveillance in thyroid cancer*

During the process of tumorigenesis, from the early stages of transformation to the emergence of clinically detectable full-blown neoplasia, the tumor cells are aided by

avoidance or subversion of detection by the immune system, known as immunosurveillance. Cells of both the innate and adaptive immune systems are engaged in the process of immune surveillance in thyroid cancer. Tumor associated macrophages (TAM)s are one of the most crucial cell type with an ambivalent role in tumor progression which has been reported in thyroid carcinogenesis (S. Park et al., 2019). In PTCs, TAMs correlated with lymph node metastasis, larger tumor size, and poor survival (W. Fang et al., 2014; Seunghwan Kim et al., 2013; Ryder et al., 2008). In PDTC, TAM density correlated with capsular invasion, extrathyroidal extension and poor survival (Ryder et al., 2008). TAMs represent more than 50% of immune cells in ATCs, forming a “microglia-like” interconnected cellular supportive network in close contact with cancer cells (Caillou et al., 2011). These TAMs secrete inflammatory cytokines such as IL-23 and IL-17 that trigger tumor-elicited inflammation that in turn promote tumor growth. TAMs also provide essential support required for tumor metastasis. DCs are responsible for sampling tumor antigens and presenting them to T cells in the draining lymph nodes. Unfortunately, tumor associated DCs are usually immature with impaired antigen presentation skill. Presence of CD1a<sup>+</sup> DCs are reported in PTC, which supports the hypothesis of immature DC and inadequate antigen presentation in TC (Tsuge et al., 2005). As discussed in the previous section, MDSCs are attracted to tumor site by multiple factors and impart a strong local as well as global immune suppressive environment. An increase in peripheral blood MDSC level was observed in ATC patients compared to healthy controls which correlated with the serum IL-10 level, pointing towards a correlation between MDSCs and systemic immunosuppression (SUZUKI et al., 2013). Other immune cells involved in immune surveillance, like natural killer (NK) cells are also sparse in ATC compared

to DTC and FTC. Optimally primed CD8<sup>+</sup> T cells execute anti-tumor activity via perforin and granzyme mediated lysis of tumor cells. Hence, tumor infiltrating T lymphocytes (TILs) are instrumental for mounting a potent anti-tumor immune response. In a study conducted with a wide cohort of DTC patients, including PTC and FTC, immunohistochemical analysis revealed that the combined enrichment of CD8<sup>+</sup> cells and Cox-2 overexpression correlated with the highest risk of disease relapse. In most of the tumor samples analyzed (68%), CD8<sup>+</sup> cells were granzyme B negative, suggesting an anergic state (Cunha et al., 2015). TILs are often associated with better prognosis as observed in melanoma (Antohe et al., 2019), ovarian cancer (Sato et al., 2005), lung cancer (Ye et al., 2017), bladder cancer (Joseph & Enting, 2019) and colorectal cancer (Glaire et al., 2019). Interestingly, a low intratumoral CD8<sup>+</sup>/Foxp3<sup>+</sup> ratio was reported in human BRAFV600E PTC, which was also associated with an increased expression of the immunosuppressive molecules arginase-1, indoleamine 2,3-dioxygenase 1 (IDO1), and programmed death-ligand 1 (PD-L1) (Angell et al., 2014). A recent study reported data on the PD-L1 expression in 407 primary TCs with a median 13.7-year of follow-up, studying the associations between PD-L1 expression and clinicopathologic features, such as TERT promoter, disease progression, and BRAF status. Tumoral PD-L1 expression was observed in 6.1% of PTCs, 7.6% of follicular thyroid cancer (FTCs), and 22.2% of ATCs. Another study noted that the proportions of PD-L1 positive follicular cells in ATCs were more than 80% (Ahn et al., 2017). These observations confirm the lack of effective immune surveillance in ATC that might promote immune escape and progression of the cancer via upregulation of the checkpoint molecule PD-L1. This molecule interacts with PD-1 on T cells and is responsible for induction of T cell exhaustion. Immune checkpoint molecules physiologically prevent

excessive immune responses and the development of autoimmunity (Ribas & Wolchok, 2018). These molecules are largely responsible for immune evasion observed in aggressive immunogenic cancer.

#### Immune checkpoint molecules in cancer

Immune checkpoint molecules physiologically prevent excessive immune responses and the development of autoimmunity. Optimal T cell responses requires three signals, which are transduced via formation of a functional immune synapse between naïve T cells and an antigen presenting cell through surface receptors and ligands (Fig 9). The first activation signal comes through ligation of MHC I/II and T cell receptor (TCR). APCs process foreign antigens into small peptides which are presented to the T cell in an MHC-bound form. This interaction is followed by ligation of co-stimulatory molecule CD28 on T cells and their cognate ligands CD80/86 on APCs. This interaction provides the second signal for optimal stimulation of the T cells. Only signal 1 in the absence of signal 2 leads to T cell anergy, when T cells lose their functionality for a prolonged period and cannot be re-stimulated. These two signals are also not enough for optimal T cell activity. The third signal comes via the cytokines secreted by APCs, that help in T cell differentiation and proliferation. IL-6, IL-12, TGF- $\beta$  are some of the cytokines produced by APCs, that help in T cell differentiation. This is the third signal for optimal T cell activation. Interestingly, in order to put a brake on T cell activity, there are certain activation induced checkpoint molecules in place controlling T cell activity. Unfortunately, prolonged expression of these immune checkpoint molecules is often observed on the T cells, especially in the case of cancer. This leads to a generalized dampening of anti-tumor T cell response and promotes immune escape. Cytotoxic T Lymphocyte Antigen

4 (CTLA4) was the first such molecule that was characterized for its immune checkpoint activity in cancer. CTLA4 is an activation induced immune checkpoint molecule that competes with CD28 for binding to CD80/86 (Linsley et al., 1991). Unfortunately, CTLA4 binds CD80/86 with much higher avidity than CD28. This leads to absence of signal 2 during T cell activation eventually leading to T cell anergy. Interestingly, ligation of CTLA4 on CD4<sup>+</sup> T cells with DCs has been shown to trigger induction of IDO1 in DCs which in turn dampens CD8<sup>+</sup> T cell responses (Munn et al., 2004). Subsequently, another immune checkpoint molecule PD-1 was discovered on T cells which interacted with PD-L1 on APCs. PD-1/PD-L1 interaction was initially implicated in case of viral infection mediated chronic exhaustion of T cells (Barber et al., 2005). Subsequent investigations revealed that the distribution and functionality of these two molecules extend far beyond viral infection and autoimmune conditions. Targeting these molecules in cancer has revolutionized the field of tumor immunotherapy. The therapeutic antibody ipilimumab, targeting CTLA-4, was the first checkpoint inhibitor to be approved by U.S. FDA in 2011 for clinical use in metastatic melanoma (Lipson & Drake, 2011; Mansh, 2011). It is undergoing clinical trials for the treatment of non-small cell lung carcinoma (NSCLC), small cell lung cancer (SCLC), bladder cancer and metastatic hormone-refractory prostate cancer. Unfortunately, patients on Ipilimumab therapy, soon developed severe immune related adverse effects (IrAE) including but not limited to diarrhea, colitis, enterocolitis, large and small intestinal perforations, rash, hypothyroidism and hypopituitarism. Most of the IrAEs were dermatological, followed by gastrointestinal and then endocrine (Tarhini, 2013). This promptly called for the development of a second immune checkpoint inhibitor targeting PD-1/PD-L1 interaction. The rationale behind this was that these two molecules activate two

unique downstream pathways in order to execute their effect which suggested a possible difference in their toxicity profile also. Two drugs, Pembrolizumab and Nivolumab targeting PD-1 were approved by U.S. FDA for unresectable melanoma in December 2014. So far, Nivolumab has been approved for NSCLC, renal cell carcinoma, Hodgkin's lymphoma, head and neck cancer, urothelial carcinoma and small cell lung cancer (<https://www.drugs.com/history/opdivo.html>). This drug has not been approved for metastatic advanced thyroid cancers, like PDTC and ATC. This could be due to the failure of successful clinical trial with these patients due to rapid progression and mortality. However, several pre-clinical studies noted moderate response to Pembrolizumab in combination with a BRAFV600E inhibitor in animal models of immune competent ATC (Brauner et al., 2016). A recent report suggested Pembrolizumab could act as a safe and effective salvage therapy when added to kinase inhibitor (KI) therapy at the earliest sign of progression or sooner in the course of KI therapy in order to attain maximum clinical and survival benefit from this combination therapy. The authors proposed that prolonged treatment with KI might alter the immune microenvironment into a less permissive type during progression (Iyer et al., 2018). Currently, Pembrolizumab is undergoing phase II clinical trials for ATC patients (NCT02688608). Nivolumab associated toxicities are also not uncommon and they also include dermatologic toxicity, gastrointestinal toxicity and endocrine toxicity. Unfortunately, late onset of neurological toxicities are also being reported with Nivolumab treatment (Diamantopoulos et al., 2017; Mirabile et al., 2019). IrAEs take at least weeks to months to appear and it usually starts with rash, but they often persist even after discontinuation of treatment. This points towards a systemic reprogramming of immune system during these

checkpoint inhibitions that is not reversed after treatment termination and might have a debilitating consequence.

CTLA4 and PD-1 are not the only molecules involved in regulation of T cell activity. There is a plethora of such immunomodulatory molecules which act in their unique way to modulate T cell responses. Most of these molecules are under strict spatio-temporal regulation which suggests that they could be tapped in a combinatorial treatment regimen, depending on the patient's response. This warrants a thorough characterization of these molecules in the context of T cell activation and inhibition and identification of novel targets which might be able to circumvent the problem of IrAE experienced with Ipilimumab and Nivolumab.

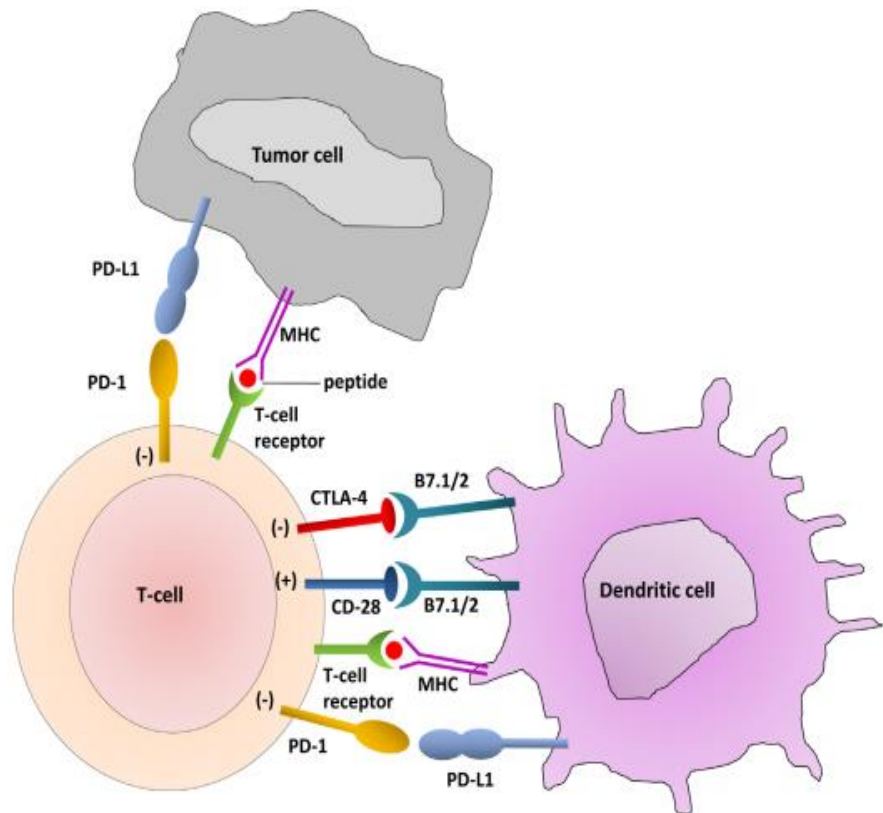


Figure 9. The immune synapses between T cell, DCs and tumor cell.  
 Adapted from: *Oncotarget*, Vol. 5, No. 12; 3956-3969

### *T cell co-signaling molecules*

T cell activation, differentiation and effector function are intricate processes, controlled by molecular interactions and biochemical signaling pathways triggered by interaction between co-stimulatory receptors and their cognate ligands (Fig 10). These molecules belong to two major families, the TNF receptor superfamily (TNFRSF) and immunoglobulin superfamily (IgSF). CTLA4 and PD-1 belong to IgSF. These receptors and ligands usually interact within families, as evidenced by interaction of CTLA4 and CD28 or CD80/86 or PD-1 with PD-L1. However, co-signaling molecule from TNFRSF, Herpes Virus Entry Mediator (HVEM) interacts with members of both the families and each interaction uniquely shapes T cell activation status. Currently, it is evident that the expression of many co-stimulatory and co-inhibitory molecules on T cell surface is induced following activation and their expression pattern changes in an overlapping manner as T cells continue to proliferate and differentiate. This underscores the importance of understanding their regulation and unique signal transduction mechanisms.



Immunomodulatory molecules from TNFRSF:

TNFRSF receptors contain one or more extra cellular cysteine-rich domains (CRDs), and their ligands contain a conserved extracellular TNF homology domain (THD). Prominent members and their interacting ligands of this family include 4-1BB: 4-1BBL, OX40: OX40L, CD27: CD70, HVEM: LIGHT, GITR: GITRL and CD30: CD30L. These interactions lead to T cell activation, proliferation and differentiation. Interaction between HVEM and LIGHT is spatiotemporally regulated in a stringent manner. HVEM is expressed mostly on naïve T cells and downregulated in activated T cells. However, the ligand of HVEM, LIGHT is a pro-inflammatory cytokine secreted from activated T cells in a transient manner and promptly downregulated following activation. It has been suggested that this mechanism has evolved to prevent *cis* interaction between HVEM and LIGHT in resting T cells and triggering of autoimmunity (del Rio et al., 2010a). Some of these molecules are being actively targeted in clinical trials for advanced cancers. Agonistic monoclonal antibodies (mAb) against GITR are in clinical trials for III or IV malignant melanoma and other solid tumors (NCT01239134). A non-randomized clinical trial of OX40 agonistic antibodies alone or in a combination with 4-1BB agonist is currently underway for locally advanced or metastatic cancers (NCT02315066). A phase 1B trial of combination therapy using 4-1BB agonistic antibody with PD-1 antagonistic antibody for solid tumors was conducted between October 2018 and February 2019. While some of these trials showed promising results, for others the results are awaited.

*Immunomodulatory molecules from IgSF:*

The CD28 and B7 families are the most well-characterized members of IgSF receptors. The members of the CD28 family interact primarily with members of the B7 family with two

exceptions: the co-inhibitory receptor B and T lymphocyte attenuator (BTLA) and CD160, both of which interact with HVEM which is a member of TNFRSF. There is another family of co-signaling molecule which has a unique structure. These are the type I transmembrane (or T cell) immunoglobulin and mucin (TIM) domain-containing molecules that are composed of both an IgV-like domain and a mucin-like domain. Prominent co-stimulatory members and their ligands of this family are CD2/signaling lymphocytic activation molecule (SLAM): SLAM, CD2: CD48/CD58, CD226: CD155/CD112 and inducible T cell co-stimulator (ICOS): B7H2. ICOS is expressed on T lymphocytes, and upon engagement with its ligand ICOSL (CD275) on APCs, they are further reinvigorated. However, its role in tumor immunology has been a matter of debate, as ICOS is also expressed on Treg lymphocytes, thus pointing to the possibility of their activation after treatment with agonistic antibody. ICOS is involved in the development and maintenance of T follicular helper cells (Tfh), Th1, Th2, Th17, Tc, and even memory effector T cells. Lack of ICOS is associated with defective germinal center formation (Tafari et al., 2001). Recent studies suggest a synergistic activity of topical ICOS costimulation at the tumor site and anti-CTLA4 antibody in a B16 melanoma model (Soldevilla et al., 2019). The authors suggested a possibility of formation of tertiary lymphoid structure at the tumor site in response to topical ICOS costimulation which might support the systemic anti-tumor T cell response. However, since reports of widespread inflammatory irAEs have already been reported with Ipilimumab therapy, further combination of this molecule with an agonistic co-stimulatory antibody should be carefully evaluated and scrupulously titrated in pre-clinical models. Some of the co-inhibitory receptors and their ligands from this family are CTLA4: B7-1/B7-2, PD-1: PD-L1, LAG3: MHCII, 2B4: CD48, PD-1H(VISTA): PD-1H receptor(unknown),

TIGIT: CD155/CD112/CD113, LAIR1: collagen and TIM3: galectin 9. Interfamily interaction is observed in BTLA/CD160: HVEM interaction. As we can see from the first glance, most of the co-inhibitory checkpoint molecules belong to this family. CTLA4 and PD-1 are the best characterized ones in this list. However, with anti-PD-1 therapy, development of TIM3 associated adaptive resistance was observed (Oweida et al., 2018). PD-1<sup>+</sup>/TIM3<sup>+</sup> T cells represent an exhausted T cell phenotype (Singer et al., 2016). This underscores the significance of the functional redundancy of these co-signaling molecules which almost precludes monotherapy targeting these molecules as a viable therapeutic option. Lymphocyte activation gene-3 (LAG-3 or CD223) is a promising target, which physiologically suppresses T-cell activation and cytokine secretion. Like CD4, LAG-3 binds to major histocompatibility complex MHC II molecules. In CD4<sup>+</sup> lymphocytes, LAG-3 signaling prevents the entry of T cells into S phase of the cell cycle, thus arresting their expansion and diminishing cytokine secretion. Two major approaches targeting LAG3 are (a) a LAG-3-Ig fusion protein (IMP321) and (b) mAbs against LAG3 (relatlimab). Multiple phase I and II clinical trials are underway evaluating efficacy of anti-LAG3 antibodies in unresectable and metastatic solid tumors, recurrent glioblastoma, relapsed hematologic malignancies under a combinatorial setting with Nivolumab. The LAG3-Ig fusion protein is in phase I trial for renal cell carcinoma (NCT00351949), pancreatic adenocarcinoma (NCT00732082), metastatic breast carcinoma (NCT00349934) and melanoma (NCT00324623). Another promising immune checkpoint target is TIGIT (T-cell immunoreceptor with immunoglobulin and ITIM domains). It is a member of the poliovirus receptor (PVR)-nectin family that inhibits T and NK cell activity and has lymphocyte-restricted expression pattern (Solomon & Garrido-Laguna,

2018). Thus, targeting TIGIT can have a multipronged effect on the immune cells in terms of NK effector functions, DC costimulatory properties, Treg response, and the CD8<sup>+</sup> cytotoxicity. It is an emerging target in the domain of immune checkpoint inhibitor therapy, which is aggressively being evaluated in multiple clinical trials. Six human anti-TIGIT mAbs of the IgG1 isotype have entered clinical trials so far. These are being evaluated for advanced metastatic solid cancers and NSCLC (Harjunpää & Guillerrey, 2019).

B and T cell lymphocyte attenuator (BTLA, CD272) is another promising target in immune checkpoint blockade therapy. This is an inhibitory receptor that is structurally and functionally related to CTLA-4 and PD-1 and is expressed by most lymphocytes. Ligation of BTLA with its ligand HVEM blocks B and T cell activation, proliferation, and cytokine production. HVEM expressed on Treg cells acts as a ligand of BTLA on effector T cells (Teff), and HVEM– BTLA interaction between these two cells suppresses effector T cell function (Tao et al., 2008). The cytoplasmic tail of BTLA resembles that of PD1, given the arrangement of two tyrosine-containing immunoreceptor (ITIM) motifs capable of recruiting SHP1 and SHP2 (Gavrieli et al., 2003). It has a third tyrosine motif that is capable of recruiting growth factor receptor-bound protein 2 (GRB2) and PI3K pathway downstream (Gavrieli & Murphy, 2006). Though HVEM can impart a positive signal to the effector T cells upon interaction with LIGHT, the inhibitory activity of HVEM through BTLA and CD160 signaling appears to be the dominant one in Teff cells, as the expression of activating ligand LIGHT is decreased in activated Teff cells and activated APCs, thus limiting its activation potential. Tumor cells exploit this pathway by either promoting the establishment of dysfunctional T cells that have chronic expression of BTLA and render them vulnerable to inactivation, or by expressing

HVEM, as observed in melanoma (Paulos & June, 2010). BTLA expression has been associated with poor prognosis in gastric cancer (Feng et al., 2015). Co-expression of HVEM and BTLA has also been reported to be associated with poor prognosis in gastric cancer (Lan et al., 2017). Gastric cancer is highly inflammatory in nature and the patients usually have significantly higher serum concentration of pro-inflammatory cytokines IL-8 and TNF $\alpha$  compared to age and gender matched controls. These observations suggested a possible association between the expression of these immunomodulatory molecules and an inflammatory immune microenvironment. HVEM expression has also been implicated in poor prognosis of colorectal cancer in a retrospective study (Inoue et al., 2015). Interestingly, a recent observations suggests that HVEM has a more widespread distribution than PD-L1 in melanoma and this was correlated with presence of BTLA<sup>+</sup> tumor infiltrating lymphocytes (Malissen et al., 2019). The authors also pointed out that BTLA can mask the effect of anti-PD-1 therapy in melanoma and a combination of anti-BTLA and anti-PD-1 would be a more rational choice depending on the immune infiltrate profile of the patient. Because of the complicated signaling mechanism, this pathway is still being investigated in pre-clinical studies.

#### *Potential of immunotherapy in ATC*

ATC has an immunologically dampened microenvironment characterized by suppressive cytokine and chemokine milieu and immune suppressive cellular infiltrate. In tumors, tissue homeostasis is often perturbed and this leads to secretion of soluble factors such as cytokines and chemokines, upregulation of reactive oxygen species (ROS), and bioactive mediators such as histamine – mostly my macrophages and mast cells, which induce leukocyte migration and

infiltration at the site of lesion. This finally culminates into an inflammatory microenvironment which promotes tumor growth. *In vitro* studies have shown that ATC cells are capable of secreting IL-4 which polarizes T cells towards Th2 phenotype and IL-10 which promotes Treg differentiation (Todaro et al., 2006). A recent *in vitro* study has demonstrated that supernatants collected from ATC cell lines have higher expression of prostaglandin E2 (PGE2) compared to PTC cell lines. PGE2 is a small lipid molecule upregulated in several cancers and induces cyclooxygenase (COX)-2 activity which in turn dampens NK cell mediated cytotoxicity in ATC. Tumor cell secreted PGE2 also interfered with functional maturity of NK cells in ATC (Park et al., 2018). NK cells are one of the major cell types responsible for successful immune surveillance in cancer. Interestingly, another report suggests perturbed NK cell function in ATC via upregulation of PD-1 and TIM3 in CD56<sup>hi</sup>CD16<sup>hi/lo</sup> NK cells which represent the less functional phenotype (Yin et al., 2018). The implications of tumor associated macrophages have already been discussed at great length in previous section and it is well established that both M1 and M2 macrophages and the cytokines secreted by them shape the prognosis of ATC by modulating T cell activity in ATC. Recent evidences from NGS studies have revealed the presence of multiple genetic lesions in ATC, which contradicts the established notion of ATC being low in mutational burden hence non-immunogenic in nature. Detailed analysis of T cell infiltrates in ATC suggests significant amount of tumor infiltrating CD8<sup>+</sup>T cells in ATC which are non-functional, mostly resulting from complex immune interactions between the co-signaling molecules in the TME. Unfortunately, owing to the rarity of the disease, there is a paucity of knowledge about these T cell immunomodulatory molecules and their regulations in ATC. Given the extremely refractory nature of ATC, it is

essential to profile these previously unexplored immunomodulatory molecules to determine their therapeutic potential in this disease.

This study was aimed at identification and characterization of novel immune checkpoint molecules in ATC and evaluation of their potential as biomarkers and potential therapeutic targets. This study focused on the mechanism of crosstalk between the immunomodulatory molecules and the inflammatory cytokine milieu commonly associated with this malignancy. We also wanted to understand how an acquired resistance against small molecule inhibitor can modulate the immune phenotype of ATC. This is a completely unexplored area of research. The classical mechanism of resistance against vemurafenib via activation of compensatory proliferation and survival pathways and additional mutations are well-characterized. There are no studies focusing on the immunological implications of these kinase inhibitors in the context of tumor cell - immunomodulatory protein expression. From the experience with PD-L1, we came to appreciate the role of tumor intrinsic immune checkpoint molecules in shaping the anti-tumor T cell response. For a better understanding of the refractory phenotype of ATC, we took a holistic approach and evaluated the expression profiles of the immunomodulatory molecules in the vemurafenib resistance scenario – commonly observed in advanced thyroid cancers.

### Hypothesis and overview of specific aims

We hypothesized that ***“Interaction between tumor cells and immune cells in tumor microenvironment (TME) confers an immunosuppressive phenotype in anaplastic thyroid cancer (ATC)”***. In order to test this hypothesis, we primarily focused on expression of immunomodulatory molecules in anaplastic thyroid cancer cell lines. We evaluated the regulation of these molecules under the influence of inflammatory mediators commonly observed in ATC. Lastly, we tested the feasibility of a combinatorial therapeutic approach targeting one of these molecules and a small molecule inhibitor against the BRAFV600E kinase in ATC.

The specific aims of this study are as follows:

### Specific aims:

**Aim 1: Expression of immunomodulatory molecules at transcript and protein levels in thyroid cancer cell lines and patient tissues**

- a. *in vitro* screening for the expression of 25 immunomodulatory molecules in 4 ATC, 3 PTC and 1 FTC cell lines at transcript level compared to normal thyroid epithelial cell line
- b. Evaluation of the expression of the immunomodulatory molecules at protein level by western blot and immunofluorescence
- c. Analysis of surface expression of HVEM, BTLA, CD160 and TIM3 in the cell lines of interest by flowcytometry
- d. Evaluation of the expression of HVEM, BTLA and CD160 in thyroid cancer tissues by immunohistochemistry

**Aim 2a: Examine the modulation of immune checkpoint molecule HVEM by inflammatory components in anaplastic thyroid cancer**

- i. Analysis of immune infiltrate composition in thyroid cancer patient tissues by immunohistochemistry
- ii. Analysis of cytokine milieu in thyroid cancer patient tissues by immunohistochemistry
- iii. Analysis of the effect of inflammatory cytokines  $TNF\alpha$ , IL-8 and  $IFN\gamma$  on expression of tumor cell – HVEM
- iv. Examine the implications of HVEM/LIGHT interaction in anaplastic thyroid cancer

**Aim 2b: Examine possible tumor intrinsic function of HVEM in anaplastic thyroid cancer**

- i. Knockdown HVEM in ATC cell line by CRISPRi
- ii. Assess the tumorigenicity profile by colony formation assay, and invasion assay

**Aim 3: Examine the feasibility of a combinatorial therapeutic approach with MEK inhibitor and antagonistic antibodies in ATC**

- a. Evaluation of the effect of vemurafenib on the expression of immunomodulatory molecules in thyroid cancer cell lines
- b. Evaluation of the expression profile of the immunomodulatory molecules in vemurafenib-resistant ATC cell lines
- c. Evaluation of the combined effect of MEKi and BRAFV600E inhibitor on expression of these molecules in thyroid cancer cells

## CHAPTER 2: MATERIALS AND METHODS

### Cell culture:

Nine thyroid cell lines were used in this study. Nthy-ori 3-1 (human follicular epithelial cell line derived from a normal thyroid and has been immortalized by SV40 large T gene; Sigma Aldrich Inc. catalog no. 90011609), 8505C (Sigma Aldrich Inc. catalog no. 94090184), BCPAP (human papillary thyroid cancer cell line), TPC-1 (human papillary thyroid cancer cell line) and CGTHW-1 (human follicular thyroid cancer cell line). BCPAP, and CGTHW-1 cell lines were purchased from DSMZ, Braunschweig, Germany. TPC-1 was obtained from American Type Culture Collection (ATCC) (Manassas, VA). Three anaplastic thyroid cancer cell lines T238, SW1736 and HTh74 and one papillary thyroid cancer cell line K1 were obtained from Dr. Rebecca Schweppe at University of Colorado Cancer Center (UCCC). The cells were tested for mycoplasma and unique STR profile at UCCC. Cells were cultured in RPMI-1640 (Mediatech, Herndon, VA) supplemented with 10% fetal bovine serum (FBS) (Atlanta Biologicals, Atlanta, GA), penicillin 10,000 IU/ml, streptomycin 10,000 µg/ml (Mediatech) and 2mM L-glutamine (Mediatech). Cells were grown at 37°C in a humidified tissue culture incubator with 5% CO<sub>2</sub> atmosphere unless noted otherwise.

### RNA extraction and quantitative PCR:

Total RNA was isolated from 60-70% confluent cells, at log phase of their growth. Cells were washed with sterile 1X PBS and harvested with 0.25% Trypsin, 0.1% EDTA (Corning MT25053CI). RNA was isolated using RNeasy Plus Mini Kit (Qiagen 74134/74136) according to the manufacturer's protocol. An additional on-column DNase digestion step was added to the protocol to ensure complete elimination of genomic DNA contamination, using the RNase

free DNase Set (Qiagen 79254) as per the manufacturer's instructions. RNA was eluted in Ultra-pure water (Thermo Fisher Scientific,10977015) and stored at -80°C until further use.

In order to design primers, sequences were obtained from the NCBI (National Center for Biotechnology Information) and the primers were designed using Integrated DNA technologies Primer Quest Tool. At least one primer was designed across an exon junction to ensure amplification of mRNA. The length of the primers was between 18-30 bases, GC content between 50%-60%, amplicon size between 70-200 base pairs. Primers with a low  $\Delta G_{max}$  (change in free energy) for secondary structures like hairpins ( $<-2$ ) and self-dimers ( $<-5$ ) were selected for the assay.

RT-PCR was run on Applied Biosystems 7900 HT and Quantstudio 5 RT-PCR Systems. RT PCR was performed using either SuperScript® III Platinum® SYBR® Green One-Step qPCR Kit w/ROX (Thermo Fisher Scientific 11746500), or qScript™ One-Step SYBR® Green qRT-PCR Kit, Low ROX (Quantabio 95089), or Power SYBR® Green RNA-to-CT™ 1-Step Kit (Thermo Fisher Scientific 4389986) according to manufacturer's protocol. The primers used for the assay are listed in table 1.

<b><u>GENES</u></b>	<b><u>FORWARD</u></b>	<b><u>REVERSE</u></b>
ICOS	TTAACAGGAGAAATCAATGGTTCTG	TGAGATCGCAGAGTATTTGCC
CD27	GAGTGTGATCCTCTTCCAAACC	CTCCAGCATCTCACTGACATAAG
HVEM	CTGGTGCTGTATCTCACCTTC	CGATAACCTGGACTGCACTT
LIGHT	TCTCTTGCTGTTGCTGATGG	GTGAGACCTTCGCTCTTGTATC
CD40L	GGATACTACACCATGAGCAACA	TTCCCGATTGGAACAGAAGG
4-1BB	CAGCATGTGTGAACAGGATTG	AAGAACAGTTTGTCCAGGGT
OX40	GCCAAGATTCGAGAGGAACA	GTGATACCTGAAGAGCAGAGAAG
DR3	CTGCCTGGCTTCTATGAACA	ACCCAGAACACACCTACTCT
GITR	TTGGCTTCCAGTGTATCGAC	GGGTGCAGTCTGTCCAAG
CD30	CAGCACCATGCCTGTAAGA	GGACAGACCTGGATCTGAACTA
TIM1	ATGAACCAGTAGCCACTTCAC	CTGGTGGGTTCTCTCCTTATTG
SLAM	GAAAGCAGGAAGGAGGATGAG	GAGTGGAGACCTGCTCATAAAG
CD2	GAGGAGTCGGAGAAATGATGAG	GGGTTGAAGCTGGAATTTGG
CD226	CCTTAACAGAAGGAGAAGGAGAG	GATTGGTAGGTTGACTGGTAGAG
LAG3	GTCCGTGTGCTGGATGAA	TGT CAG ACC CAT GTC CAA TG
CTLA4	ATGGACACGGGACTCTAC	GGC ACG GTT CTG GAT CAA TTA
PD1	CCGCACGAGGGACAATAG	CTTCTCTCGCCACTGGAA
B7-1/CD80	GCAGAGAGAGAAGGAGGAATG	GGTGGGACCTTCAGATC
CD160	CTATTCACAGAGACAGGGAACACTAC	CTGAACTGAGAGTGCCTTCAT
BTLA	ACCCTGGCTCCTGTATAG	TGC TTT CCT TGG TGC CTT C
PD1-H/VISTA	GGTGCAGACAGGCAAAGA	TAGACCAGGAGCAGGATGAG
LAIR1	CCGCATTGACTCAGTAAGAGAAG	AGAGCTTTCTTTACCCAGCAG
TIM3	TGCTGCTACTACTTACAAGGTC	GTGTAGAAGCAGGGCAGATAG
2B4	GGTGTATCAGGGCAAAGGATG	ACCTTCGTCTGTATGCTGTTTTG
TIGIT	CTCGCCTCAGGAATGATGAC	GGAGGAGAGGTGACATTGTAAG
PDL1	ACCAGCACACTGAGAATCAAC	GGTAGTTCTGGGATGACCAATTC
PD1	CCGCACGAGGGACAATAG	CTTCTCTCGCCACTGGAAAT

Table 1. List of primers used for qRT PCR

#### Western Blot:

Cells were harvested at 60-70% confluence for western blot analyses. Cell culture media was discarded, and the cells were washed with 1X PBS and scraped off the culture flask/dish. Cell pellets were resuspended in RIPA buffer (50 mM Tris-HCl, pH 7.4, 150 mM NaCl, 0.2% sodium deoxycholate, 0.1% SDS, 0.5% NP-40) supplemented with HALT protease/phosphatase inhibitor cocktail (Thermo Fisher Scientific 78440). Samples were placed on ice for 45 minutes with intermittent vortexing. Subsequently, the lysates were centrifuged for 30 minutes at 14000 rpm at 4°C. Protein concentrations were determined using the Bio-rad Protein Assay Dye Reagent Concentrate (Bio-Rad #5000006). Fifteen micrograms of total protein were loaded per sample and resolved on 10% SDS-PAGE under reducing conditions (presence of  $\beta$ -mercaptoethanol) and transferred onto Immobilon-P membranes (Millipore #IPVH00010) using the Transblot Turbo RTA Transfer Kit (Biorad 1704272) in the Transblot Turbo System for 7 minutes. Membranes were blocked using 5% dried milk in 1X TBST (200 mM Tris-HCl, 150mM NaCl, pH 7.4, and 0.1% Tween-20 added fresh/liter of 1XTBS (TBS-T)) for 2 hours on a shaker at room temperature for non-phosphorylated proteins and in 5% BSA instead of milk for phosphorylated proteins. Membranes were incubated with primary antibodies overnight at a 1:1000 dilution (unless indicated otherwise) in 2% bovine serum albumin made in 1X TBST at 4°C. The next day, membranes were washed three times with 1X TBST for 5 minutes, followed by incubation with horse radish peroxidase (HRP) conjugated secondary antibodies (Thermo Fisher Scientific), at a dilution of 1:10,000 in 2% dried milk or BSA in 1X TBST, for 2 hours, on a shaker, at room temperature. After 4 washes, 10 minutes each, in 1XTBST, the membranes were developed using western blotting substrate (Radiance Q Chemiluminescent Substrate, Azure Biosystems; 10147-296) and detected on Next Advance Celvin

Chemiluminescence Imaging System and band intensities were analyzed using the ImageJ software. List of primary antibodies used for this work is in table 2. For detection of nuclear and cytoplasmic proteins, cytoplasmic and nuclear protein extracts were prepared from untreated and treated cells using NE-PER nuclear and cytoplasmic extraction reagent kit by Thermo Fisher (cat # 78833). Cellular extracts (15µg protein for nuclear and cytoplasmic extracts) were resolved in 12% SDS-PAGE under reducing conditions as described in our earlier work (Rajoria et al., 2010). The above mentioned protocol was followed for subsequent immunoblotting steps.

<b>Antibody</b>	<b>Manufacturer</b>	<b>Catalog number</b>	<b>Dilution</b>
HVEM	Abcam	ab62462	1:1000
BTLA	Abcam	ab181406	1:1000
CD160	Abcam	ab128954	1:1000
TIM3	Abcam	ab47997	1:1000
LGALS9B	Abcam	ab69630	1:1000
p-STAT1	Cell Signaling Technology	9167S	1:1000
STAT1	Cell Signaling Technology	14994S	1:1000
IRF 1	Cell Signaling Technology	8478S	1:1000
Phospho-I $\kappa$ B $\alpha$	Cell Signaling Technology	2859S	1:1000
I $\kappa$ B $\alpha$	Cell Signaling Technology	9242S	1:1000
NF $\kappa$ B	Cell Signaling Technology	8242S	1:1000
Phospho-c-Jun	Cell Signaling Technology	9261S	1:1000
c-Jun	Cell Signaling Technology	9162	1:1000
Phospho-JNK	Cell Signaling Technology	9251s	1:1000
JNK	Cell Signaling Technology	9252	1:1000
Phospho P38 MAPK	Cell Signaling Technology	4511T	1:1000
P38 MAPK	Cell Signaling Technology	8690P	1:1000
JunD	Cell Signaling Technology	5000S	1:1000
ADAM17	Cell Signaling Technology	3976S	1:1000
Phospho-ERK	Cell Signaling Technology	4376S	1:1000
ERK	Cell Signaling Technology	4695S	1:1000
Phospho-MEK	Cell Signaling Technology	9154S	1:1000
MEK	Cell Signaling Technology	9126S	1:1000
Phospho-c-Raf	Cell Signaling Technology	9427S	1:1000
c-Raf	Cell Signaling Technology	9422S	1:1000
Phospho ELK	Cell Signaling Technology	9181S	1:1000
ELK	Cell Signaling Technology	9182	1:1000
Lamin B1	Cell Signaling Technology	13435S	1:1000
GAPDH	Cell Signaling Technology	5174S	1:2000

Table 2. List of antibodies used in western blots

**Immunofluorescence:**

Cells were seeded in 8 chamber slides at a density of 15,000 cells/well in 250µl complete growth media and incubated at 37°C and 5% CO<sub>2</sub> in a humidified tissue culture incubator overnight. Post adherence or treatment period, the chambers were washed gently with 1X PBS three times. Cells were fixed with 200µl/well of 4% paraformaldehyde for ten minutes at room temperature. This was followed by three washes with 300µl/well of 1X PBS. Subsequently, cells were permeabilized with 0.2% Triton\_X\_100 (Thermo Scientific 85111) in 1X PBS for 10 minutes at room temperature. At the end of incubation, wells were washed three times with 1X PBS, followed by the addition of 250µl/well blocking solution (0.1% Triton\_X\_100 +10% Goat Serum (Sigma G9023) + 1% BSA in 1X PBS) for 30 minutes at room temperature. For TIM3, cells were blocked in BSA only as the primary antibody was raised in goat. Blocking solution was gently removed and primary antibody added (100µl/well) in 1% BSA in PBS. Slides were sealed with parafilm and incubated overnight at 4°C. The following day, wells were washed three times with 300µl/well in 1X PBS and incubated with fluorochrome conjugated secondary antibodies (Goat Anti Rabbit Alexa Fluor 647, Rabbit Anti-Goat Alexa Fluor 488; 1:250 in 1% BSA in 1X PBS) and incubated for 45 minutes in the dark. Wells were washed five times with 300µl/well in 1X PBS. Slides were mounted in Vectashield containing DAPI (Vector Labs H-1200) and imaged on a Nikon Ti microscope at 200X and 400X magnification.

**Flow cytometry:**

For surface phenotype assessment, cells were harvested by scraping off the culture vessels in 1X PBS. The cells were washed twice with 1X PBS and stained using conjugated primary

antibodies (concentrations, incubation times, and catalog numbers listed in table 3) in FACS buffer (1:20 BSA Stock Solution (Miltenyi 130-091-376) in 1X PBS). Next, cells were washed twice in FACS buffer and fixed with 4% paraformaldehyde for 15 minutes at room temperature. Cells were washed with 1ml FACS buffer and finally resuspended in 500µl FACS buffer for analyses on the MoFlo flow cytometer (Beckman Coulter) or BD FACS Celesta and data were analyzed using FlowLogic software (Miltenyi).

<u>Antibody</u>	<u>Fluorochrome</u>	<u>Concentration</u>	<u>Incubation time (minutes)</u>	<u>Company (Catalog Number)</u>
HVEM	FITC	1:10	10	Miltenyi (130-101-595)
BTLA	PerCP/Cy5.5	1:10	20	Biolegend (344514)
CD160	Alexa Fluor 647	1:10	30	R&D Systems (FAB6700R)
TIM3	PE	1:50	10	Miltenyi (130-117-364)

Table 3. List of antibodies used in flow cytometry

**Immunohistochemistry:**

For immunohistochemistry (IHC), formalin-fixed and paraffin embedded tumor samples and normal tissues were obtained from Cooperative human tissue network (CHTN). Antibodies used I IHC are listed in table 4. antibodies were titrated at different concentrations in with positive control tissues recommended by the manufacturer for each antibody. Briefly, tissue slides were heated to 60°C for 15 mins, deparaffinized using xylene, and hydrated through a graded series of ethanol treatments with descending concentrations and then rinsed in distilled water. Antigen retrieval was accomplished by boiling in 10 mM sodium citrate buffer of pH 6.0 for 10 min or by using EDTA antigen retrieval buffer based on the antibody and according to manufacturer’s instruction for each antibody. Endogenous peroxidase activity

was quenched by 30 min incubation in 3% H<sub>2</sub>O<sub>2</sub>. Non-specific binding was blocked with 10% normal horse serum made in 3% BSA-PBS for one hour at room temperature. Next, sections were incubated with primary antibodies in 1% horse serum made in 3% BSA-PBS overnight at 4°C in a humidified chamber. The tissues were incubated with biotinylated horse anti-rabbit or anti-mouse IgG secondary antibodies (Vector labs, Burlingame, CA, USA) made in 1% horse serum/3% BSA-PBS at 1:500 dilution for 45 mins at room temperature. Avidin–biotin-complex (ABC) peroxidase method (ABC Elite Kit, Vector Labs, Burlingame, CA, USA) was employed for detection. The complex was used at 1:1000 dilution made in 1% horse serum in 3% BSA-PBS for one hour at RT. Final color was developed with the DAB peroxidase substrate kit (Vector Labs, Burlingame, CA, USA) for 15 mins or more at RT. The sections were then counterstained with hematoxylin, decolorized in Define Mx-aq, washed in Buffer blue (Scott's water) followed by dehydration in graded alcohols with ascending concentrations and finally xylene. Positive and negative controls were run at the same time for each the antibody tested. To avoid variations, we used same incubation time for each antibody. Images were taken at 10X and 20X magnification using Nikon Eclipse Ti-E inverted microscope. Stained tissues were examined by a licensed pathologist. Hematoxylin and eosin stained sections were examined to determine the tumor area. Immunomodulatory molecules HVEM, BTLA, CD160, were examined in the follicular cells of the thyroid cancer tissue sections and normal thyroid tissue sections. Percent positive cells were determined subsequently. A pan-T cell marker CD3 was used to determine intra tumoral T cell infiltration. Percentage of Th cells, and T cytotoxic cells was determined by examining serial sections and estimating the percentages of CD4 and CD8 positive cells respectively, out of CD3 positive lymphocytes. Percentage of T regulatory cells

was determined by estimating FoxP3 nuclear staining positive population of lymphocytes among the CD3, and CD4 positive cells. IDO1, IL-10 and IL-17 positivity was determined by the number of cells positive for the antigens among the tumor area in the malignant samples and follicular regions in normal thyroid tissue.

<u>Antibody</u>	<u>Manufacturer</u>	<u>Catalog number</u>	<u>Dilution</u>
HVEM	Thermo Fisher	PA5-20237	1:1000
BTLA	Abcam	ab181406	1:400
CD160	Abcam	ab128954	1:200
TIM3	Abcam	ab47997	1:250
LGALS9B	Abcam	ab69630	1:250
IL-10	Abcam	ab34843	1:750
IL-17	Abcam	ab79056	1:200
IDO1	Abcam	ab55305	1:400
CD3	Abcam	ab5690	1:2000
CD4	Abcam	ab133616	1:4000
CD8	Abcam	ab4055	1:500
FoxP3	Abcam	ab20034	1:200

Table 4. List of antibodies used in immunohistochemistry

**IL-8, TNF $\alpha$ , IFN $\gamma$  and rhLIGHT Treatment:**

Nthy-ori-3-1, 8505C, T238 and SW1736 were grown up to 60-70% confluence in complete growth media. Subsequently, cells were treated with 50ng/ml IL-8 (R&D systems; 208-IL-010/CF) and 10ng/ml TNF $\alpha$  (R&D Systems; 210-TA/CF) separately and in combination for 24 hours in serum free clear RPMI (Corning 17-105-CV) devoid of L-Glutamine for 24 hours. Conditioned media was collected and stored at -80°C until further use. For rhLIGHT treatments, cells growing at 70% confluence were starved for 24 hours in clear RPMI (Corning 17-105-CV) with 2% Charcoal-stripped Fetal Bovine Serum (CS-FBS) (Sigma F6765) to synchronize their cell cycle and subsequently treated with 100ng/ml rhLIGHT (R&D Systems; 664-LI-025) in 5% charcoal stripped FBS-clear RPMI media for another 24 hours. Cell pellets

were collected for western blot analyses. For IFN $\gamma$  (R&D Systems; 285-IF-100/CF) treatment, the rhLIGHT treatment protocol was followed and cells were processed after the stipulated time period based on experimental needs.

#### Fractionation of Nuclear and cytoplasmic extracts from thyroid cancer cells

Cytoplasmic and nuclear protein extracts were prepared from untreated and treated cells using NE-PER nuclear and cytoplasmic extraction reagent kit by Thermo Fisher (cat # 78833). Cellular extracts (15 $\mu$ g protein for nuclear and cytoplasmic extracts) were resolved in 12% SDS-PAGE under reducing conditions as described in our earlier work (Rajoria et al., 2010). Briefly, the proteins were transferred to Immobilon-P membranes using the Transblot Turbo RTA Transfer Kit (Biorad 1704272) in the Transblot Turbo System for 7 minutes. Membranes were blocked with 5% dried milk in TBST [200 mM Tris-HCl, pH 7.4, 150 mM NaCl, and 0.01% Tween-20 added fresh/liter of 1 $\times$  TBS (TBST)] for 2 hours on a shaker at room temperature. Subsequently, the membranes were incubated overnight at 4°C with primary antibodies. Membranes were washed three times with TBST and incubated with the respective horseradish peroxidase (HRP) conjugated secondary antibody for 2 hours at room temperature in TBST containing 2% milk. After four washes with TBST, membranes were developed using western blotting substrate (Radiance Q Chemiluminescent Substrate, Azure Biosystems; 10147-296) and detected on Next Advance Celvin Chemiluminescence Imaging System and band intensities were analyzed using the ImageJ software.

#### Enzyme-linked immunosorbent assay (ELISA):

Conditioned media collected from IL-8 and TNF $\alpha$  treated cells were concentrated with Pierce™ Protein Concentrator PES, 10K MWCO; 88517). Human HVEM/TNFRSF14 DuoSet

ELISA kit (R&D Systems; DY356) and DuoSet ELISA Ancillary Reagent Kit 2 (R&D Systems; DY008) were used for detection of soluble HVEM in IL-8 and TNF $\alpha$  treated cell-culture conditioned media according to manufacturer's protocol. Plates were coated with 100 $\mu$ l of captured antibody overnight at room temperature. The following day, plates were washed with 400 $\mu$ l/well wash buffer three times. Plates were blocked with reagent diluent with a volume of 300 $\mu$ l/well for 1 hour at room temperature. Subsequently, plates were washed with wash buffer for three times. 100 $\mu$ l samples or standards were added to the designated wells and incubated for 2 hours at room temperature. Plates were washed three times with wash buffer and incubated with 100 $\mu$ l detection antibody for 2 hours at room temperature. Plates were washed thrice with wash buffer and incubated with 100 $\mu$ l of streptavidin-HRP for 20 minutes at room temperature in dark. 100  $\mu$ l substrate solution was added subsequently, and plates were incubated for 20 minutes at room temperature in dark. The reaction was stopped by adding 50 $\mu$ l stop solution (2N H<sub>2</sub>SO<sub>4</sub>). The plate was read immediately at 450nm and 570 nm. Four parametric standard curves were constructed with the standards as recommended by the manufacturer and the concentrations were computed using GraphPad Prism 8.

HVEM knockdown by CRISPRi:

*Generation of CRISPRi plasmid:*

Primers for single guide RNAs targeting the promoter region of HVEM were selected from the Weissman lab repository (MA et al., 2016). Five sets of forward and reverse primers were chosen for the gene. The primers were ligated by polynucleotide kinase (PNK) to create the sgRNA cassette. The sgRNA cassette was ligated with Bsmbl (New England Biologicals;

R0580S) digested, PCR purified dCas9-KRAB-GFP plasmid (Addgene # p71237). The map of the vector is depicted in figure 11. (Subcloning Efficiency™ DH5α™ Competent Cells (New England Biologicals; C2988) *E.coli* were transformed with the 1ug of ligation mixture using standardized protocol. The transformation mix was spread evenly on LB Agar plate with 50µg/ml Ampicillin. Following day, colony PCR was performed from 5 separate colonies to confirm the transformation. Plasmid was isolated using QIAprep Spin Miniprep Kit (cat: 27104) according to manufacturer's protocol. Sequence of the plasmid was verified by Genewiz (South Plainfield, NJ) before generation of lentiviral particles.

*Generation of lentiviral particles and viral transduction:*

HEK293 FS cells were grown up to 80% confluence. Subsequently, the cells were transfected with lentiviral packaging plasmids psPAX2 (Addgene#12259), VSV-G expressing envelope vector pCI VSVG (Addgene#1733) and the CRISPRi plasmid using TransIT®-LT1 Transfection Reagent (Mirus # 2300) according to manufacturer's instruction. The following morning, the media was replenished with complete growth media. Cells were cultured for 24 hours and supernatants were collected at different time points for transduction of the thyroid cancer cell lines. After 24 hours, supernatants with lentiviral particles were collected from transfected HEK293 FS cells and filtered through 0.45µm filter and added to 8505C with polybrene (catalog number) at a concentration of 1:250 from 10mg/ml stock solution. Non-specific sequence was used as control. The sequences are provided in table 5. Viral supernatant was titrated for optimal transduction efficiency and a dilution of 50% was used for final transduction. Cells were monitored with fluorescent microscopy for GFP and sorted after 48 hours for GFP<sup>+</sup> cells. Sorted cells were cultured and used for subsequent experiments.

All the procedures were approved by Institutional Biosafety Committee, New York Medical College (Protocol number: 02-2019-1).

<b>Primers for sgRNA cassette</b>	<b>Primer sequences (with restriction enzyme sites)</b>
TNFRSF14-gRNA1_F	caccGCAGCTGCCCCGTGGACGGAG
TNFRSF14-gRNA1_R	aaacCTCCGTCCACGGGCAGCTGC
TNFRSF14-gRNA2_F	caccGCCACATCCGGCCAAATGG
TNFRSF14-gRNA2_R	aaacCCATTTGGCCGGATGTGGGC
TNFRSF14-gRNA3_F	caccGGGAGGAGGTCTGCTGGGTA
TNFRSF14-gRNA3_R	aaacTACCCAGCAGACCTCCTCCC
TNFRSF14-gRNA4_F	caccGCGGATGTGGGCACTTCTGG
TNFRSF14-gRNA4_R	aaacCCAGAAGTGCCACATCCGC
TNFRSF14-gRNA5_F	caccGGCAGGATGAACTCCAGCAG
TNFRSF14-gRNA5_R	aaacCTGCTGGAGTTCATCCTGCC

Table 5. Primer sequences for sgRNA cassette targeting HVEM promoter

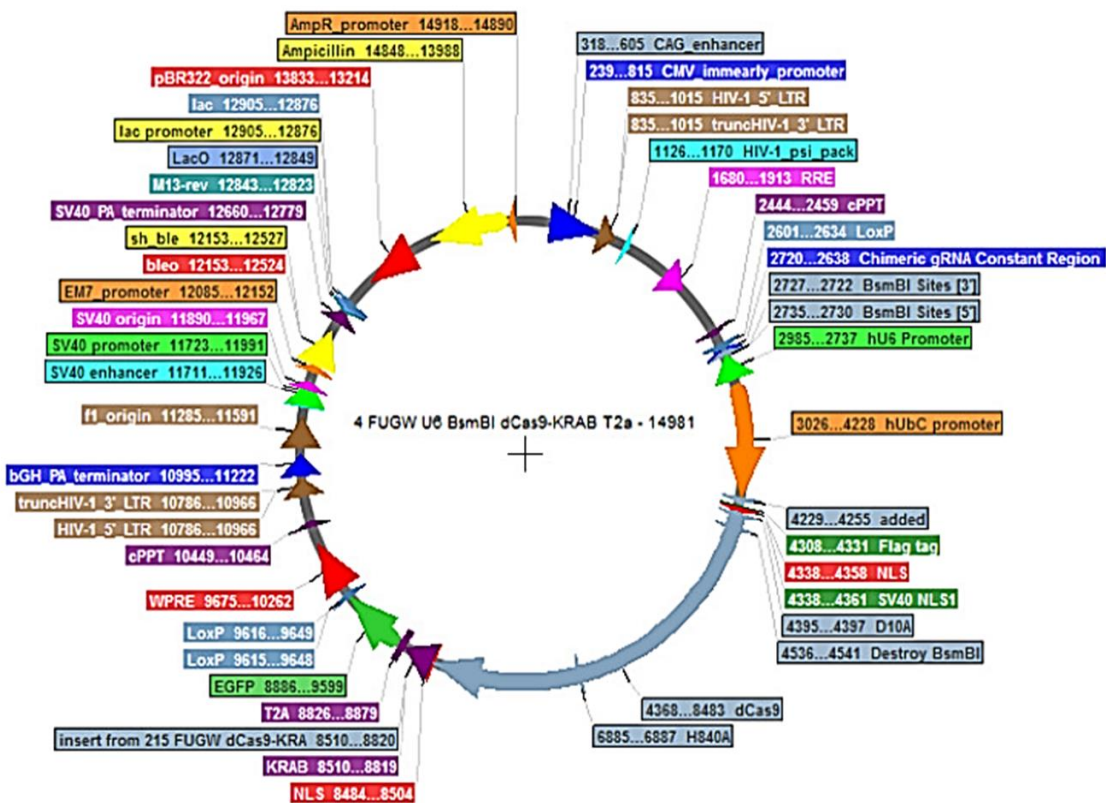


Figure 11. Map of dCas9-KRAB-GFP plasmid

#### Colony formation assay:

Cells were trypsinized and resuspended in complete growth media at a density of 200 cells/ml. 1 ml of cell suspension was added to each well of a 24 well dish. Cells were incubated at 37°C for 7 days in a humidified tissue culture incubator with 5% CO<sub>2</sub>. Formation of colonies (a group of 50 or more cells) were monitored using a bright-field microscope. Once the colonies reached an optimum size for counting (colonies with >50 cells), cells were washed twice with 1X PBS and fixed with 100% methanol for 20 minutes at room temperature. Cells were washed twice with distilled water (dH<sub>2</sub>O). Next, cells were stained with 0.5% crystal violet in 25% methanol for 5 minutes at room temperature. Crystal violet was washed carefully with dH<sub>2</sub>O until all the excess dye was removed. Plate was inverted on a paper towel overnight for drying and counted the next day using brightfield microscope. Number of colonies were plotted using GraphPad Prism 8.

#### Trans well invasion assay:

BD Biocoat Control Inserts (BD Biosciences, Bedford, MA) with 8- $\mu$ m pore membrane filters were coated with 300 $\mu$ g/ml of BD Matrigel Matrix (BD; 356231) according to manufacturer's protocol. Cells were harvested at log phase of their growth and seeded at a density of 2.5X10<sup>4</sup> cells/well in 500 $\mu$ l RPMI1640 with L-Glutamine and 0.1% BSA. An equal number of control (uncoated) permeable supports were included by using sterile forceps to transfer the permeable supports into empty wells. 750 $\mu$ l of complete growth media with 10% FBS was added to the bottom well as a chemoattractant. Cell invasion chambers were incubated overnight in a humidified tissue culture incubator at 37°C and 5% CO<sub>2</sub> atmosphere. Next morning, non-invaded cells were removed by gentle scrubbing with a moistened cotton swab. Cells were fixed by transferring permeable supports into the 100% methanol for 2 minutes

and stained with 1% Toluidine Blue in 1% borax for 2 minutes. The permeable support membranes were rinsed with dH<sub>2</sub>O to remove excess stain. The permeable support membranes were air dried and imaged using brightfield microscopy. Images were analyzed using Image J software and data were plotted using GraphPad Prism.

#### **Generation of PLX4032 resistant T238 and SW1736:**

PLX 4032 sensitive T238 and SW1736 were cultured in complete growth media with 15µM PLX4032 for 10 days. Gradually, the dose was escalated to 20, 30 and finally 60µM over a period of 3 months. Cell culture media was changed every 5 days and the old media and dead cells were thoroughly washed with sterile 1X PBS before adding fresh media. Doubling time was checked and a comparable doubling time with the sensitive phenotype was achieved at a concentration of 30µM. Both the cell lines were cultured in 30µM PLX4032 for a total of 7 months, by the end of which they were considered as the PLX4032 resistant variants.

#### **XTT assay:**

PLX4032 sensitive T238 and SW1736 were seeded at a density of 6000 cells/well and 10,000 cells/well of 96 well dishes in 200µl complete growth media. Cells were allowed to adhere overnight. Next day, complete growth media was replaced with 5% Charcoal-stripped Fetal Bovine Serum (CS-FBS) (Sigma F6765) containing clear RPMI, devoid of L-Glutamine (Corning 17-105-CV). Cells were treated with 0.5, 1, 5, 10, 20, and 50µM of PLX4032 (vemurafenib) for determination of IC<sub>50</sub> values for 96 hours. In order to determine IC<sub>50</sub> value of PLX4032 in the resistant T238 and SW1736, cells were treated with 5, 10, 20, 40, 80, 160, 320, and 640µM of PLX4032 for 96 hours. After incubation, a mixture of 1mg/ml yellow tetrazolium salt XTT (2,3-Bis-(2-Methoxy-4-Nitro-5-Sulfophenyl)-2H-Tetrazolium-5-Carboxanilide) (Thermo Fisher;

X6493) and 3mg/ml of phenazimemethosulfate was added to the microculture wells. After 4-6 hours of additional incubation at 37°C, cell viability was assessed. Live cells reduce the tetrazolium salt to formazan, which is spectrophotometrically measured at A450 nm and A630nm. The latter reading is for correcting the background noise and is subtracted from 450nm reading to get the final value.

#### Cell cycle analyses:

Cells were cultured in complete growth media up to 60% confluence. Then, the cells were starved with 2% Charcoal-stripped Fetal Bovine Serum (CS-FBS) (Sigma F6765) containing clear RPMI, devoid of L-Glutamine (Corning 17-105-CV) for 24 hours. Following this, cells were scraped off the culture vessel in their culture media to include floating cells in mitotic phase also. Cell suspension was spun at 1500 rpm for ten minutes at room temperature and cell pellets were re-suspended in 50µl of 1X PBS. 5ml Ice cold 70% ethanol was added dropwise to the cell suspension with constant low speed vortexing and stored at -20°C for a minimum of 2 hours for fixation. Ethanol was washed by 20 ml 1X PBS wash twice. Cells were washed again in 1X PBS and finally re-suspended in a staining solution of 1µg/ml DAPI in 1X PBS and stored overnight at 4°C in the dark. The cells were analyzed for their DNA content on the Beckman Coulter MoFlo.

#### BRAF<sup>i</sup> and MEK<sup>i</sup> treatment:

For BRAF<sup>i</sup> and MEK<sup>i</sup> treatments, cells were cultured up to 70-80% confluence and starved for 24 hours in 2% Charcoal-stripped Fetal Bovine Serum (CS-FBS) (Sigma F6765) containing clear RPMI, devoid of L-Glutamine (Corning 17-105-CV). Vemurafenib (PLX4032) (Selleck Chemicals; S1267) and Trametinib (GSK1120212) (Selleck Chemicals; S2673) were

reconstituted in DMSO at a concentration of 10mM and 1mM. Cells were treated with the drugs individually or in combination in 5% CS-FBS containing RPMI devoid of L-Glutamine at a concentration of 15 $\mu$ M Vemurafenib and 400nM Trametinib for 24 hours at 37°C in a humidified tissue culture incubator with 5% CO<sub>2</sub>. At the end of treatment period, cells were processed based on experimental needs.

### CHAPTER3: RESULTS

Specific aim 1: Expression of immunomodulatory molecules at transcript and protein levels in thyroid cancer cell lines and patient tissues

**EXPERIMENTAL DESIGN:** Eight human thyroid cancer cell lines were used for these *in vitro* experiments. Four ATC cell lines: 8505C, T238, SW1736 and HTh74; three PTC cell lines: TPC-1, BCPAP and K1; one FTC cell line: CGTH-W-1 and one immortalized normal thyroid follicular epithelial cell line Nthy-ori-3-1. The goal was to cover different histological subtypes of thyroid cancers of follicular/parafollicular origin and identify the molecules selectively overexpressed in ATC. Cells were harvested at the log phase of their growth and we looked at the expression of twenty-five immunomodulatory molecules by qRT PCR. From this initial screening, five molecules were shortlisted, and protein levels were further looked at by western blot. Sub-cellular localization of the protein was confirmed by immunofluorescence. Next, their surface expression was assessed by flow cytometry. Lastly, the expression of these molecules was evaluated in thyroid cancer tissues. 4µm thick serial sections were obtained from the Cooperative Human Tissue Network. Immunohistochemical analyses were done for the expression of HVEM, BTLA and CD160 in these tissues. Slides were imaged under 100X and 200X magnification and scored by a pathologist for positive staining in follicular and parafollicular cells.

*1a. in vitro screening for the expression of twenty-five immunomodulatory molecules in four ATC, three PTC and one FTC cell lines at transcript level compared to normal thyroid epithelial cell line*

**Rationale:** ATC is an extremely aggressive and de-differentiated form of thyroid cancer which is not amenable to surgery or radioiodine therapy which are the primary treatment choices for thyroid cancer (Smallridge et al., 2012). Immune checkpoint-blockade has reinvigorated

the field of cancer immunotherapy and showed great promise in a wide range of malignancies including but not limited to advanced melanoma, non-small cell lung cancer, Merkel cell carcinoma (Bhatia & Berry, 2016), head and neck squamous cell carcinoma (Forster & Devlin, 2018), urothelial and kidney cancers (Soria et al., 2018), (Massard et al., 2016) hepatocellular carcinoma (Shrestha et al., 2019) and gastric cancer (Özdemir et al., 2019). Recent findings on tumor intrinsic expression of immune checkpoint proteins and their complex interplay with cellular signaling (Marcucci et al., 2017; Meng et al., 2018) highlight their importance in preserving tumor cell biology along with immunomodulation. This therapeutic option is under- explored in ATC patients. Owing to the inherently heterogenous nature of thyroid cancer, it became important to profile different histological subtypes for expression of these molecules to see if ATC exhibits any unique set of molecules which might be clinically relevant for these patients.

a. Immunomodulatory molecules have differential expression across different histological subtypes of thyroid cancer with selective upregulation of HVEM, BTLA, CD160, OX40, TIM1, TIM3 and PD-L1 in ATC

RNA was isolated from the cells at 60-70% confluence and qRT-PCR were done for the expression of twenty-five immunomodulatory molecules. Expression was compared to normal thyroid follicular epithelial cell line Nthy-ori-3-1. We observed a unique expression pattern of immunomodulatory molecules in each cell line. Multiple Student's 't' tests were used to compare mean fold change between Nthy-ori-3-1 and thyroid cancer cell lines. Alpha level was set at 0.05 for the 't' tests. Interestingly, we observed certain patterns in ATC cell lines for some of the co-stimulatory molecules, like 4-1BB, CD27, CD40L, DR3 ICOS, CD2, CD226 all of which were down regulated in ATC cell lines compared to normal (Fig 12). Among

immune checkpoint molecules, CTLA4 and LAG3 were downregulated in ATC. Interestingly, two co-stimulatory molecules, HVEM and TIM1 were significantly over expressed in ATC cell lines T238, SW1736 and HTh74 and PTC cell line K1 compared to normal. K1 is an aggressive PTC cell line which is positive for BRAFV600E and PIK3CA E542K. It has silent mutations in HRAS and P53. Interestingly, the binding partners of HVEM, BTLA and CD160 were also upregulated in T238, SW1736, HTh74 and K1 compared to normal. We also noted overexpression of PD-L1 and TIM3 in ATC cell lines and K1 (Fig 13).

**Conclusion:** Thyroid cancer cell lines have differential expression of immunomodulatory molecules at transcript level. Players of HVEM/BTLA/CD160 signaling axis are over expressed in ATC cell lines compared to normal.

## EXPRESSION OF COSTIMULATORY MOLECULES

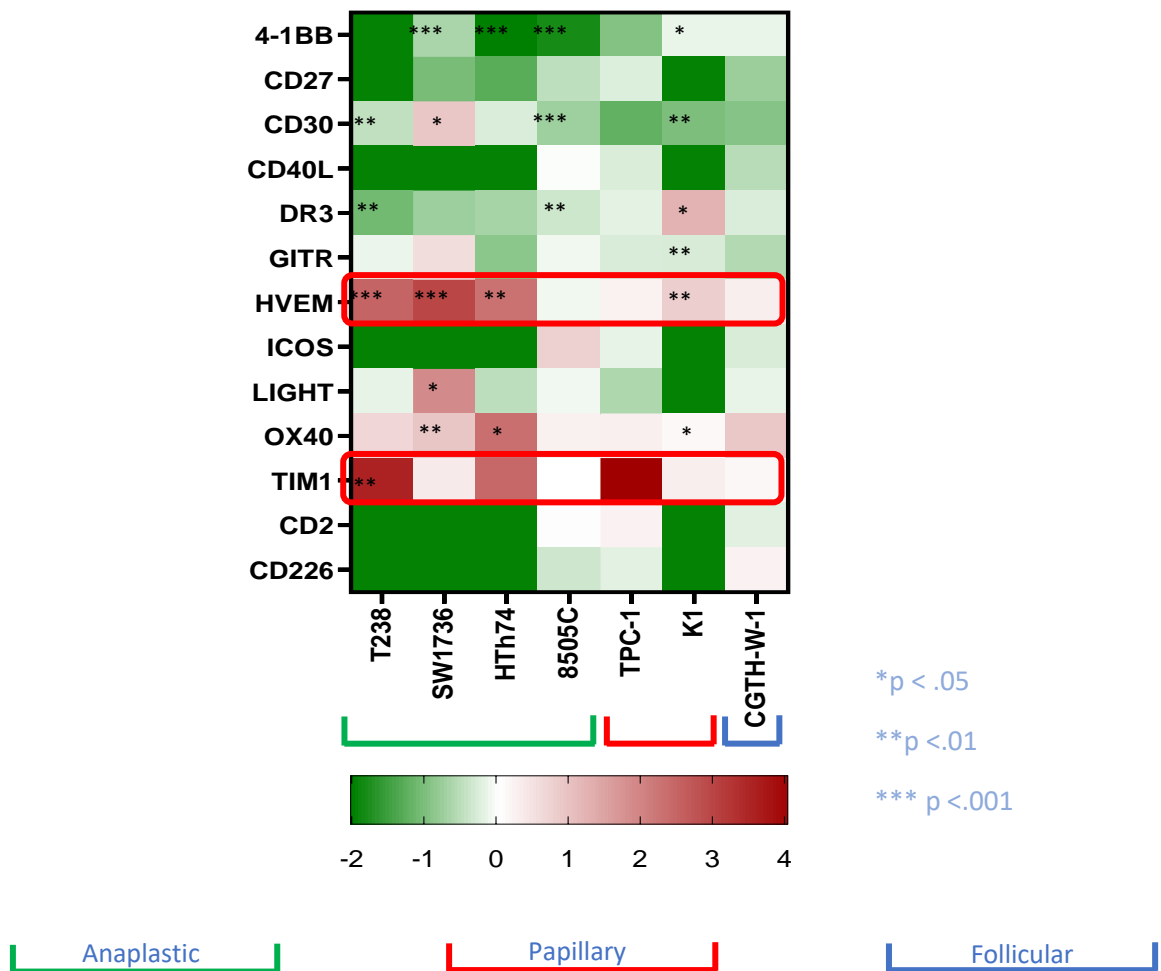


Figure 12. Expression of co-stimulatory molecules in thyroid cancer cell lines. qRT-PCR for expression of co-stimulatory molecules in different thyroid cancer cell lines compared to normal thyroid epithelial cell line Nthy-ori-3-1. Results are depicted as mean fold change from N=3 biological replicates. Multiple student's t tests were performed for comparison of mean fold change between normal and cancer cell lines. \*p<0.05 \*\*p<0.01 \*\*\*p<0.001

## EXPRESSION OF COINHIBITORY MOLECULES

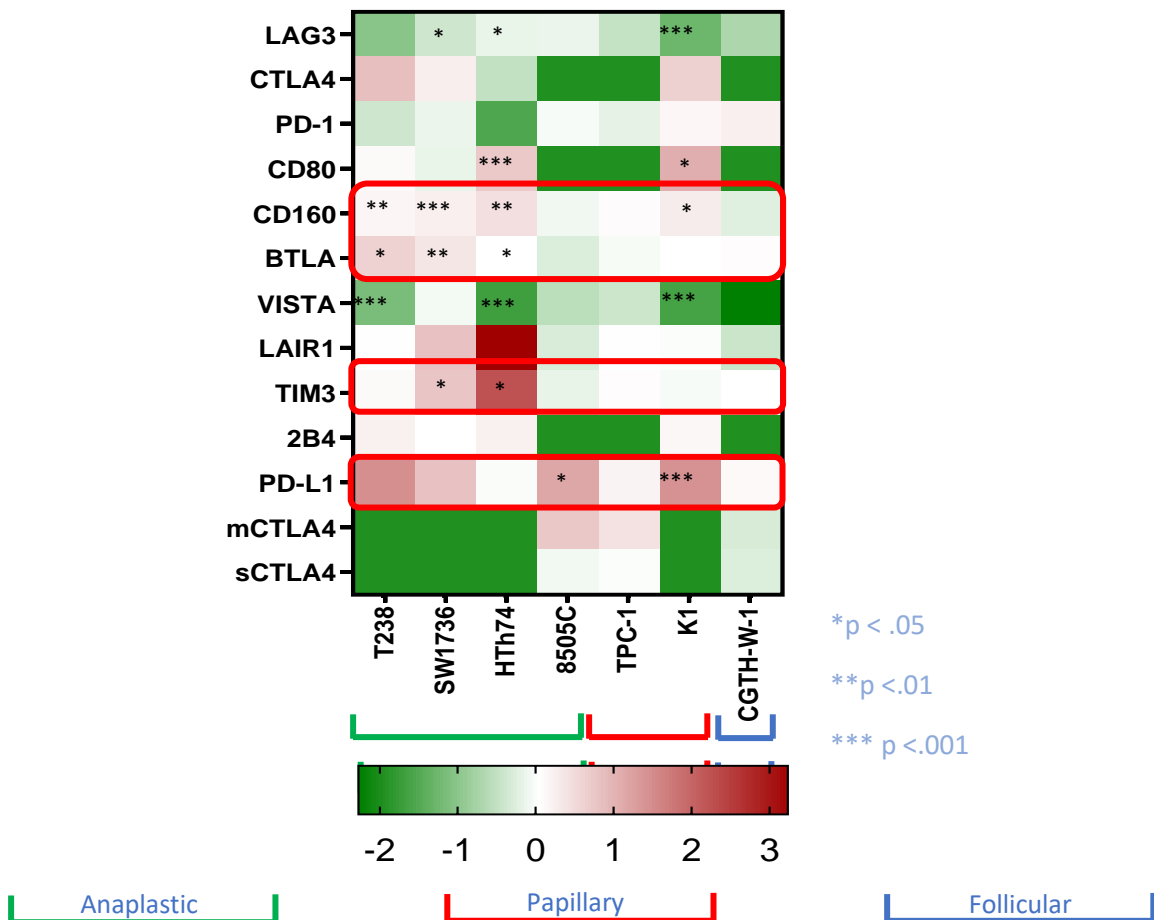


Figure 13. Expression of immune-checkpoint molecules in thyroid cancer cell lines. qRT-PCR for expression of immune-checkpoint molecules in different thyroid cancer cell lines compared to normal thyroid epithelial cell line Nthy-ori-3-1. Result depicted is mean fold change from N=3 biological replicates. Multiple student's t tests were performed for comparison of mean fold change between normal and cancer cell lines. \*p<0.05 \*\*p<0.01 \*\*\*p<0.001

*1b. Evaluation of the expression of the immunomodulatory molecules at protein level by western blot and immunofluorescence*

**Rationale:** Our qRT-PCR, study confirmed over expression of certain co-stimulatory and immune-checkpoint molecules in ATC among which HVEM was the most prominent one. HVEM is expressed in a variety of immune cells including T cells, B cells, natural killer cells, dendritic cells and endothelial cells. There are no reports suggesting expression of HVEM in stromal cells. BTLA and CD160 are two members of immunoglobulin superfamily that interacts with HVEM and dampens immune activation in T cells. High expression of these genes in tumor cells was suggestive of a possible immune interaction in the tumor microenvironment mediated by the tumor cells. Formation of active immune synapse is of course contingent upon expression of the proteins in these cells. It was therefore important to determine whether these proteins are being actively translated in the cells.

b. HVEM, BTLA and CD160 proteins are expressed in thyroid cancer cell lines

Whole cell lysates were prepared from the cell lines at 60-70% confluence and expression of HVEM, BTLA, CD160 and TIM3 were evaluated by western blot analyses. For statistical analyses, one-way ANOVA was performed with Tukey's post-test with alpha level set at 0.05. ATC cell lines T238, SW1736, HTh74 and 8505C had moderately higher expression of HVEM, BTLA and CD160 (Fig 14) compared to Nthy-ori-3-1. While, TPC-1 had negligible expression of these proteins, another PTC cell line K1 had significant expression. K1 is PTC cell line that has BRAFV600E mutation and PIK3CAE542K mutation and represents aggressive form of papillary thyroid cancer. Immunofluorescence staining revealed cytoplasmic distribution of HVEM and BTLA in T238, SW1736 and HTh74. ATC cell line 8505C had comparatively low cytoplasmic

distribution of these proteins (Fig 15). The PTC cell line K1 also had significant amount of cytoplasmic distribution of these proteins which corroborates with the first qRT-PCR result that we observed. We noted a heterogeneous distribution of the proteins within the cells in each cell line suggesting a heterogeneous distribution of these proteins in the cells. In some cells, we noted more condensation of the proteins on the membranes whereas in some, it was mostly cytoplasmic. Surprisingly, we could not detect cytoplasmic expression of CD160 by immunocytochemistry.

**Conclusion:** Anaplastic thyroid cancer cells and aggressive variant of papillary thyroid cancer cells have constitutive cytoplasmic expression of HVEM and BTLA protein.

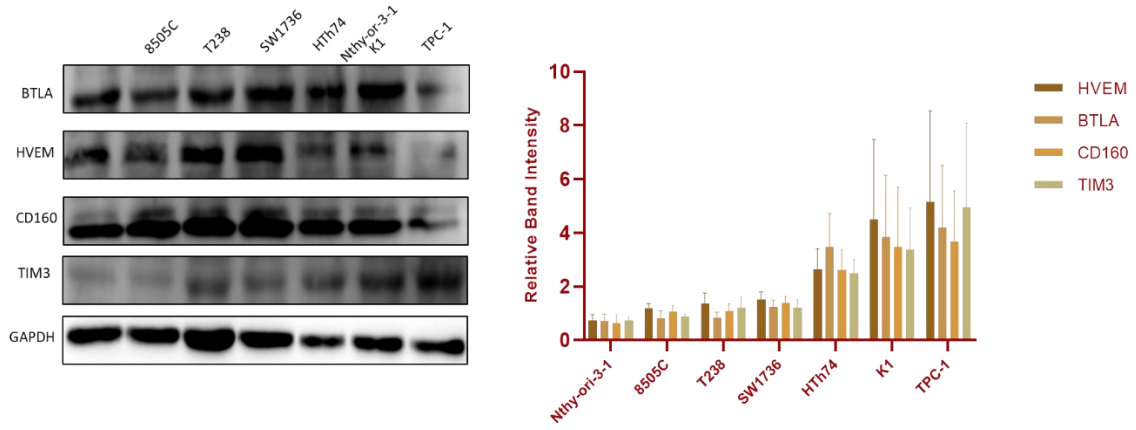


Figure 14. Expression of immunomodulatory proteins in thyroid cancer cell lines. Whole cell lysate was prepared from thyroid cancer cell lines at 70% confluence. Western blot was conducted for expression of HVEM, BTLA, CD160, TIM3 and GAPDH. Image representative of N=3 biological replicates.

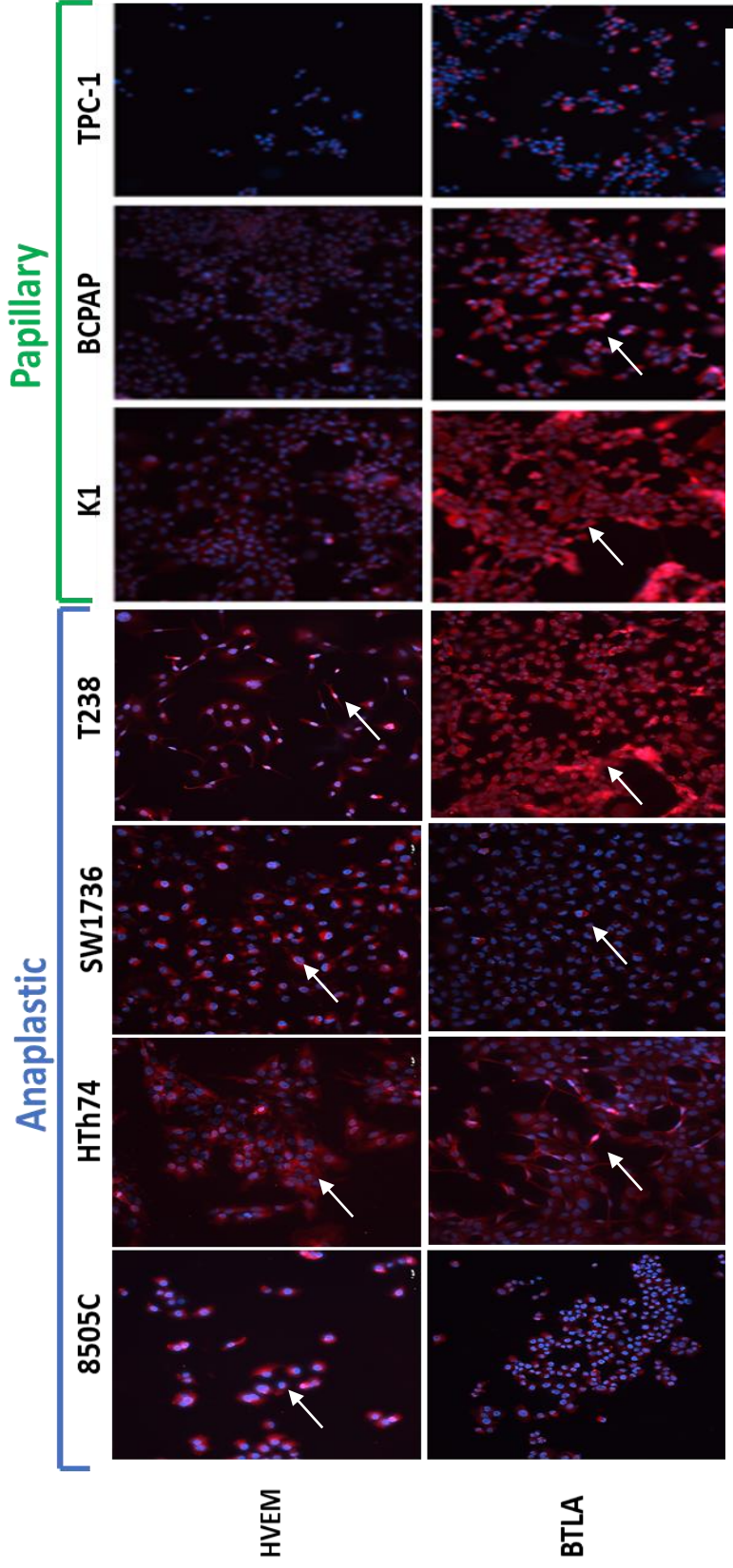


Figure 15. Sub-cellular localization of HVEM and BTLA in thyroid cancer cell lines. Immunofluorescence staining was done on permeabilized thyroid cancer cell lines for expression of HVEM and BTLA. Nuclei are stained with DAPI (blue) and target proteins are stained with Alexa Fluor 594 conjugated secondary (red). Arrows point to representative positive cells. Magnification: 200X.

### **1c. Analysis of surface expression of HVEM, BTLA, CD160 and TIM3 in the cell lines of interest by flowcytometry**

**Rationale:** High expression of HVEM, BTLA, CD160, TIM3 and PD-L1 was observed during our qRT PCR study. With immunofluorescence studies, we confirmed varied constitutive cytoplasmic expression of HVEM and BTLA in the anaplastic thyroid cancer cell lines with some membrane condensation suggesting the possibility of their presence on the surface. In order to form an active synapse with the ligands on the immune cells and participate in immunomodulation, these proteins must be expressed on the cell surface. Naturally, the next logical step was to assess the surface expression of these protein in the cell lines of interest.

c. Immunomodulatory proteins HVEM, BTLA, CD160 and TIM3 are present on the surface of the anaplastic thyroid cancer cell lines

In order to assess the surface expression of these proteins in the cell lines, four color flow cytometry was performed with the cell lines without permeabilization. We looked at surface expression of HVEM, BTLA, CD60 and TIM3. We looked at the percentage of positive cells and, level of surface expression in the cells by mean fluorescent intensity (MFI). An overlay was generated for each protein to distinguish the positive population from isotype control (Fig 16). For each protein, we observed two distinct peaks suggesting a heterogenous population composed of high and low expressors. This corroborates with our previous findings with immunofluorescence, where we noted differential expression of the proteins between the cells in each cell line. Among the molecules, HVEM had the highest expression in T238, SW1736 and HTh74. BTLA and CD160 had comparable expression among the cell lines (Fig 17). Interestingly, TIM3 was the molecule with second highest expression after HVEM. TIM3

expression was detected at transcript level and in western blot, immunofluorescence was unable to detect any cytoplasmic expression of this protein. T238 and HTh74 were the cell lines that had high expression of TIM3. CD160 expression was significantly higher in HTh74 compared to normal. HTh74 had the highest percentages of cells positive for the expression of the immunomodulatory molecules. Approximately 54.48% cells were positive for HVEM, 40% of the cells were positive for BTLA and almost 66% of the cells were positive for CD160 in HTh74 (Fig 18). Approximately 48% of the cells were positive for TIM3. A heterogeneous expression of the molecules was observed across different cell lines which might account for the inherently heterogeneous nature of the cell lines and indicates the unique immune phenotype of each cell line. Mean fluorescent intensity of HVEM was significantly higher in ATC cell lines compared to Nthy-ori-3-1. This observation was very significant as these were basal level of expression of these proteins in these cells. Some of these genes have binding sites for IRF1, STAT1 and STAT3 in their promoter. This could be suggestive of an IFN $\gamma$  or IL8 inducible expression pattern which would be very significant in an inflammatory microenvironment commonly observed in cancer like ATC where these cytokines are abundant.

**Conclusion:** Anaplastic thyroid cancer cells have a heterogeneous surface expression of HVEM, BTLA, CD160 and TIM3. Constitutively higher surface expression of HVEM was observed in ATC cell lines compared to normal. There is a heterogeneity in the distribution of these molecules in the cells which can result from the inherently heterogeneous nature of the cancer cells.

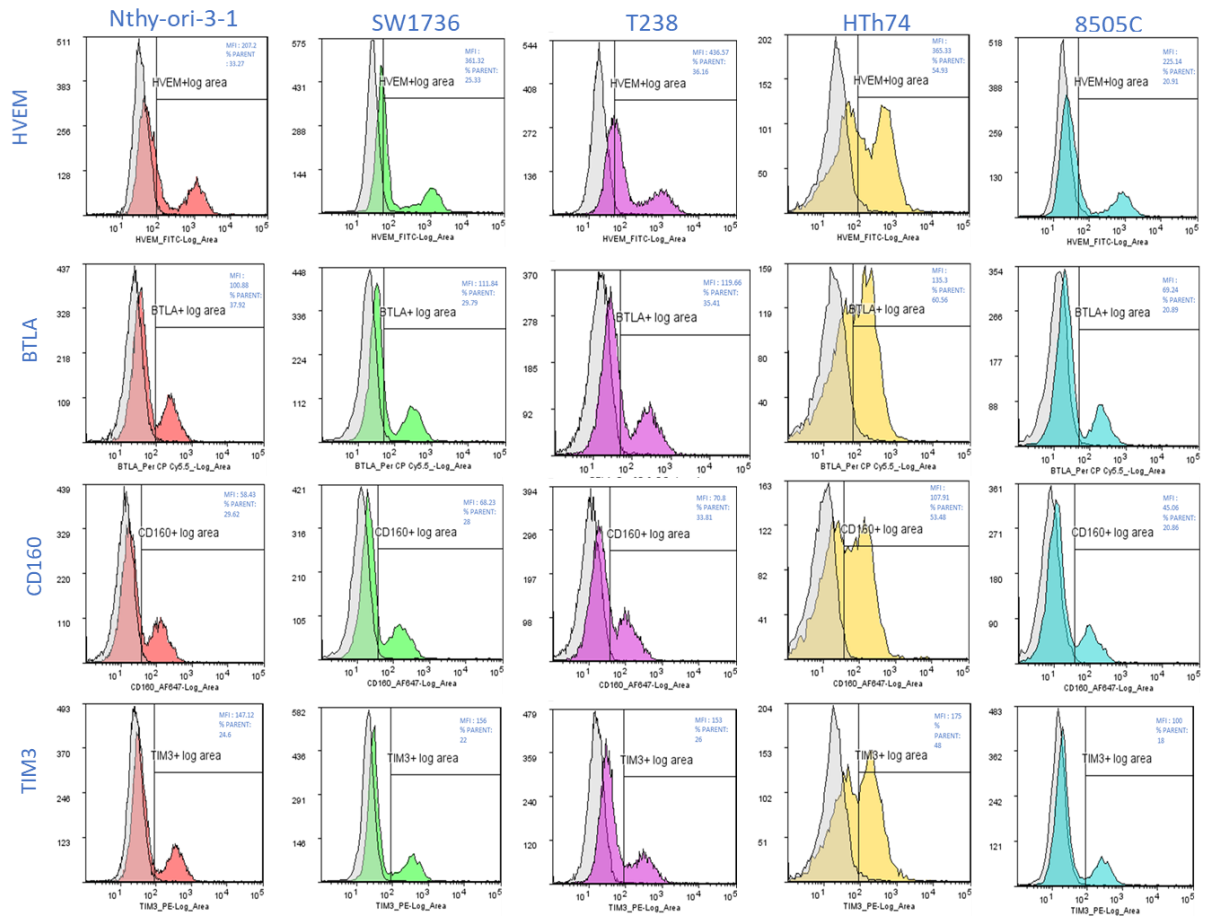


Figure 16. Constitutive expression of cell surface immunomodulatory molecules by anaplastic thyroid cancer cell lines. Flow cytometry was performed for expression of HVEM, BTLA, CD160 and TIM3. Grey: Isotype control; colored histogram: stained cells. Image is representative of 3 independent experiments.

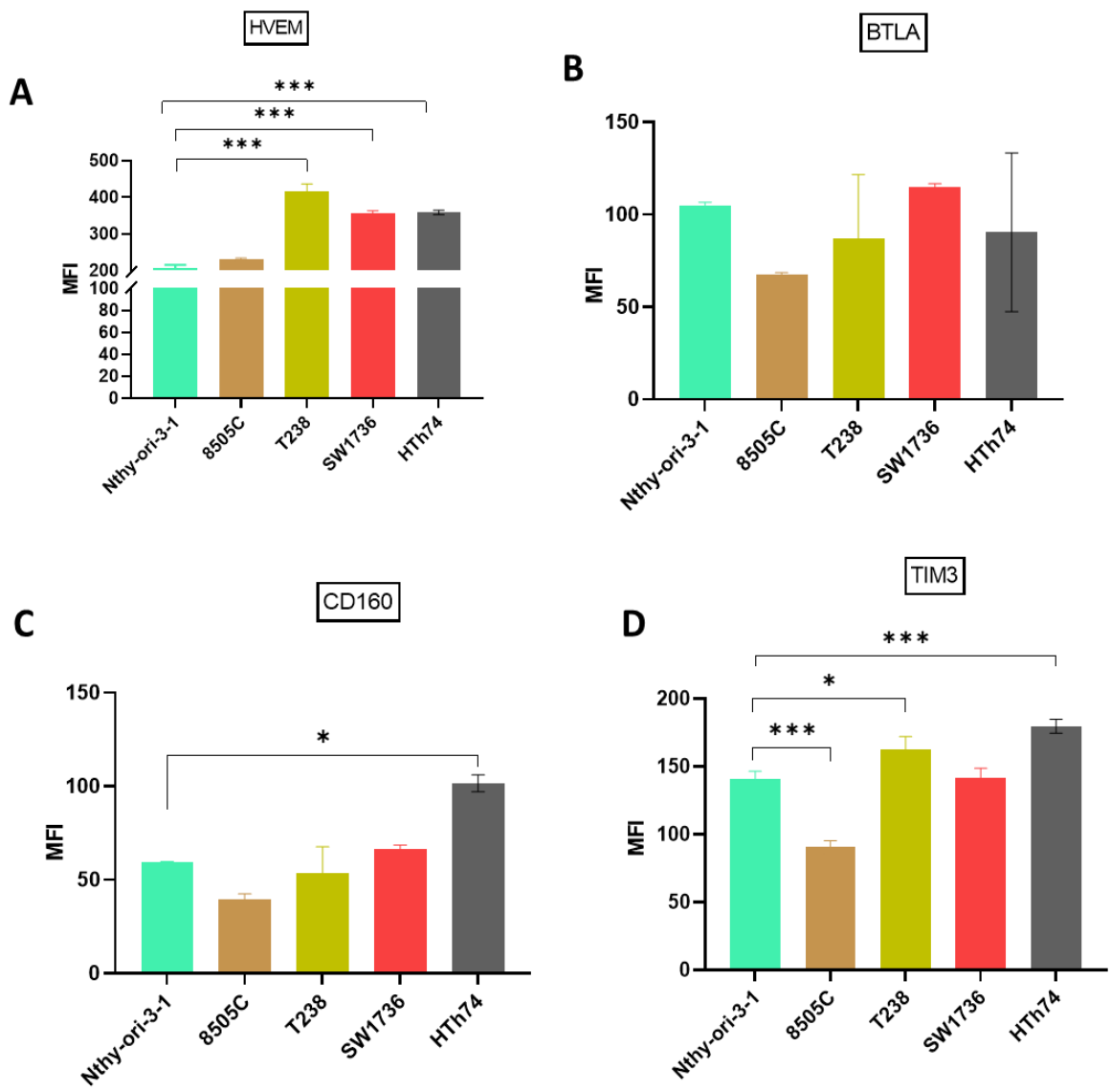


Figure 17. Constitutive surface expression of immunomodulatory molecules in ATC cell lines. Flow cytometry was carried out with non-permeabilized cell lines with a cocktail of four-color fluorochrome conjugated antibodies. The bars represent the average MFI  $\pm$  SEM from N=3 biological replicates. One-way ANOVA with Tukey's posttest was conducted for statistical analyses. \*\*p<0.01 \*\*\*\*p<0.0001

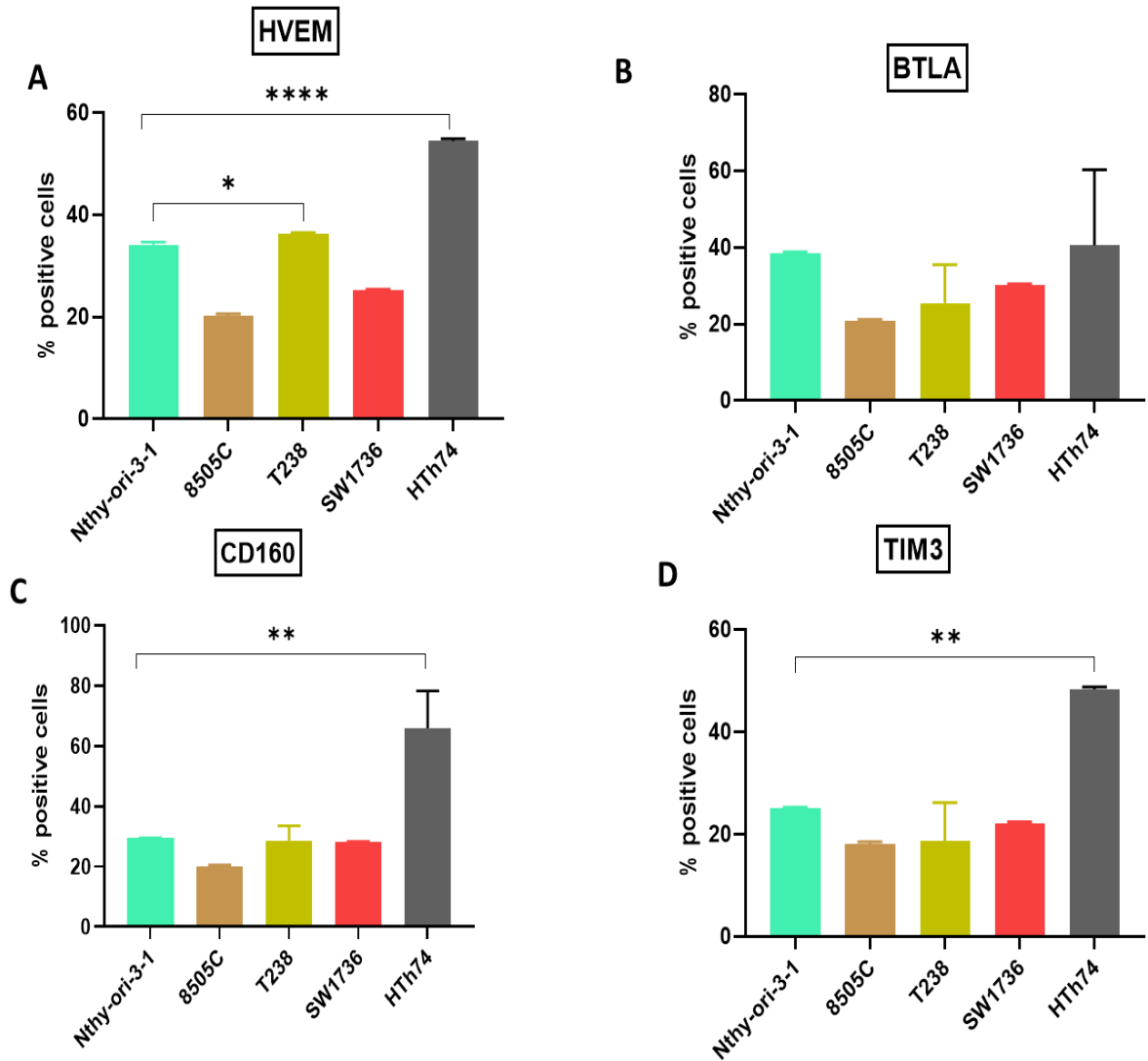


Figure 18. Percentage of cells positive for expression of immunomodulatory molecules. Flow cytometry was carried out with non-permeabilized cell lines with a cocktail of four-color fluorochrome conjugated antibodies comprising of anti-HVEM, anti-BTLA, anti-CD160 and anti-TIM3. Graphs represent percentage of cells positive for the expression of the specified proteins. The bars represent mean  $\pm$  SEM of % positive cells from N=3 biological replicates. One-way ANOVA with Tukey's posttest was conducted for statistical analyses. \*\* $p < 0.01$  \*\*\*\* $p < 0.0001$

*1d. Evaluation of the expression of immunomodulatory molecules of interest in thyroid cancer tissues by immunohistochemistry*

**Rationale:** From our initial study, we confirmed expression of Immunomodulatory molecules HVEM, BTLA, CD160 and TIM3 in the tumor cells both at transcript and protein level. Classically, these molecules were known to be expressed by the cells of the innate and adaptive immune system, particularly antigen presenting cells (APC) and T cells. However, there is ample evidence that tumor cells also express these molecules intrinsically and play crucial role in determining the tumor phenotype (Marcucci et al., 2017). Presence of these molecules on tumor cells indicates their possible participation in processes beyond immunomodulation. Since ATC has a very complex tumor microenvironment enriched with different types of infiltrating immune cells, the presence of these immunomodulatory molecules on the tumor cells can enable a more complex interaction between the tumor cells and the immune microenvironment that might promote immune evasion. There is a lack of knowledge regarding tumor intrinsic expression of such immunomodulatory molecules in ATC and our initial findings from *in vitro* studies suggested a strong possibility that these proteins might be expressed in the follicular cells of thyroid cancer tissues as well.

d. Immunomodulatory molecules HVEM, BTLA and CD160 are abundantly expressed in the follicular cells of ATC and aggressive PTC

In order to assess the expression of these proteins, we procured 10 formalin fixed paraffin embedded tissue samples from the University of Pennsylvania, Eastern Coast, Cooperative human tissue network (CHTN). The samples consisted of four PTC tissues, four ATC tissues and two normal tissues. Both PTC and ATC tissue samples were malignant in nature. ATC tissues had extensive necrotic centers and typical spindle and giant cell morphology. All of

them had extensive extrathyroidal extensions and involvement of local skeletal muscles and high degree of angio-invasion. One ATC tissue had a papillary counterpart with tall cell variant. PTC tissues were classical variants except for one which was a tall cell variant. One of the patients with PTC had minimal lymphocytic thyroiditis at the time of diagnosis. Immunohistochemistry was performed for detection of HVEM, BTLA and CD160 on 4µm thick serial sections.

We observed considerably higher expression of HVEM in both ATC (Fig 19 A-D) and PTC (figure 19 E-H) tissues compared to normal (figure 19 I). Tumor infiltrating immune cells also scored positive for the staining, but for our scoring, we strictly focused on the follicular and parafollicular cells for positive staining. Percentage of tumor cells positive for the staining was considered for scoring. HVEM staining was predominantly cytoplasmic in the follicular cells. BTLA expression was also significantly higher in both ATC (figure 20 A-D) and PTC (figure 20 E-H) tissues compared to normal (figure 20 I). Interestingly, for BTLA, we observed not only high cytoplasmic expression, but membrane condensation also, suggesting their surface expression. Follicular cells of normal thyroid tissue had minimal expression of BTLA. The colloid inside the follicle showed brown color, but that should be considered as non-specific staining. CD160 expression was also predominantly cytoplasmic with some membrane condensation in ATC (Figure 21 A-D), suggesting their presence on the surface. PTC tissues also had comparable expression of CD160 (figure 21 E-H). a quantitative representation of the results is summarized in figure 22.

**Conclusion:** Follicular cells in ATC and aggressive variant of PTC have high expression of immunomodulatory molecules HVEM, BTLA and CD160. This suggests the possibility of an

immunologically active microenvironment in this aggressive form of thyroid cancer which might be amenable to therapeutic intervention.

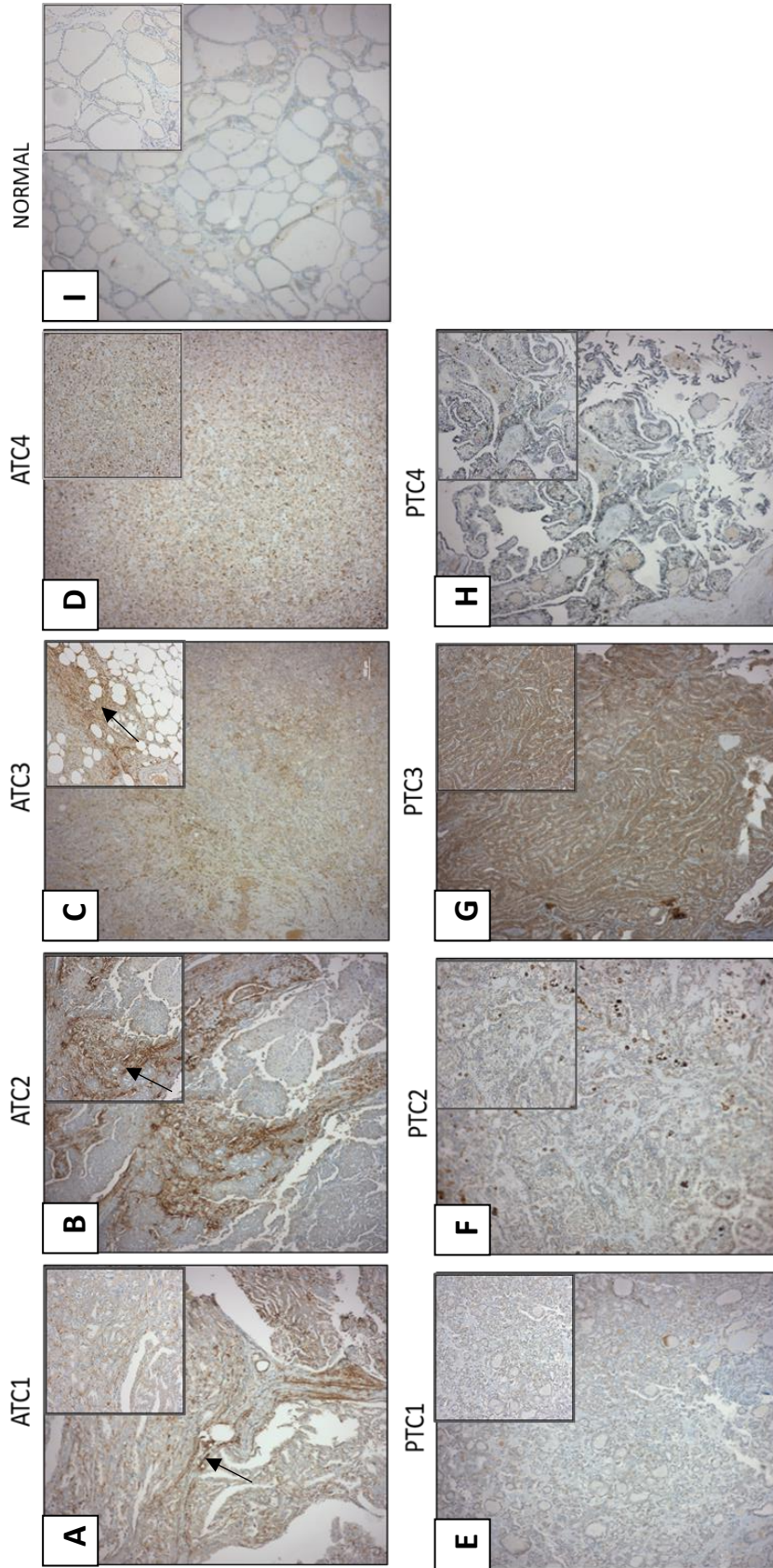
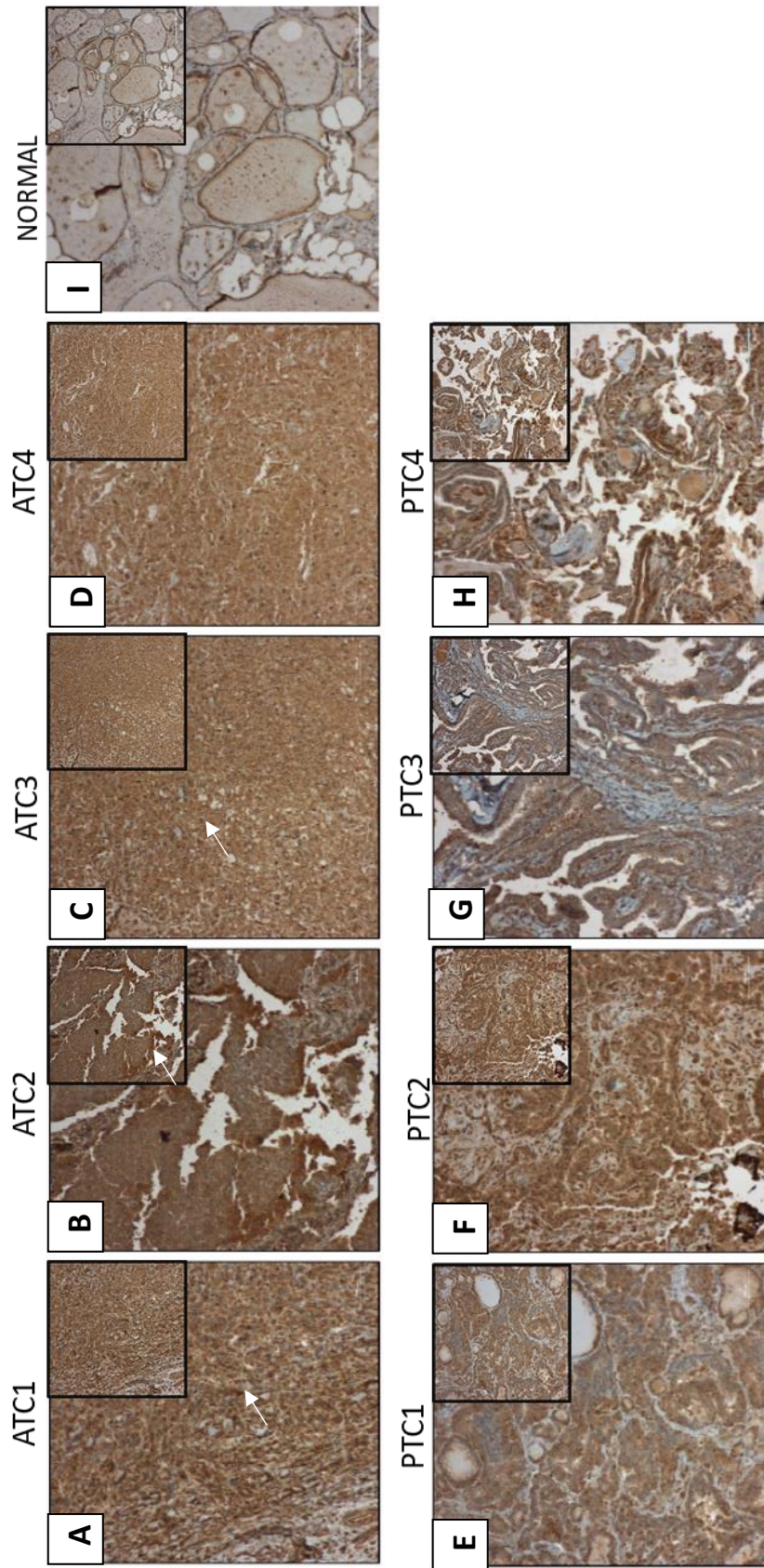


Figure 19. Expression of HVEM in follicular cells of ATC and PTC. ATC tissues (A-D); PTC tissues (E-H) and normal (I). Positive staining is represented by brown color. Membrane condensations are indicated with black arrow. Magnification: 100X. Inset: 200x magnification



**Figure 20. Expression of BTLA in follicular cells of ATC and PTC.** ATC tissues (A-D); PTC tissues (E-H) and normal (I). positive staining is represented by brown color. Membrane condensations are indicated with white arrow. Magnification: 100X. Inset: 200x magnification

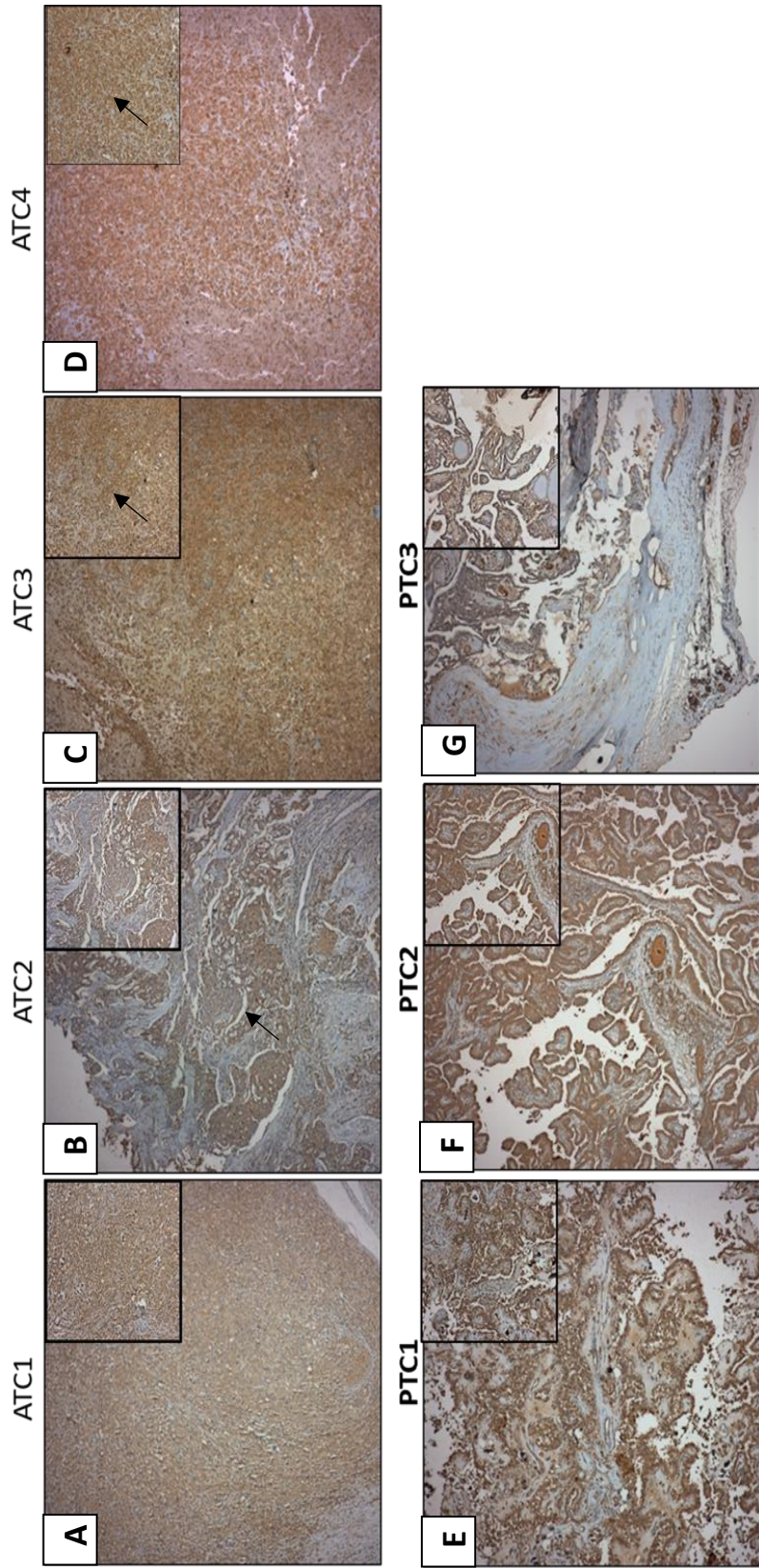


Figure 21. Expression of CD160 in follicular cells of ATC and PTC. ATC tissues (A-D); PTC tissues (E-H). positive staining is represented by brown color. Magnification: 100X. Inset: 200x magnification

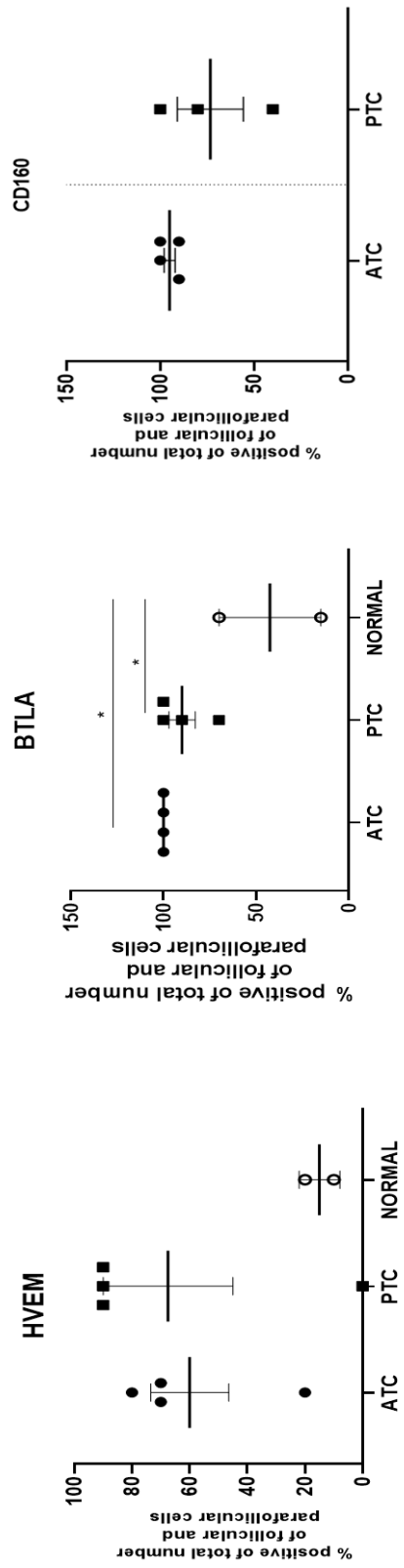


Figure 22. Expression of HVEM, BTLA and CD160 in follicular cells of ATC and PTC. Line and bars represent Mean±SEM. Student's t test was used to determine statistical significance \*p<0.05

### *Summary*

- Thyroid cancer cell lines differentially express T cell co-stimulatory and immune checkpoint molecules
- HVEM, BTLA, CD160, TIM3 and PD-L1 are significantly overexpressed in thyroid cancer cell lines 8505C, T238, Sw1736 and HTh74 compared to normal thyroid epithelial cells
- HVEM, BTLA, CD160 and TIM3 proteins are constitutively expressed in the thyroid cancer cell lines and HVEM has the highest level of surface expression
- HVEM, BTLA and CD160 has abundant expression in follicular and parafollicular cells of thyroid cancer tissues
- Membrane condensations of HVEM and BTLA on follicular cells of the ATC tissues suggests their surface expression and possible involvement in immunomodulation in TME

### *Conclusion:*

**Profiling of T cell co-stimulatory and immune checkpoint molecules resulted in the identification of HVEM/BTLA/CD160 pathway as a putative immunotherapeutic target in ATC.**

Specific aim 2a: Examine the modulation of HVEM by inflammatory components in anaplastic thyroid cancer

**EXPERIMENTAL DESIGN:** Our previous studies confirmed the expression of immunomodulatory proteins HVEM, BTLA and CD160 in the follicular cells of ATC and PTC. Next, we wanted to examine the tumor immune microenvironment to have a better idea of the possible interaction between the immunomodulatory molecules expressed on follicular cells and the infiltrating immune cells. First, we conducted immunohistochemistry to assess the composition of the immune infiltrate in these tissues. First, we looked for tumor infiltrating CD3<sup>+</sup>, CD8<sup>+</sup>, CD4<sup>+</sup> and FOXP3<sup>+</sup> T cells. Next, we wanted to look at the cytokine milieu and did IHC staining for immune suppressive cytokines IL10 and IDO1 and the pro-inflammatory cytokine IL17. Previous studies have confirmed that the immunomodulatory proteins are regulated by different cytokines and this phenomenon partially accounts for the responsiveness or lack thereof towards immunotherapy (Bertrand et al., 2017; Li et al., 2018; Zheng et al., 2019a). ATC is well known to have a high density of TAMs and a mixed population of M1 and M2 macrophages. Activated M1 macrophages secrete various pro-inflammatory cytokines among which IL8 and TNF $\alpha$  are the prominent ones. We evaluated the effect of these two cytokines on expression of HVEM using an *in vitro* cell culture model system. Cells were treated with these cytokines separately and in combination and surface expression of HVEM was assessed by flow cytometry and soluble HVEM in the conditioned media was measured by ELISA. Lastly, we wanted to see if HVEM on tumor cells transduces the signaling cascade after binding its cognate ligand LIGHT. To test this, cells were treated with recombinant human LIGHT and various effectors of HVEM/LIGHT signaling were looked at by western blot.

*2ai) Analysis of immune infiltrate composition in thyroid cancer patient tissues by immunohistochemistry*

**Rationale** Tumor-infiltrating T cells are a hallmark of ongoing immune surveillance in cancer and are of immense prognostic and therapeutic value. Patients with higher frequency of tumor-infiltrating T lymphocytes (TILs) generally display favorable prognosis (Fridman et al., 2017). The tumor immune microenvironment is a spatially organized landscape where immune cells are found in their specific niche. Both ATC and PTC have been shown to have an immunologically active microenvironment with tumor infiltrating macrophages (Caillou et al., 2011; W. Fang et al., 2014) and NK cells (A. Park et al., 2018, 2019). Owing to the refractory nature of ATC, it is logical to envision a weak immune surveillance in this cancer which fails to elicit a proper anti-tumor immune response. This can be attributed to lower CD8<sup>+</sup> T cell infiltration or increased number of regulatory T cells. Very little is known about infiltration status of CD8<sup>+</sup> and FoxP3<sup>+</sup> regulatory T cells in ATC. In order to understand the immune contexture in ATC accurately, it was crucial to assess the infiltration status of the immune cells as a first step.

**ai). ATC and aggressive variants of PTC have significantly higher tumor infiltrating CD8<sup>+</sup>T cells compared to normal tissue**

Immunohistochemistry was conducted on 4µm thick serial sections of the formalin fixed paraffin embedded tissues used before for the assessment of immunomodulatory molecules. Slides were reviewed by a licensed pathologist for quantitative assessment of tumor infiltrating CD3, CD4, and CD8 lymphocytes. Percentage of CD3<sup>+</sup> cells among tumor infiltrating lymphocytes were determined first, followed by percentage of CD4<sup>+</sup> and CD8<sup>+</sup> cells among

the CD3<sup>+</sup> lymphocytes. Ordinary One-Way ANOVA followed by a Tukey's posttest was used to compare infiltration between all three groups with an alpha level of 0.05. 82.5% of tumor infiltrating lymphocytes in ATC were CD3<sup>+</sup> lymphocytes (Fig 23 A-D) which was significantly higher compared to normal tissue (25%) (Fig 25 A-D). 80% of the CD3<sup>+</sup> lymphocytes were CD8<sup>+</sup> (Fig 23 E-H) in ATC. 67.5% of mononuclear cells in PTC were CD3<sup>+</sup> (Fig 24 A-D) and among them close to 80% were CD8<sup>+</sup> (Fig 24 E-H). This also was significantly higher compared to normal tissue (Fig 25 C-D), but the overall numbers were lower than ATC. ATC had higher amount of CD4<sup>+</sup> T lymphocytes compared to PTC, but it did not reach statistical significance (Fig 28). Interestingly, the CD8<sup>+</sup> T cells had mostly intra-tumoral distribution in both ATC and PTC, whereas CD4<sup>+</sup> T cells were found mostly around the tumoral margin, not inside the tumor. However, in patient ATC3, we observed some negligible intratumoral infiltration of CD4<sup>+</sup> T cells. Normal thyroid tissue was devoid of any CD8<sup>+</sup> T cells, which is expected. We did not detect significant amount of FoxP3<sup>+</sup> regulatory T cells in either ATC (Fig 26 A-C) or PTC tissues (Fig 26 D-G) and the number was very small in normal thyroid tissue as well (Fig 27). FoxP3<sup>+</sup> T<sub>regs</sub> are very potent. So, there is a possibility that these small number of cells might be sufficient to contribute towards the immune suppressive microenvironment. A quantitative summary of the findings is depicted in figure 29.

**Conclusion:** Our findings suggested that ATC and aggressive variants of PTC have a T cell inflamed immune microenvironment characterized by presence of ample amount of tumor infiltrating T cells, including CD8<sup>+</sup> T cells which play the most significant role in mounting anti-tumor immune response. This underscores the importance of our earlier findings on presence of immunomodulatory molecules on the tumor cells, suggesting a possible interaction

between the tumor cells and the infiltrating T cells via engagement of HVEM, BTLA and CD160. Engagement of BTLA and CD160 on the activated T cells with HVEM on either antigen presenting cells or tumor cells or vice versa can render the T cells non-functional and incapable of mounting an effective anti-tumor immune response. This phenomenon might contribute to immune evasion in ATC.

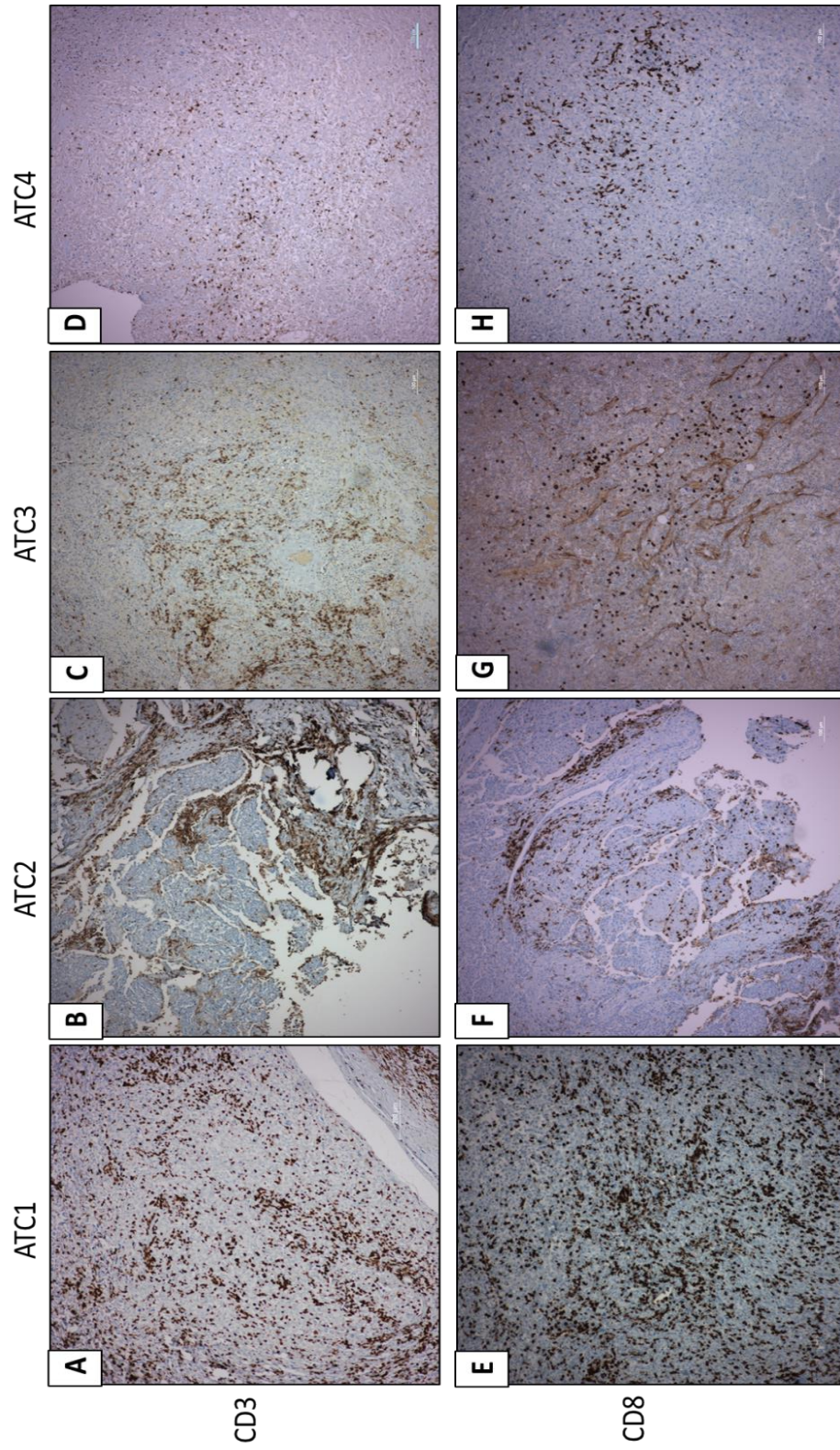


Figure 23. Tumor infiltrating CD3 and CD8 lymphocytes in ATC. CD3+ T cells (A-D); CD8+ T cells (E-H). positive staining is represented by brown color. Lower magnification (100X) is used to cover more surface area and to get a better estimate of the extent of infiltration.

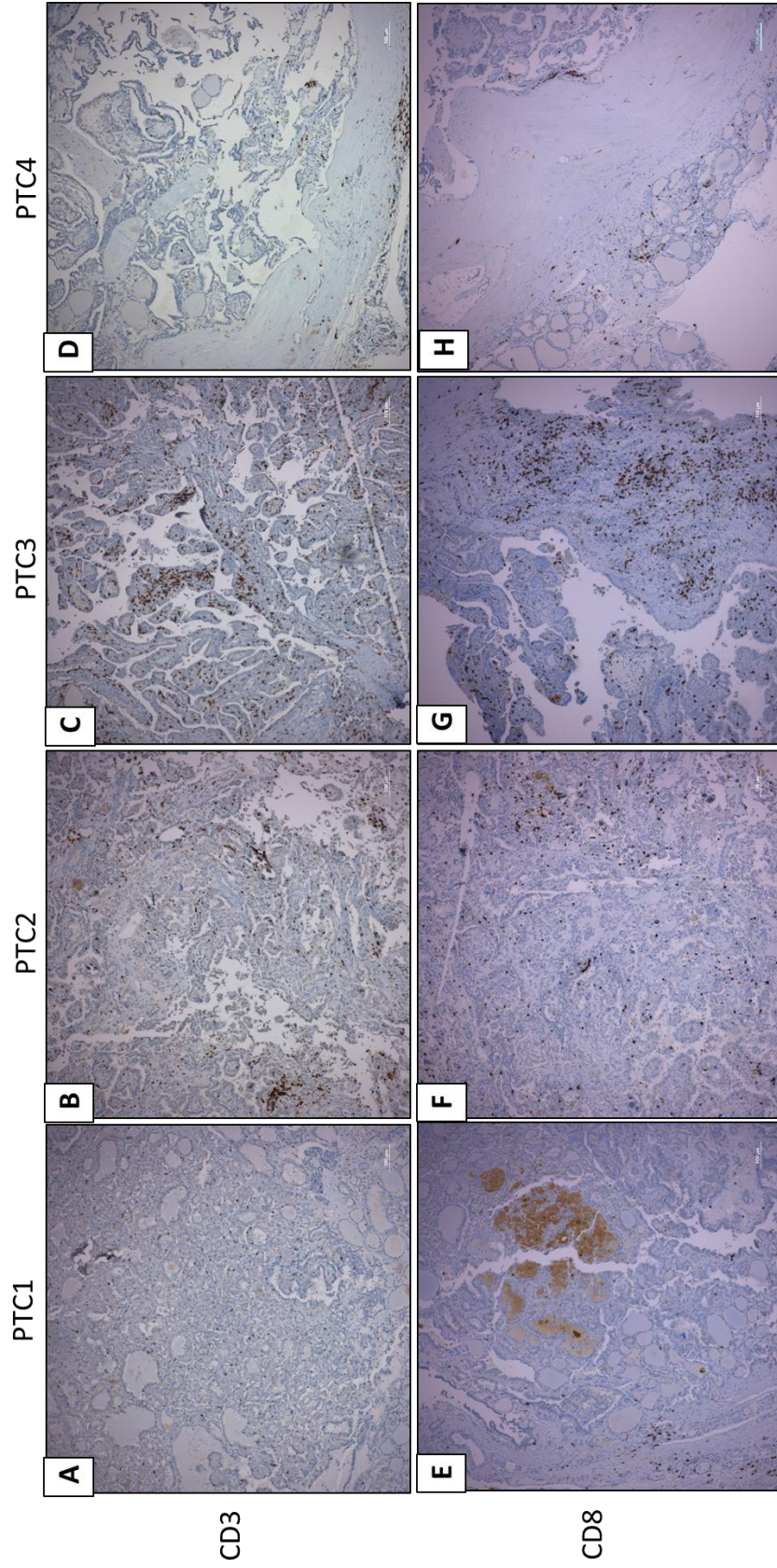


Figure 24. Tumor infiltrating CD3 and CD8 lymphocytes in PTC. CD3+ T cells (A-D); CD8+ T cells (E-H). positive staining is represented by brown color. Lower magnification (100X) is used to cover more surface area and to get a better estimate of the extent of infiltration.

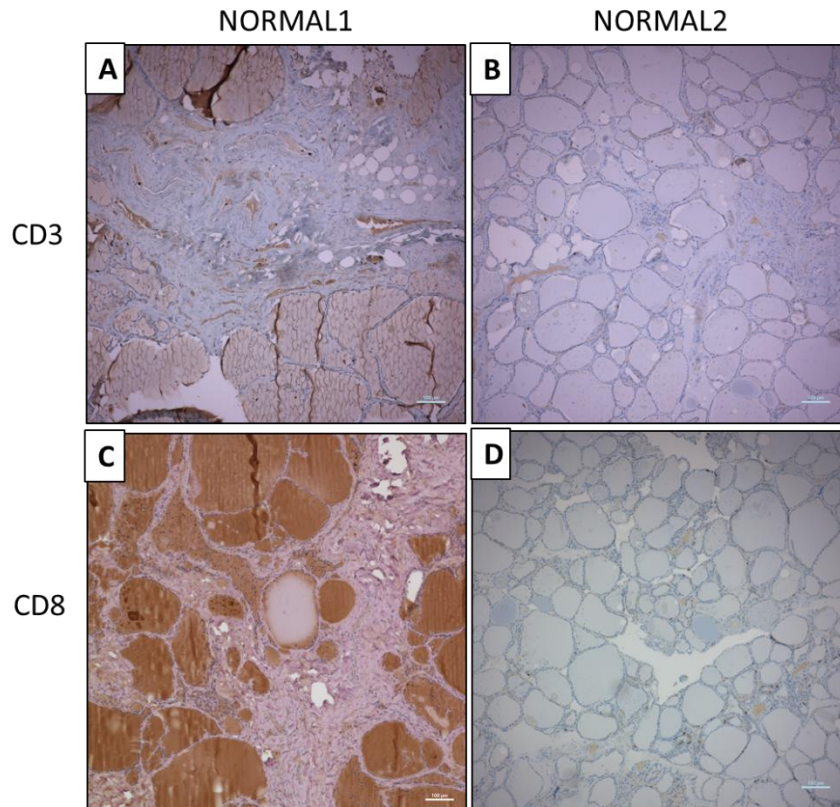
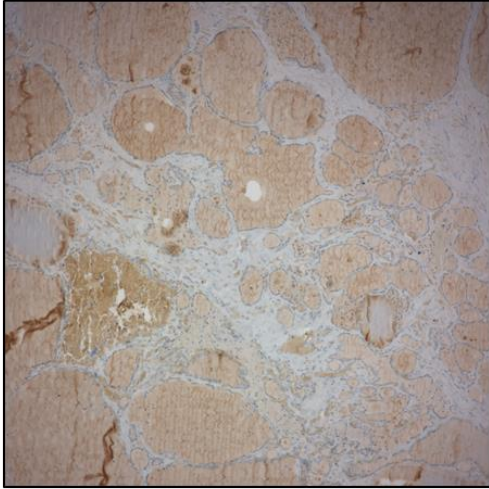


Figure 25. CD3 and CD8 lymphocytes infiltration in normal thyroid tissue. CD3+ T cells (A-B); CD8+ T cells (C-D). Positive staining is represented by brown color. The colloid inside the follicle shows non-specific brown staining. Lower magnification (100X) is used to cover more surface area and to get a better estimate of the extent of infiltration.

NORMAL1



NORMAL2

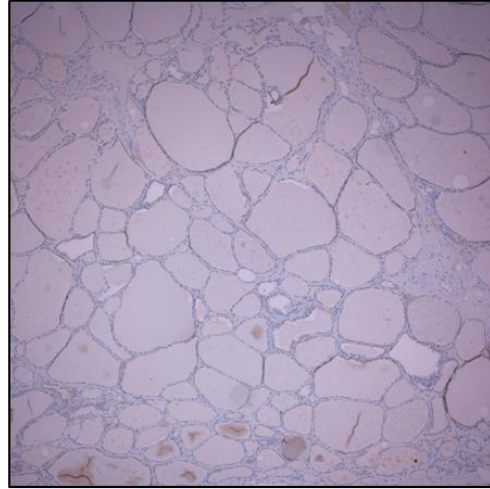


Figure 26. Infiltration of FoxP3+ lymphocytes in normal thyroid tissue. FoxP3+ cells in two normal thyroid tissues. Positive staining is represented by brown color. Lower magnification (100X) is used to cover more surface area and to get a better estimate of the extent of infiltration.

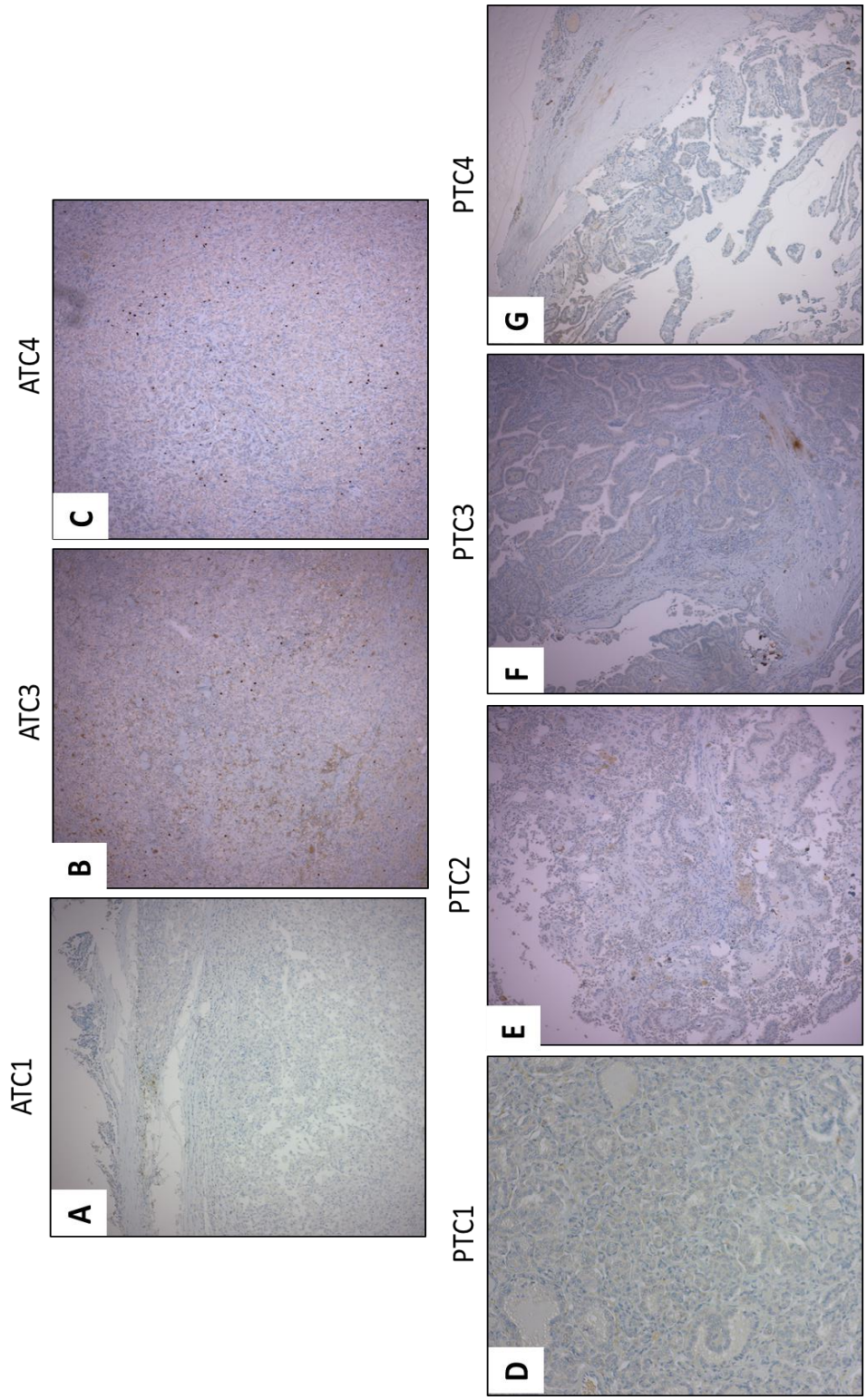


Figure 27. Tumor infiltrating FoxP3+ lymphocytes in ATC and PTC. FoxP3+ cells in ATC (A-C); FoxP3+ cells in PTC (D-G). positive staining is represented by brown color. Lower magnification (100X) is used to cover more surface area and to get a better estimate of the extent of infiltration.

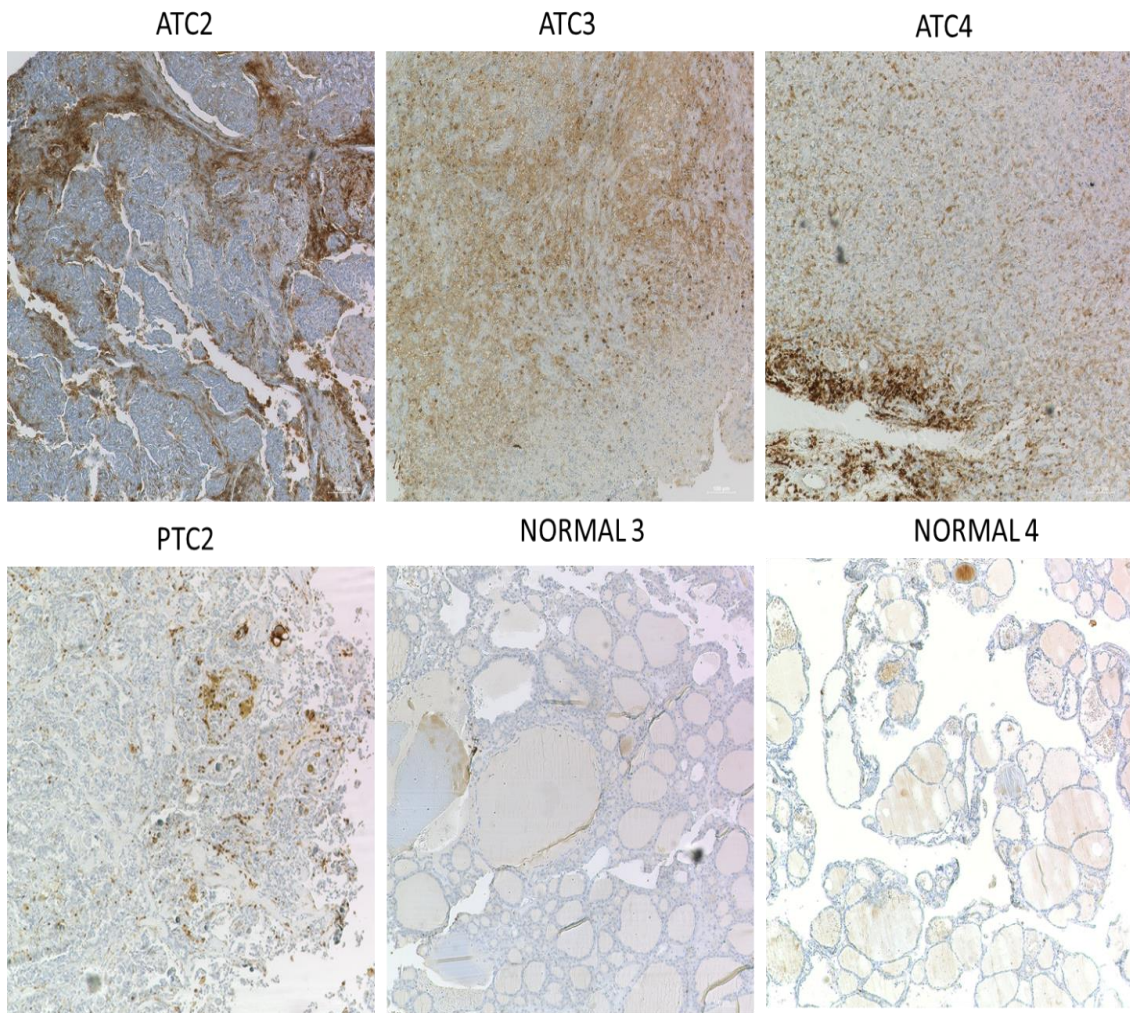


Figure 28. Tumor infiltrating CD4+ lymphocytes in ATC, PTC and normal thyroid tissue. Representative images of tumor infiltrating CD4+ cells in thyroid tissues. Positive staining is represented by brown color. Lower magnification (100X) is used to cover more surface area and to get a better estimate of the extent of infiltration.

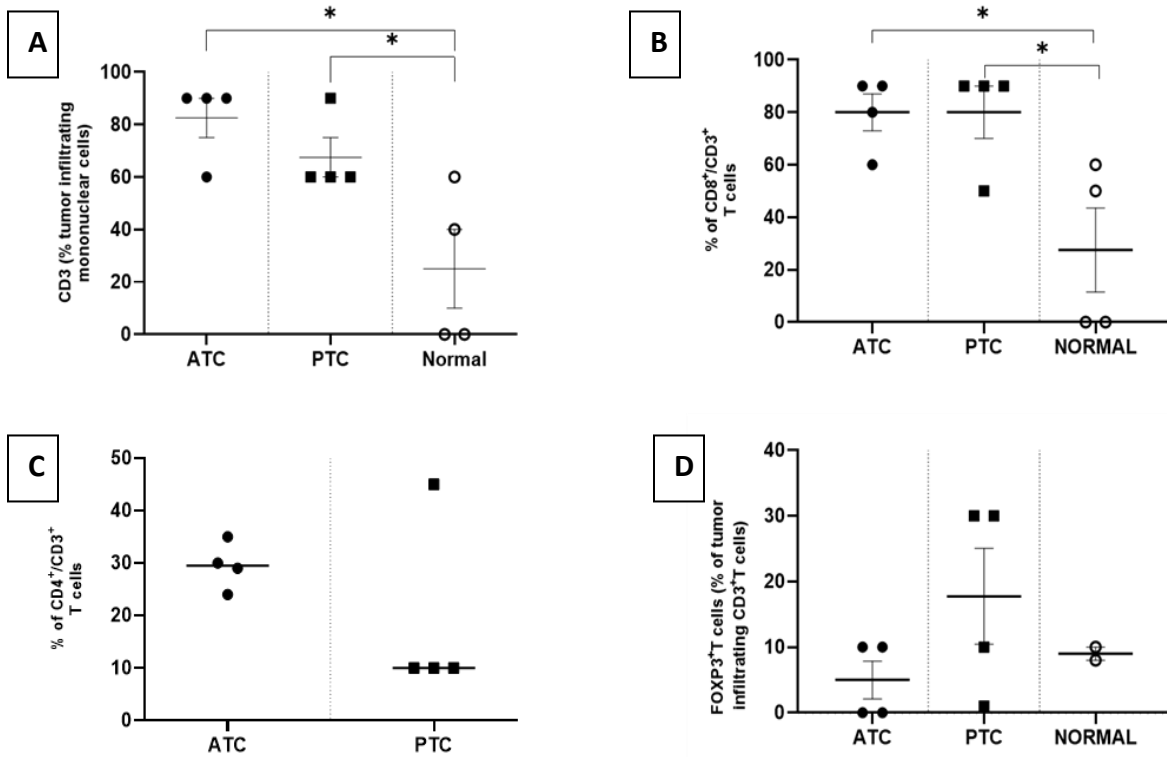


Figure 29. T cell infiltration in ATC, PTC and normal thyroid tissues. (A) Percent CD3+ lymphocytes and (B) percent CD8+/CD3+ lymphocytes in ATC and PTC compared to normal thyroid tissue (C) Percent CD4+/CD3+ lymphocytes in ATC and PTC (D) percent FoxP3+/CD3+ lymphocytes in ATC, PTC and normal thyroid tissues. Ordinary One-Way ANOVA followed by a Tukey's test was used to compare infiltration between three groups. The line and bars represent Mean±SEM. \*p<0.05

*2a ii) Analysis of cytokine milieu in thyroid cancer patient tissues by immunohistochemistry*

**Rationale:** ATC and WDTC-derived cell lines secrete a wide range of cytokines and chemokines with pleiotropic functions, such as GM-CSF, IL-1 $\alpha$ , IL-6, CXCL8/IL-8, monocyte chemoattractant protein-1 (MCP-1), and TNF- $\alpha$  (Guarino et al., 2010), some of which control the tumor cells in an autocrine manner (Kulbe et al., 2009; Long et al., 2016). Pro-inflammatory cytokines, like IL17 has been implicated in poor prognosis of thyroid cancer (Carvalho et al., 2017). Indoleamine 2,3-dioxygenase (IDO1), a cytoplasmic single chain oxidoreductase responsible for one of the rate-limiting steps of tryptophan metabolism is one such crucial immune regulator which has been linked with immune suppressive phenotype observed in PDTC (Rosenbaum et al., 2018). IDO1 has been indicated to have immune suppressive effect on cytotoxic T cells in PTC and MTC (Moretti et al., 2014). Another such immune suppressive cytokine commonly associated with impaired cytotoxic T cell activity, is IL-10. Interestingly, the immunomodulatory molecule BTLA has also been implicated in upregulation of IL10 synthesis (Zhang et al., 2019). All these different cytokines in TME act as immune regulators and can contribute to adaptive immune resistance in TC. Expression pattern of these cytokines is not well characterized in ATC, most probably owing to the rarity of the disease. In order to understand the immune contexture of the TME of ATC in the context of impaired CD8<sup>+</sup>T cell activity, we characterized the expression of some of these immune suppressive cytokines in ATC and some aggressive variants of PTC tissues.

**aii) IDO1 and IL17 have higher expression in both ATC and aggressive variants of PTC compared to normal**

We performed Immunohistochemistry on 4 $\mu$ m thick serial sections of the formalin fixed paraffin embedded tissues. Slides were reviewed by a licensed pathologist for an assessment of IDO1 positive immunoreactivity. Percentages of immune reactive follicular and parafollicular cells and PMNs were determined among different histological subtypes. For quantitative assessment, we focused on the IDO1 positive follicular cells. IDO1 positive immune cells were only considered for qualitative evaluation. Ordinary One-Way ANOVA followed by a Tukey's posttest was used to compare the percentages between all three groups with an alpha level of 0.05. We observed much higher expression of IDO1 in both ATC (Fig 30 A-D) and PTC (Fig 30 E-H) compared to normal (Fig 30 I). A stronger IL17 immunoreactivity was also observed in both ATC (figure 31 A-D) and PTC (figure 31 E-H) compared to normal (figure 31 I). The same trend was observed in case of IL10 (figure 32).

**Conclusion:** Our findings suggest that ATC and aggressive variants of PTCs have a mix of pro-inflammatory and immunosuppressive microenvironment. High expression of IDO1 is indicative of an immune environment which is usually associated with immune tolerance. IL17 expression suggests an ongoing inflammatory process in the TME and a different type of immune response which supports differentiation of CD4<sup>+</sup> T cells into Th17 cells. Interestingly, differentiation of Th17 cells occur in presence of IL6, IL21 and TGF $\beta$  (D. F. G. Carvalho et al., 2017), two of which are secreted by the tumor cells themselves. Also, IL-17 promotes secretion of inflammatory cytokines such as IL-6, TNF $\alpha$  and chemokines such as IL-8, MCP 1 from different types of cells including keratinocytes, endothelial cells, epithelial cells and

macrophages. Previous studies in our lab has shown, that the conditioned media from TC cell lines are enriched with a plethora of cytokines among which IL6, IL8 and TNF $\alpha$  are the prominent ones. This underscores the significance of tumor cell – immune cell interaction in maintaining a subdued immune microenvironment rendering the effector cells dysfunctional.

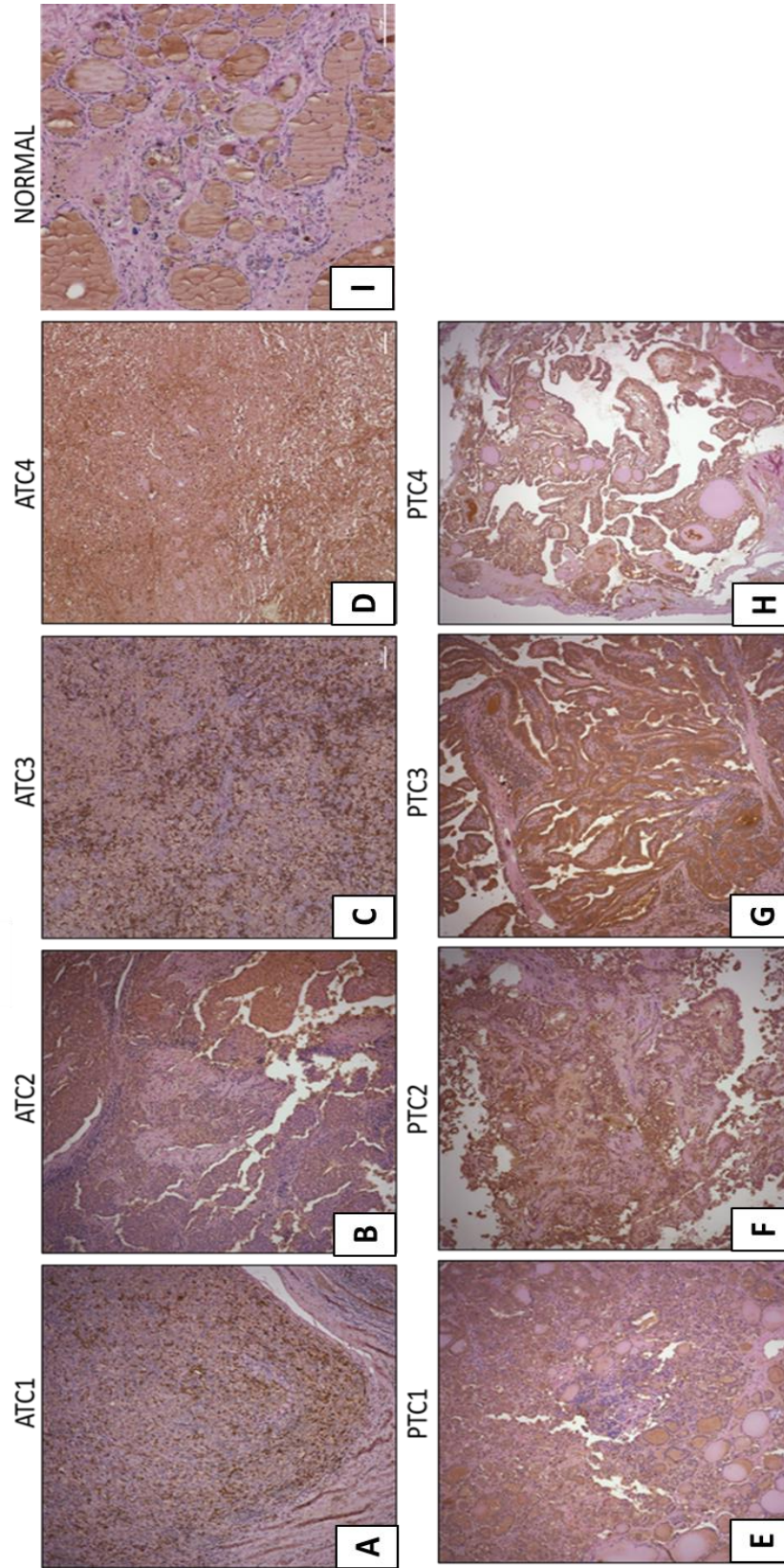


Figure 30. Expression of IDO1 in ATC and PTC. ATC (A-D); PTC (E-H); normal (I). Positive staining is represented by brown color. Lower magnification (100X) is used to cover more surface area and to get a better estimate of the extent of immune reactivity.

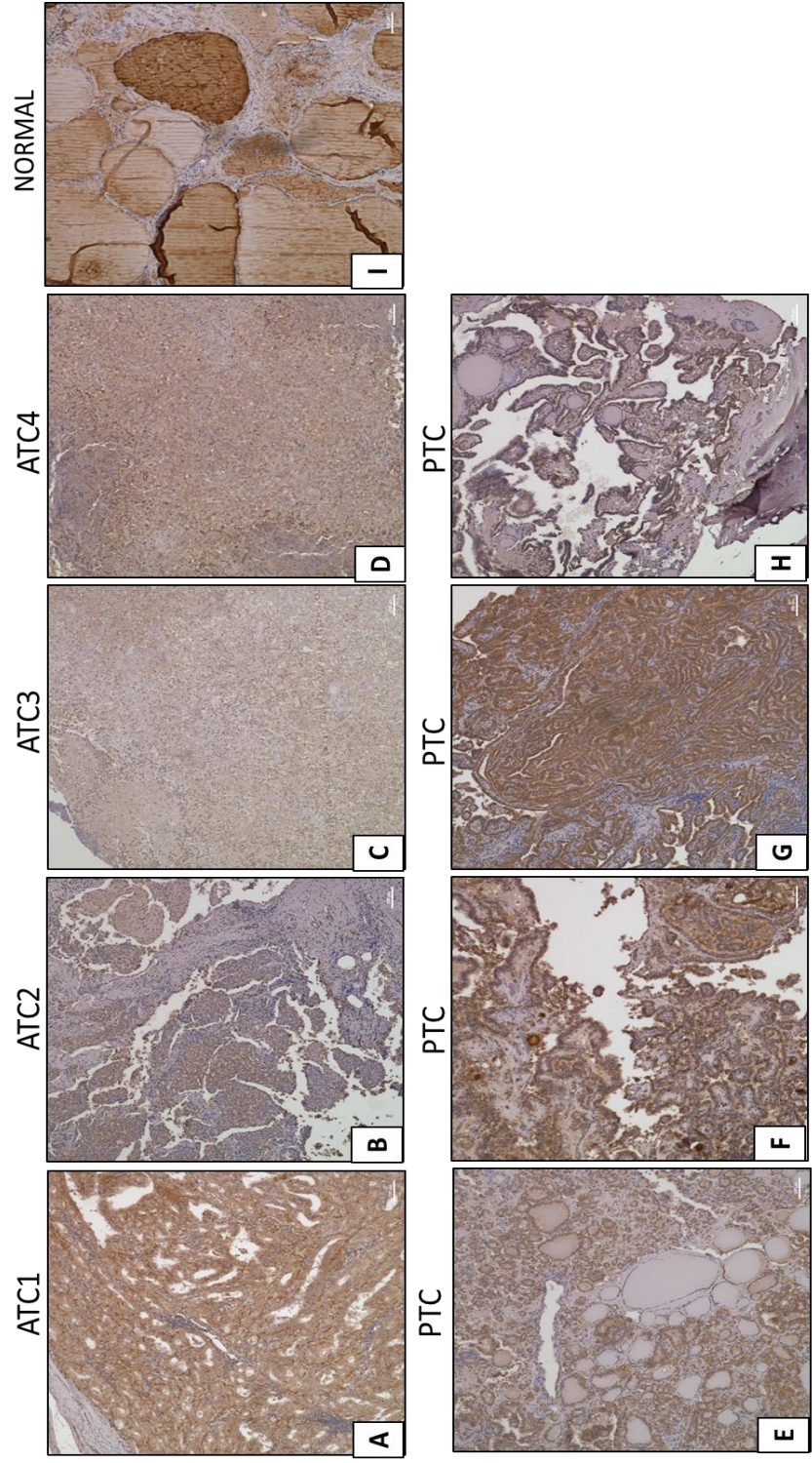


Figure 31. Expression of IL17 in ATC and PTC. ATC (A-D); PTC (E-H); normal (I). Positive staining is represented by brown color. Lower magnification (100X) is used to cover more surface area and to get a better estimate of the extent of immune reactivity. The colloid inside the follicle in normal thyroid tissue shows non-specific brown staining.

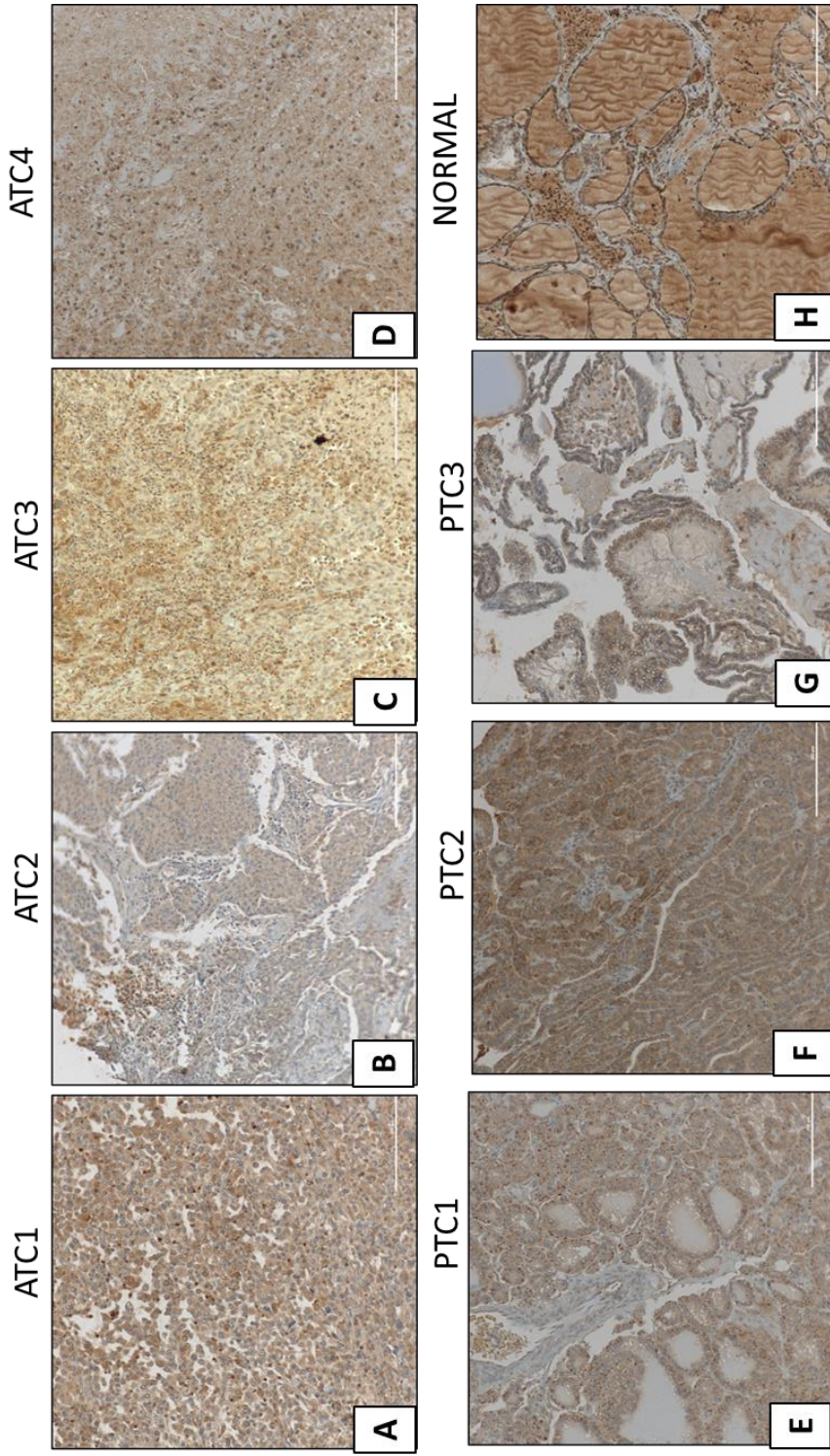


Figure 32. Expression of IL10 in ATC and PTC. ATC (A-D); PTC (E-G); normal (H). Positive staining is represented by brown color. Lower magnification (100X) is used to cover more surface area and to get a better estimate of the extent of immune reactivity. Colloid inside the follicle of normal thyroid tissue shows non-specific brown staining.

*2aiii) Analysis of the effect of inflammatory cytokines TNF $\alpha$ , IL-8 and IFN $\gamma$  on expression of tumor cell – HVEM*

**Rationale:** Thyroid cancer cell lines secrete pro-inflammatory cytokines such as IL-8 and IL-6 and high circulating level of these cytokines are usually associated with poor prognosis in thyroid cancer (Basolo et al., 2002; Rotondi et al., 2018). Circulating level of these cytokines are considered as a biomarker for response to various immunotherapies, including immune checkpoint inhibitor therapy (Nakamura, 2019). Targeting IL-6 has recently been shown to sensitize colorectal cancer cells to anti-PD-L1 treatment in a preclinical study (Li et al., 2018). This suggests a complex interplay between the cytokine milieu and expression of the immunomodulatory molecules in TME. Recent studies indicate that IL-8 can regulate expression of immune checkpoint protein PD-L1 in gastric cancer cells (Sun et al., 2018). Additionally, TNF $\alpha$  has recently been implicated in upregulation of the immunomodulatory molecule TIM3 on NK cells, rendering them non-functional in esophageal cancer (Zheng et al., 2019b). A recent study by Bertrand *et al.* found that TNF $\alpha$  blockade can overcome therapeutic resistance to anti-PD-1 therapy in experimental melanoma (Bertrand et al., 2017). We hypothesized that the pro-inflammatory immune microenvironment in ATC might reinforce crosstalk between the cytokines and the tumor cell - immunomodulatory molecules which might promote immune escape.

- **IL8 and TNF $\alpha$  induce transcription of HVEM, but reduces its surface expression on ATC cell lines**

ATC cell line 8505C was cultured in complete growth medium up to 60% confluence. Then the cells were starved in completely serum free clear RPMI for 24 hours for cell cycle synchronization. Then the cells were treated with 50ng/ml IL-8, 10ng/ml TNF $\alpha$  and a combination of both for 24 hrs. RNA was isolated and qRT PCR was performed for expression of HVEM. Data were normalized to GAPDH of the control group. One-way ANOVA was performed with Tukey's posttest and a P value set at 0.05. We observed that both IL-8 and TNF $\alpha$  induced transcription of HVEM (Fig 33). Statistically significant upregulation was observed only with TNF $\alpha$  treatment.

Next, we wanted to assess if these inflammatory cytokines modulate surface expression of HVEM in these ATC cell lines. Flow cytometry was done following the same treatment procedure on 8505C, T238, SW1736, HTh74 and Nthy-ori-3-1. Percentage of HVEM positive cells and mean fluorescent intensity (MFI) were analyzed. Cells were not permeabilized for these studies. Interestingly, we observed reduction in surface expression of HVEM following treatment with IL-8 and TNF $\alpha$  (Fig 34). TNF $\alpha$  treated group had a 25% reduction in HVEM positive population and 47% decrease in MFI in HTh74 (Fig 34). In T238, there was a 52.6% decrease in HVEM positive population and 17% decrease in MFI in TNF $\alpha$  treated group (Fig 34). In SW1736, there was 48.6% reduction in HVEM positive group, but there was no change in MFI (Fig 35). In 8505C also, we observed similar trend, but it did not reach statistical significance (figure 35). This differential effect might be attributed to the inherently

heterogeneous nature of the cell lines. This phenomenon was not observed in normal thyroid epithelial cell line Nthy-ori-3-1 (Fig 36), suggesting there might be some unique mechanism at play in the cancer cells which is not active in the normal cells. For statistical analyses, one-way ANOVA was done with Tukey's posttest and P value set at 0.05.

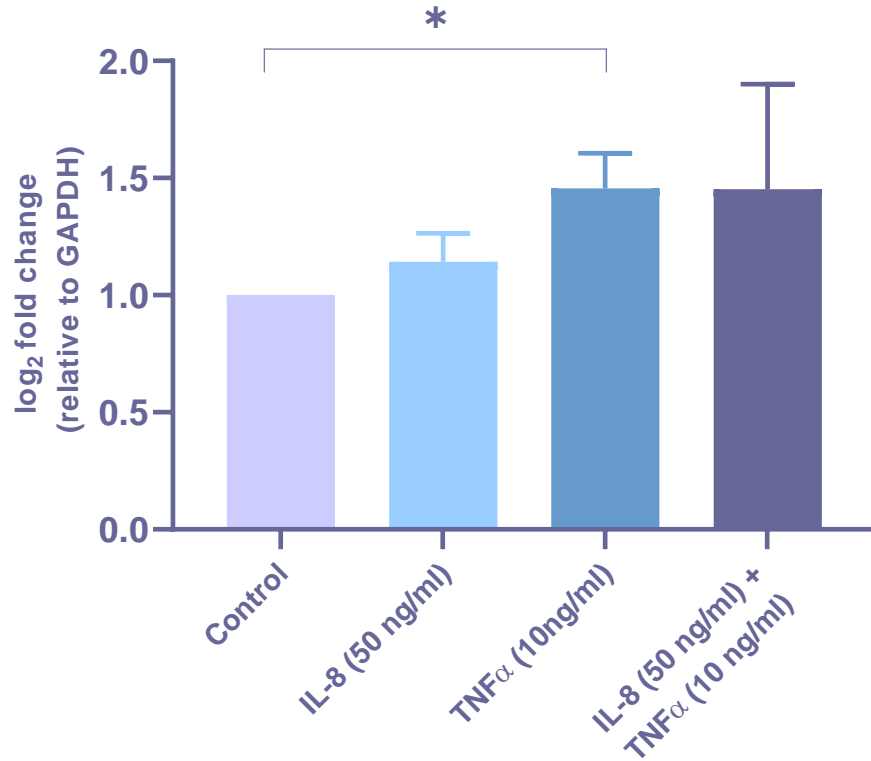


Figure 33. IL-8 and TNF $\alpha$  mediated regulation of HVEM transcription in 8505C. Cells were synchronized by starvation for 24 hrs followed by the indicated treatments for 24 hrs. qRT PCR was performed with total RNA for expression of HVEM. \*p<0.05

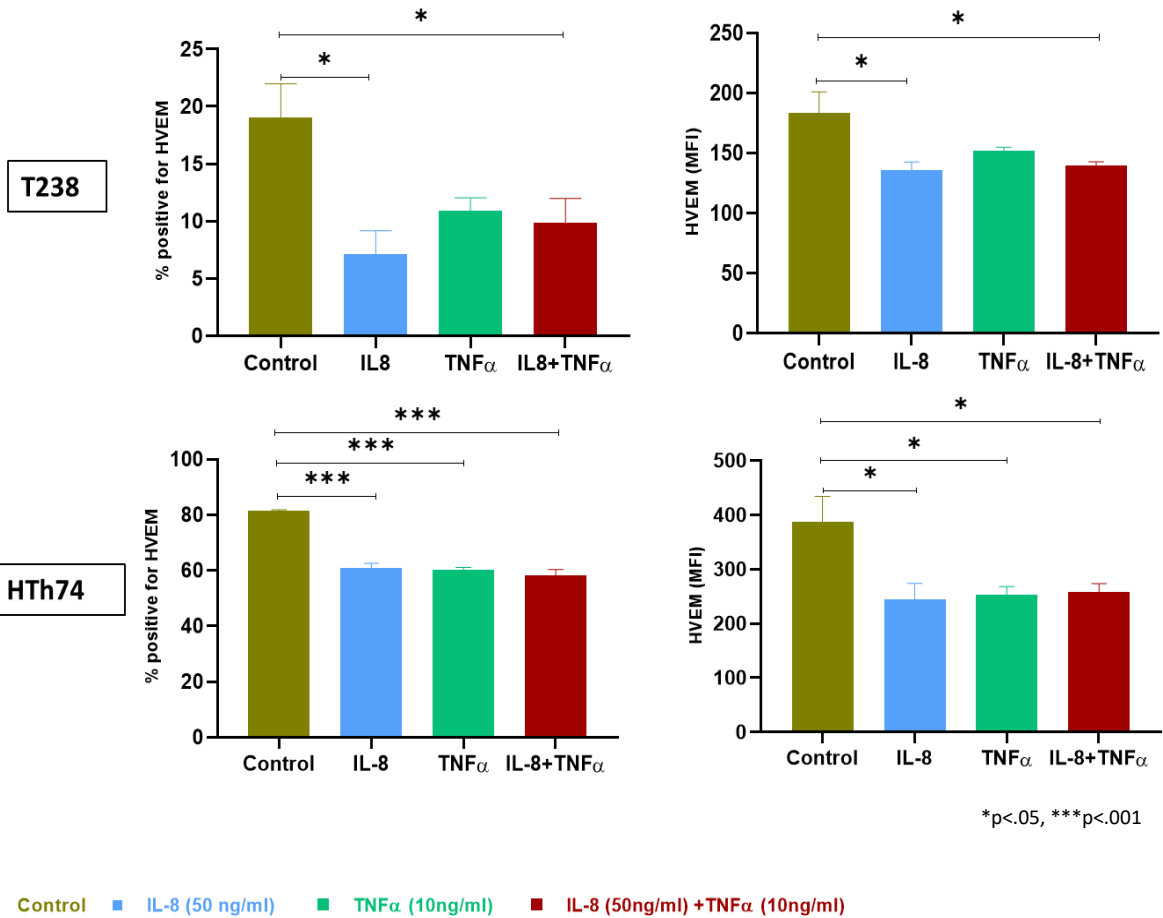
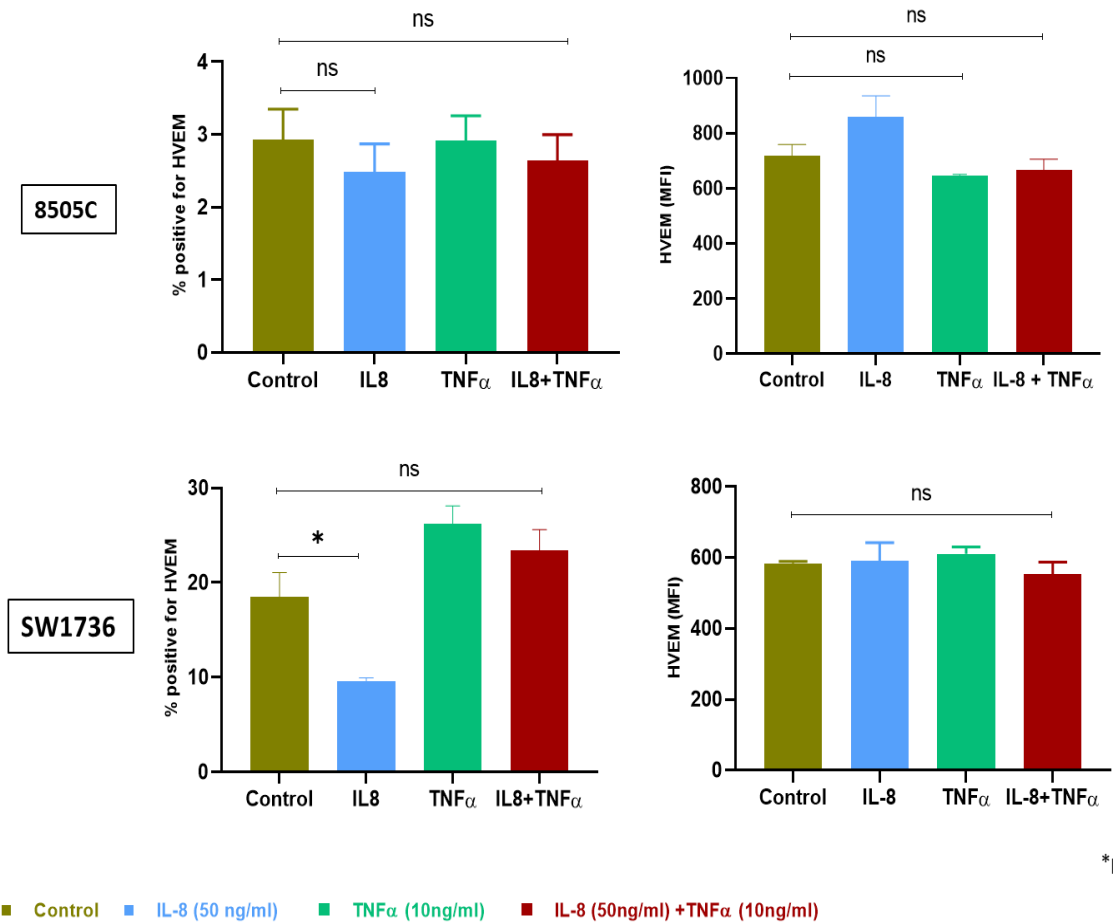
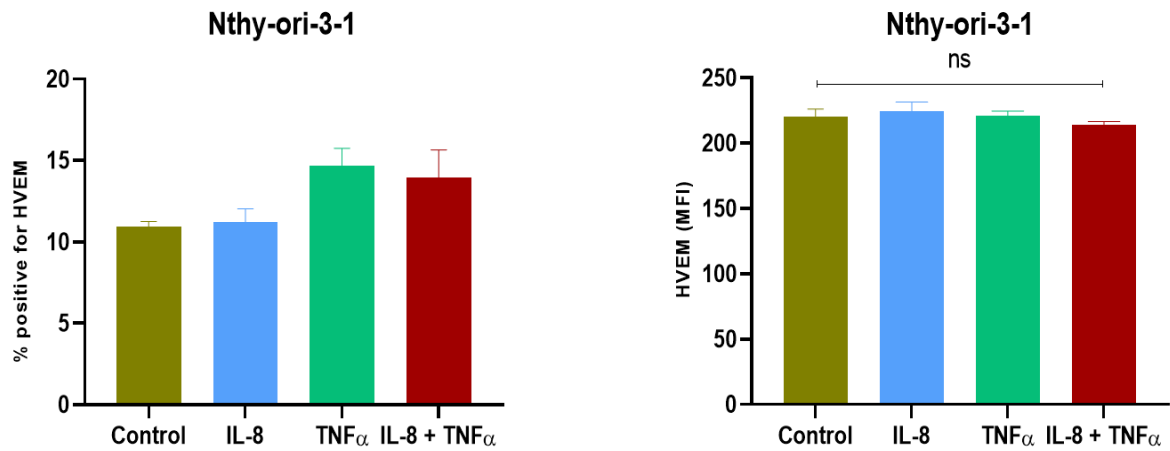


Figure 34. IL-8 and TNF $\alpha$  mediated regulation of surface HVEM in T238 and HTh74. Cells were synchronized by starvation for 24 hrs followed by the indicated treatments for 24 hrs. Flow cytometry was conducted for surface expression of HVEM. Upper panel: T238; lower panel: HTh74. Bars represent mean $\pm$ SEM from n=3 biological replicates. One-way ANOVA with a Tukey's posttest was used to determine statistical significance. \*p<0.05 \*\*\*p<0.001



\*p<.05

Figure 35. IL-8 and TNF $\alpha$  mediated regulation of surface HVEM in 8505C and SW1736. Cells were synchronized by starvation for 24 hrs followed by the indicated treatments for 24 hrs. Flow cytometry was conducted for surface expression of HVEM. Upper panel: 8505C; lower panel: SW1736. Bars represent mean $\pm$ SEM from n=3 biological replicates. One-way ANOVA with a Tukey's posttest was used to determine statistical significance. \*p<0.05 \*p<0.05



**Figure 36. IL-8 and TNF $\alpha$  mediated regulation of surface HVEM in normal thyroid epithelial cell line Nthy-ori-3-1.** Cells were synchronized by starvation for 24 hrs. followed by the indicated treatments for 24 hrs. Flow cytometry was conducted for surface expression of HVEM. Bars represent mean $\pm$ SEM from n=3 biological replicates. One-way ANOVA with a Tukey's posttest was used to determine statistical significance.

- **IL-8 and TNF $\alpha$  treatment enhances soluble HVEM in conditioned media of ATC cell lines**

Our previous findings from qRT PCR confirmed upregulation of HVEM at transcript level in presence of IL-8 and TNF $\alpha$ . Still we observed a reduction in surface expression of HVEM in the presence of these two cytokines. Since HVEM does not have a soluble splice variant, this observation pointed towards the possibility of a post-translational event controlling surface expression of HVEM protein in ATC cell lines. HVEM is a member of TNF receptor superfamily that has conserved cleavage site for Tumor Necrosis Factor-Alpha Converting Enzyme (TACE). This is a member of 'A Disintegrin And Metalloprotease', or ADAM, family. This enzyme is known to be involved in cleaving the ectodomain of TNF $\alpha$  and TNF $\alpha$  receptors – a process often known as shedding. The detailed regulation of this enzyme is not well studied yet but is thought to be regulated by TNF $\alpha$ . Since we observed a reduction in surface expression of HVEM after treatment of IL-8 and TNF $\alpha$ , we wanted to see if we could detect any soluble HVEM in the conditioned media of ATC cell lines from the same treatment groups. We saved the conditioned media from the treatment groups from which we did flow cytometry and conducted sandwich ELISA for detection of soluble HVEM. The capture antibody used for this assay was targeted against the ectodomain of the HVEM protein. One-way ANOVA with Tukey's posttest was conducted for statistical analyses with a p value of 0.05. Surprisingly, we detected soluble HVEM in the conditioned media of ATC cell lines (Fig 37 A-C). There was an increase in concentration of soluble HVEM after IL-8 and TNF $\alpha$  treatment which complimented

the trend of decreasing surface expression upon these cytokine treatments. We detected soluble HVEM in conditioned media from Nthy-ori-3-1 also (Fig 38), but the concentration was lower than the ATC cell lines T238 and 8505C. We evaluated level of ADAM17 by western blot from IL-8 and TNF $\alpha$  treated two ATC cell lines T238 and SW1736. An increase in ADAM17 level was observed after IL-8 and TNF $\alpha$  treatment (Fig 39) in the cell lines.

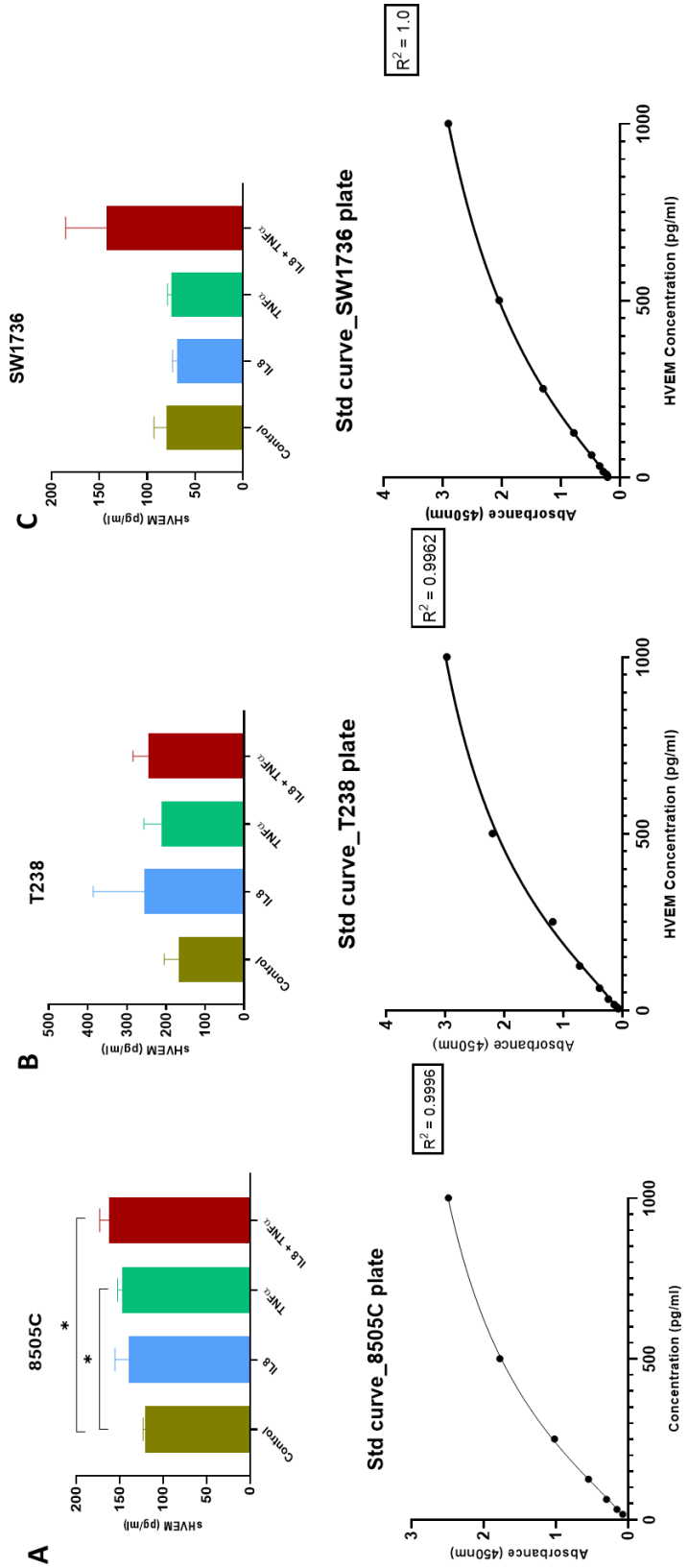
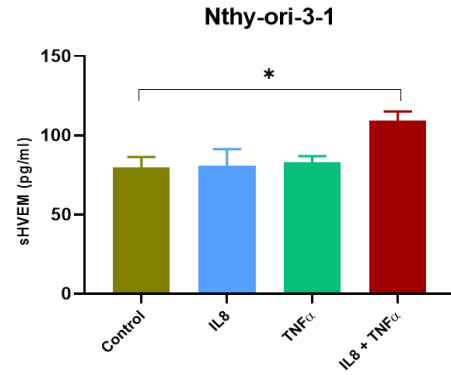
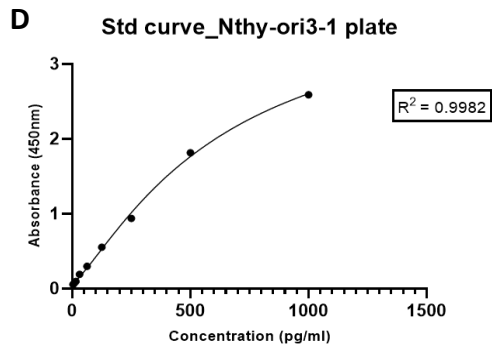


**Figure 37. Soluble HVEM in conditioned media from ATC cell lines.** Cells were synchronized for 24 hrs. by starvation, followed by indicated treatments for 24 hrs. Soluble HVEM was detected in the conditioned media by ELISA. Bars represent mean $\pm$ SEM from n=3 biological replicates. One-way ANOVA with a Tukey's posttest was used to determine statistical significance. \*p<0.05



■ Control 
 ■ IL8 (50ng/ml) 
 ■ TNF alpha(10ng/ml) 
 ■ IL8 (50ng/ml) + TNF alpha (10ng/ml)

Figure 38. Soluble HVEM in conditioned media from Nthy-ori-3-1. Cells were synchronized for 24 hrs. by starvation, followed by indicated treatments for 24 hrs. Soluble HVEM was detected in the conditioned media by ELISA. Bars represent mean $\pm$ SEM from n=3 biological replicates. One-way ANOVA with a Tukey's posttest was used to determine statistical significance. \*p<0.05

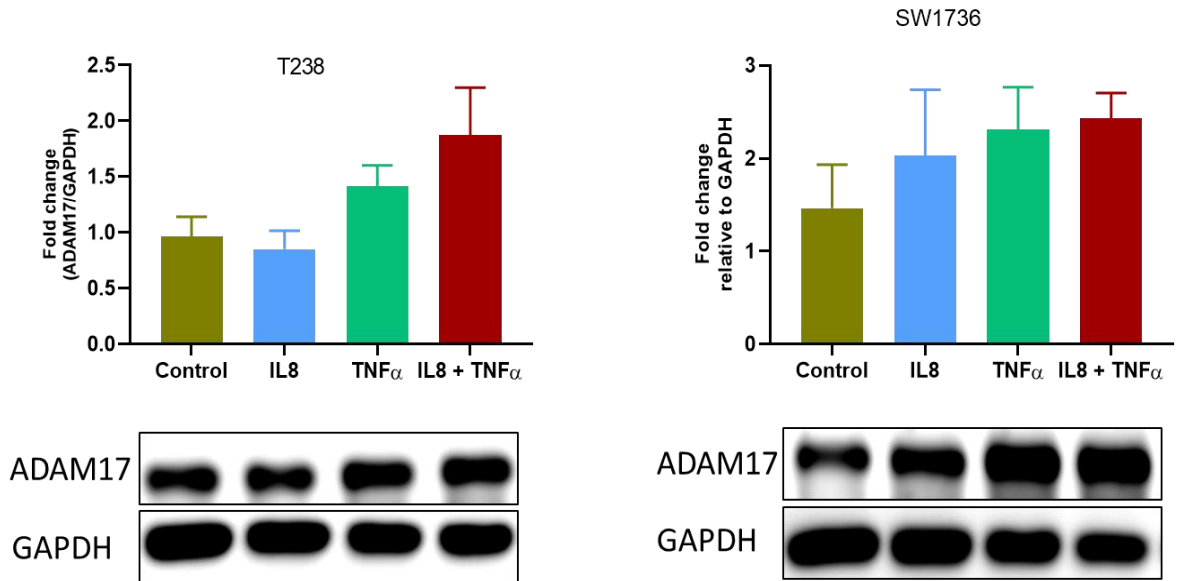


Figure 39. IL-8 and TNF $\alpha$  mediated regulation of ADAM17 in ATC cell lines. Cells were synchronized by starvation for 24 hrs followed by the indicated treatments for 24 hrs. Western blot was conducted from whole cell-lysate for expression of ADAM17. Bars represent mean $\pm$ SEM from n=3 biological replicates. One-way ANOVA with a Tukey's posttest was used to determine statistical significance.

**•IFN $\gamma$  induces HVEM, BTLA and CD160 expression at the transcript level in ATC cell lines**

IFN $\gamma$  is one of the most prominent pro-inflammatory cytokines secreted by immune cells, such as CD8<sup>+</sup> T lymphocytes (CTLs) following antigen stimulation of T cell receptor (TCR), Th1 polarized CD4<sup>+</sup> T helper cells, NKT cells, macrophages and some other types of immune cells that are highly relevant in cancer. Malignant cells take advantage of the homeostatic pathways induced by IFN $\gamma$  and attenuate the anti-tumor immune response. More than 200 genes are induced by IFN $\gamma$ , including but not limited to PD-L1, PD-L2, IDO1 and CTLA-4. These are some of the crucial players involved in cancer cell - immune evasion (Mimura et al., 2017)(Minn & Wherry, 2016). Our previous immunohistochemical studies confirmed infiltration of both CD8<sup>+</sup> and C4<sup>+</sup> T cells in ATC tissues. Previous studies from our laboratory has confirmed a mixed infiltration of M1 and M2 macrophages in ATC. A low level of IFN $\gamma$  is often present in tumor microenvironment because of a pre-existing non-productive immune response against the tumor or forced by therapeutic intervention. This is often associated with development of adaptive resistance in tumor cells (Topalian et al., 2015). Since we have already seen that anaplastic thyroid cancer microenvironment has infiltration of IFN $\gamma$ -secreting immune cells, we hypothesized that IFN $\gamma$  might be inducing the expression of these immune checkpoint molecules in the tumor cells contributing to the development of immune evasive phenotype.

In order to test this hypothesis, we first wanted to examine if the cell lines are IFN $\gamma$  sensitive. Western blot was a better choice, because it could help us confirm activation of downstream mediators of IFN $\gamma$  signaling pathway. ATC cell lines HTh74 and SW1736 were treated with 5, 10 and 20ng/ml of IFN $\gamma$  for 24 hrs. Whole cell lysate was prepared and western blot was done

for the expression of IRF1, and pSTAT1 in the cell lines. We observed induction of pSTAT1 and IRF1 after IFN $\gamma$  treatment in both the cell lines (Fig 40 A-C) confirming that these cell lines were sensitive. Since this was just a confirmation of IFN $\gamma$  sensitivity, this experiment was performed just once. Next, we wanted to assess the effect of IFN $\gamma$  treatment on the expression level of HVEM, BTLA and CD160 in the ATC cell lines. We treated the cell lines with indicated concentrations of IFN $\gamma$  for 24 hrs and isolated RNA after the stipulated period. PD-L1 was also included in the assay as a positive control, since it is already well established as a IFN $\gamma$  inducible gene (Chen et al., 2012; Mojic et al., 2018). The expression level of each gene was compared to the untreated group and log<sub>2</sub> of fold changes were used for plotting the graph. We observed an upregulation in the transcript level of HVEM, BTLA, and PD-L1 in both the cell lines (Fig 41 A-H). Interestingly, we observed more than a 2-fold upregulation in HVEM with both 5 and 10 ng/ml IFN $\gamma$  in SW1736 (Fig 41 A). More than 2-fold increase was observed in case of BTLA in SW1736. CD160 was induced upon treatment with 5ng/ml IFN $\gamma$ , which subsequently declined with 10ng/ml of IFN $\gamma$  treatment. This is congruent with reports on upregulated IRF2 after IFN $\gamma$  signal transduction, which in turn negatively regulates expression of interferon gamma receptor 1 (IFNGR1) in cancer cells leading to loss of sensitivity towards IFN $\gamma$  (Wang et al., 2008). Similar induction pattern was observed in PD-L1. A distinct induction pattern was observed in case of HTh74 (Fig 42). We observed more than 7-fold induction of HVEM at both the concentrations of IFN $\gamma$  in this cell line, whereas only a marginal induction was observed in BTLA. Dramatic increase in PD-L1 was observed in both the cases. However, induction of CD160 was not observed in HTh74. This points towards unique mechanism of regulation of the genes in each cell line. Next, we wanted to assess if

IFN $\gamma$  induces surface expression of HVEM in ATC. For this, we treated HTh74 with 5ng/ml IFN $\gamma$  for 48 hrs. and conducted flow cytometry for surface expression of HVEM. IFN $\gamma$  treatment caused a significant increase in HVEM positive cells and mean fluorescent intensity of HVEM (Fig 43).

**Conclusion:** Our study suggested that inflammatory cytokines TNF $\alpha$  and IL-8 modulate expression of HVEM in anaplastic thyroid cancer cell lines. Also, ATC cell lines secrete this immunomodulatory protein which might be mediated by a metalloprotease ADAM17. We also confirmed that HVEM, BTLA and CD160 have IFN $\gamma$  inducible gene expression in ATC cell lines SW1736 and HTh74. Increase in surface expression of HVEM in HTh74 in response to IFN $\gamma$  stimulation suggests a probable mechanism of development of adaptive resistance in ATC under the pressure of an inflammatory immune microenvironment. Interestingly, ADAM17 is also an IFN $\gamma$  inducible protein, which might suggest a possibility of increased solubilization of HVEM in the presence of all these pro-inflammatory cytokines. Overall, our findings suggest a complex interplay between the immunomodulatory molecules on ATC cells and the pro-inflammatory cytokines IL-8, TNF $\alpha$  and IFN $\gamma$ .

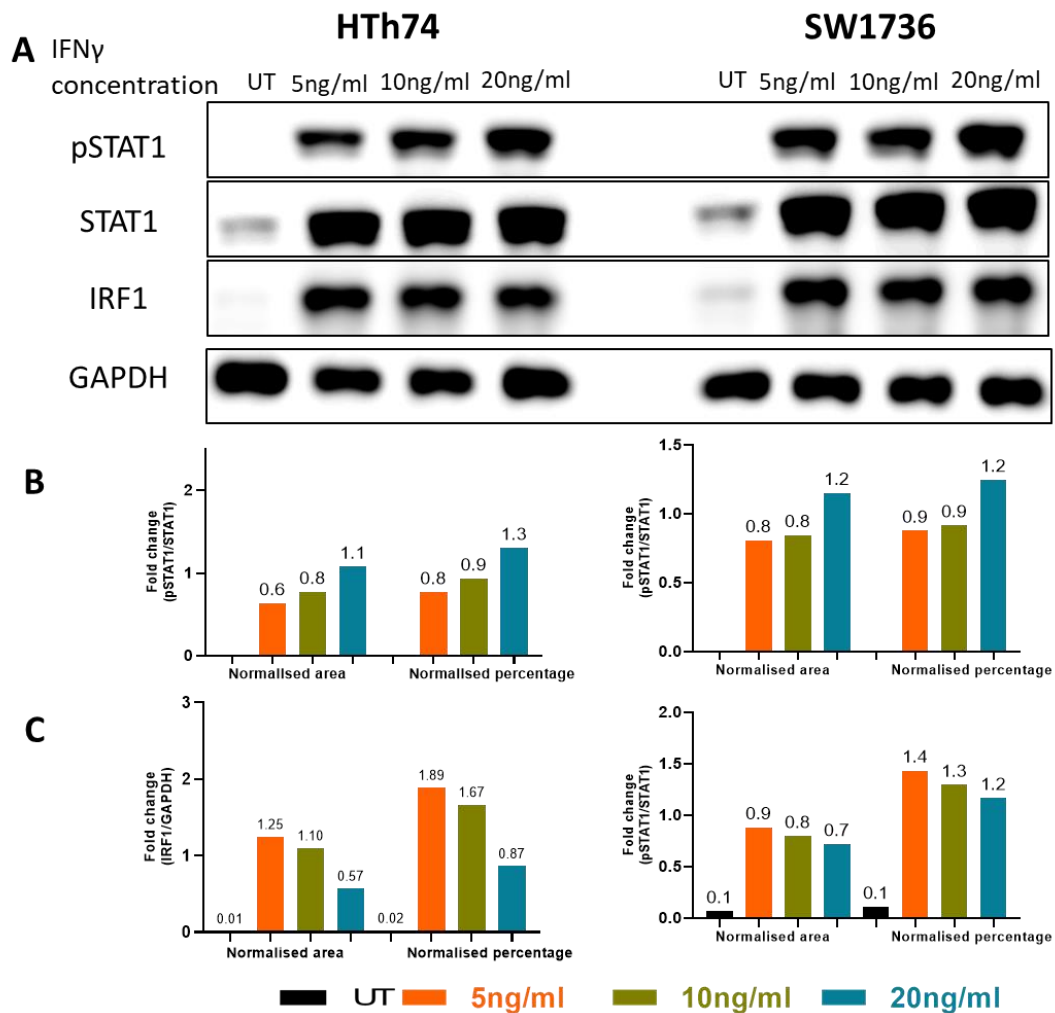


Figure 40. IFN $\gamma$  sensitivity of HTh74 and SW1736. Cells were synchronized by starvation for 24 hrs followed by the indicated treatments for 24 hrs. Western blot was conducted from whole cell-lysate for expression of pSTAT1, STAT1 and IRF1 (A). Relative band intensity of pSTAT1 (B) and IRF1(C).

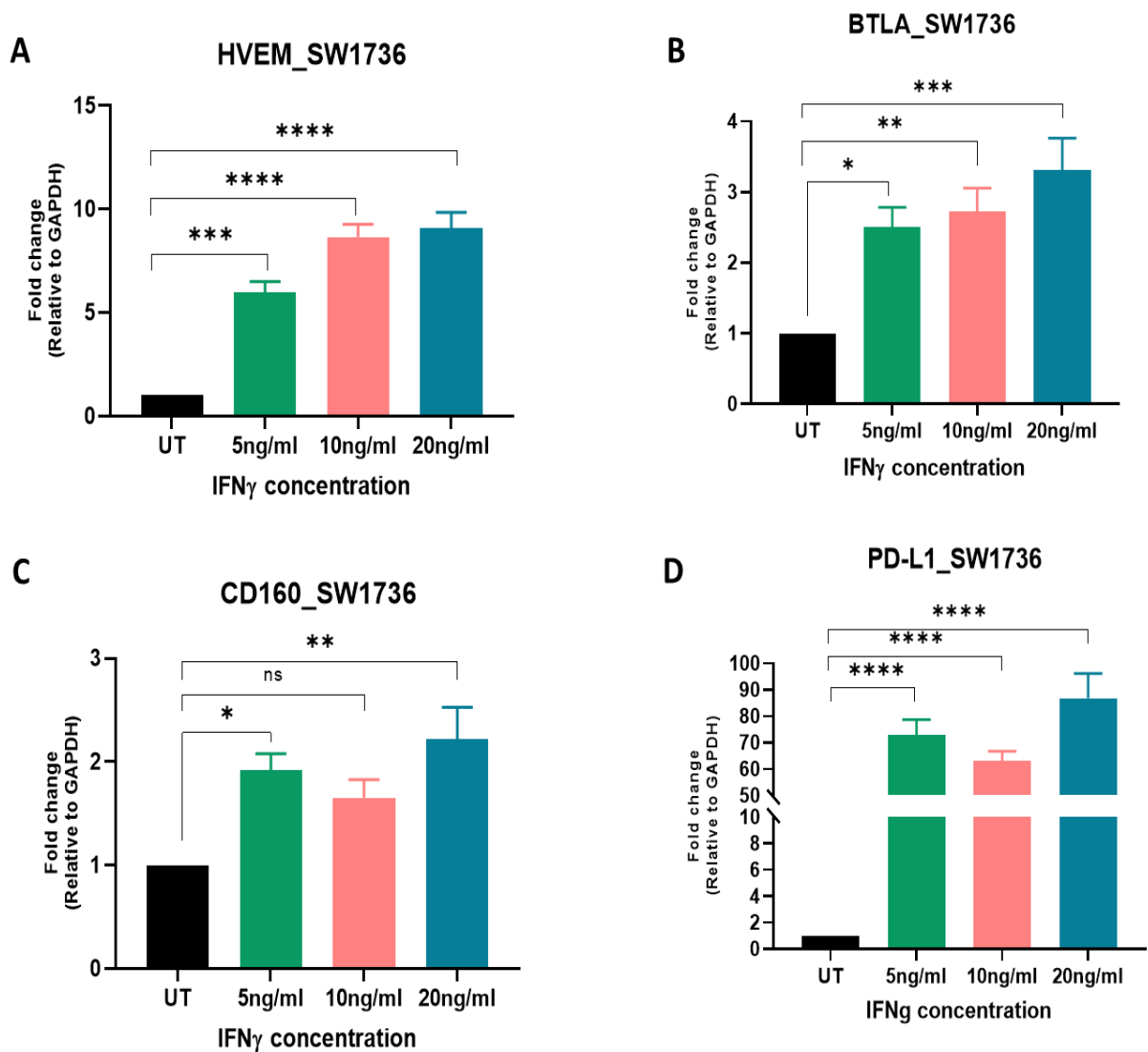


Figure 41. IFN $\gamma$  inducible gene expression of HVEM, BTLA, CD160, and PD-L1 in ATC cell lines. Cells were synchronized by starvation for 24 hrs followed by the indicated treatments for 24 hrs. Total RNA was isolated and qRT PCR was conducted for expression of HVEM (A), BTLA (B), CD160 (C) and PD-L1 (D). Bars represent mean $\pm$ SEM from n=3 biological replicates. One-way ANOVA with a Tukey's posttest was used to determine statistical significance. \*p<.05, \*\*p<.01, \*\*\*p<.001, \*\*\*\*p<.0001

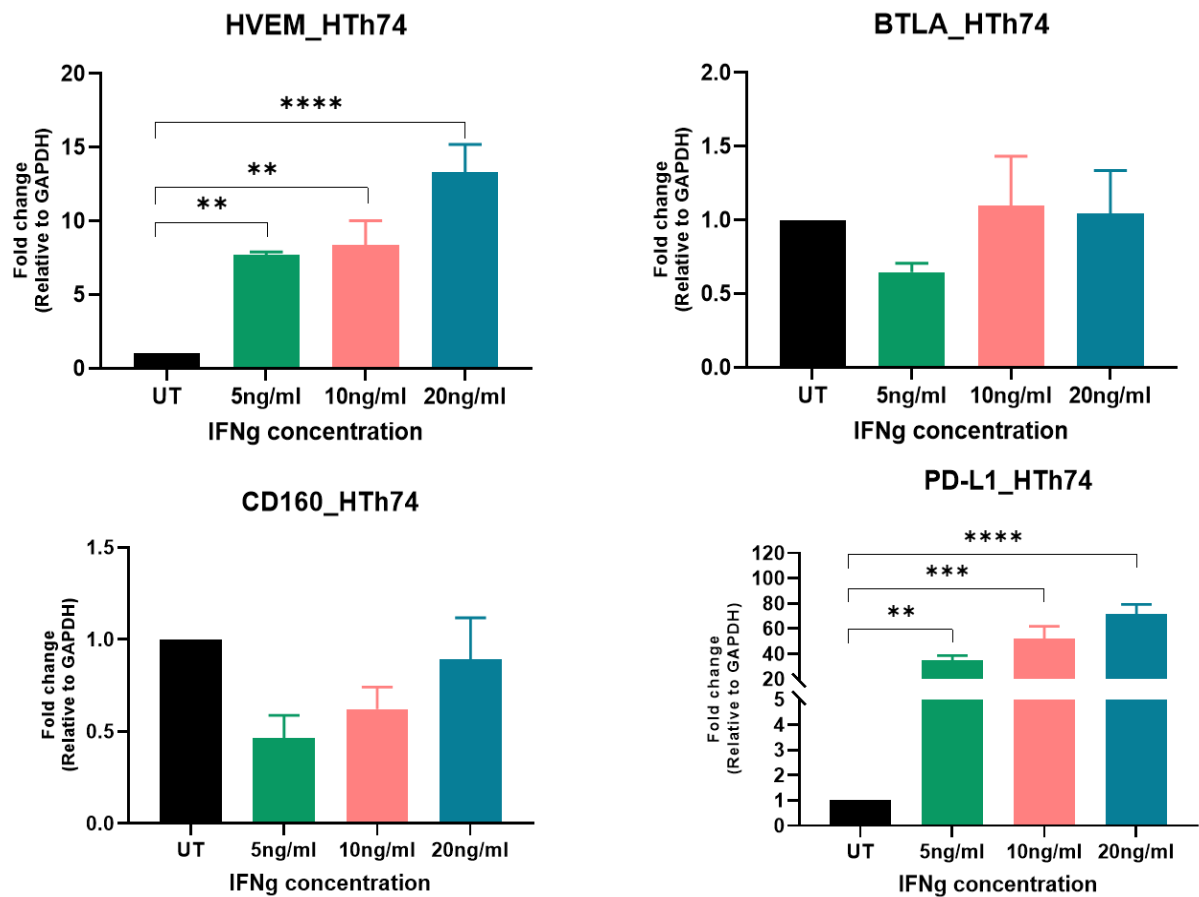


Figure 42. IFN $\gamma$  inducible gene expression of HVEM, BTLA, CD160, and PD-L1 in ATC cell lines. Cells were synchronized by starvation for 24 hrs followed by the indicated treatments for 24 hrs. qRT PCR was conducted from RNA for expression of HVEM (A), BTLA (B), CD160 (C) and PD-L1 (D). Bars represent mean $\pm$ SEM from n=3 biological replicates. One-way ANOVA with a Tukey's posttest was used to determine statistical significance. \*\*p<.01, \*\*\*p<.001, \*\*\*\*p<.0001

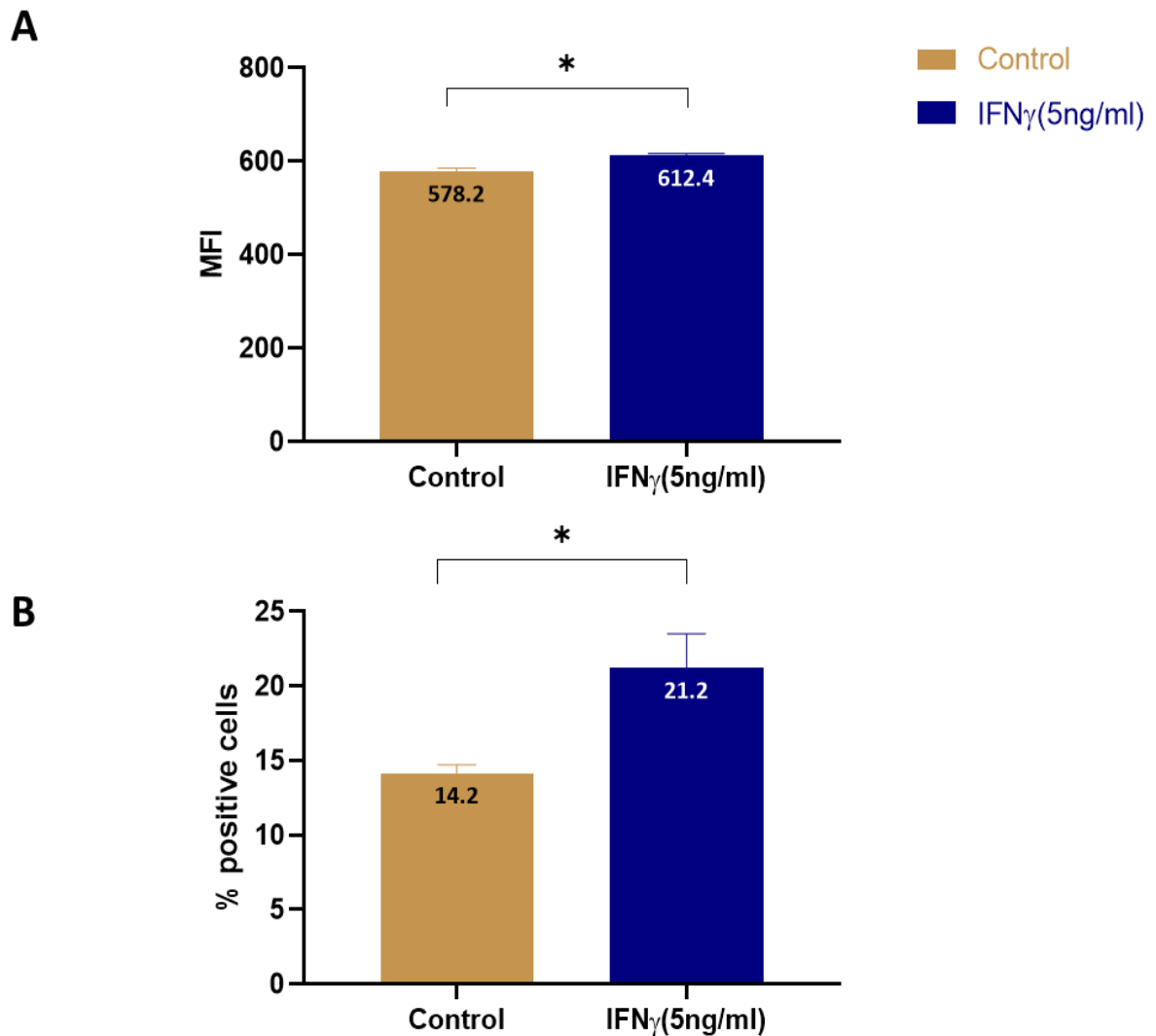


Figure 43. IFN $\gamma$  inducible surface expression of HVEM in ATC cell line HTh74. Cells were synchronized by starvation for 24 hrs. followed by the indicated treatment for 24 hrs. Flow cytometry was conducted for surface expression of HVEM. Bars represent mean $\pm$ SEM from n=3 biological replicates. One-way ANOVA with a Tukey's posttest was used to determine statistical significance. \*p<.05

*2aiv) Examine the implications of HVEM/LIGHT interaction in anaplastic thyroid cancer*

**Rationale:** Our previous experiments confirmed expression of immunomodulatory molecule HVEM in the anaplastic thyroid cancer cell lines. Given the fact that this is a highly inflammatory cancer and there is an abundance of pro-inflammatory cytokines in the TME, we wanted to assess if HVEM plays any tumor intrinsic role in ATC. Upon interaction with its TNFSF ligand LIGHT, HVEM transduces a stimulatory signal in HVEM expressing immune cells leading to proliferation, activation and cytokine secretion via upregulation of NF $\kappa$ B and AP-1 transcription factors (Marsters et al., 1997). NF $\kappa$ B is an extremely crucial transcription factor involved in myriads of pro-tumorigenic processes. Interestingly, members of TNFR superfamily are identified as activators of JNK and p38 MAP kinase signaling pathways which are collectively named stress-activated MAP kinases. Activation of these kinases culminates in enhanced cellular proliferation in tumor cells. We wanted to see if HVEM/LIGHT interaction triggers this signaling in ATC cell lines which might support tumor cell proliferation.

**aiv) HVEM/LIGHT interaction triggers stress activated MAP kinases and increases level of phosphorylated I $\kappa$ B $\alpha$  in ATC cell lines**

ATC cell lines SW1736, T238 and 8505C and normal thyroid epithelial cell line Nthy-ori-3-1 were cultured up to 60% confluence level and they were serum starved for 24hrs. Following starvation, they were treated with 100ng/ml of recombinant human LIGHT (rhLIGHT) for 24 hrs. in a humidified incubator with 5% CO<sub>2</sub>. Whole cell lysate was prepared from the cells and western blot was conducted for expression of pJNK, p-c-Jun, JunD, pI $\kappa$ B $\alpha$ , p-P38 MAPK and ADAM17. Induction of stress related MAPK was observed in all 3 ATC cell lines, but not in Nthy-ori-3-1. Significantly higher pJNK and JunD were observed in the rhLIGHT treated group

in SW1736 (Fig 44 B, E – middle panel). rhLIGHT treated SW1736 had significantly higher level of phosphorylated I $\kappa$ B $\alpha$  compared to untreated group (Fig 44 A – middle panel) which was consistent in both T238 and 8505C (Fig 44 A – first and third panel). This trend was observed in Nthy-ori-3-1 also but was not consistent for all biological replicates and did not reach statistical significance (Fig 44 A, last panel). An increase in the level of JunD was observed in SW1736, but not in T238 and 8505C (Fig 44E). Relative band intensities were calculated, and data were plotted (Fig 45). Phosphorylated I $\kappa$ B $\alpha$  results in its ubiquitination-mediated degradation leading to nuclear translocation of NF $\kappa$ B. Since we observed higher level of phosphorylated I $\kappa$ B $\alpha$  after treatment with rhLIGHT, we wanted to evaluate nuclear translocation of NF $\kappa$ B. We followed the same experimental procedure as before and treated Nthy-ori-3-1 and 8505C with rhLIGHT for 24 hrs. Following the treatment, nuclear and cytoplasmic fractions were isolated, and lysates were prepared. Western blot was conducted with the lysates for evaluation of NF $\kappa$ B expression. Expression was normalized to housekeeping proteins GAPDH and lamin B1. An increase nuclear accumulation of NF $\kappa$ B was observed after treatment with rhLIGHT in ATC cell line 8505C, but not in Nthy-ori-3-1 (Fig 46).

**Conclusion:** Interaction of HVEM with its cognate ligand rhLIGHT triggers differential activation of stress induced MAPKs in anaplastic thyroid cancer cell lines. Also, we observed nuclear translocation of NF $\kappa$ B on treatment with rhLIGHT in ATC cell line 8505C.

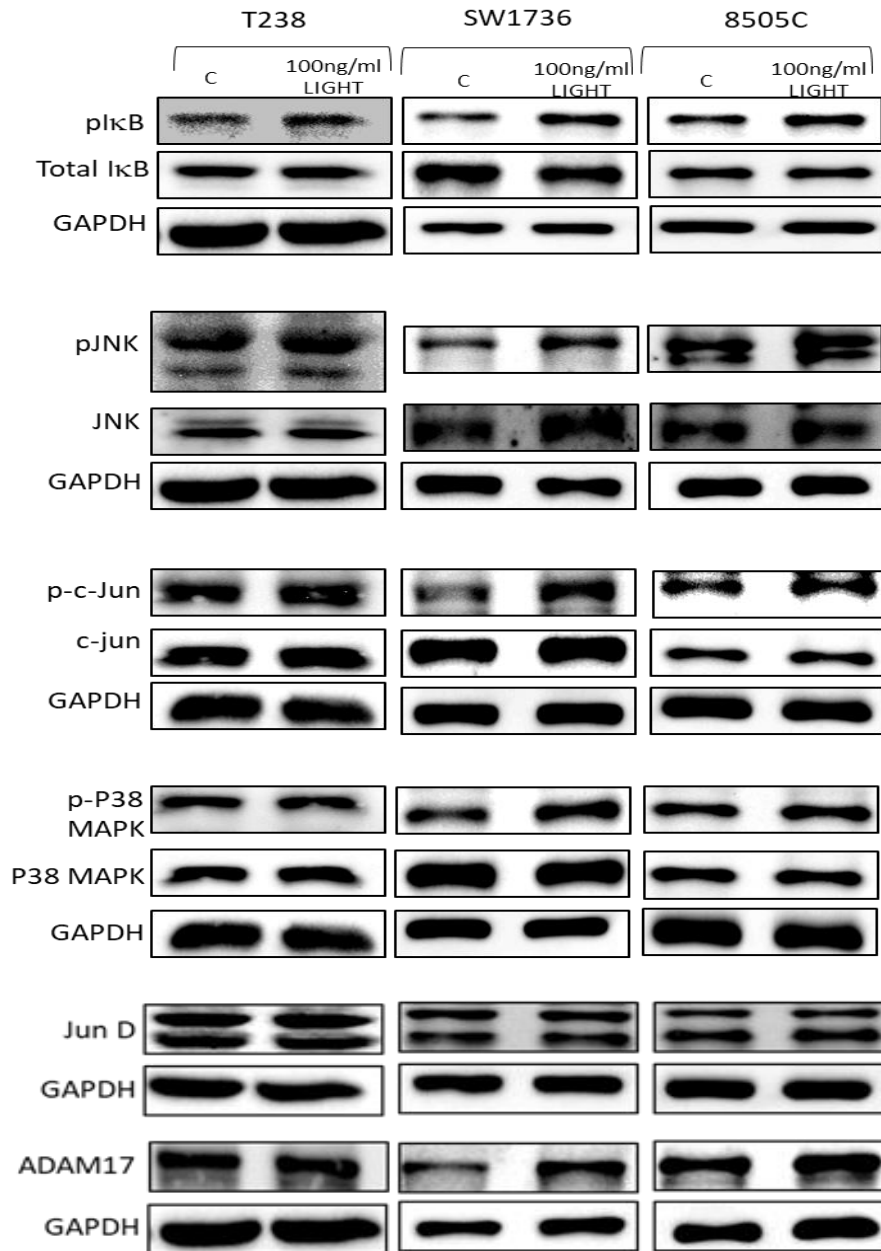


Figure 44. Activation of stress related MAPK on rhLIGHT treatment in ATC cell lines. Cells were synchronized by starvation for 24 hrs followed by the indicated treatment for 24 hrs. Whole cell lysate was prepared and western blot was conducted for expression of IκBα (A), JNK (B), c-Jun (C) and P738 MAPK (D). Representative image from n=3 biological replicates

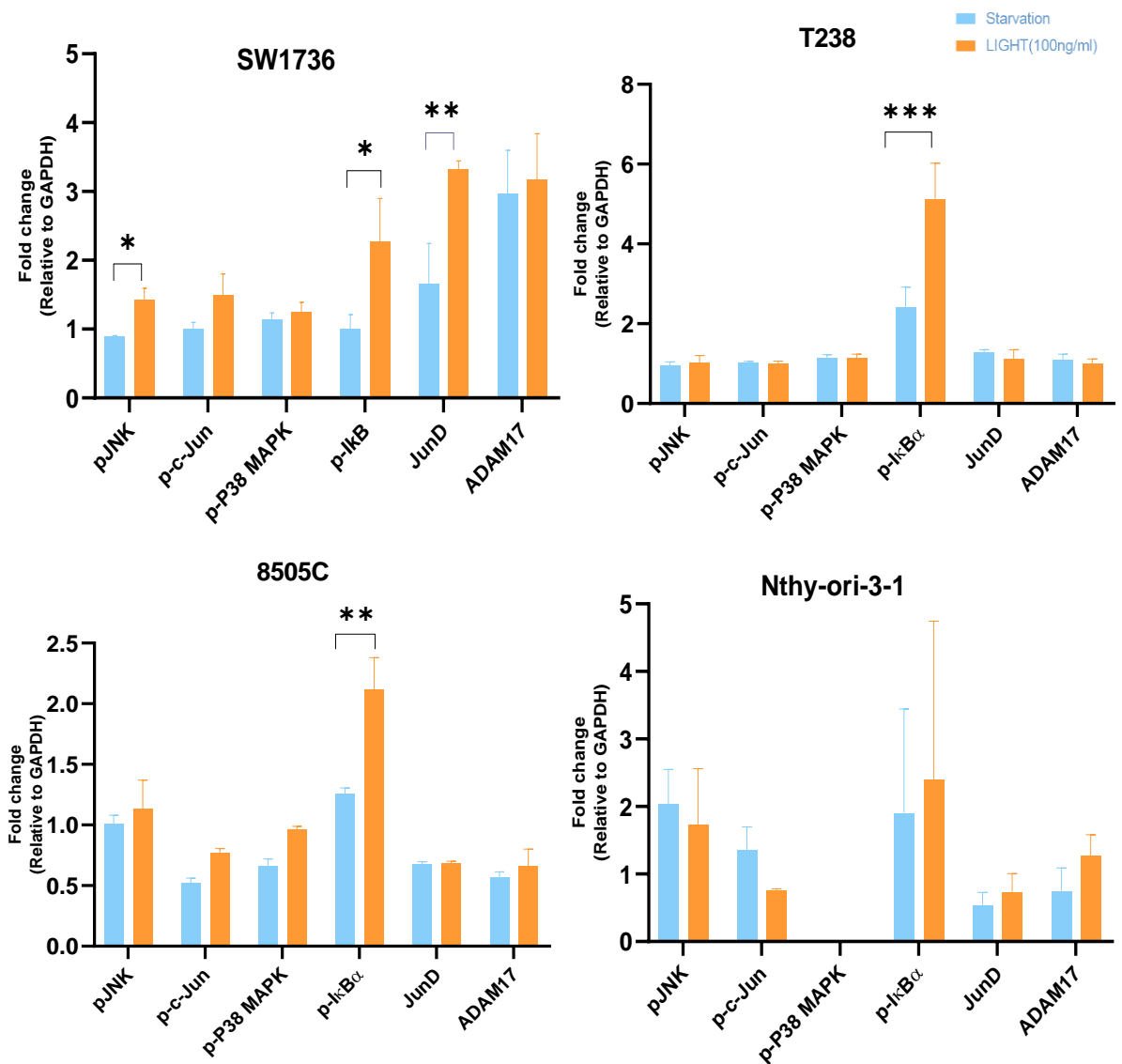


Figure 45. **Relative expression of stress related MAPKs, pI $\kappa$ B and ADAM17 upon LIGHT treatment.** Cells were synchronized by starvation for 24 hrs. followed by the indicated treatment for 24 hrs. Whole cell lysate was prepared and western blot was conducted for expression of the proteins. Bars represent mean $\pm$ SEM from n=3 biological replicates. One-way ANOVA with a Tukey's posttest was used to determine statistical significance. \*p<.05, \*\*p<.01, \*\*\*p<.001

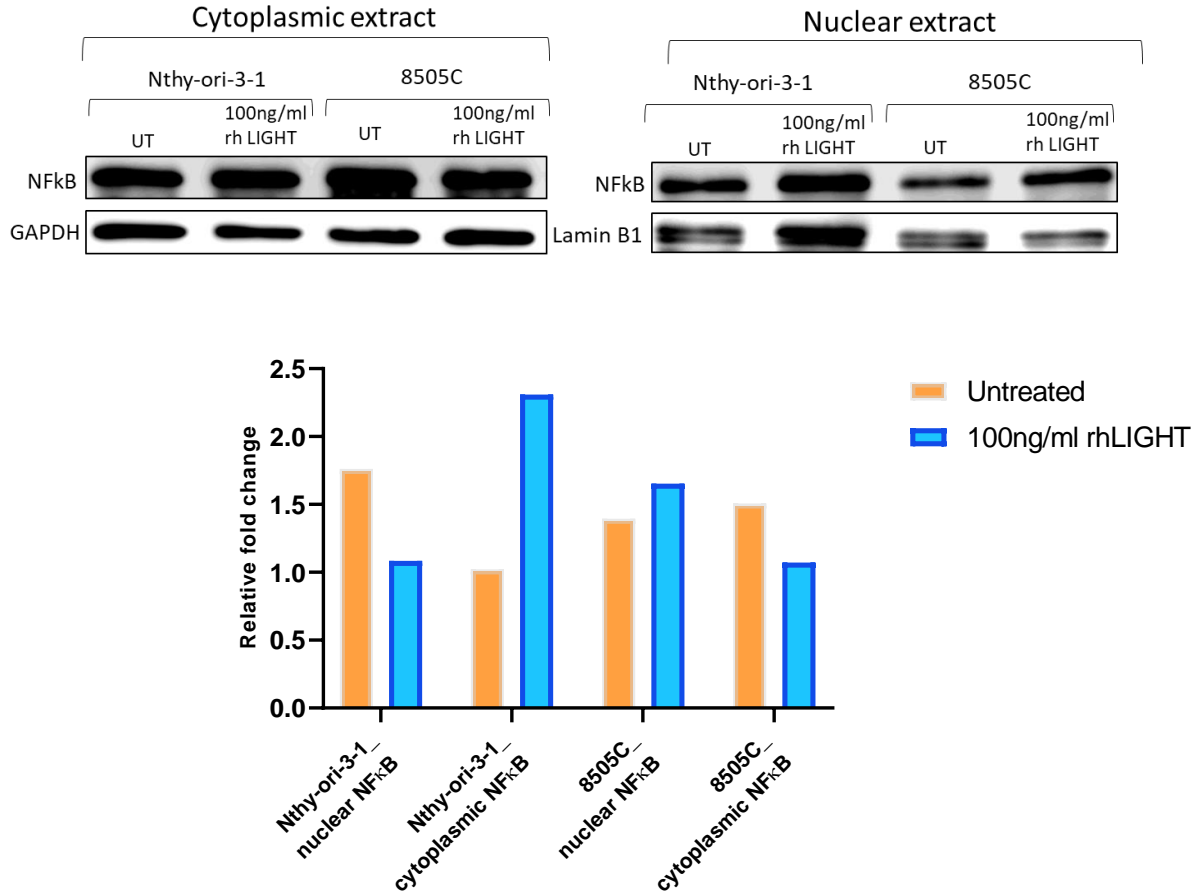


Figure 46. **Nuclear translocation of NFκB on rhLIGHT treatment in 8505C and Nthy-ori-3-1.** Western blots of nuclear and cytoplasmic extracts derived from thyroid cancer cells treated with rhLIGHT for 24 hours. GAPDH served as a loading control for cytoplasmic extracts, whereas, Lamin B1 was used as a loading control for nuclear extracts. The graphical representation of the optical density is below the western blots. (n=2)

Specific aim 2b: Examine possible tumor intrinsic function of HVEM in anaplastic thyroid cancer

**EXPERIMENTAL DESIGN:** Previous findings suggest a possible role of HVEM in supporting pro-tumorigenic signaling pathways in the presence of an inflammatory microenvironment. Next, we wanted to assess if HVEM has any tumor intrinsic function. We generated stable HVEM-knockdown 8505C by CRISPRi. Five 20 nucleotides long single guide RNAs targeting the promoter of HVEM were designed and cloned into CRISPRi plasmid (Gilbert et al., 2014) Any sg RNA targeting more than one site was discarded from the initial list. sgRNA cassettes were generated by PCR, using the forward and reverse primer. The PCR product was purified using a PCR purification kit and the concentration of DNA was measured using nanodrop. The PCR products were digested using Bsmbl and the CRISPRi vector backbone was also digested separately. The products were ligated using T4 DNA ligase using the manufacturer's protocol. One Shot TOP10 chemically competent E. coli cells were transformed with the ligation mix. For generation of lentiviral particles, HEK293 cells were co-transfected with sgRNA-ligated CRISPRi backbone plasmid (Addgene#p71237), the packaging plasmids pVSVg (Addgene#1733) and psPAX2 (Addgene#12259). Lentiviral particles were harvested from the cell culture media and filtered through 0.45 $\mu$ m PES filters. This supernatant was added to 8505C and GFP expressing cells were sorted after 48 hrs. the sorted cells were expanded further and seeded for experiment. HVEM level was checked before and after sorting. 5000 cells were seeded/well of a 24 well dish and they were cultured in complete medium in humidified incubator with 5% CO<sub>2</sub> for two weeks. Number of colonies were counted in each well and compared to non-specific control. For invasion assay, 2.5 X 10<sup>4</sup> cells were seeded in each well of Matrigel coated invasion chamber with a pore size of 0.8 $\mu$ m and cultured in

humidified incubator with 5% CO<sub>2</sub> for 8hrs. and percentage of invaded cells out of total number of migrated cells was calculated.

*2bi) Knockdown HVEM in ATC cell line by CRISPRi*

**Rationale:** With increasing knowledge on the immune checkpoint molecules and their mechanism of actions, it has become more evident that these molecules are expressed on a substantial fraction of tumor cells in different kinds of tumors. It was believed that the primary function of tumor cell-associated immune checkpoint molecules would be the modulation of antitumor immune responses aiding in the process of immune escape. Over past few years however, it has become evident that the expression of immune checkpoint molecules on tumor cells has significant consequences on the tumor- physiology also. Expression of these molecules have been proven to play fundamental role in development of malignant traits (Dong et al., 2018; Marcucci et al., 2017; Meng et al., 2018; Xiong et al., 2019; Zhou et al., 2018). Our previous findings on high tumor cell expression of HVEM, BTLA and CD160 both *in vitro* and in clinical samples suggested the possibility of tumor intrinsic role of this protein. We wanted to conduct some preliminary investigation to see if ablation of HVEM affects the tumorigenic potential of ATC cell line 8505C in any way.

**bi) CRISPRi successfully knocked down HVEM in ATC cell line 8505C**

Among the five guides that were designed initially, we followed up guide RNA 3 for our experiments. Similar results were obtained with guide RNA 2. Total RNA was isolated from the cells and qRT PCR was performed for expression of HVEM. Since, this was a qualitative assessment, experiment was not performed in biological triplicate. We observed a 100-fold reduction in level of HVEM transcript in HVEM knockdown cells (HVEM<sup>KD</sup> 8505C) compared

to the scrambled control (NS.1) (Fig 47). No change in cellular morphology was observed in the knockdown cells. There was no indication of cellular stress also. Both the transgenic cell lines had higher proliferation index compared to wild type 8505C, which can be explained by the fact that, during expansion of our transgenic cells, the highly proliferative cells with higher translational potential were selected for.

**Conclusion:** HVEM was successfully stably silenced in 8505C by CRISPRi technique.

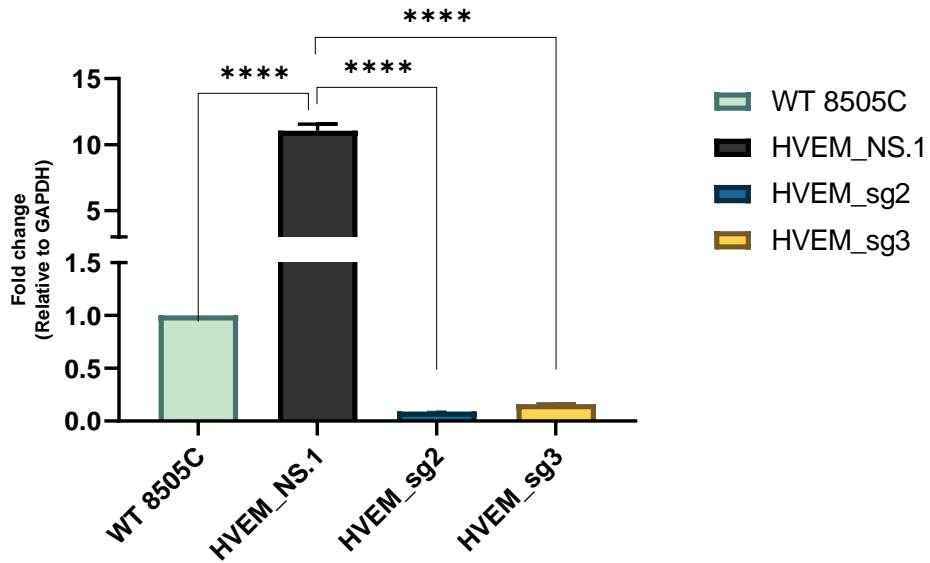


Figure 47. **CRISPRi mediated stable knockdown of HVEM in 8505C.** RNA was isolated from WT 8505C, 8505C transduced with scrambled control (NS.1) and HVEM<sup>KD</sup> 8505C transduced with HVEM promoter specific guides sg2 and sg3. qRT PCR was done for the expression of HVEM. Data was normalized to WT 8505C. Bars represent mean±SEM from n=3 biological replicates. One-way ANOVA with a Tukey's posttest was used to determine statistical significance. \*\*\*\*p<.0001

*2bii) Assess the tumorigenicity profile by colony formation assay and invasion assay*

**Rationale:** Anaplastic thyroid cancer has an extremely aggressive phenotype which is associated with increased rate of proliferation and metastatic potential. Our previous studies pointed to the fact that HVEM is capable of transducing proliferative signals in the ATC cell lines upon interacting with its cognate ligand LIGHT via upregulation of stress induced MAPKs, such as JNK, c-Jun, P38 MAPK and Jun D. HVEM/LIGHT interaction also seemed to trigger nuclear translocation of NF $\kappa$ B in 8505C which is germane to any metastatic or proliferative process. A reciprocal relationship has been reported between immune checkpoint proteins and development of malignant traits, such as EMT (Taube et al., 2010). We wanted to conduct some preliminary experiments to test potential tumor-intrinsic function of HVEM in ATC cells.

*2bii.i) HVEM knocked down 8505C (HVEM<sup>KD</sup> 8505C) has reduced colony forming capacity*

5000 cells were seeded in each well of a 24 well dish and cultured for 14 days in complete media. Number of colonies with at least more than 50 cells were counted in each well. The assay was conducted with three biological replicates. HVEM<sup>KD</sup> 8505C had reduced colony forming capacity. Surprisingly, though HVEM<sup>KD</sup> 8505C had a 6% increase in their proliferation potential, the number of colonies were significantly lower and of smaller size compared to wild type 8505C or 8505C with scrambled control. Number of colonies were counted/well for analysis (Fig 48).

*2bii.ii) HVEM<sup>KD</sup> 8505C has reduced invasive potential*

In order to assess the invasion potential of the HVEM<sup>KD</sup> 8505C, we conducted Matrigel invasion assay. This assay provides an excellent *in vitro* system to study cellular invasion. Invasion chambers coated with Matrigel matrix provide the cells with the settings that allow assessment of their invasive capacity *in vitro*. Matrigel matrix serves as a reconstituted

basement membrane *in vitro*, occluding the pores of the membrane and blocking non-invasive cells from migrating through the membrane. In contrast, invasive cells like malignant cells secrete proteases that enzymatically degrade the Matrigel matrix and enable invasion through the membrane pores. Invasion chambers with a pore size of 0.8 $\mu$ m was used for this assay. Cells were cultured to 70 to 80% confluence before to sub-culturing into the Matrigel coated trans well. The chambers were coated with Matrigel and  $2.5 \times 10^4$  cells were seeded/well. Cells were cultured for 8 hrs. Following the culture, cells were fixed and stained with 1% Toluidine Blue in 1% borax and counted. Four fields were counted per well in all the replicates. Quantification was done using Image J software. A 20% reduction in the number of invaded cells was observed in the HVEM<sup>KD</sup> 8505C compared to the control (Fig 49).

**Conclusion:** Taken together, our preliminary studies suggest that HVEM might be involved in certain pro-tumorigenic processes such as, cellular proliferation and maintenance of invasive phenotype in ATC cell line 8505C.

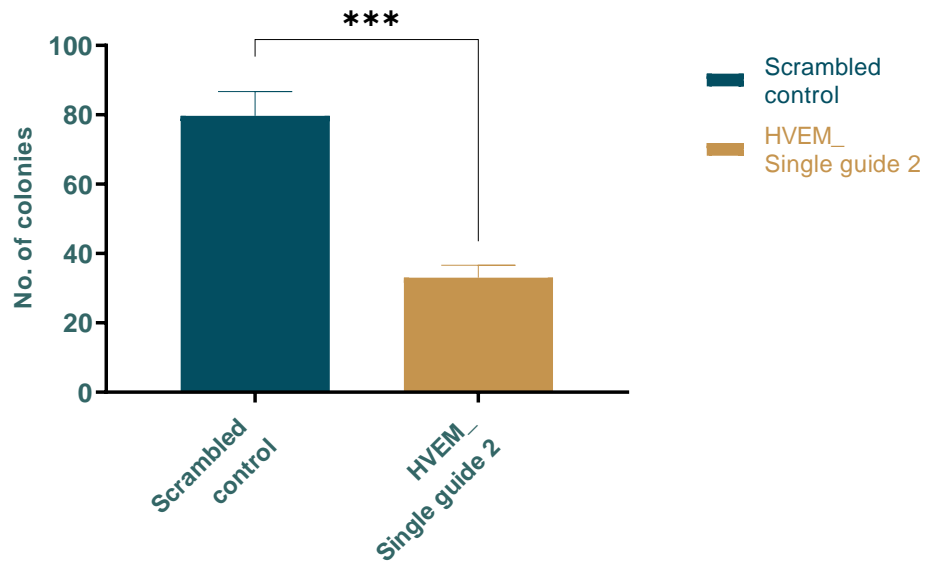


Figure 48. Colony formation assay in HVEM<sup>KD</sup> 8505C. 5000 Cells were seeded in each well of a 24 well dish and cultured for 14 days in complete media. Number of colonies were counted in each well. Bars represent mean ± SEM from n=3 biological replicates. One-way ANOVA with a Tukey's posttest was used to determine statistical significance. \*\*\*p<0.001

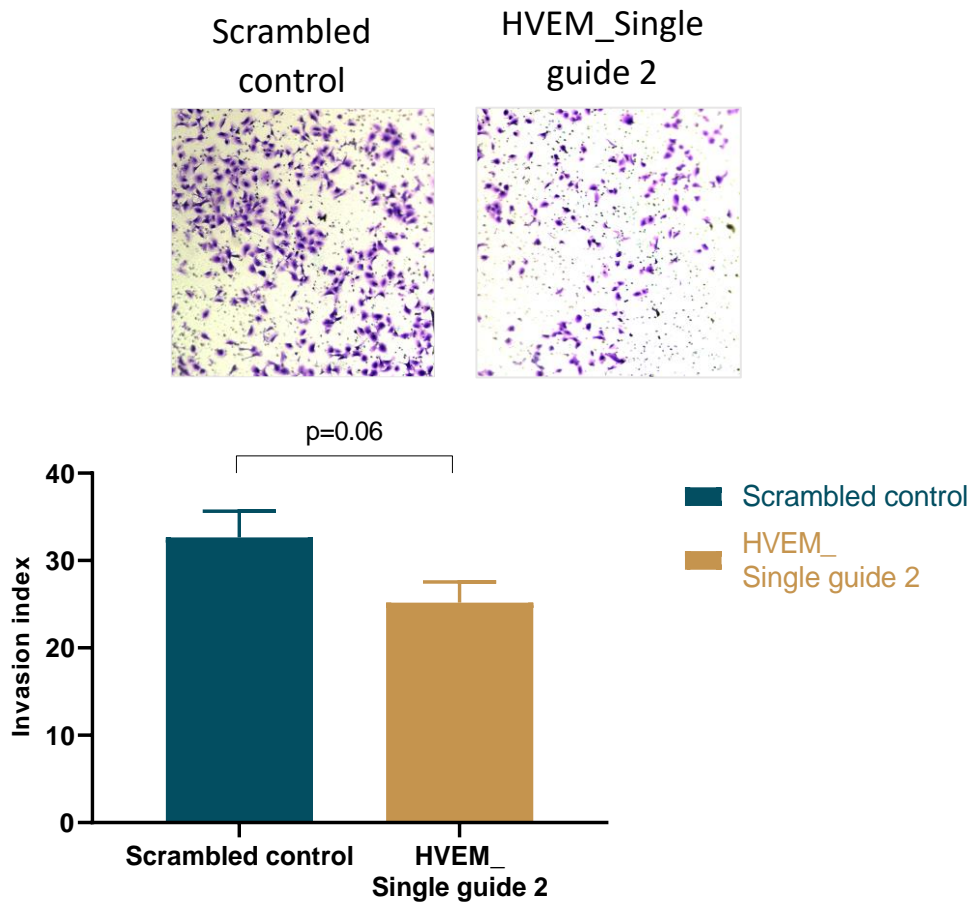


Figure 49. Matrigel invasion assay with HVEM<sup>KD</sup> 8505C. 2.5 X 10<sup>4</sup> cells were seeded/well of Matrigel coated trans-well inserts in serum starved media and complete growth media with 10% FBS was used as a chemoattractant in the bottom wells. Cells were cultured for 8 hrs. followed by fixation and staining as described above. Quantitative data is expressed relative to invasion ability of 8505C transfected with scrambled control. bars represent mean +/-SEM from N=3 biological replicates. Student's t test was used to determine statistical significance.

### *Summary*

- Anaplastic thyroid cancer and aggressive variants of papillary thyroid cancers have significantly higher amount of tumor infiltrating T lymphocytes, among which more than 80% are CD8<sup>+</sup> T cells
- The immune microenvironment in ATC and aggressive PTC has a mix of immunosuppressive and pro-inflammatory microenvironment with abundant expression of IL10, IDO1 and IL17.
- Pro-inflammatory cytokines TNF $\alpha$ , IL-8 and IFN $\gamma$  modulates expression of immunomodulatory molecule HVEM and is associated with its solubilization
- The interaction between HVEM and its cognate ligand LIGHT induces stress activated MAPK mediators in ATC cell lines
- HVEM/LIGHT interaction leads to an increase in the level of pI $\kappa$ B $\alpha$  and nuclear translocation of NF $\kappa$ B in ATC cell line 8505C
- CRISPRi efficiently silenced HVEM in a stable manner in 8505C without inducing any cellular stress or change in cellular morphology
- HVEM might have some potential role in cellular proliferation in ATC which is evidenced by reduced colony forming ability of HVEM<sup>KD</sup> 8505C
- Reduced invasive potential in HVEM<sup>KD</sup> 8505C suggested that HVEM might play some role in maintenance of invasive characteristics in ATC

## *Conclusion*

**Tumor immune contexture in ATC confirms a T cell inflamed microenvironment with a combination pro and anti-inflammatory cytokine milieu and HVEM expression in ATC is closely interlinked with pro-inflammatory cytokines IL-8, TNF $\alpha$  and IFN $\gamma$ . HVEM fundamentally supports tumorigenesis and its interaction with the cognate ligand LIGHT triggers activation of tumor associated MAPK signaling in ATC.**

Specific aim 3: Examine the feasibility of a combinatorial therapeutic approach with MEK inhibitor and antagonistic antibodies in ATC

**EXPERIMENTAL DESIGN:** Like most of the malignancies, ATC is also accompanied with multiple genetic lesions among which BRAFV600E the third most common after TERT and P53. Presence of this genetic lesion makes ATC patients suitable candidates for BRAFV600E directed targeted therapy with small molecule inhibitors. We wanted to evaluate the effect of the BRAFV600E directed kinase inhibitor – Vemurafenib or PLX4032 on expression of immunomodulatory molecules in ATC cell lines. In order to do this, we treated the thyroid cancer cell lines with 10 $\mu$ M PLX4032 and looked for the expression of 25 immunomodulatory molecules by qRT PCR. Next, we assessed the expression of the molecules of interest at protein level, by western blot and immunocytochemistry. Unfortunately, acquired resistance to this drug is inevitable and often reported. In order to emulate the resistance scenario, we generated PLX4032 resistant ATC cell lines T238r and SW1736r over 8 months by a process of dose escalation. Expression of the immunomodulatory molecules of interest were evaluated by qRT PCR in both PLX4032 – sensitive and resistant cell lines. Surface expression of HVEM was assessed by flow cytometry. Activation of compensatory signaling molecules responsible for MAPK pathway reactivation was evaluated by western blot. Next, we combined MEK inhibitor Trametinib in the treatment module and evaluated surface expression of the immunomodulatory molecules in ATC cell lines under a combinatorial therapeutic scenario. Since the immunomodulatory molecules of our interest are T cell activation induced, we conducted a tumor cell – PBMC co-culture study to evaluate the immune activation of T cells by ATC.

*3a. Evaluation of the effect of vemurafenib on the expression of immunomodulatory molecules in thyroid cancer cell lines*

**Rationale:** Vemurafenib is a widely used anti-cancer drug that targets constitutively active BRAFV600E. Unfortunately, reports of acquired resistance are extremely common. Interestingly, most of the studies on resistance mechanism against PLX4032 focus on reactivation of MAPK pathways during development of resistance, but there is a paucity of studies characterizing immunological implications of this treatment and their contribution to development of therapeutic resistance from the perspective of tumor cells. BRAFV600E inhibition-induced upregulation of PDL1 in tumors of patients with metastatic melanoma have been reported (Frederick et al., 2013). Owing to the extremely refractory nature of ATC, we wanted to evaluate possible immunological implications of this drug on a panel of thyroid the cancer cell lines in the context of expression of immunomodulatory molecules. ATC cell line 8505C, T238, SW1736 and PTC cell line BCPAP and K1 were positive for BRAFV600E and the rest had wild type BRAF. TPC-1 had RET/PTC translocation which is often implicated in hyperactive MAPK signaling.

*a.1 Vemurafenib treatment modulates expression of multiple immunomodulatory molecules including HVEM, BTLA and CD160 in thyroid cancer cell lines at transcript level*

In order to evaluate the possible immunomodulatory effect of PLX4032 on the thyroid cancer cells, we treated our thyroid cancer cell line panels with 10 $\mu$ M PLX4032 following 24hrs. serum starvation. Representative image of cell cycle synchronization is depicted in figure 50 (A-B). Tumor cells are inherently heterogeneous in nature and cells are usually at different phases of cell cycle. We knew complete synchronization is not possible in cancer cells by serum starvation as they can still carry on division without external growth stimuli. Since we wanted to discern the specific effect of vemurafenib treatment, we did not want to introduce

any additional toxicity by hydroxyurea or nocodazole treatment before treatment with vemurafenib. Serum starvation protocol followed in the experiments were standardized in our lab previously. RNA was isolated from the cells after PLX4032 treatment and qRT PCR was conducted for expression of CD27, CD30, OX40, TIM1, 4-1BB and DR3 among the co-stimulatory molecules and CTLA4, PD-1, PD-L1, LAG3, 2B4, CD160, BTLA, LAIR1, VISTA and TIM3 among the co-inhibitory or immune checkpoint molecules. Interestingly, while most of the molecules were downregulated after PLX4032 treatment, CD160, BTLA, TIM3, 2B4 and VISTA were upregulated in 8505C after PLX4032 treatment (Fig 51A). CD160 and BTLA both are ligands of HVEM and can transduce an inhibitory signal in the T cells upon interaction. BTLA is increasingly being appreciated in the field of immuno-oncology as a potential target for development of new immunotherapeutic drugs. Anti-BTLA antibodies are in clinical trial for metastatic unresectable solid tumors (NCT04137900). Interestingly, TIM3 and VISTA were also upregulated in PTC cell line TPC-1(Fig 51B) and FTC cell line CGTH-W-1(Fig 52A). Upregulation of BTLA was observed only in 8505C and CGTH-W-1. Except for DR3, all the immunomodulatory molecules were downregulated in PTC cell line BCPAP (Fig 52B). TIM3 is an immunoglobulin superfamily receptor which has four ligands, including galectin-9 (Gal-9), carcinoembryonic antigen cell adhesion molecule 1 (CEACAM-1), high-mobility group protein B1 (HMGB1), and phosphatidylserine (PS). Tim-3 expression on CD8<sup>+</sup> TILs is often linked with PD-1 expression. Tim-3<sup>+</sup> PD-1<sup>+</sup> CD8<sup>+</sup> T cells represent a “deeply” exhausted T cell population as compared to just PD-1<sup>+</sup> positive CD8<sup>+</sup> T cells. High levels of Tim-3 expression on CD8<sup>+</sup> T cells have been associated with a poor prognosis for tumor progression. Also, TIM3/Galectin 9 interaction triggers exhaustion in TIM3 expressing T cells. TIM3 and galectin 9 have been

reported to have a cis interaction and active autocrine loop in human myeloid leukemia stem Cells which drives leukemic progression (Kikushige, 2016). We wanted to confirm this observation in other ATC cell lines also, and for that, we conducted the same treatment in T238, SW1736 and HTh74. We also treated another PTC cell line K1. 8505C, T238, SW1736 and K1 had BRAFV600E mutation. We included HTh74 to discern any differential effect PLX4032 might have between BRAFV600E positive and negative ATC cell lines. For this assessment, we looked at five genes including the ones that displayed upregulation in our previous experiment – CD160, BTLA, TIM3, HVEM and LGALS9B. We observed the same trend of upregulated BTLA, CD160, TIM3 in T238, SW1736, K1 and HTh74 (Fig 53A-D). Interestingly, HVEM and galectin 9 were also upregulated in T238, SW1736 and K1 (Fig 53A-C), but not in HTh4 (Fig 53D).

*a.2 Vemurafenib does not have any impact on the expression of HVEM or BTLA proteins in ATC*

10,000 cells were seeded/well an eight-chamber slide and cultured overnight in complete growth media. They were starved for 24 hrs. in serum free media and treated with either vehicle or 10 $\mu$ M PLX4032 for 24 hrs. Cells were fixed with 4% paraformaldehyde and permeabilized with Triton X. Immunofluorescence was conducted for the expression of HVEM and BTLA proteins. We did not observe any change in level of HVEM, BTLA and TIM3 in ATC cell lines (Fig 54-57). Whole cell lysate was prepared from the same treatment groups and western blot was conducted for the expression of HVEM, BTLA, TIM3 and LGALS9B (Fig 58).

**Conclusion:** BRAFV600E inhibitor vemurafenib or PLX4032 induces upregulation of immunomodulatory molecules in thyroid cancer cell lines at transcript level. Transient treatment with vemurafenib does not change the expression of these proteins in the cells. This points towards induction of an immunosuppressive molecular signature in ATC during treatment with PLX4032. This type of immunosuppressive environment usually correlates with worse clinical outcomes. This phenomenon supports the rationale for monitoring immune profile of the patients alongside clinical course and clinical responses to treatments and tailor the therapeutic regimen based on the patient-specific molecular and immune signature.

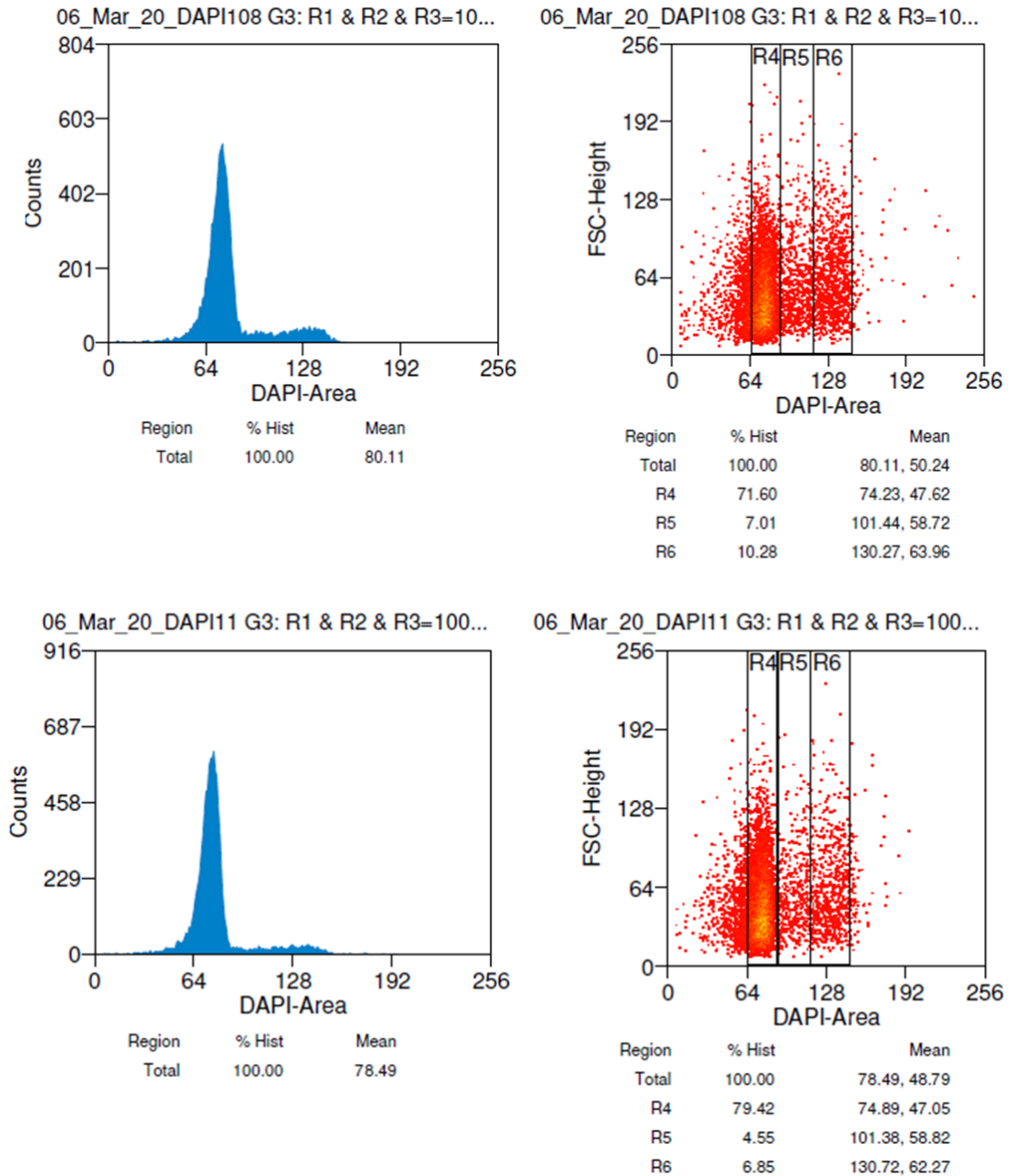


Figure 50. Representative image of cell cycle synchronization in SW1736 **after 24hrs. of serum starvation**. Cells were cultured in complete growth media up to 60-70% confluence and cultured for another 24 hours in clear RPMI with 2% charcoal stripped FBS. Cells were fixed with ice cold 70% alcohol for at least 2 hours and stained with DAPI for DNA content analyses.

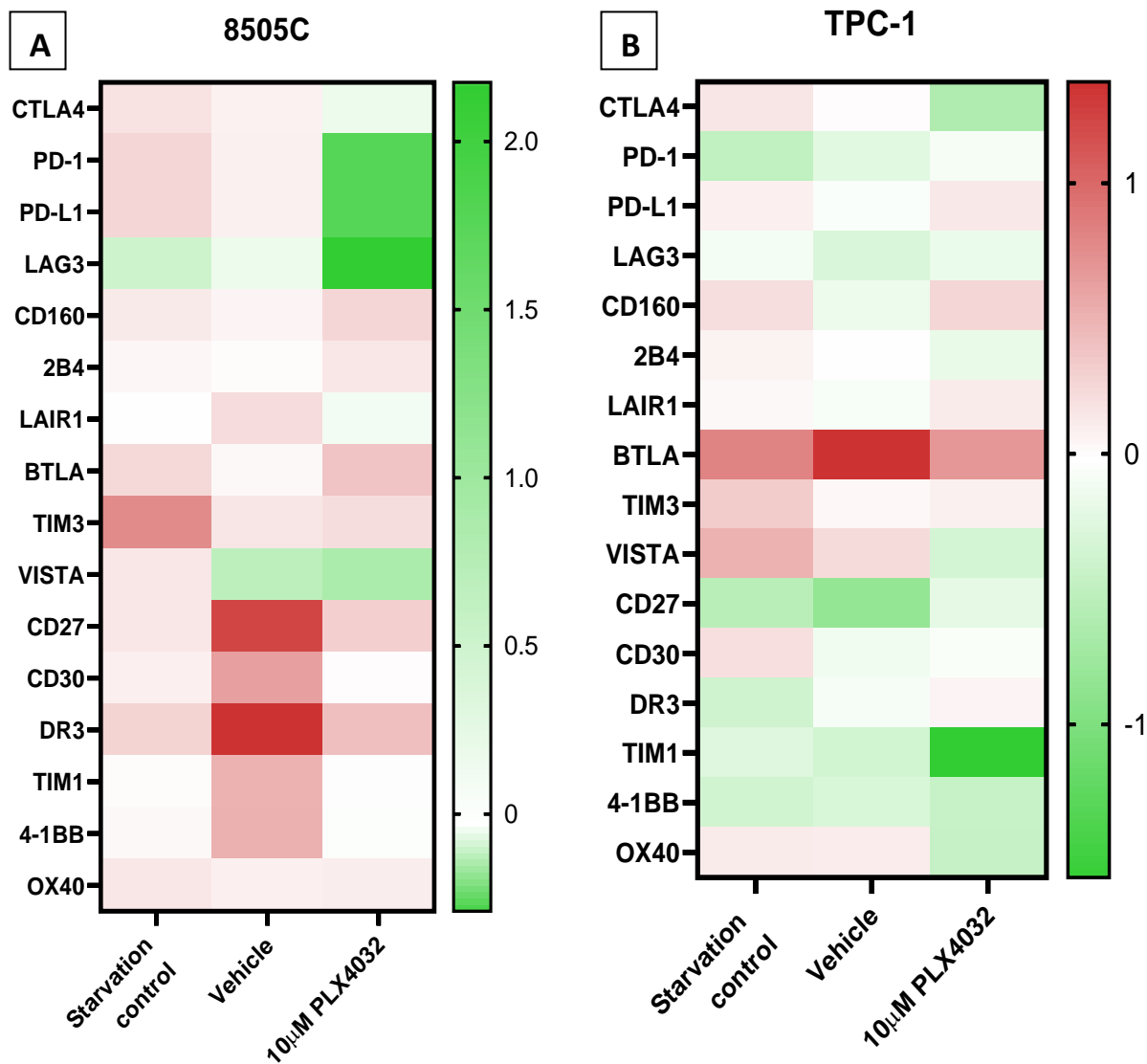


Figure 51. Effect of PLX4032 on expression of immunomodulatory molecules in ATC. Cells were grown up to 60-70% confluence and serum starved for 24 hrs. Following starvation, cells were treated with 10µM PLX4032 for 24 hrs. Same concentration of DMSO was used as vehicle control. Total RNA was isolated, and levels of the indicated immunomodulatory molecules were determined by qRT PCR in 8505C (A) and TPC-1 (B). Mean ± SEM from n=3 biological replicates. One-way ANOVA with a Tukey's posttest was used to determine statistical significance.

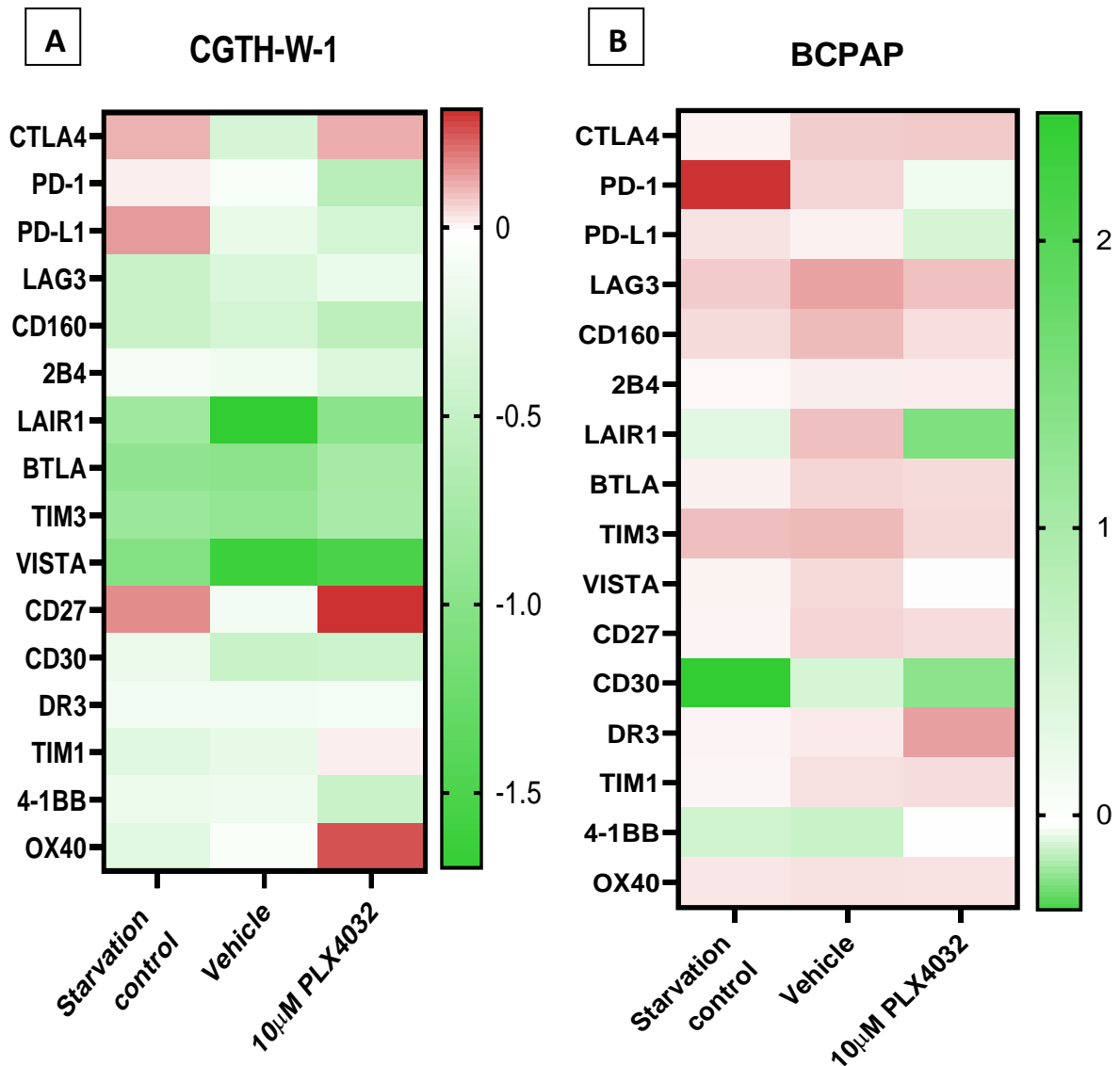


Figure 52. Effect of PLX4032 on expression of immunomodulatory molecules in FTC and PTC. Cells were grown up to 60-70% confluence and serum starved for 24 hrs. Following starvation, cells were treated with 10µM PLX4032 for 24 hrs. Same concentration of DMSO was used as vehicle control. Total RNA was isolated, and levels of the indicated immunomodulatory molecules were determined by qRT PCR in CGTH-W-1 (C) and BCPAP (D). Mean ± SEM from n=3 biological replicates. One-way ANOVA with a Tukey's posttest was used to determine statistical significance.

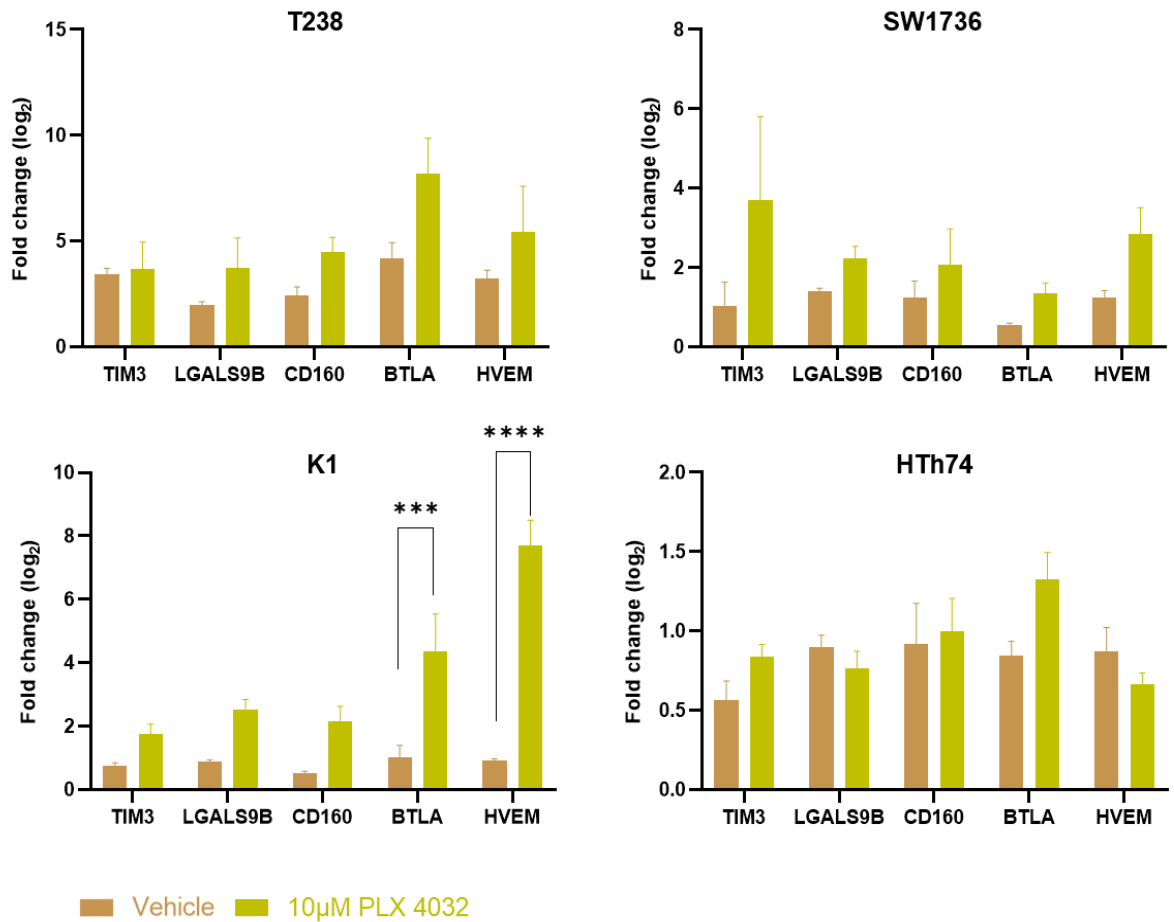
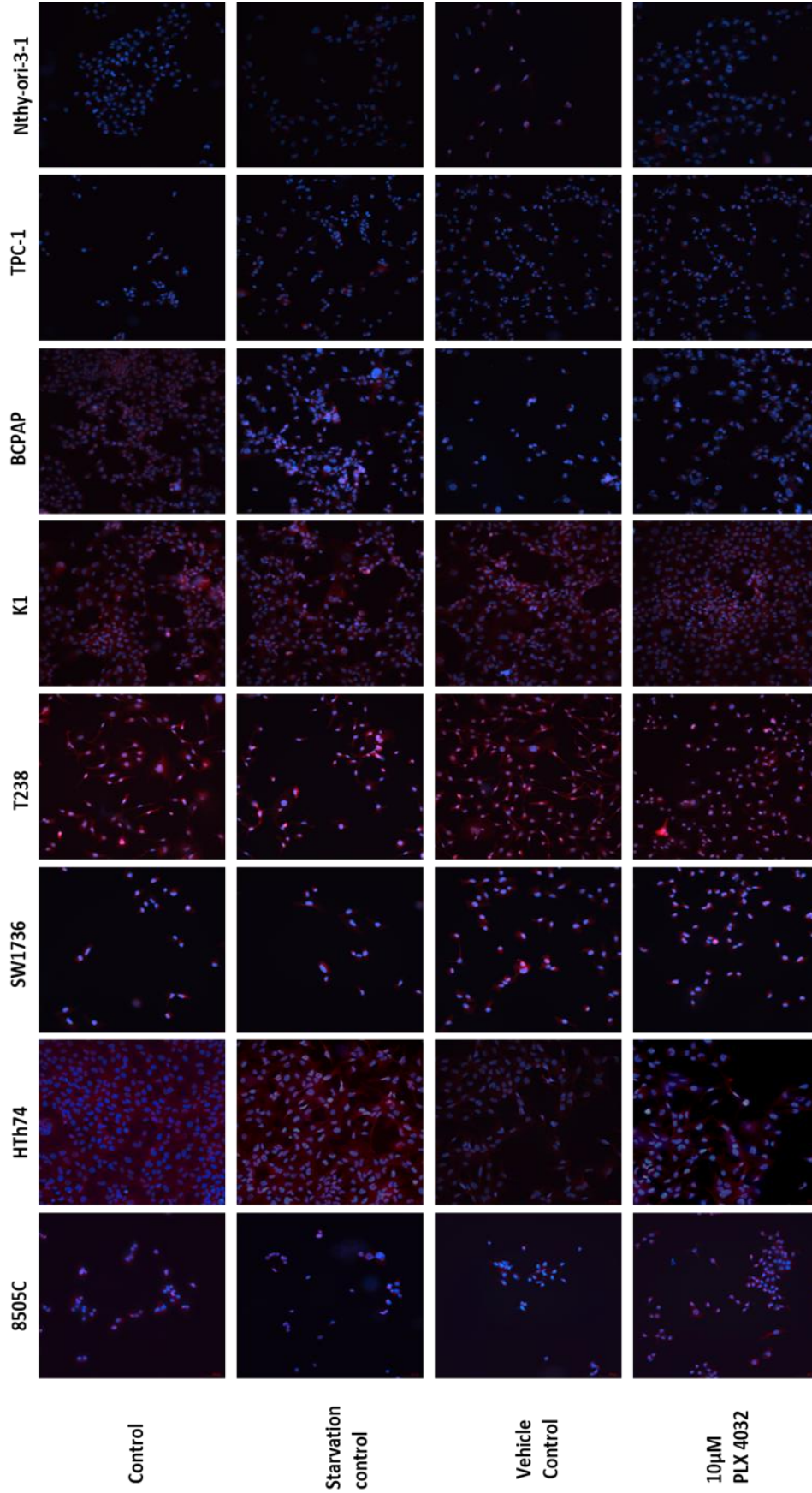


Figure 53. **PLX4032-mediated modulation of HVEM, BTLA, CD160, TIM3 and LGALS9B in thyroid cancer cell lines.** Cells were grown up to 60-70% confluence and serum starved for 24 hrs. Following starvation, cells were treated with 10µM PLX4032 for 24 hrs. Same concentration of DMSO was used as vehicle control. Total RNA was isolated, and levels of the indicated immunomodulatory molecules were determined by qRT PCR in T238 (A), SW1736 (B), K1 (C) and HTh74 (D). Bars represent mean ± SEM from n=3 biological replicates. One-way ANOVA with a Tukey's posttest was used to determine statistical significance. \*\*\*p<.001 \*\*\*\*p<.0001

**A**



**Figure 54. Expression of HVEM in thyroid cancer cell lines after PLX4032 treatment.** 10,000 cells were seeded/well of an eight-chambered slide and cultured overnight. Cells were serum starved for 24 hrs. and treated with PLX4032 for another 24 hrs. Immunofluorescence was carried out to detect target protein. Red: Target protein; blue: DAPI

**B**

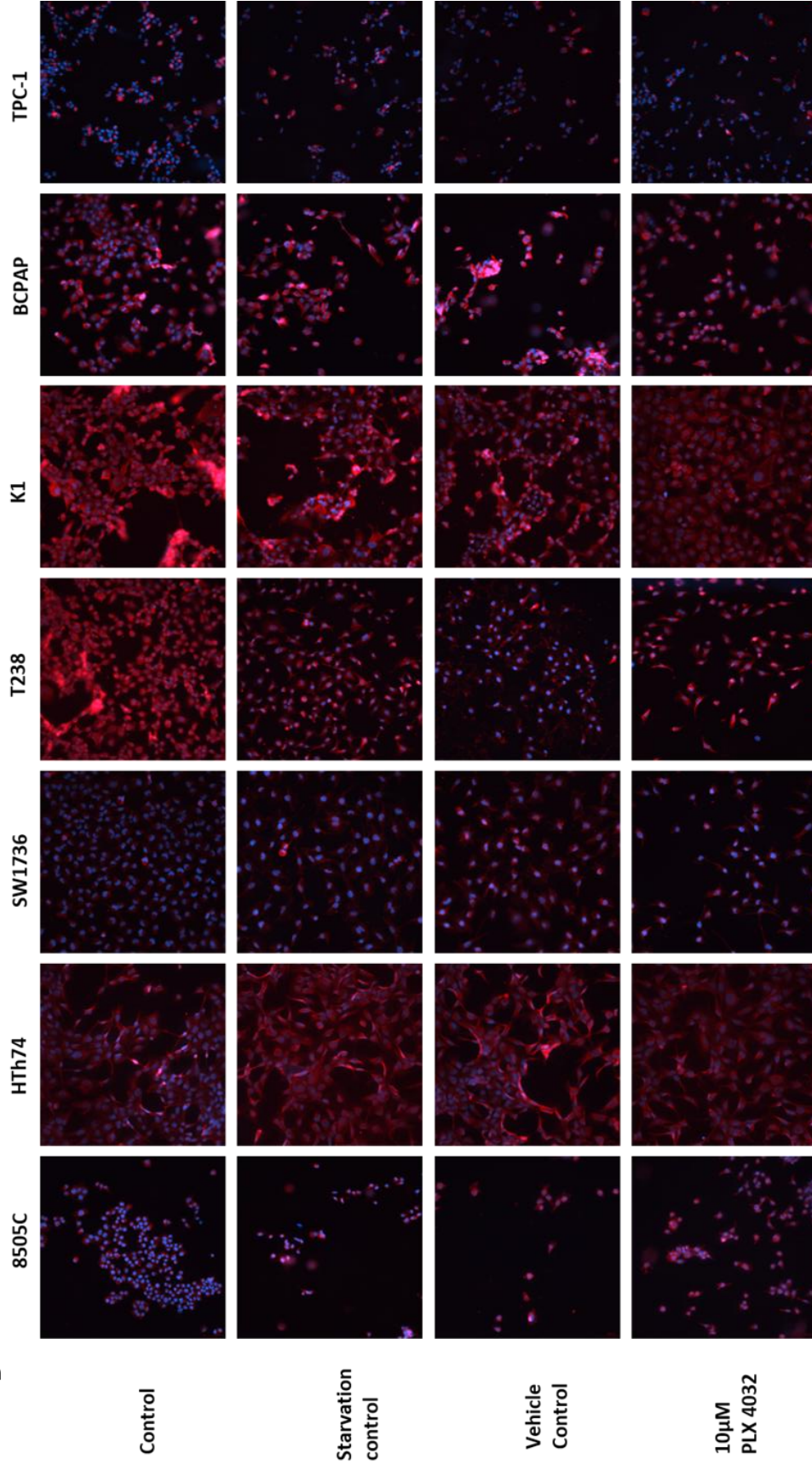


**Figure 55. Expression of BTLA in thyroid cancer cell lines after PLX4032 treatment.** 10,000 cells were seeded/well of an eight-chambered slide and cultured overnight. Cells were serum starved for 24 hrs. and treated with PLX4032 for another 24 hrs. Immunofluorescence was carried out to detect target protein Red: Target protein; blue: DAPI

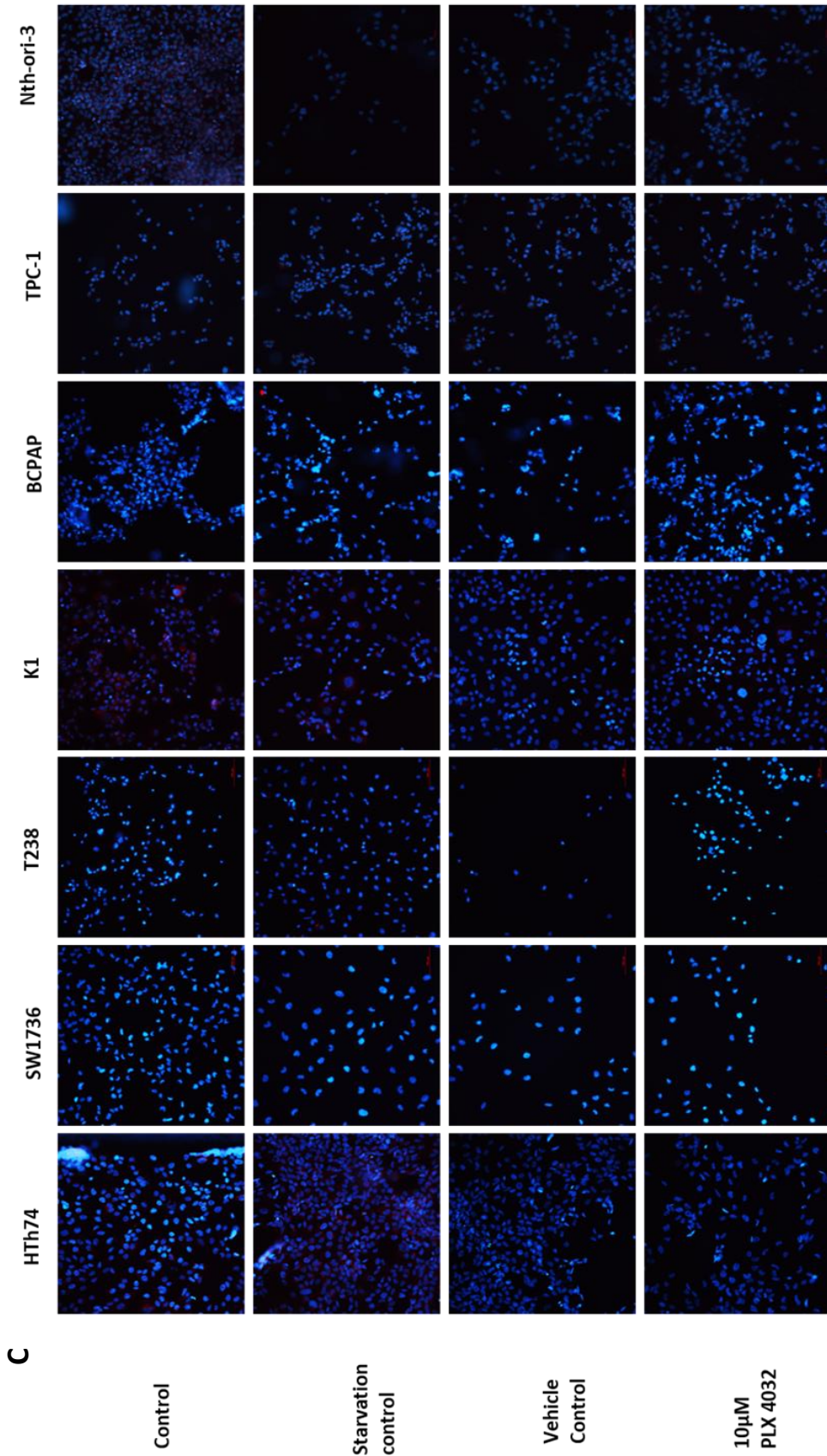


Figure 56. Expression of CD160 in thyroid cancer cell lines after PLX4032 treatment. 10,000 cells were seeded/well of an eight-chambered slide and cultured overnight. Cells were serum starved for 24 hrs. and treated with PLX4032 for another 24 hrs. Immunofluorescence was carried out to detect target protein. Red: Target protein; blue: DAPI

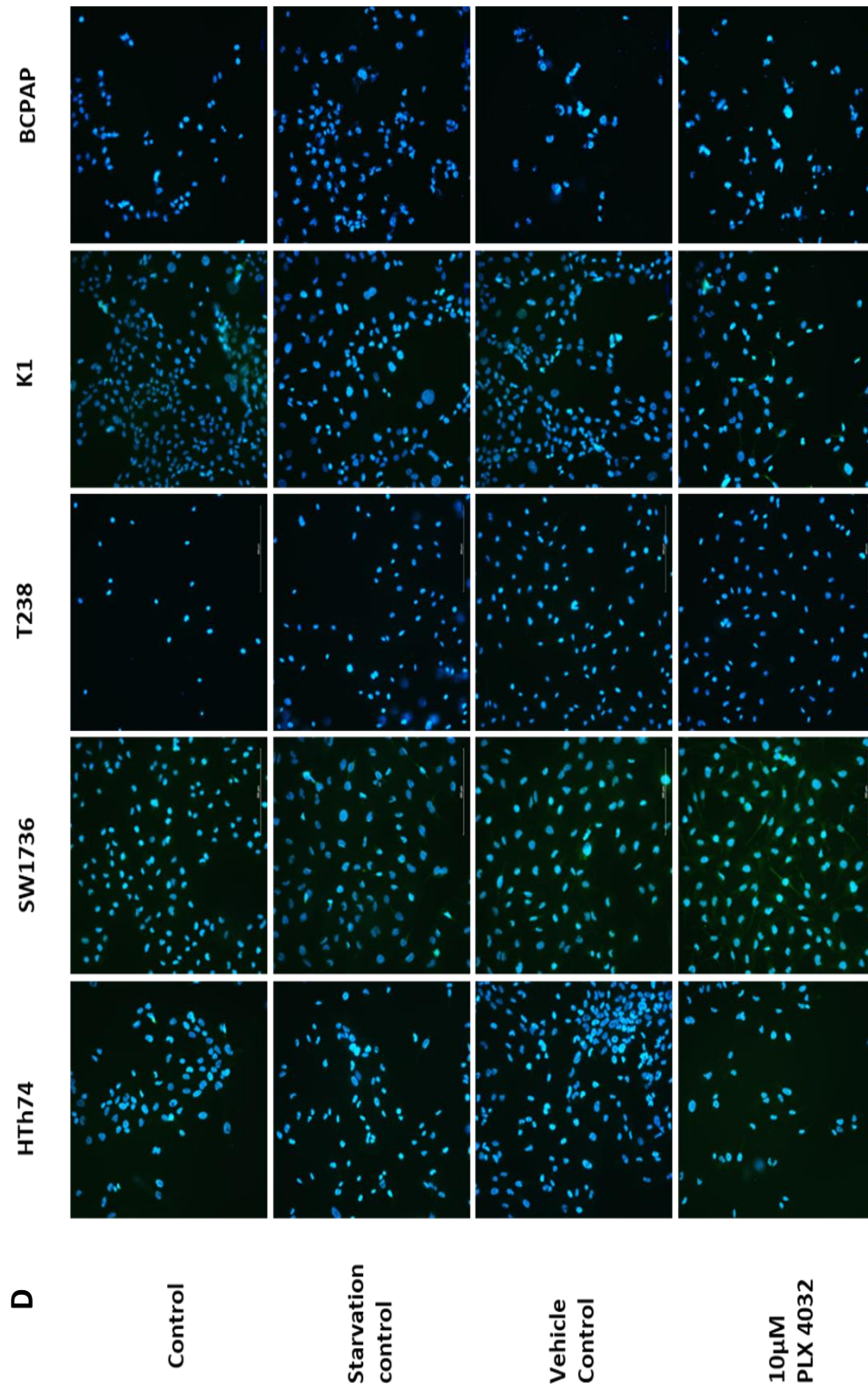
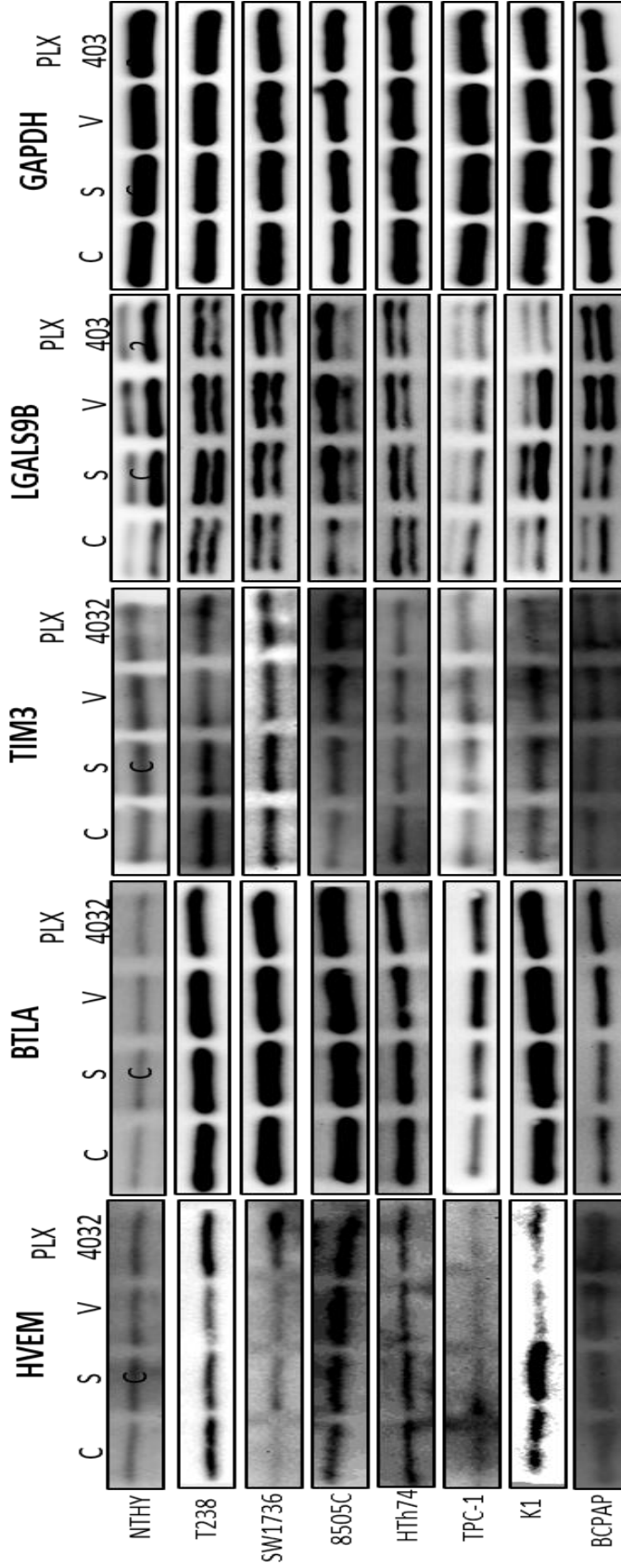


Figure 57. Expression of TIM3 in thyroid cancer cell lines after PLX4032 treatment. 10,000 cells were seeded/well of an eight-chambered slide and cultured overnight. Cells were serum starved for 24 hrs. and treated with PLX4032 for another 24 hrs. Immunofluorescence was carried out to detect (A) HVEM (B) BTLA (C) CD160 and (D) TIM3. Red/Green: Target protein; blue: DAPI



**Figure 58. PLX4032-mediated modulation of the expression of immunomodulatory molecules in thyroid cancer cell lines.**

Cells were grown up to 60-70% confluence and serum starved for 24 hrs. Following starvation, cells were treated with 10 $\mu$ M PLX4032 for 24 hrs. Whole cell lysate was used for western blot for detection of HVEM, BTLA, TIM3 and LGALS9B. C: Cells grown in complete growth media; SC: Cells cultured in starvation media; V: Vehicle control; PLX 4032: Treatment with PLX4032; Representative image from N=3 biological replicates.

*3b. Evaluation of the expression profile of the immunomodulatory molecules in vemurafenib-resistant ATC cell lines*

**Rationale:** BRAFV600E mutation is closely associated with aggressive clinical and pathologic features of thyroid cancer such as lymphatic metastases, extrathyroidal capsular invasion, advanced clinical stage, recurrence, and morbidity. From our previous studies, we have confirmed the expression and complex regulation of immunomodulatory molecules in ATC at basal level and in a pro-inflammatory immune microenvironment respectively. We have also observed a cause and effect relationship between the small molecule inhibitor of BRAFV600E and expression of immunomodulatory molecules in thyroid cancer cell lines at transcript level. Since development of acquired resistance against PLX4032 has been reported in multiple studies, including thyroid cancer, we wanted to see if the expression of immunomodulatory molecules is subject to change during development of resistance.

**b. PLX4032 resistant cell lines have significantly higher expression of immunomodulatory molecules at transcript level and protein level**

In order to emulate the scenario of acquired resistance, two ATC cell lines T238 and SW1736 were treated intermittently with escalating dose of PLX4032 over 7 months. The sensitive cells were also cultured parallelly for the entire period and passaged the same number of times as the resistant cells. The initial dose was 15 $\mu$ M and final dose was 30 $\mu$ M. SW1736 showed heightened tolerance to PLX4032 and were proliferative even at 60 $\mu$ M PLX4032. But we chose 30 $\mu$ M as the maintenance concentration as this is already a physiologically high concentration. We conducted all the experiments with 30 $\mu$ M as maintenance concentration. The development of resistance was confirmed by higher IC<sub>50</sub> values against the drug (Fig 59).

PLX4032 resistant T238 had almost three times higher IC<sub>50</sub> value compared to its PLX4032 - sensitive version. SW1736 had more than 10 times the IC<sub>50</sub> value compared to its PLX4032 - sensitive version. This was observed during the induction phase as well. SW1736 had inherently higher resistance against PLX4032 as we observed higher drug tolerance in SW1736 during the treatment. Western blot analyses confirmed higher basal expression pCRAF in the resistant cell lines which partially suggests compensatory mechanism for reactivation of MAPK pathway in response to BRAF inhibition, triggering hyperactive ERK in them (Fig 60). Both resistant and sensitive cells were treated with 15 and 30µM PLX4032 following 24 hrs. of serum starvation. Whole cell lysate was prepared, and western blot analyses confirmed higher level of pMEK and pERK in both the resistant cell lines even at a concentration of 30µM which was enough to ablate their expression in the sensitive phenotype (Fig 61). Total RNA was isolated from both PLX4032 sensitive and resistant T238 and SW1736 and qRT PCR was performed for the expression of HVEM, BTLA, CD160, TIM3, LGALS9B (galectin 9) and PD-L1. Dramatically higher expression of the immunomodulatory molecules was observed in PLX4032 resistant cell lines compared to their sensitive counterpart (Fig 62). In order to assess the surface expression, flow cytometry was performed with the resistant cell lines for expression of HVEM, BTLA and CD160. PLX4032 resistant T238 had significantly higher expression of HVEM compared to its sensitive counterpart and PLX4032 resistant SW1736 had significantly higher surface expression of all three proteins (Fig 63). The proportion of cells positive for expression of these immunomodulatory molecules were almost double in the resistant phenotype compared to normal.

**Conclusion:**

Acquired resistance to PLX4032 or vemurafenib is associated with increased expression of HVEM, BTLA, CD160, TIM3 and LGALS9B in BRAFV600E positive ATC cell lines at transcript level. Resistance-associated increase in surface expression of HVEM suggests an increased immunomodulatory potential of the PLX4032 resistant ATC cells in the tumor microenvironment which might support immune evasion.

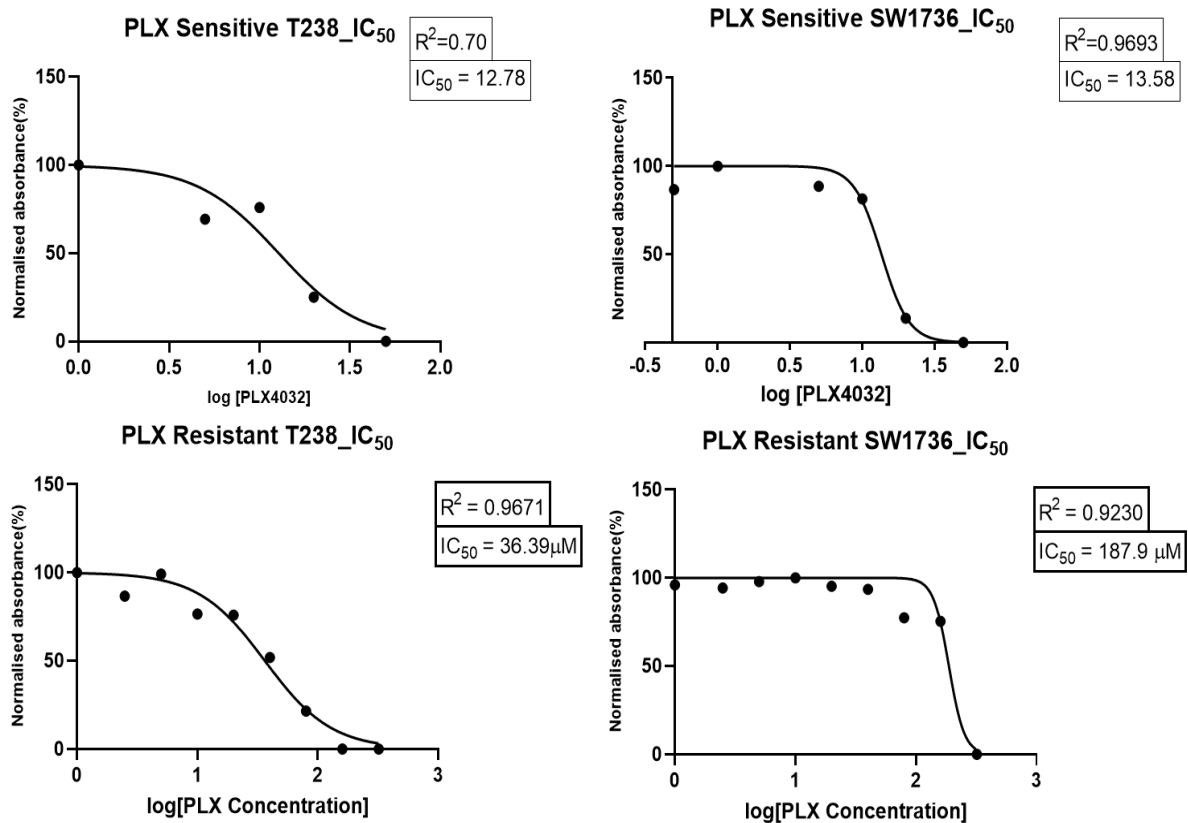


Figure 59. Induction of PLX4032 resistance in ATC cell lines. Two ATC cell lines T238 and SW1736 we cultured in complete growth media containing PLX4032 over 7 months in a dose escalation setting. The initial concentration was 15 $\mu M$  and the final concentration was 30 $\mu M$ . SW1736 had stronger resistance to PLX4032. For T238 and SW1736, 8000 and 10,000 cells were seeded/well of a 96 well dish respectively. Cells were treated with different concentrations of PLX4032 ranging from 2.5 $\mu M$  to 320 $\mu M$  and XTT assay was performed to determine  $IC_{50}$  values.

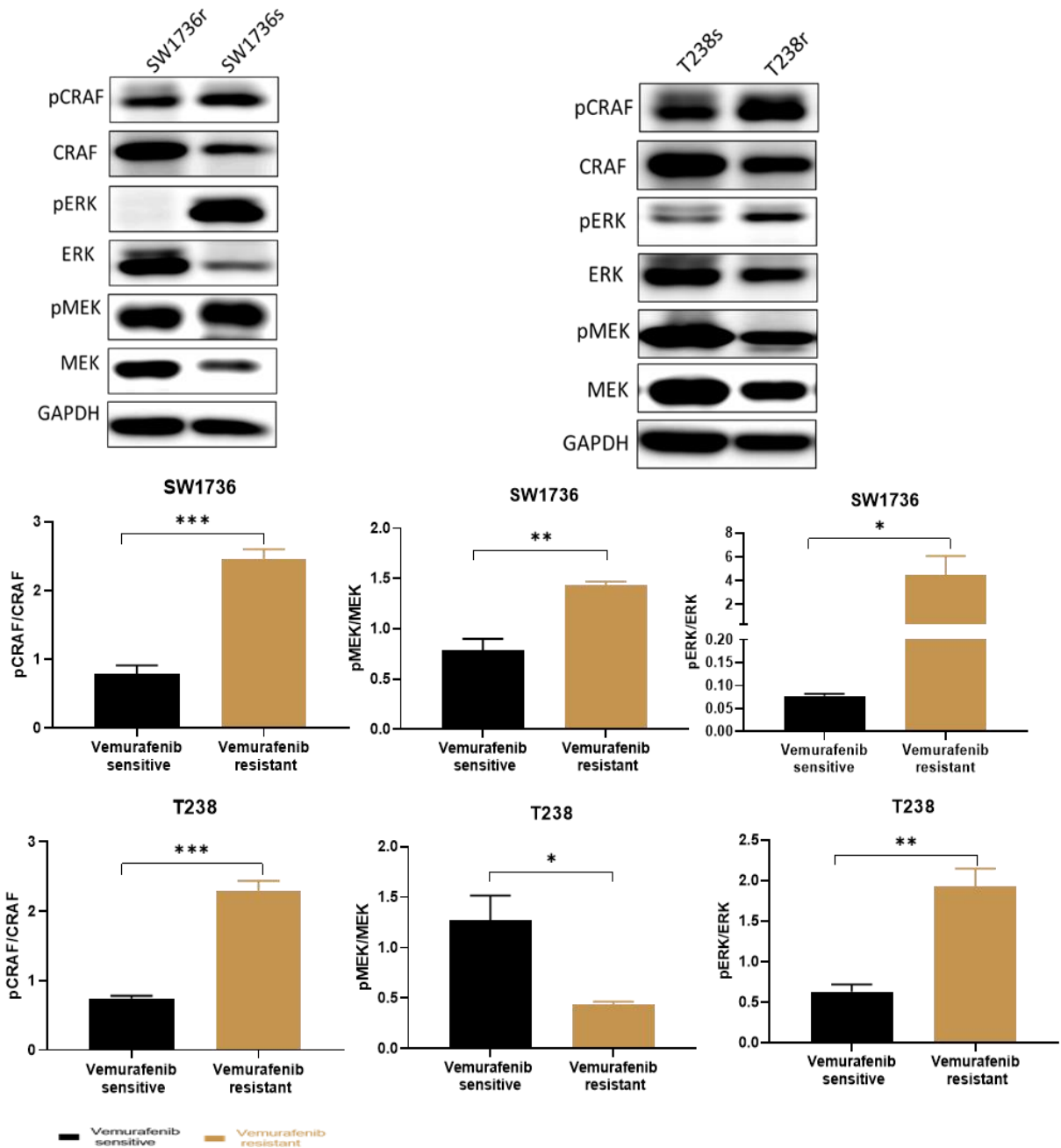


Figure 60. Activation of compensatory pathways in PLX4032 resistant ATC cell lines leading to hyperactivation of ERK. PLX4032 resistant and sensitive T238 and SW1736 were cultured in complete growth media up to 70% confluence. Whole cell lysate was prepared, and western blot was performed for expression of pCRAF, pMEK and pERK. Data representative of N=3 biological replicates. T238r: PLX4032 resistant T238; T238s: PLX4032 sensitive T238; SW1736r: PLX4032 resistant SW1736; SW1736s: PLX4032 sensitive SW1736. Student's t test was performed to evaluate statistical significance. \*p<.05, \*\*p<.01, \*\*\*p<.001

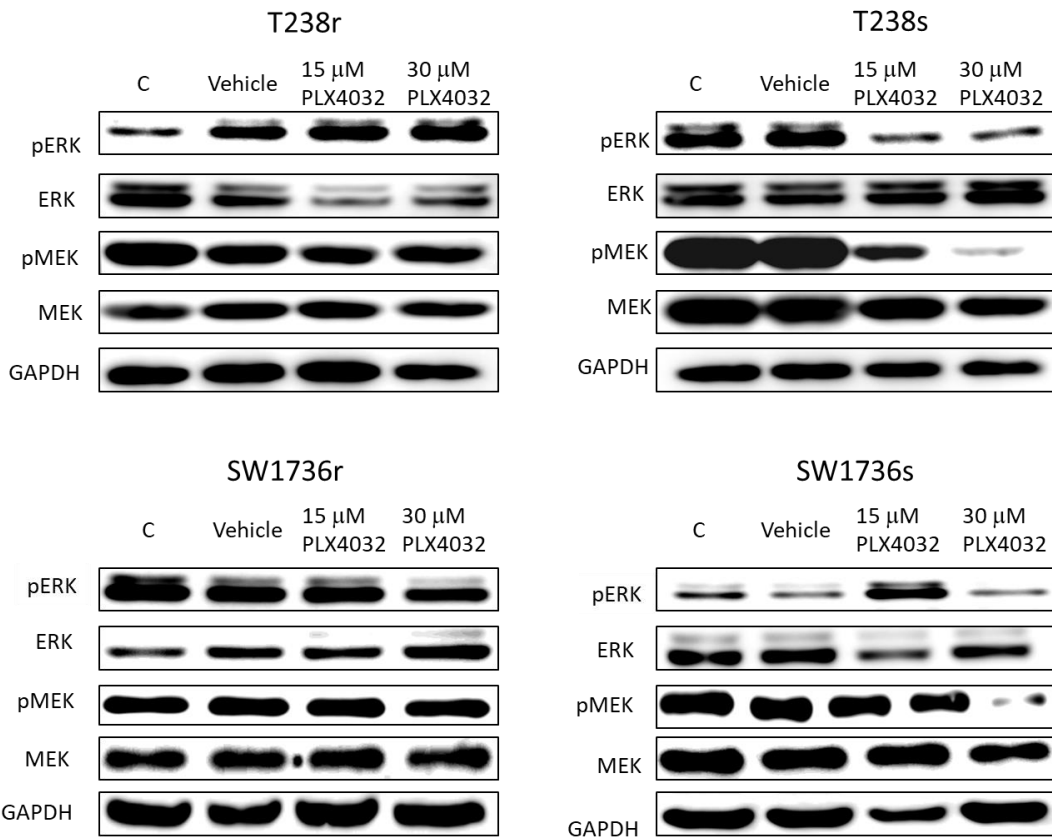


Figure 61. PLX4032 resistant ATC cell lines are characterized by hyperactivated MEK and ERK at higher concentrations of PLX4032. PLX4032 resistant and sensitive T238 and SW1736 were cultured in complete growth media up to 60% confluence. Cells were serum starved for 24hrs. followed by treatment with indicated dosages of PLX4032 for 24 hrs. Whole cell lysate was prepared and western blot was performed for expression of MEK and ERK. Data representative of N=3 biological replicates. T238r: PLX4032 resistant T238; T238s: PLX4032 sensitive T238; SW1736r: PLX4032 resistant SW1736; SW1736s: PLX4032 sensitive SW1736

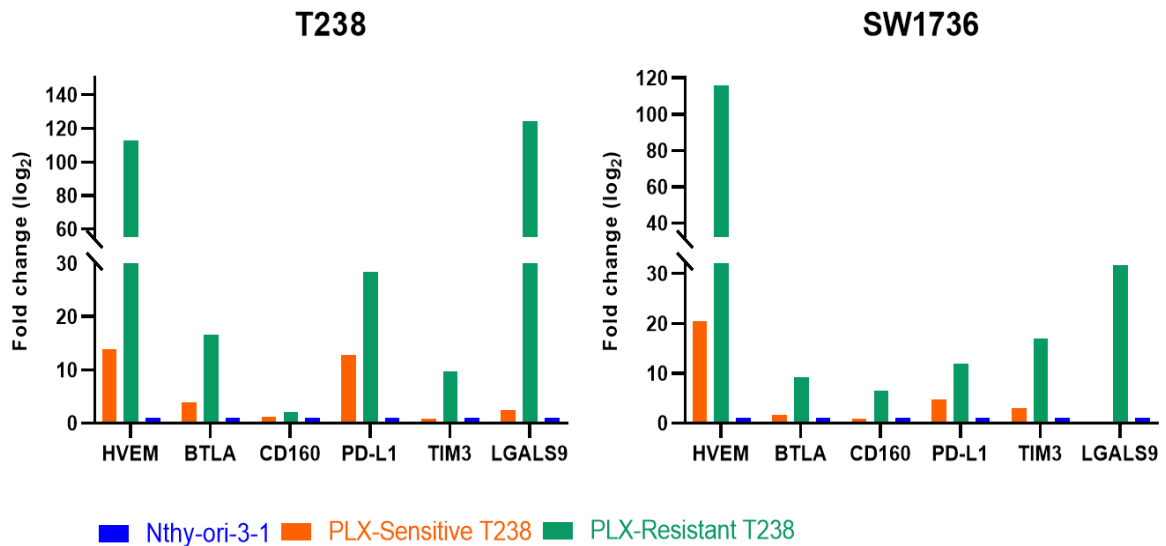


Figure 62. Higher expression of immunomodulatory molecules in vemurafenib (PLX4032) resistant ATC cell lines. PLX4032 resistant and sensitive T238 and SW1736 were grown in complete growth media up to 70% confluence and total RNA was isolated. qRT PCR was conducted for the expression of HVEM, BTLA, CD160, TIM3 and galectin 9 (LGALS9). Expression levels were compared to normal thyroid epithelial cell line Nthy-ori-3-1.

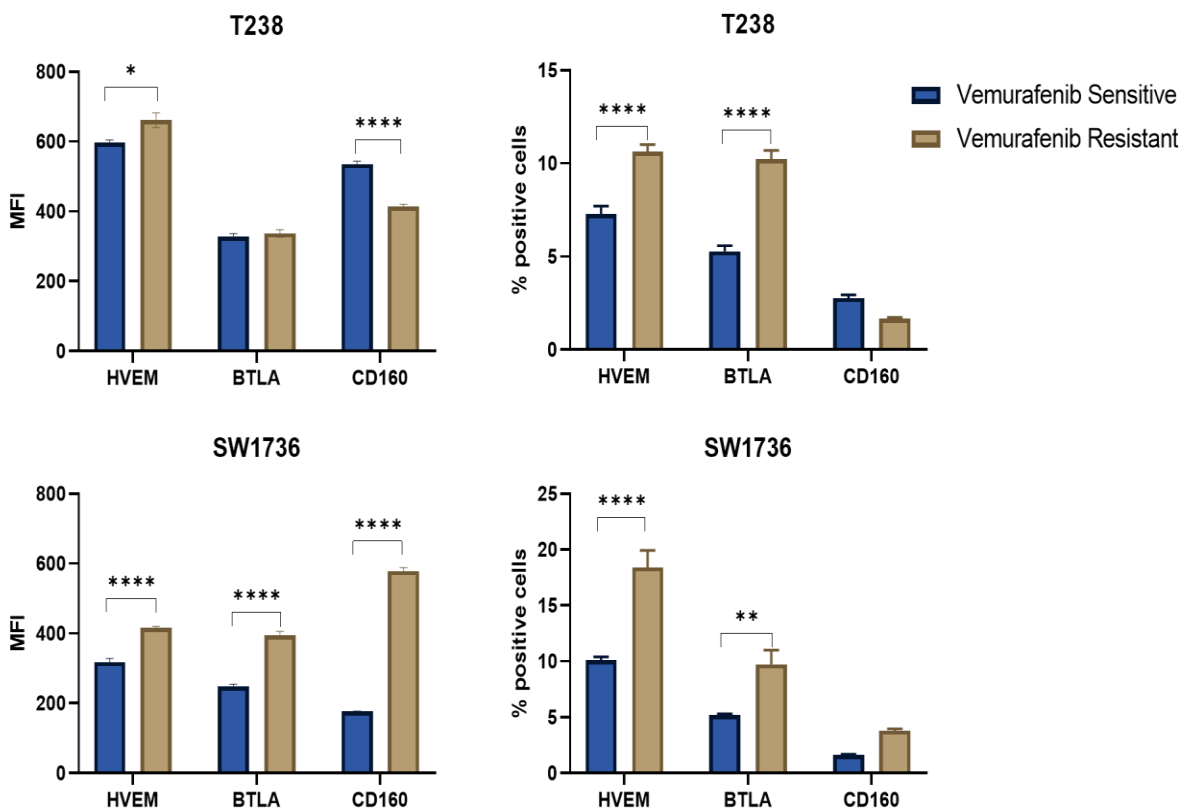


Figure 63. Higher surface expression of HVEM, BTLA and CD160 in Vemurafenib (PLX4032) resistant ATC cell lines. Flow cytometry was conducted on unpermeabilized PLX4032 - sensitive and PLX-4032-resistant T238 and SW1736 for expression of HVEM, BTLA and CD160. Bars represent mean  $\pm$  SEM from n=3 biological replicates. \*p<0.05, \*\*p<0.01, \*\*\*\*p<.0001

*3c. Evaluation of the combined effect of MEKi and BRAFV600E inhibitor on expression of these molecules in thyroid cancer cells*

Previous findings have already suggested expression of hyperactive MEK and ERK in PLX4032 resistant T238 and SW1736. MEK inhibitor Trametinib has been approved by FDA for anaplastic thyroid cancer in combination with Dabrafenib which is a BRAFV600E inhibitor. Immunological implications of this combination therapy are completely unknown in ATC. As our previous studies indicated that prolonged PLX4032 treatment could induce resistance in ATC cell lines and trigger dramatic change in expression profile of the immunomodulatory molecules, we wanted to see if the combination therapy with a MEKi can help circumvent this issue. Both sensitive and resistant T238 were treated with a combination of 15 $\mu$ M PLX4032 and 400nM Trametinib. Surface expression of HVEM was assessed by flow cytometry. A mild reduction in surface expression of HVEM was observed upon combination of PLX4032 and Trametinib in the PLX4032 sensitive phenotype which was lost in the resistant phenotype (Fig 64). Monotherapy with 15 $\mu$ M PLX4032 or 400nM Trametinib had no effect on expression of HVEM in resistant T238. In case of SW1736, the same pattern was observed in the resistant cells, however, we could see an intrinsically more resistant phenotype in SW1736 sensitive cells from their lack of responsiveness to trametinib. This explains the unusually high IC<sub>50</sub> values observed in the PLX4032 resistant SW1736 cells in our XTT assay. When the treatment groups were compared parallelly between the PLX4032 sensitive and resistant groups, we observed that the surface expression of HVEM was unaltered among different treatment groups in the resistant phenotype and expression of HVEM was significantly higher in them compared to the sensitive phenotype (Fig 65). This indicates that these patients might be able to benefit from immune checkpoint blockade therapy targeting

HVEM/BTLA axis. The lack of responsiveness to the combination therapy in the resistant cells could be attributed to the activation of compensatory pathways like HGF/MET (Knauf et al., 2018b) leading to the activation of transcription factors such as STAT3 which plays extremely crucial role in expression of HVEM.

**Conclusion:** Combination therapy including BRAFV600E inhibitor PLX4032 and MEK inhibitor trametinib has modest impact on expression of HVEM in the PLX4032 sensitive tumor cells. However, once the cells acquire resistance against BRAFV600Ei, this combination therapy is not sufficient to control the expression of HVEM and the patient might develop a unique and unforeseen immune interaction at the tumor site. These patients might benefit from additional intervention with antagonistic antibodies targeting interaction of HVEM with its cognate co-inhibitory ligand BTLA on T cells in combination with small molecule inhibitors.

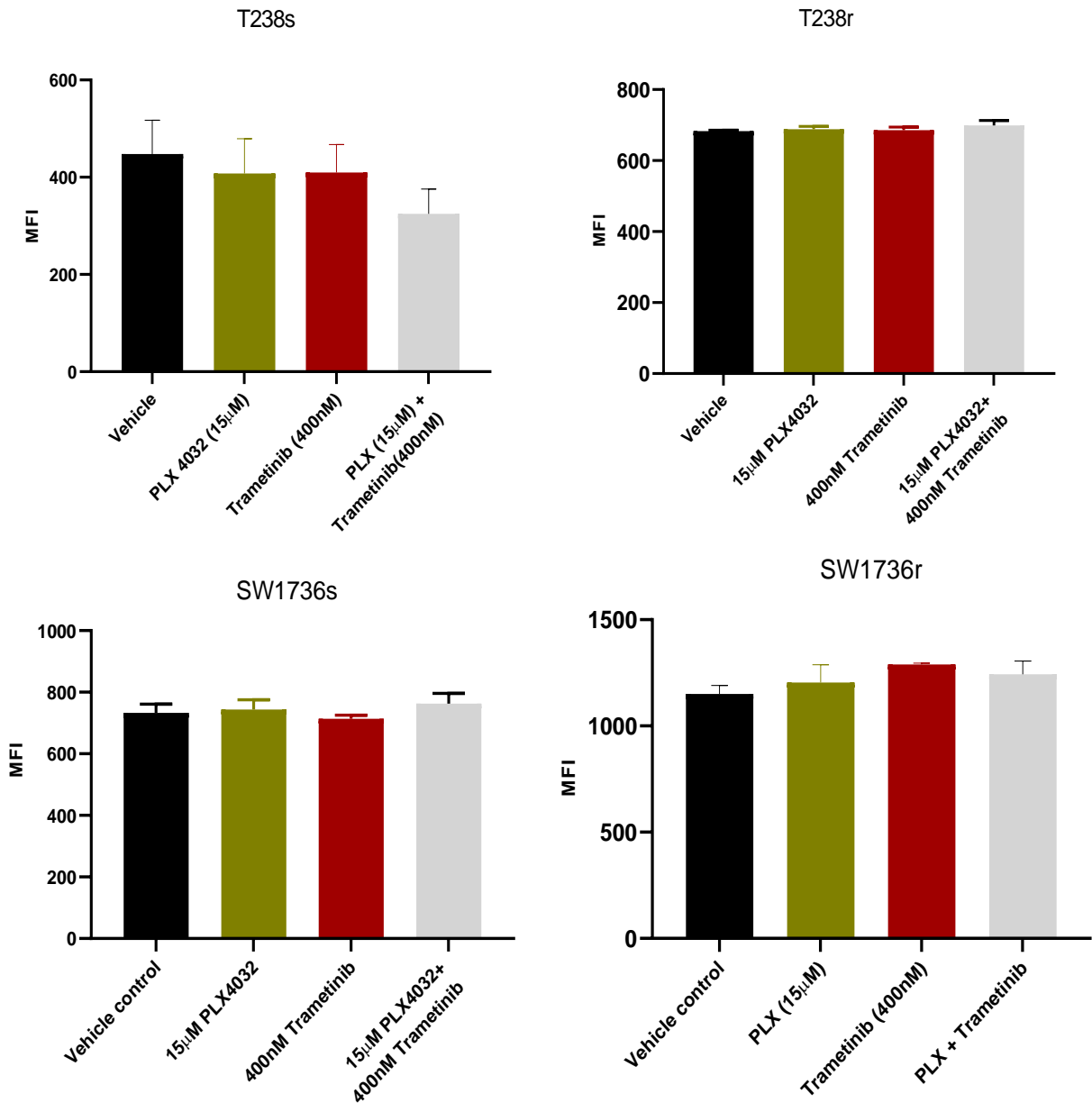


Figure 64. Differential effect of BRAFV600E and MEK inhibitors on surface expression of HVEM in PLX4032-sensitive and PLX4032-resistant T238 and SW1736. PLX4032 sensitive and resistant T238 and SW1736 were cultured up to 60% confluence and serum starved for 24 hrs. Subsequently, they were treated with 15µM PLX4032 and 400nM Trametinib alone or in combination for 24 hrs. Flow cytometry was conducted on unpermeabilized cells for expression of HVEM. Bars represent mean  $\pm$  SEM from n=3 biological replicates. One-way ANOVA with a Tukey's posttest was used to determine statistical significance.

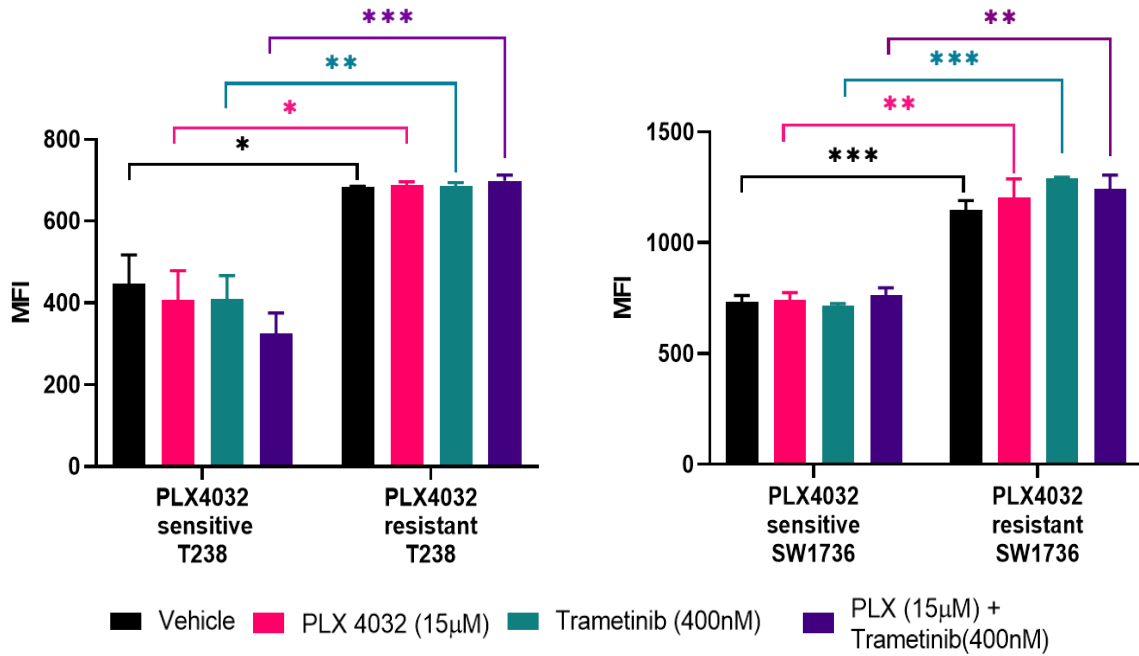


Figure 65. Persistent expression of HVEM upon combination treatment with PLX4032 and trametinib. PLX4032 sensitive and resistant T238 and SW1736 were cultured up to 60% confluence and serum starved for 24 hrs. Subsequently, they were treated with 15µM PLX4032 and 400nM Trametinib alone or in combination for 24 hrs. Flow cytometry was conducted on unpermeabilized cells for expression of HVEM. Bars represent mean  $\pm$  SEM from n=3 biological replicates. One-way ANOVA with a Tukey's posttest was used to determine statistical significance.

## *Summary*

- Transient treatment with BRAFV600E inhibitor vemurafenib or PLX4032 induces differential upregulation in immunomodulatory genes in anaplastic thyroid cancer
- PLX4032 treatment does not modulate expression of HVEM, BTLA or TIM3 proteins in thyroid cancer cells
- Adaptive resistance to PLX4032 is associated with hyperactive CRAF in resistant ATCs leading to hyperactivation of MEK and ERK
- Adaptive resistance to PLX4032 induces further upregulation of immunomodulatory molecules in anaplastic thyroid cancer with increased surface expression of HVEM
- Surface expression of HVEM becomes significantly higher once the cells acquire resistance against PLX4032 or vemurafenib and this expression persists even after the combination therapy with trametinib

## *Conclusion*

**Transient treatment with vemurafenib or PLX4032 upregulates expression of certain immunomodulatory genes and a significantly higher constitutive surface expression of HVEM persists in PLX4032 resistant cells upon combination therapy with BRAFV600Ei and MEKi**

## OVERALL SUMMARY

**Specific aim 1:** Profiling of T cell co-stimulatory and immune checkpoint molecules resulted in the identification of HVEM/BTLA/CD160 pathway as a putative immunotherapeutic target in ATC as evidenced by the following observations:

- Thyroid cancer cell lines differentially express T cell co-stimulatory and immune checkpoint molecules
- HVEM, BTLA, CD160, TIM3 and PD-L1 are significantly overexpressed in thyroid cancer cell lines 8505C, T238, Sw1736 and HTh74 compared to normal thyroid epithelial cells
- HVEM, BTLA, CD160 and TIM3 proteins are constitutively expressed in the thyroid cancer cell lines and HVEM has the highest level of surface expression
- HVEM, BTLA and CD160 has abundant expression in follicular and parafollicular cells of thyroid cancer tissues
- Membrane condensations of HVEM and BTLA on follicular cells of the ATC tissues suggests their surface expression and possible involvement in immunomodulation in TME

**Specific aim 2:** Tumor immune contexture in ATC confirms a T cell inflamed microenvironment with a combination pro and anti-inflammatory cytokine milieu and HVEM expression in ATC is closely interlinked with pro-inflammatory cytokines IL-8, TNF $\alpha$  and IFN $\gamma$ . HVEM fundamentally supports tumorigenesis and its interaction with the cognate ligand LIGHT triggers activation of tumor associated MAPK signaling in ATC. This was evidenced by the following observations:

- Anaplastic thyroid cancer and aggressive variants of papillary thyroid cancers have significantly higher amount of tumor infiltrating T lymphocytes, among which more than 80% are CD8<sup>+</sup> T cells
- The immune microenvironment in ATC and aggressive PTC has a mix of immunosuppressive and pro-inflammatory microenvironment with abundant expression of IL10, IDO1 and IL17.
- Pro-inflammatory cytokines TNF $\alpha$ , IL-8 and IFN $\gamma$  modulates expression of immunomodulatory molecule HVEM and is associated with its solubilization
- The interaction between HVEM and its cognate ligand LIGHT induces stress activated MAPK mediators in ATC cell lines
- HVEM/LIGHT interaction leads to a moderate increase in the level of pI $\kappa$ B $\alpha$  and nuclear translocation of NF $\kappa$ B in ATC cell line 8505C

- HVEM might have some potential role in cellular proliferation in ATC which is evidenced by reduced colony forming ability of HVEM<sup>KD</sup> 8505C
- Reduced invasive potential in HVEM<sup>KD</sup> 8505C suggested that HVEM might play some role in maintenance of invasive characteristics in ATC

**Specific aim 3:** Transient treatment with vemurafenib or PLX4032 upregulates expression of HVEM, CD160, BTLA, LGALS9B and TIM3 at transcript level and a significantly higher constitutive surface expression of HVEM protein persists in PLX4032 resistant cells upon combination therapy with BRAFV600Ei and MEKi trametinib. This was evidenced by the following observations:

- Transient treatment with BRAFV600E inhibitor vemurafenib or PLX4032 induces differential upregulation in immunomodulatory genes in anaplastic thyroid cancer
- PLX4032 treatment does not modulate expression of HVEM, BTLA or TIM3 proteins in thyroid cancer cells
- Adaptive resistance to PLX4032 is associated with hyperactive CRAF in resistant ATCs leading to hyperactivation of MEK and ERK and reactivation of MAPK pathway
- Adaptive resistance to PLX4032 induces further upregulation of immunomodulatory molecules in anaplastic thyroid cancer with increased surface expression of HVEM

- Surface expression of HVEM becomes significantly higher once the cells acquire resistance against PLX4032 or vemurafenib and this expression persists even after the combination therapy with trametinib

#### CHAPTER 4: DISCUSSION:

ATC is refractory to current conventional therapeutic modalities

ATC is one of the deadliest human solid tumors that accounts for less than 2% of thyroid carcinoma. It has a very rapid course of progression and it has extremely poor treatment outcomes, accounting for 15–40% of TC related deaths (Corrigan et al., 2019; Ferrari et al., 2020). According to American Thyroid Association, all ATCs are considered as stage T4. Further classification depends primarily on extent of extrathyroidal involvement. At stage IVA, the tumor is intrathyroidal. IVB represents tumor with gross extra thyroidal extension or cervical lymph node metastases, and ATC with distant metastases is stage IVC (Hoang et al., 2013). The main risk factors for ATC include age>65 years, a long-standing goiter and a history of radiation exposure to the neck or chest. The primary factors contributing to the prognosis are, age, sex, local tumor extension (T stage) and presence of distant metastasis (M stage). Male patients over 65 years with extrathyroidal involvement usually have extremely poor prognosis compared to patients without distant metastasis.

#### *Diagnosis of ATC: A difficult clinical challenge*

The histological diagnosis of ATC is extremely difficult. Histological variations are common from patient to patient and intra-tumoral variations are also observed. These tumors usually contain a heterogeneous mixture of spindled, epithelioid and pleomorphic giant cells among which spindle-cells are most common followed by the giant cell pattern (Y. Nikiforov et al., 2012). Immunohistochemical analyses for epithelial cell markers are commonly performed to discern the cellular differentiation status. Usually a weak and focal immunoreactivity against cytokeratin is observed in ATC. some other common markers used are thyroglobulin and TTF-

1, both of which are negative in ATC. Thyroglobulin staining can be ambiguous in case of ATC, since entrapment of normal follicular cells at the invasive front of the carcinoma is often observed in ATC. The normal follicular cells often secrete thyroglobulin which diffuses into the neoplastic cells leading to a false positive staining. The most frequent symptoms of ATC are mostly related to its enlarged mass and the mechanical compression on surrounding organs associated with it. Some of the most frequently observed symptoms are hoarseness, cervical pain, dysphagia, dyspnea and stridor. Given the rapid progression of the disease, ATC requires multimodal therapeutic approach by surgeons, radiation oncologists, and medical oncologists.

#### *Limited surgical options for ATC patients*

First-line curative treatment includes surgical resection. External beam radiation therapy (EBRT) with chemotherapy is generally administered postoperatively or utilized as definitive therapy for unresectable cases (Huang et al., 2019; Sun et al., 2013). In general, patients with intrathyroidal and extrathyroidal ATC without involvement of aerodigestive tracts are considered for surgery, but patients with involvement of aerodigestive tracts are not even considered for surgery according to ATA guidelines (Smallridge et al., 2012). Hence, surgery in ATC patients is recommended only for patients at stage IVA and IVB disease and when gross tumor resection (at least R1) can be achieved (Smallridge et al., 2012). However, significant debulking of the tumor is associated with a dismal improvement in overall survival of the patients though the reports are ambiguous because of heterogenous treatment approaches taken post-surgery.

*Radioiodine ablation therapy (RAIT) and EBRT: Limited potential with grim outcome in ATC*

For DTC, radioiodine therapy is the next choice of treatment following surgery. Since expression of NIS is lost in ATC patients, they are precluded from this option and external beam radiation therapy (EBRT) is the next choice of treatment which is often associated with side effects such as redness of the skin, sore throat, dry mouth, altered taste perception, pain on swallowing, local hair loss and fatigue. Unfortunately, this is not a viable option for patients with distant metastasis which is quite common in ATC.

*Chemotherapy in ATC: Debilitating side effects*

Common chemotherapeutic agents like combination of doxorubicin and taxanes and/or platins has shown some efficacy in controlling the tumor mass, but this is associated with severe toxicity including but not limited to bone marrow suppression, tissue ulceration, necrosis and acute cardio-toxicity (StatPearls, 2019). Cytotoxic agents, such as gemcitabine and vinorelbine, have shown activity against multiple ATC cell lines in *in vitro* studies, but these drugs have not made it to the clinical practice owing to their inadequacy in controlling the progression of advanced ATC. The failure of conventional chemotherapy, alone and in combination with radiotherapy, to stall the progression of ATC and to improve patient outcomes with reduced toxicity led to the development of novel, molecularly targeted drugs designed to target specific genetically aberrant oncoproteins in the patients. These small molecule inhibitors have shown promising result in a wide range of malignancies and seemed to hold great promise in TC.

*Small molecule inhibitors: Big problem of resistance*

Most of these drugs target serine threonine kinases and tyrosine kinases commonly overexpressed in ATC, such as BRAFV600E, VEGFR, EGFR, PDGFR and RET. BRAFV600E-positive PTCs display the constitutively activated RAF/ERK pathway which leads to repression of downstream pathways responsible for regulation of many thyroid-specific genes, leading to cellular de-differentiation, tumor progression and acquisition of more aggressive phenotypes eventually leading to ATC. Successful clinical trials with two such small molecule inhibitors of the MAPK pathway led to the development of a combination therapy with BRAFV600E inhibitor dabrafenib and MEK inhibitor trametinib, which was later approved by FDA for ATC in May 2018. Unfortunately, both intrinsic and acquired resistance against these drugs have been reported. One of the reasons of intrinsic resistance to BRAFV600E inhibitor vemurafenib in PTC is copy number gain of myeloid cell leukemia 1, chromosome 1q gene (MCL1) and a loss of the tumor suppressor cyclin dependent kinase inhibitor 2A (CDKN2A), which confer resistance to vemurafenib treatment due to impairment of the B-Cell CLL/Lymphoma 2 (BCL2)-regulated apoptotic pathway (Duquette et al., 2015). The PIK3CA<sup>H1047R</sup> activating mutation is commonly associated with the de-differentiation process involved in progression of PTC into ATC. In TCs harboring both BRAFV600E and PIK3CA<sup>H1047R</sup> mutation, the latter paradoxically hyperactivates ERK signaling, thus conferring resistance to BRAFi (Antonello et al., 2017).

### *Immune contexture in ATC: scope of immunotherapy*

#### *ATC has complex cytokine milieu*

The association between an inflammatory microenvironment and DTC has been implicated in multiple studies (Cunha et al., 2014), (Graceffa et al., 2019). The immune microenvironment in TC is extremely complex in nature with a combination of pro and anti-inflammatory cytokines and immune cell infiltrates (Varricchi et al., 2019). Our study revealed an immunosuppressive microenvironment in ATC with high expression of IL10 and IDO1. IL10 is an extremely potent immunosuppressive cytokine secreted by TAMs and tumor cells themselves in both PTC and ATC (Todaro et al., 2006). This cytokine has pleiotropic effects in both immunoregulation and inflammation. It dampens the expression of Th1 cytokines, MHC class II antigen presentation, and costimulatory molecules on macrophages. IDO1 is an enzyme that catalyzes the first and rate-limiting step in tryptophan catabolism to N-formyl-kynurenine. Expression of this enzyme in DCs, monocytes and macrophages regulate T cell activity by controlling peri-cellular catabolism of tryptophan and limiting its availability to T cells. This is a prominent immunosuppressive cytokine responsible for dampening anti-tumor T cell response. High expression of IDO1 in our clinical samples corroborate with previous reports of upregulated IDO1 during thyroid carcinogenesis (Moretti et al., 2014). In this study, the authors observed 5-10-fold higher expression of IDO1 and more T<sub>reg</sub> polarization in ATC compared to PTC. The study also confirmed that expression of IDO1 in the tumor cells was IFN $\gamma$  inducible. This depicts another possible mechanism of induction of immune tolerance in ATC.

#### *ATC has T cell inflamed immune microenvironment*

Further profiling of the immune infiltrate in our clinical samples revealed significantly higher number of TILs compared to normal, more than 80% of which were CD8<sup>+</sup> T cells. We also noted CD4<sup>+</sup> T cells, but they were not intra-tumoral. A recent study suggests existence of two distinct immune phenotypes in TC – PDTC like and ATC like. In their study, they observed significantly higher number of CD8<sup>+</sup> T cells in ATC, compared to PDTC (Giannini et al., 2019). They also noted higher expression of CCL2, CCL3, CCL4, CCL5, CXCL9 and CXCL10 in ATC compared to PDTC. We detected more TILs in ATC. compared to PTC, which might be attributed to preferential secretion of CXCL9 and CXCL10 by the ATC cells, which act as chemoattractant for T cells. Interestingly, their study detected simultaneous upregulation of several T cell exhaustion markers such as TIM3, LAG3 and TIGIT and co-stimulatory molecules, like GITR, 4-1BB and OX-40 at a high extent ATC, and to a lesser extent in PTC, but not at all in PDTC. Our observation corroborated this study and we believe the immune microenvironment of ATC should be categorized as T cell-inflamed or “hot” as opposed to the traditional belief of being “cold”. This observation opens up the immense possibility of immune checkpoint blockade therapy for these patients. One of our primary objectives was to explore this new avenue to find a novel therapeutic approach.

#### **Immune modulatory molecules in ATC: an unexplored realm**

The last decade of immune checkpoint inhibitor therapy have revolutionized the field of tumor immunotherapy. Ipilimumab, an anti-CTLA-4 antibody, was the first immune checkpoint inhibitor (ICI) to be FDA-approved in 2011 for metastatic melanoma. Subsequently, five other immune checkpoint-targeted therapies have been approved, all directed against PD-1 or PD-L1, for the treatment of melanoma, non-small cell lung cancer

(NSCLC), renal cell carcinoma (RCC) and several other tumor types, in monotherapy and combinatorial regimen. Several clinical trials investigating PD-1/ PD-L1 inhibitors as monotherapy or in combination in ATC are presently underway (NCT02688608, NCT03181100, NCT03211117, NCT03246958,). One of the major hallmarks of immunotherapy is the durability of the responses that can be translated into survival benefit for the patient. ICI prolonged survival in patients, however the response was not universal.

A substantial variation in responsiveness towards ICI is observed among patients with same malignancy and among different malignancies. The degree of responsiveness often correlates with tumor mutational burden (TMB), though it alone is not sufficient to predict clinical response. High TMB with additional elevated level of tumor neoantigen expression plays a crucial role in antitumor immunity. However, there are several tumor-intrinsic and tumor-extrinsic factors that shape the final response. Extrinsic factors include quality of T cell infiltrates, composition of cytokines, percentage of immune suppressor cells such as MDSCs. All of these eventually shape the immune response in a highly individualized manner. High percentage of TAMs and immune suppressive cytokines are well established features of the immune landscape in ATC. Some preliminary studies have shown promising results with PD-1 blockade, but they are not yet approved for ATC.

*Immune Related Adverse Effects (irAE): The unprecedented consequences*

Unfortunately, with CTLA4 and PD-1/PD-L1 ICI therapy, there is an increasing number of reports of severe adverse effects including immune mediated pneumonitis, immune mediated colitis, immune mediated neuropathies, and severe cardiac toxicity, some of which

are sustained after completion of therapy. preliminary studies suggest that irAEs are triggered by antigens that are common to both tumor and the inflamed organ. This results in the destruction of both the diseased and normal tissue by the unleashed T cells. In a recent post-mortem study, infiltrating T-cells and macrophages were found in the myocardial tissue and the cardiac conduction system of two metastatic melanoma patients who developed fulminant myocarditis after nivolumab plus ipilimumab treatment (Johnson et al., 2016). A prospective study with NSCLC patients on anti-PD-1 antibodies revealed 34.2% patients had dermatologic irAEs. Interestingly, TCR clonotype from normal skin and tumor biopsies of 4 patients revealed shared T cell clones between two tissues. There were 9 shared antigens between these two tissues that might have elicited the response (Flatz et al., 2019). Due to these unforeseen shortcomings of the therapies based on the use of the anti-CTLA-4, PD-1, or PD-L1 monoclonal antibodies, both as monotherapy and in combination regimens, the additional co-inhibitory pathways are being evaluated as novel pharmacological targets.

*Second generation of immune checkpoint molecules in ATC:*

In this study we performed a thorough profiling of four ATC cell lines for expression of novel immune checkpoint molecules and identified HVEM/CD160/BTLA as a potential target. Constitutively high expression of HVEM, BTLA and CD160 genes were detected in the ATC cell lines. Our flow cytometry analyses confirmed the surface expression of these molecules which indicates that they can engage the infiltrating T lymphocytes and APCs via their cognate receptors. HVEM act as a bidirectional switch which can transduce either co-stimulatory or inhibitory signal into the T cells depending on the receptor/ligand it is interacting with. HVEM

itself is a ligand for the TNF superfamily members LIGHT. Binding of T cell-expressed LIGHT to HVEM expressed by APCs results in enhanced T cell proliferation and cytokine production. On the contrary, when HVEM engages BTLA – a member of the immunoglobulin superfamily – or CD160 on T cells, it triggers inhibitory signals resulting in decreased T cell proliferation and cytokine production (del Rio et al., 2010b) (Fig 66).

Tumor cell-expression of HVEM has recently been reported in ovarian serous adenocarcinoma tissues. In this study expression of HVEM was evaluated in 40 ovarian serous adenocarcinoma tissue samples by IHC. 72.5% of the cases were positive for expression of HVEM. Tumors at stage III and IV had significantly higher cytoplasmic expression of HVEM and the expression also positively correlated with lymph node metastasis (Fang et al., 2017). In our study, HVEM expression was identified in both the cytoplasm and plasma membrane of follicular cancer cells in ATC tissues, but there was no expression in normal thyroid follicular cells. High HVEM expression was also observed in the PTC tissues in our study which were aggressive variants with previous history of thyroiditis and with capsular invasion and extrathyroidal extensions. Takashi *et al.* looked at HVEM expression in 234 colorectal cancer (CRC) by IHC. 49.6% of the cases had intermediate expression of HVEM and 19.2% of the cases had strong HVEM expression. They also found that HVEM positivity correlated with disease stage and they concluded that HVEM could act as an independent prognostic factor for CRC (Inoue et al., 2015). The authors observed a graded expression pattern of HVEM, where normal colonic epithelium had a minimal expression followed by 24% adenomas positive for HVEM and more than 50% of CRC samples had high HVEM expression (Inoue et al., 2015). Interestingly, we observed high cytoplasmic and membrane expression of BTLA and CD160

also. Again, we did not detect any expression in normal thyroid follicular cells. BTLA expression was marginally higher in ATC than PTC. Expression of these proteins in the aggressive forms of TC, indicates that HVEM/BTLA pathway might be actively involved in development and progression of aggressive variants of PTCs into ATC.

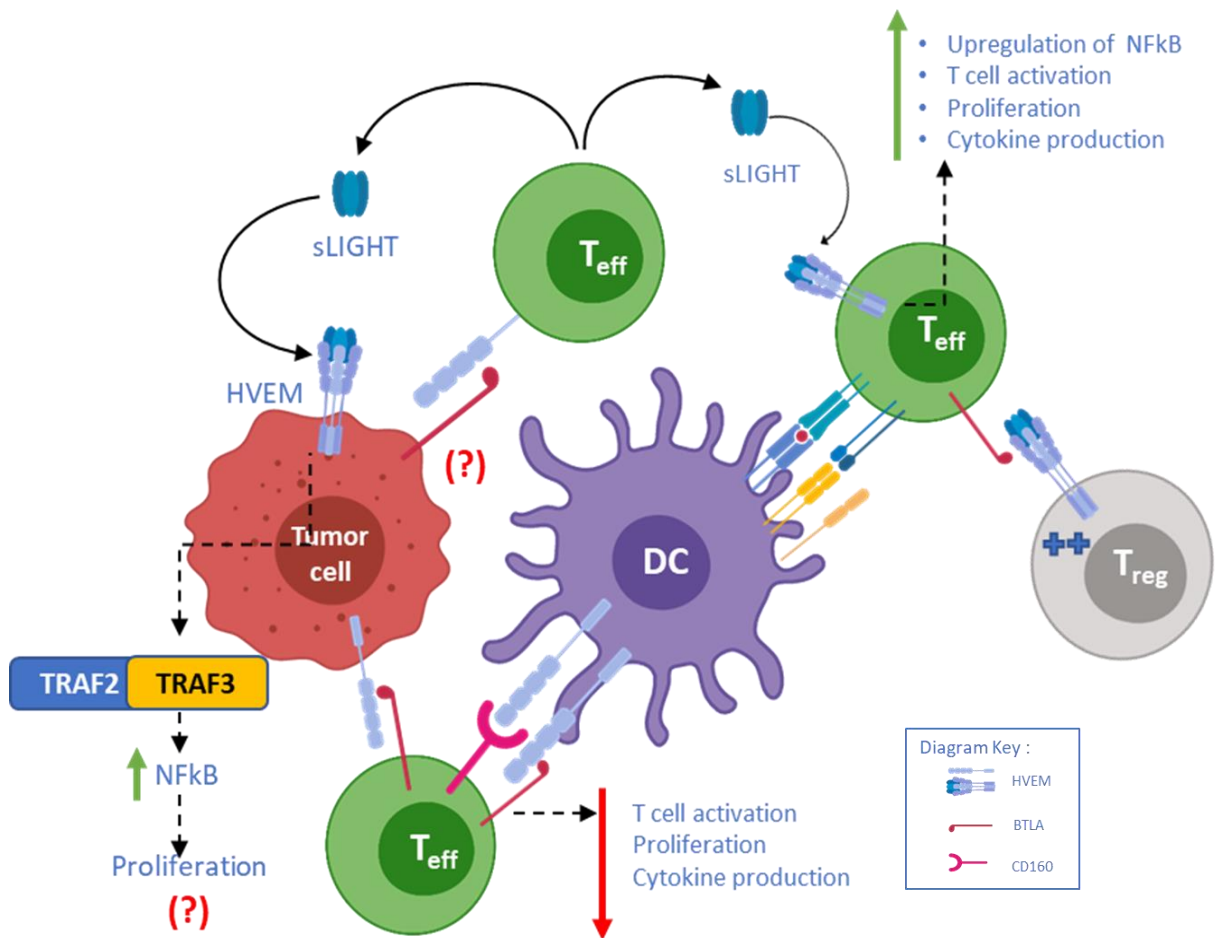


Figure 66. HVEM/BTLA/CD160/LIGHT Signaling in T cells and antigen presenting cells. HVEM is expressed on antigen presenting cells (e.g. DC) and interacts with inhibitory ligand BTLA on T cells resulting in a dampened T cell activity. Activated T cells secrete LIGHT, which is activating ligand of HVEM. Upon interaction with soluble LIGHT, HVEM triggers downstream activation of NFκB and proliferation in T cells. Interaction between effector T cell-BTLA and T<sub>reg</sub>-HVEM promotes T<sub>reg</sub> differentiation. HVEM: Herpes Virus Entry Mediator; BTLA: B & T Lymphocyte Antigen; LIGHT: lymphotoxin-like inducible protein that competes with glycoprotein D for herpes virus entry on T cells; T<sub>eff</sub>: Effector T cell; T<sub>reg</sub>: Regulatory T cell; DC: Dendritic cell

### Inflammation and immune checkpoint molecules: a complex interplay

Until recently, the crosstalk between cytokines and immune checkpoint proteins was underappreciated. Recent reports focusing on a complex regulation of PD-L1 by IL-6 and IL-8 reinvigorated the perception of a complex interplay between the cytokine milieu and the immune checkpoint molecules. The concentration of cytokines varies significantly between serum and tumor tissues. A study by *Young et al.* on CRC reported almost four times higher concentration of intra-tumoral IL-8 than its serum level (Kim et al., 2014). Serum concentration of IL-8 and TNF $\alpha$  is usually higher in inflammatory cancers and higher concentration of IL-8 has been reported in ATC.

Our study has also established HVEM, BTLA and CD160 as IFN $\gamma$  inducible genes. There is a heterogeneous level of sensitivity observed across the different cell lines which could be attributed to the inherently heterogeneous nature of the tumor cells. This was an interesting observation and it points towards the possibility of upregulation of these molecules in presence of IFN $\gamma$  secreted by activated T cells and other immune cells in the TME. Previous study in our lab has shown that the thyroid cancer cells secrete several pro-inflammatory cells that have pleiotropic functions and are capable of supporting tumor growth and upregulate proliferation. IL-8 and TNF $\alpha$  are two most prominent pro-inflammatory cytokines secreted by TC cells and the tumor infiltrating M1 macrophages commonly observed in ATC. We observed a complex regulation of HVEM in ATC cell lines by IL-8 and TNF $\alpha$ . In our study, IL-8 and TNF $\alpha$  upregulated HVEM expression at transcript level which can be attributed to multiple binding sites for STAT3 and RELA/NF $\kappa$ B p65 in the promoter of HVEM (Fig 67).

Interestingly, we observed solubilization of HVEM post- IL-8 and TNF $\alpha$  treatment. HVEM ELISA confirmed presence of soluble HVEM in the conditioned media from ATC cell lines. Interestingly, we observed increased expression of a metalloprotease ADAM17 in the ATC cell lines when subjected to the inflammatory cytokine treatment, especially TNF $\alpha$ . This enzyme is responsible for ectodomain shedding of members of TNFSF and TNFRSF (Ward-Kavanagh et al., 2016) (Fig 68). There is an increasing appreciation of ADAM17 in carcinogenesis and is being implicated in different malignancies such as lung adenocarcinoma, breast cancer, colon cancer and so on (Düsterhöft et al., 2019; Moss & Minond, 2017; Pavlenko et al., 2019; Saad et al., 2019). Our preliminary observation suggests that we might be able to detect soluble HVEM in ATC patients' sera which could potentially act as a biomarker. However, we need to analyze patient sera and compare with age, gender matched control to reach a definitive conclusion.

Overall, the studies conducted in specific aim 2 confirms an immunologically active T cell inflamed immune microenvironment in ATC and a complex regulation of HVEM by the inflammatory cytokine milieu, leading to its solubilization.

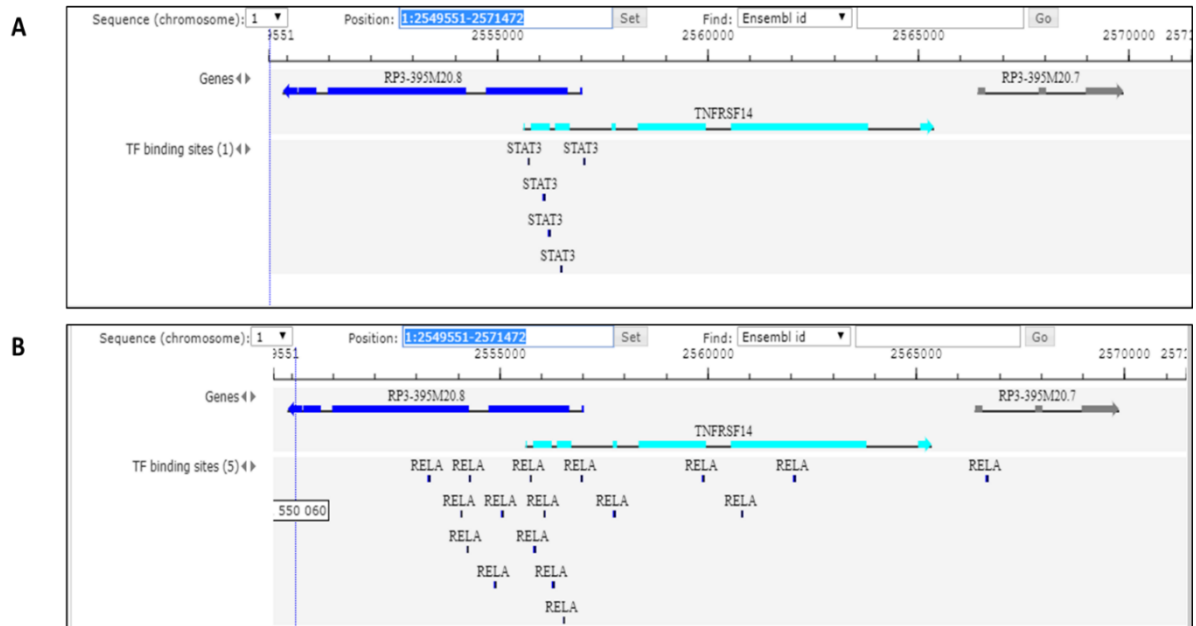


Figure 67. STAT3 (A) and NFκB (B) binding sites in HVEM promoter. Source: GTRD: a database on gene transcription regulation—2019 update. I.S. Yevshin, R.N. Sharipov, S.K. Kolmykov, Y.V. Kondrakhin, F.A. Kolpakov. *Nucleic Acids Res.* 2019 Jan 8;47(D1): D100-D105.

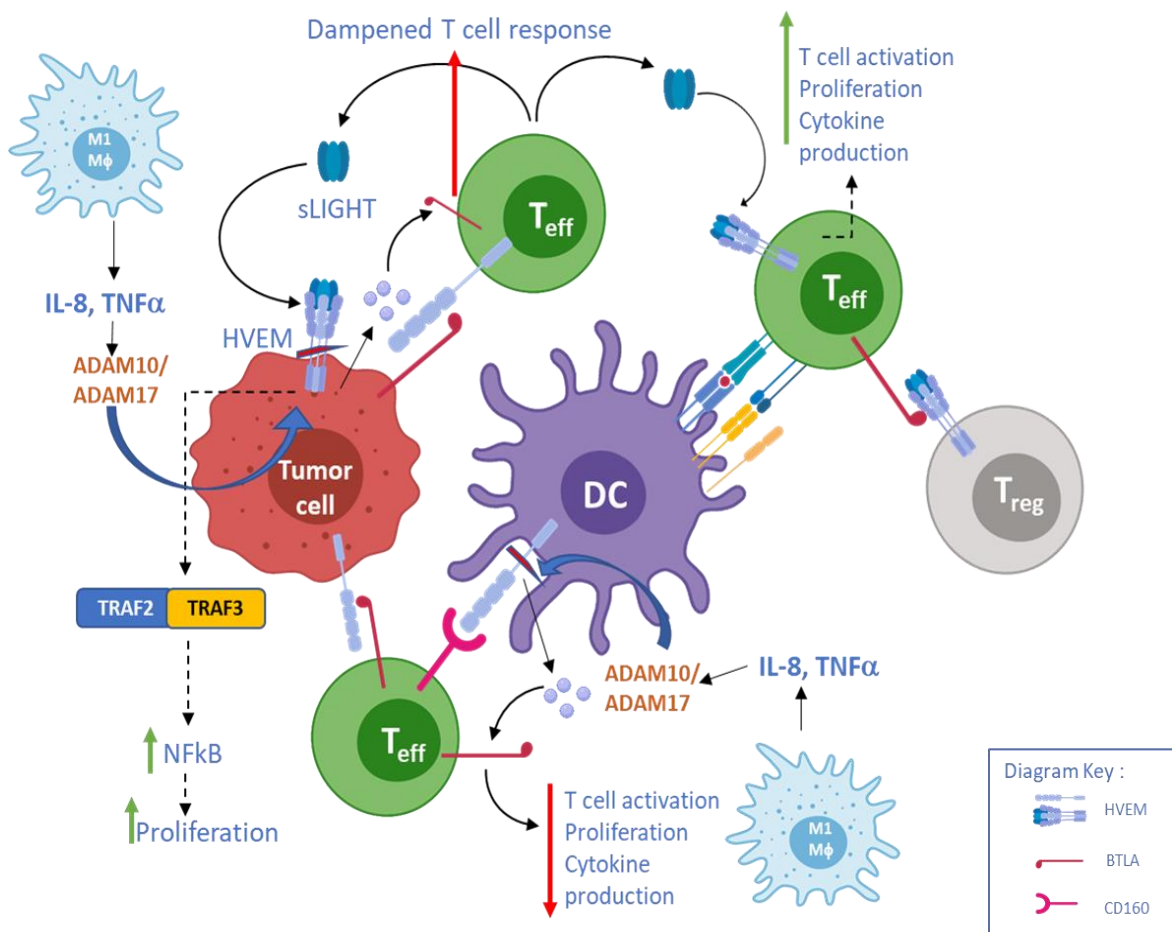


Figure 68. **ADAM17 mediated ectodomain shedding in HVEM.** Inflammatory cytokine IFN $\gamma$  upregulates ADAM17 metalloprotease which cleaves the functional ectodomain of HVEM. This functional ectodomain retains its interaction motifs for BTLA, CD160 and LIGHT. This facilitates dampening of distal T cells' activity via soluble HVEM/BTLA or soluble HVEM/CD160 interaction. HVEM: Herpes Virus Entry Mediator; BTLA: B & T Lymphocyte Antigen; LIGHT: lymphotoxin-like inducible protein that competes with glycoprotein D for herpes virus entry on T cells; T<sub>eff</sub>: Effector T cell; T<sub>reg</sub>: Regulatory T cell; DC: Dendritic cell

### HVEM: Potential involvement in supporting tumorigenesis in ATC

HVEM functions as a bidirectional switch, acting both as a receptor capable of signal-transduction and as a ligand eliciting signaling. This functional dichotomy results from the distinct ligand binding sites on HVEM. HVEM gene has 8 exons encoding a type 1 transmembrane glycoprotein with four pseudo repeats of the cysteine-rich domain (CRD) (1-4 from the N-terminus) in its extracellular domain, distinctive of the TNFRSF. The disulfide bonds in the CRD form an elongated, ladder-like structure. The signaling potential of HVEM resides in a relatively short cytoplasmic tail, with a binding site for the TNFR-associated factor (TRAF) family of ubiquitin E3 ligases that triggers activation of NF- $\kappa$ B, which is critical for controlling genes involved in cell survival and inflammation.

The ectodomain of HVEM has distinct interaction sites for BTLA /CD160 and LIGHT/LT $\alpha$ . LIGHT and LT $\alpha$  binding sites reside in CRD2 and CRD3, whereas BTLA and CD160 interaction happens through CRD1. Soluble LIGHT is not competitive for BTLA or CD160 binding; however, membrane LIGHT displaces HVEM-BTLA interactions, probably by steric hindrance due to space constraints on the cell surface. Engagement of either BTLA or LIGHT can trigger activation of NF $\kappa$ B in HVEM expressing cell. HVEM has been implicated in promoting macrophage migration and vascular smooth muscle cell proliferation via upregulation of PI3K/Akt (Wei et al., 2006). LIGHT was found to induce PI3K-Akt phosphorylation in osteoclast precursor cells, supporting differentiation of osteoclasts (Hemingway et al., 2013).

We were intrigued by these findings and our previous observations of high constitutive expression of HVEM in ATC cell lines and tissues in specific aim 1. In order to discern possible tumor intrinsic function of HVEM in ATC, we took two different approaches. First, we

evaluated the response generated in ATC, by HVEM/LIGHT interaction and secondly, we knocked down HVEM in one ATC cell line and tested its tumorigenicity profile.

We report for the first time, the activation of stress induced MAPKs in ATC cell lines resulting from HVEM/LIGHT interaction. In our model, we had treated the cells with recombinant human LIGHT to emulate the tumor microenvironment, where secretion of LIGHT from activated tumor infiltrating T cells would trigger the same response in HVEM expressing tumor cells. We observed phosphorylation of c-Jun, JNK and P38 MAPK in the ATC cell lines after treatment with LIGHT. Activation of stress induced MAPKs have been reported in TNF/TNFR interaction, but this specific interaction and its outcome in tumor cells is not reported yet. HVEM/LIGHT interaction triggered phosphorylation of  $\text{I}\kappa\text{B}\alpha$  and nuclear translocation of NF $\kappa$ B which could lead to several processes involved in tumorigenesis, such as proliferation, secretion of a several growth factors and angiogenic factors and metastasis. Increased Ki67 staining after rhLIGHT treatment suggests enhanced proliferative potential of the cells post treatment. All these processes are of high clinical significance in ATC given its rapid progression and high metastatic potential.

Silencing HVEM in ATC cell lines dampened their proliferation potential and invasive property in our model system. Both the number and size of colonies formed by HVEM-knockdown cell were smaller compared to control. These observations from specific aim 2 and 3 strongly suggest that HVEM can independently contribute to tumor progression via interaction with its cognate ligands in the TME or by some other mechanisms yet unknown. Interestingly, HVEM can have *cis* interaction with BTLA which can also trigger activation of NF $\kappa$ B via the

same pathway. We have seen co-expression of HVEM and BTLA in the ATC cell lines, which points towards this possibility, but this was not addressed in this current study.

#### Targeting HVEM/BTLA/CD160/LIGHT axis and genetic lesions in ATC: a case for combinatorial approach

BRAFV600E is the most common genetic lesion associated with aggressive and highly proliferative cancers. As a ligand independent activator of MAPK, BRAFV600E is thought to induce “oncogene addiction” in thyroid cancer and melanoma. In previous sections we have discussed the small molecule inhibitors currently in use and in clinical trials for ATC. However, eventual development of resistance is inevitable. Resistance against small molecule inhibitors can manifest itself in three different forms: innate, acquired and adaptive. Innate and acquired resistance are often associated with novel mutations and expansion of mutated clonal population in response to the drug respectively. Adaptive resistance is very interesting in that, they rewire the signaling mechanism in order to bypass the effect of the specific inhibitor.

Adaptive resistance is often associated with reactivation of the same molecular pathway or activation of compensatory pathways which transform the tumor into a more resistant phenotype and alters its microenvironment at the same time. One such mechanism responsible for acquired resistance against BRAFV600E inhibitors in ATC, is activation of HGF/MET axis (Knauf et al., 2018a). Interestingly, this study noted a higher expression of HGF with increased copy number of MET in murine model of ATC, suggesting the activation of an autocrine loop supporting tumor growth. Increasing reports of acquired and intrinsic resistance against the small molecule inhibitors emphasize the need for development of

alternative therapeutic approach for ATC patients. A good indicator of development of adaptive resistance is, reactivation of MAPK pathway via activation of CRAF. We observed significantly higher expression of active CRAF in PLX4032 resistant phenotype compared to the sensitive phenotype in our study.

Immunological consequences of this adaptive resistance are not well characterized and completely unknown in ATC. We believed a better understanding of the adaptive resistant phenotype would help us identify better actionable targets in these patients that could be targeted in a combinatorial therapeutic approach. Two BRAFV600E inhibitor (PLX4032) resistant cell lines were generated in the lab over 7 months of slowly escalated drug treatment. BRAFV600Ei – PLX4032 resistant ATC cell lines in our study, had a completely different expression profile of the immunomodulatory compared to the sensitive phenotype. Expression of HVEM was more than 100-fold higher in the resistant cell lines compared to the sensitive cell lines. BTLA had more than 10-fold upregulation in the resistant cell lines compared to normal. PD-L1, TIM3 and LGALS9B expression were highly upregulated in the resistant phenotype. This suggests activation of cellular processes during development of resistance that finally culminates into upregulation of these immunomodulatory molecules.

These observations underscore the importance of a multipronged approach while considering a new treatment modality for a patient who started out as a BRAFV600Ei sensitive phenotype but eventually developed resistance. It is of utmost importance to profile the tumor intermittently as the patient is on one specific small molecule inhibitor for a prolonged period. The development of adaptive resistance might alter the tumor phenotype in a way that the tumor becomes more amenable to another type of therapeutic intervention.

When we treated both the sensitive and resistant cell lines with a combination of BRAFV600E inhibitor PLX4032 and MEK inhibitor trametinib, expression of HVEM was mildly dampened in the sensitive phenotype, but was persistent in the resistant cells. Most of the compensatory pathways activated during development of BRAFV600Ei resistance eventually leads to upregulation of ERK. Activation of HGF/MET pathway or activation of STAT3 during development of resistance eventually culminates into upregulation of ERK (Brighton et al., 2018; Byeon et al., 2016; Knauf et al., 2018a; Titz et al., 2016). This indicates that, an ERK inhibitor might be more suitable for hyperproliferative cancers where the patients are prone to develop resistance against standard BRAF and MEK inhibitors. A recent study using ERK inhibitor LY3214996 in a panel of cell lines including melanoma, colorectal cancer, pancreatic cancer, and NSCLC, demonstrated preferential *in vitro* sensitivity towards the inhibitor in the cell lines harboring ERK pathway alterations (BRAF, KRAS, NRAS, MEK1, or NF1 mutations) (Bhagwat et al., 2020). As discussed before, recent multicenter NGS studies have confirmed that most these genetic lesions are extremely frequent in ATC, which indicates that ERK inhibitors might be a better drug of choice as small molecule inhibitor. A careful examination needs to be done to assess the potential off target effect of ERK inhibitors in ATC. Expression of HVEM and BTLA in ATC patients, and their further upregulation in the resistant phenotype, suggest that these patients might benefit from a combination of antagonistic antibodies targeting HVEM/BTLA signaling axis and ERK inhibitors depending on their tumor profile.

*The rational combinatorial approach:*

The expression profile of the components of HVEM/BTLA/CD160 axis in ATC strongly suggest an alternate therapeutic avenue that could be explored in these patients. The ideal outcome of this therapeutic approach should be increased activation of effector T cells accompanied with diminished tumor cell proliferation and re-differentiation (Fig 69).

A combination of ERK inhibitor and antagonistic antibodies targeting HVEM/BTLA axis seems to be a rational combination based on the following observations:

1. Anaplastic thyroid cancer cells have high constitutive expression of HVEM, BTLA and CD160 on their surface which can be targeted by antibodies
2. Antagonistic antibody targeting BTLA can disrupt the *cis* interaction between HVEM and BTLA on the tumor cells and *trans* interaction between tumor cells and T cells, thus preventing activation of NF $\kappa$ B in the tumor cells in the first case and dampening of anti-tumor immune response in the latter
3. Blocking BTLA would also prevent differentiation of effector T cells into regulatory T cells and in turn help immune activation
4. As we observed in our study, anaplastic thyroid cancer cells can develop resistance against BRAFV600E inhibitor, and the resistant cells have much higher expression of HVEM, BTLA, CD160, TIM3, galectin9 genes and significantly higher surface expression of HVEM protein
5. A combination of BRAFV600E inhibitor vemurafenib (PLX4032) and MEK inhibitor (trametinib) does not modulate the expression of HVEM in the resistant tumor cells

6. Introduction of an ERK inhibitor with anti-BTLA antibody might help induce redifferentiation in the de-differentiated follicular cells which would be accompanied with increased expression of NIS and re-sensitize the patient towards radioiodine ablation therapy
7. Also, inhibition of ERK would downregulate the transcription of crucial transcription factors responsible for upregulation of HVEM and BTLA in the tumor cells, such as c-Jun, STAT3, c-fos, ATF2, c-Myc.

**Our study has identified HVEM/BTLA axis as a potential immunotherapeutic target in anaplastic thyroid cancer.** Development of adaptive resistance to targeted therapies is inevitable and a combination therapy targeting the immune microenvironment can forestall therapeutic resistance in ATC and provide a promising outcome.



## CHAPTER 5: APPENDIX

### PRESENTATIONS RESULTING FROM THIS THESIS

1. **Sanjukta Chakraborty**, Tara Jarboe, Dina Dadafarin, Jan Geliebter, Augustine Moscatello, Raj K Tiwari. Implications of HVEM/BTLA/LIGHT signaling in anaplastic thyroid cancer. [abstract]. In: Proceedings of the American Association for Cancer Research Annual Meeting 2020 (rescheduled for August 2020 due to COVID-19)
2. **Sanjukta Chakraborty**, Rachana R. Maniyar, Sina Dadafarin, Ghada Ben Rahoma, Sarnath Singh, Augustine Moscatello, Jan Geliebter, Raj K. Tiwari. Combinatorial immune checkpoint inhibitor therapy in anaplastic thyroid cancer [abstract]. In: Proceedings of the American Association for Cancer Research Annual Meeting 2019; 2019 Mar 29-Apr 3; Atlanta, GA
3. **Sanjukta Chakraborty**, Rachana R. Maniyar, Neha Y. Tuli, Ghada Ben Rahoma, Sarnath Singh, Ameet Kamat, Craig Berzofsky, Cameron Budenz, Augustine Moscatello, Jan Geliebter, Raj K. Tiwari; Identification of novel immunotherapeutic targets in anaplastic thyroid cancer; In: Proceedings of the 109th Annual Meeting of the American Association for Cancer Research; 2018 Apr 14-18; Chicago, Illinois. Abstract # 2762
4. **Sanjukta Chakraborty**, Rachana R. Maniyar, Neha Y. Tuli, Ghada Ben Rahoma, Cameron Budenz, Sarnath Singh, Jan Geliebter and Raj Tiwari; Functional pairing of immunomodulatory targets in anaplastic thyroid cancer; In: Proceedings of the American Association for Cancer Research Annual Meeting 2017; 2017 Apr 1-5; Washington, DC. Abstract# 5676

## BIBLIOGRAPHY

- Abubaker, J., Jehan, Z., Bavi, P., Sultana, M., A-Harbi, S., Ibrahim, M., Al-Nuaim, A., Ahmed, M., Amin, T., Al-Fehaily, M., Al-Sanea, O., Al-Dayel, F., Uddin, S., & Al-Kuraya, K. S. (2008).** Clinicopathological Analysis of Papillary Thyroid Cancer with PIK3CA Alterations in a Middle Eastern Population. *J Clin Endocrinol Metab*, 93, 611–618. <https://doi.org/10.1210/jc.2007-1717>
- Agrawal, N., Akbani, R., Arman Aksoy, B., Ally, A., Arachchi, H., Asa, S. L., Todd Auman, J., Balasundaram, M., Balu, S., Baylin, S. B., Behera, M., Bernard, B., Beroukhim, R., Bishop, J. A., Black, A. D., Bodenheimer, T., Boice, L., Bootwalla, M. S., Bowen, J., ... Zou, L. (2014).** Integrated Genomic Characterization of Papillary Thyroid Carcinoma. *Cell*, 159, 676–690. <https://doi.org/10.1016/j.cell.2014.09.050>
- Ahn, S., Kim, T. H., Kim, S. W., Ki, C. S., Jang, H. W., Kim, J. S., Kim, J. H., Choe, J. H., Shin, J. H., Hahn, S. Y., Oh, Y. L., & Chung, J. H. (2017).** Comprehensive screening for PD-L1 expression in thyroid cancer. *Endocrine-Related Cancer*, 24, 97–106. <https://doi.org/10.1530/ERC-16-0421>
- Al-Salamah, S. M., Khalid, K., & Bismar, H. A. (2002).** Incidence of differentiated cancer in nodular goiter. *Saudi Medical Journal*, 23, 947–952. <http://www.ncbi.nlm.nih.gov/pubmed/12235469>
- Angell, T. E., Lechner, M. G., Jang, J. K., LoPresti, J. S., & Epstein, A. L. (2014).** MHC class I loss is a frequent mechanism of immune escape in papillary thyroid cancer that is reversed by interferon and selumetinib treatment in Vitro. *Clinical Cancer Research*, 20, 6034–6044. <https://doi.org/10.1158/1078-0432.CCR-14-0879>
- Antohe, M., Nedelcu, R. I., Nichita, L., Popp, C. G., Cioplea, M., Brinzea, A., Hodoroagea, A., Calinescu, A., Balaban, M., Ion, D. A., Diaconu, C., Bleotu, C., Pirici, D., Zurac, S. A., & Turcu, G. (2019).** Tumor infiltrating lymphocytes: The regulator of melanoma evolution (Review). *Oncology Letters*, 17, 4155–4161. <https://doi.org/10.3892/ol.2019.9940>
- Antonello, Z. A., Hsu, N., Bhasin, M., Roti, G., Joshi, M., Van Hummelen, P., Ye, E., Lo, A. S., Karumanchi, S. A., Bryke, C. R., & Nucera, C. (2017).** Vemurafenib-resistance via de novo RBM genes mutations and chromosome 5 aberrations is overcome by combined therapy with palbociclib in thyroid carcinoma with BRAFV600E. *Oncotarget*, 8, 84743–84760. <https://doi.org/10.18632/oncotarget.21262>
- Aschebrook-Kilfoy, B., Schechter, R. B., Tina Shih, Y.-C., Kaplan, E. L., C-H Chiu, B., Angelos, P., & Grogan, R. H. (2013).** *The Clinical and Economic Burden of a Sustained Increase in Thyroid Cancer Incidence*. <https://doi.org/10.1158/1055-9965.EPI-13-0242>
- Balasubramaniam, S., Ron, E., Gridley, G., Schneider, A. B., & Brenner, A. V. (1969).** Association between Benign Thyroid and Endocrine Disorders and Subsequent Risk of Thyroid Cancer among 4.5 Million U.S. Male Veterans. *J Clin Endocrinol Metab*, 97, 2661–2669. <https://doi.org/10.1210/jc.2011-2996>
- Barber, D. L., Wherry, E. J., Masopust, D., Zhu, B., Allison, J. P., Sharpe, A. H., Freeman, G. J., & Ahmed, R. (2005).** Restoring function in exhausted CD8 T cells during chronic viral infection. *Nature*, 439, 682–687.
- Basolo, F., Giannini, R., Toniolo, A., Casalone, R., Nikiforova, M., Pacini, F., Elisei, R., Miccoli, P.,**

- Berti, P., Faviana, P., Fiore, L., Monaco, C., Pierantoni, G. M., Fedele, M., Nikiforov, Y. E., Santoro, M., & Fusco, A.** (2002). Establishment of a non-tumorigenic papillary thyroid cell line (FB-2) carrying the RET/PTC1 rearrangement. *International Journal of Cancer*, 97, 608–614. <https://doi.org/10.1002/ijc.10116>
- Benavenga, S., Tuccari, G., Ieni, A., & Vita, R.** (2018). Thyroid Gland: Anatomy and Physiology. In *Encyclopedia of Endocrine Diseases* (2nd ed., Issue April). Elsevier Inc. <https://doi.org/10.1016/b978-0-12-801238-3.96022-7>
- Bertrand, F., Montfort, A., Marcheteau, E., Imbert, C., Gilhodes, J., Filleron, T., Rochaix, P., Andrieu-Abadie, N., Levade, T., Meyer, N., Colacios, C., & Ségui, B.** (2017). TNF $\alpha$  blockade overcomes resistance to anti-PD-1 in experimental melanoma. *Nature C*, 8, 1–13. <https://doi.org/10.1038/s41467-017-02358-7>
- Bevenga, S., & Robbins, J.** (1996). Altered Thyroid Hormone Binding to Plasma Lipoproteins in Hypothyroidism. *Thyroid*, 6, 595–600. <https://doi.org/10.1089/thy.1996.6.595>
- Bhagwat, S. V., McMillen, W. T., Cai, S., Zhao, B., Whitesell, M., Shen, W., Kindler, L., Flack, R. S., Wu, W., Anderson, B., Zhai, Y., Yuan, X. J., Pogue, M., Van Horn, R. D., Rao, X., McCann, D., Dropsey, A. J., Manro, J., Walgren, J., ... Peng, S. Bin.** (2020). ERK Inhibitor LY3214996 Targets ERK Pathway-Driven Cancers: A Therapeutic Approach Toward Precision Medicine. *Molecular Cancer Therapeutics*, 19, 325–336. <https://doi.org/10.1158/1535-7163.MCT-19-0183>
- Bhatia, S., & Berry, S.** (2016). PD-1 Blockade with Pembrolizumab in Advanced Merkel-Cell Carcinoma. *Johns Hopkins University School of Medicine and Kimmel Cancer Center*, 374, 2542–2552. <https://doi.org/10.1056/NEJMoa1603702>
- Bible, K. C., & Ryder, M.** (2016). Evolving molecularly targeted therapies for advanced-stage thyroid cancers. *Nature Reviews Clinical Oncology*, 13, 403–416. <https://doi.org/10.1038/nrclinonc.2016.19>
- Blagih, J., Zani, F., Chakravarty, P., Hennequart, M., Pilley, S., Hobor, S., Hock, A. K., Walton, J. B., Morton, J. P., Gronroos, E., Mason, S., Yang, M., McNeish, I., Swanton, C., Blyth, K., & Vousden, K. H.** (2020). Cancer-Specific Loss of p53 Leads to a Modulation of Myeloid and T Cell Responses. *Cell Reports*, 30, 481-496.e6. <https://doi.org/10.1016/j.celrep.2019.12.028>
- Bommarito, A., Richiusa, P., Carissimi, E., Pizzolanti, G., Rodolico, V., Zito, G., Criscimanna, A., Di Blasi, F., Pitrone, M., Zerilli, M., Amato, M. C., Spinelli, G., Carina, V., Modica, G., Latteri, A., Galluzzo, A., & Giordano, C.** (2011). BRAF V600E mutation, TIMP-1 upregulation, and NF- $\kappa$ B activation: Closing the loop on the papillary thyroid cancer trilogy. *Endocrine-Related Cancer*, 18, 669–685. <https://doi.org/10.1530/ERC-11-0076>
- Brauner, E., Gunda, V., Borre, P., Vanden, Zurakowski, D., Kim, Y. S., Dennett, K. V., Amin, S., Freeman, G. J., & Parangi, S.** (2016). Combining BRAF inhibitor and anti PD-L1 antibody dramatically improves tumor regression and anti tumor immunity in an immunocompetent murine model of anaplastic thyroid cancer. *Oncotarget*, 7. [www.impactjournals.com/oncotarget](http://www.impactjournals.com/oncotarget)
- Brighton, H. E., Angus, S. P., Bo, T., Roques, J., Tagliatela, A. C., Darr, D. B., Karagoz, K., Sciaky, N., Gatz, M. L., Sharpless, N. E., Johnson, G. L., & Bear, J. E.** (2018). New mechanisms of resistance to MEK inhibitors in melanoma revealed by intravital imaging. *Cancer Research*, 78, 542–557. <https://doi.org/10.1158/0008-5472.CAN-17-1653>

- Brose, M. S., Robinson, B., Bermingham, C., Puvvada, S., Borgman, A. E., Krzyzanowska, M. K., Capdevila, J., & Sherman, S. I.** (2019). A phase 3 (COSMIC-311), randomized, double-blind, placebo-controlled study of cabozantinib in patients with radioiodine (RAI)-refractory differentiated thyroid cancer (DTC) who have progressed after prior VEGFR-targeted therapy. *Journal of Clinical Oncology*, 37, TPS6097–TPS6097. [https://doi.org/10.1200/jco.2019.37.15\\_suppl.tps6097](https://doi.org/10.1200/jco.2019.37.15_suppl.tps6097)
- Brose, M. S., Worden, F. P., Newbold, K. L., Guo, M., & Hurria, A.** (2017). Effect of age on the efficacy and safety of lenvatinib in radioiodine-refractory differentiated thyroid cancer in the phase III select trial. *Journal of Clinical Oncology*, 35, 2692–2699. <https://doi.org/10.1200/JCO.2016.71.6472>
- Byeon, H. K., Na, H. J., Yang, Y. J., Kwon, H. J., Chang, J. W., Ban, M. J., Kim, W. S., Shin, D. Y., Lee, E. J., Koh, Y. W., Yoon, J. H., & Choi, E. C.** (2016). c-Met-mediated reactivation of PI3K/AKT signaling contributes to insensitivity of BRAF(V600E) mutant thyroid cancer to BRAF inhibition. *Molecular Carcinogenesis*, 55, 1678–1687. <https://doi.org/10.1002/mc.22418>
- Cabanillas, M. E., De Souza, J. A., Geyer, S., Wirth, L. J., Menefee, M. E., Liu, S. V., Shah, K., Wright, J., & Shah, M. H.** (2017). Cabozantinib as salvage therapy for patients with tyrosine kinase inhibitor-refractory differentiated thyroid cancer: Results of a multicenter phase II international thyroid oncology group trial. *Journal of Clinical Oncology*, 35, 3315–3321. <https://doi.org/10.1200/JCO.2017.73.0226>
- Caillou, B., Talbot, M., Weyemi, U., Pioche-Durieu, C., Ghuzlan, A., Bidart, J. M., Chouaib, S., Schlumberger, M., & Dupuy, C.** (2011). Tumor-Associated macrophages (TAMs) form an interconnected cellular supportive network in anaplastic thyroid carcinoma. *PLoS ONE*, 6. <https://doi.org/10.1371/journal.pone.0022567>
- Carvalho, D. F. G., Zanetti, B. R., Miranda, L., Hassumi-Fukasawa, M. K., Miranda-Camargo, F., Crispim, J. C. O., & Soares, E. G.** (2017). High IL-17 expression is associated with an unfavorable prognosis in thyroid cancer. *Oncology Letters*, 13, 1925–1931. <https://doi.org/10.3892/ol.2017.5638>
- Carvalho, D. P., & Dupuy, C.** (2017). Thyroid hormone biosynthesis and release. *Molecular and Cellular Endocrinology*, 458, 6–15. <https://doi.org/10.1016/j.mce.2017.01.038>
- Chen, J., Feng, Y., Lu, L., Wang, H., Dai, L., Li, Y., & Zhang, P.** (2012). Interferon- $\gamma$ -induced PD-L1 surface expression on human oral squamous carcinoma via PKD2 signal pathway. *Immunobiology*, 217, 385–393. <https://doi.org/10.1016/j.imbio.2011.10.016>
- Cheng, S. Y., Leonard, J. L., & Davis, P. J.** (2010). Molecular aspects of thyroid hormone actions. *Endocrine Reviews*, 31, 139–170. <https://doi.org/10.1210/er.2009-0007>
- Cho, A., Chang, Y., Ahn, J., Shin, H., & Ryu, S.** (2018). Cigarette smoking and thyroid cancer risk: a cohort study. *British Journal of Cancer*, 119, 638–645. <https://doi.org/10.1038/s41416-018-0224-5>
- Cohen, Y., Xing, M., Mambo, E., Guo, Z., Wu, G., Trink, B., Beller, U., Westra, W. H., Ladenson, P. W., & Sidransky, D.** (2003). *BRAF Mutation in Papillary Thyroid Carcinoma*. <https://academic.oup.com/jnci/article-abstract/95/8/625/2520710>
- Cooper, D. S., Doherty, G. M., Haugen, B. R., Kloos, R. T., Lee, S. L., Mandel, S. J., Mazzaferri, E. L.,**

- McClever, B., Sehrman, S. I., & Tuttle, R. M.** (2006). Management Guidelines for Patients with Thyroid Nodules and Differentiated Thyroid Cancer. *Thyroid*, 16, 109–142.  
<https://doi.org/10.1089/thy.2014.0460>
- Corrigan, K. L., Williamson, H., Elliott Range, D., Niedzwiecki, D., Brizel, D. M., & Mowery, Y. M.** (2019). Treatment outcomes in anaplastic thyroid cancer. *Journal of Thyroid Research*, 2019.  
<https://doi.org/10.1155/2019/8218949>
- Cunha, L. L., Marcello, M. A., Nonogaki, S., Morari, E. C., Soares, F. A., Vassallo, J., & Ward, L. S.** (2015). CD8+ tumour-infiltrating lymphocytes and COX2 expression may predict relapse in differentiated thyroid cancer. *Clinical Endocrinology*, 83, 246–253.  
<https://doi.org/10.1111/cen.12586>
- Cunha, L. L., Marcello, M. A., & Ward, L. S.** (2014). The role of the inflammatory microenvironment in thyroid carcinogenesis. *Endocrine-Related Cancer*, 21. <https://doi.org/10.1530/ERC-13-0431>
- Davies, L., Ouellette, M., Hunter, M., & Welch, H. G.** (2010). The increasing incidence of small thyroid cancers: Where are the cases coming from? *Laryngoscope*, 120, 2446–2451.  
<https://doi.org/10.1002/lary.21076>
- Davies, L., & Welch, H. G.** (2014). Current thyroid cancer trends in the United States. *JAMA Otolaryngology - Head and Neck Surgery*, 140, 317–322.  
<https://doi.org/10.1001/jamaoto.2014.1>
- del Rio, M. L., Lucas, C. L., Buhler, L., Rayat, G., & Rodriguez-Barbosa, J. I.** (2010a). HVEM/LIGHT/BTLA/CD160 cosignaling pathways as targets for immune regulation. *Journal of Leukocyte Biology*, 87, 223–235. <https://doi.org/10.1189/jlb.0809590>
- del Rio, M. L., Lucas, C. L., Buhler, L., Rayat, G., & Rodriguez-Barbosa, J. I.** (2010b). HVEM/LIGHT/BTLA/CD160 cosignaling pathways as targets for immune regulation. *Journal of Leukocyte Biology*, 87, 223–235. <https://doi.org/10.1189/jlb.0809590>
- Dettmer, M. S., Schmitt, A., Komminoth, P., & Perren, A.** (2019). Poorly differentiated thyroid carcinoma. *Der Pathologe*, 1–8. <https://doi.org/10.1007/s00292-019-0600-9>
- Di Desidero, T., Orlandi, P., Gentile, D., & Bocci, G.** (2019). Effects of Pazopanib Monotherapy vs. Pazopanib and Topotecan Combination on Anaplastic Thyroid Cancer Cells. *Frontiers in Oncology*, 9, 1–9. <https://doi.org/10.3389/fonc.2019.01202>
- Diamantopoulos, P. T., Gaggadi, M., Kassi, E., Benopoulou, O., Anastasopoulou, A., & Gogas, H.** (2017). Late-onset nivolumab-mediated pneumonitis in a patient with melanoma and multiple immune-related adverse events. *Melanoma Research*, 27, 391–395.  
<https://doi.org/10.1097/CMR.0000000000000355>
- Dong, P., Xiong, Y., Yue, J., Hanley, S. J. B., & Watari, H.** (2018). B7H3 As a promoter of metastasis and promising therapeutic target. *Frontiers in Oncology*, 8, 1–8.  
<https://doi.org/10.3389/fonc.2018.00264>
- Duquette, M., Sadow, P. M., Husain, A., Sims, J. N., Antonello, Z. A., Fischer, A. H., Song, C., Castellanos-Rizaldos, E., Mike Makrigiorgos, G., Kurebayashi, J., Nose, V., Van Hummelen, P., Bronson, R. T., Vinco, M., Giordano, T. J., Dias-Santagata, D., Pandolfi, P. P., & Nucera, C.** (2015). Metastasis-associated MCL1 and P16 copy number alterations dictate resistance to vemurafenib in a BRAFV600E patient-derived papillary thyroid carcinoma preclinical model.

*Oncotarget*, 6, 42445–42467. <https://doi.org/10.18632/oncotarget.6442>

- Durante, C., Haddy, N., Baudin, E., Leboulleux, S., Hartl, D., Travagli, J. P., Caillou, B., Ricard, M., Lumbroso, J. D., De Vathaire, F., & Schlumberger, M.** (2006). Long-term outcome of 444 patients with distant metastases from papillary and follicular thyroid carcinoma: Benefits and limits of radioiodine therapy. *Journal of Clinical Endocrinology and Metabolism*, 91, 2892–2899. <https://doi.org/10.1210/jc.2005-2838>
- Düsterhöft, S., Lokau, J., & Garbers, C.** (2019). The metalloprotease ADAM17 in inflammation and cancer. *Pathology Research and Practice*, 215, 152410. <https://doi.org/10.1016/j.prp.2019.04.002>
- Dwight, T., Thoppe, S. R., Foukakis, T., Lui, W. O., Wallin, G., Höög, A., Frisk, T., Larsson, C., & Zedenius, J.** (2003). Involvement of the PAX8/peroxisome proliferator-activated receptor  $\gamma$  rearrangement in follicular thyroid tumors. *Journal of Clinical Endocrinology and Metabolism*, 88, 4440–4445. <https://doi.org/10.1210/jc.2002-021690>
- Eberhardt, N. L., Grebe, S. K. G., Mclver, B., & Reddi, H. V.** (2010). The role of the PAX8/PPAR $\gamma$  fusion oncogene in the pathogenesis of follicular thyroid cancer. *Molecular and Cellular Endocrinology*, 321, 50–56. <https://doi.org/10.1016/j.mce.2009.10.013>
- El Lakis, M., Giannakou, A., Nockel, P. J., Wiseman, D., Gara, S. K., Patel, D., Sater, Z. A., Kushchayeva, Y. Y., Klubo-Gwiedzinska, J., Nilubol, N., Merino, M. J., & Kebebew, E.** (2019). Do patients with familial nonmedullary thyroid cancer present with more aggressive disease? Implications for initial surgical treatment. *Surgery (United States)*, 165, 50–57. <https://doi.org/10.1016/j.surg.2018.05.075>
- Etit, D., Faquin, W. C., Gaz, R., Randolph, G., Delellis, R. A., & Pilch, B. Z.** (2008). Histopathologic and Clinical Features of Medullary Microcarcinoma and C-Cell Hyperplasia in Prophylactic Thyroidectomies for Medullary Carcinoma A Study of 42 Cases. In *Arch Pathol Lab Med* (Vol. 132).
- Evaluation of Efficacy, Safety of Vandetanib in Patients With Differentiated Thyroid Cancer - Study Results - ClinicalTrials.gov.* (n.d.). Retrieved February 23, 2020, from <https://clinicaltrials.gov/ct2/show/results/NCT01876784>
- Fakhrudin, N., Jabbour, M., Novy, M., Tamim, H., Bahmad, H., Farhat, F., Zaatari, G., Aridi, T., Kriegshauser, G., Oberkanins, C., & Mahfouz, R.** (n.d.). *BRAF and NRAS Mutations in Papillary Thyroid Carcinoma and Concordance in BRAF Mutations Between Primary and Corresponding Lymph Node Metastases*. <https://doi.org/10.1038/s41598-017-04948-3>
- Fang, W., Ye, L., Shen, L., Cai, J., Huang, F., Wei, Q., Fei, X., Chen, X., Guan, H., Wang, W., Li, X., & Ning, G.** (2014). Tumor-associated macrophages promote the metastatic potential of thyroid papillary cancer by releasing CXCL8. *Carcinogenesis*, 35, 1780–1787. <https://doi.org/10.1093/carcin/bgu060>
- Fang, Y., Ye, L., Zhang, T., He, Q. Z., & Zhu, J. L.** (2017). High expression of herpesvirus entry mediator (HVEM) in ovarian serous adenocarcinoma tissue. *Journal of B.U.ON.*, 22, 80–86. [www.jbuon.com](http://www.jbuon.com)
- Faria, M., Matos, P., Pereira, T., Cabrera, R., Cardoso, B. A., Bugalho, M. J., & Silva, A. L.** (2017). RAC1b overexpression stimulates proliferation and NF- $\kappa$ B-mediated antiapoptotic signaling in

thyroid cancer cells. *PLoS ONE*, 12, 1–13. <https://doi.org/10.1371/journal.pone.0172689>

- Feng, X. Y., Wen, X. Z., Tan, X. J., Hou, J. H., Ding, Y., Wang, K. F., Dong, J., Zhou, Z. W., Chen, Y. B., & Zhang, X. S.** (2015). Ectopic expression of B and T lymphocyte attenuator in gastric cancer: A potential independent prognostic factor in patients with gastric cancer. *Molecular Medicine Reports*, 11, 658–664. <https://doi.org/10.3892/mmr.2014.2699>
- Ferrari, S. M., Elia, G., Ragusa, F., Ruffilli, I., La Motta, C., Paparo, S. R., Patrizio, A., Vita, R., Benvenga, S., Materazzi, G., Fallahi, P., & Antonelli, A.** (2020). Novel treatments for anaplastic thyroid carcinoma. *Gland Surgery*, 9, S28–S42. <https://doi.org/10.21037/gs.2019.10.18>
- Fischer, K. R., Durrans, A., Lee, S., Sheng, J., Li, F., Wong, S. T. C., Choi, H., El Rayes, T., Ryu, S., Troeger, J., Schwabe, R. F., Vahdat, L. T., Altorki, N. K., Mittal, V., & Gao, D.** (2015). Epithelial-to-mesenchymal transition is not required for lung metastasis but contributes to chemoresistance. *Nature*, 527, 472–476. <https://doi.org/10.1038/nature15748>
- Flatz, L., Berner, F., Bomze, D., Diem, S., Ali, O. H., Fässler, M., Ring, S., Niederer, R., Ackermann, C. J., Baumgaertner, P., Pikor, N., Cruz, C. G., Van De Veen, W., Akdis, M., Nikolaev, S., Läubli, H., Zippelius, A., Hartmann, F., Cheng, H. W., ... Speiser, D. E.** (2019). Association of Checkpoint Inhibitor-Induced Toxic Effects with Shared Cancer and Tissue Antigens in Non-Small Cell Lung Cancer. *JAMA Oncology*, 5, 1043–1047. <https://doi.org/10.1001/jamaoncol.2019.0402>
- Forster, M. D., & Devlin, M. J.** (2018). Immune checkpoint inhibition in head and neck cancer. *Frontiers in Oncology*, 8, 1–9. <https://doi.org/10.3389/fonc.2018.00310>
- Foukakis, T., Au, A. Y. M., Wallin, G., Geli, J., Forsberg, L., Clifton-Bligh, R., Robinson, B. G., Lui, W. O., Zedenius, J., & Larsson, C.** (2006). The Ras effector NORE1A is suppressed in follicular thyroid carcinomas with a PAX8-PPAR $\gamma$  fusion. *Journal of Clinical Endocrinology and Metabolism*, 91, 1143–1149. <https://doi.org/10.1210/jc.2005-1372>
- Frederick, D. T., Piris, A., Cogdill, A. P., Cooper, Z. A., Lezcano, C., Ferrone, C. R., Mitra, D., Boni, A., Newton, L. P., Liu, C., Peng, W., Sullivan, R. J., Lawrence, D. P., Hodi, F. S., Overwijk, W. W., Lizée, G., Murphy, G. F., Hwu, P., Flaherty, K. T., ... Wargo, J. A.** (2013). BRAF inhibition is associated with enhanced melanoma antigen expression and a more favorable tumor microenvironment in patients with metastatic melanoma. *Clinical Cancer Research*, 19, 1225–1231. <https://doi.org/10.1158/1078-0432.CCR-12-1630>
- Fridman, W. H., Zitvogel, L., Sautès-Fridman, C., & Kroemer, G.** (2017). The immune contexture in cancer prognosis and treatment. *Nature Reviews Clinical Oncology*, 14, 717–734. <https://doi.org/10.1038/nrclinonc.2017.101>
- Fukushima, T., Suzuki, S., Mashiko, M., Ohtake, T., Endo, Y., Takebayashi, Y., Sekikawa, K., Hagiwara, K., & Takenoshita, S.** (2003). BRAF mutations in papillary carcinomas of the thyroid. *Oncogene*, 22, 6455–6457. <https://doi.org/10.1038/sj.onc.1206739>
- Ganly, I., Makarov, V., Deraje, S., Dong, Y., Reznik, E., Seshan, V., Nanjangud, G., Eng, S., Bose, P., Kuo, F., Morris, L. G. T., Landa, I., Blecua, P., Albornoz, C., Riaz, N., Nikiforov, Y. E., Patel, K., Umbricht, C., Zeiger, M., ... Chan, T. A.** (2018). Integrated genomic analysis of Hürthle cell cancer reveals oncogenic drivers, recurrent mitochondrial mutations, and unique chromosomal landscapes HHS Public Access. *Cancer Cell*, 34, 256–270. <https://doi.org/10.1016/j.ccell.2018.07.002>

- Gavrieli, M., & Murphy, K. M.** (2006). Association of Grb-2 and PI3K p85 with phosphotyrosine peptides derived from BTLA. *Biochemical and Biophysical Research Communications*, 345, 1440–1445. <https://doi.org/10.1016/j.bbrc.2006.05.036>
- Gavrieli, M., Watanabe, N., Loftin, S. K., Murphy, T. L., & Murphy, K. M.** (2003). Characterization of phosphotyrosine binding motifs in the cytoplasmic domain of B and T lymphocyte attenuator required for association with protein tyrosine phosphatases SHP-1 and SHP-2. *Biochemical and Biophysical Research Communications*, 312, 1236–1243. <https://doi.org/10.1016/j.bbrc.2003.11.070>
- Giannini, R., Moretti, S., Ugolini, C., Macerola, E., Menicali, E., Nucci, N., Morelli, S., Colella, R., Mandarano, M., Sidoni, A., Panfili, M., Basolo, F., & Puxeddu, E.** (2019). Immune Profiling of Thyroid Carcinomas Suggests the Existence of Two Major Phenotypes: An ATC-Like and a PDTC-Like. *The Journal of Clinical Endocrinology and Metabolism*, 104, 3557–3575. <https://doi.org/10.1210/jc.2018-01167>
- Gilbert, L. A., Horlbeck, M. A., Adamson, B., Villalta, J. E., Chen, Y., Whitehead, E. H., Guimaraes, C., Panning, B., Ploegh, H. L., Bassik, M. C., Qi, L. S., Kampmann, M., & Weissman, J. S.** (2014). *Genome-Scale CRISPR-Mediated Control of Gene Repression and Activation*. <https://doi.org/10.1016/j.cell.2014.09.029>
- Glaire, M. A., Domingo, E., Sveen, A., Bruun, J., Nesbakken, A., Nicholson, G., Novelli, M., Lawson, K., Oukrif, D., Kildal, W., Danielsen, H. E., Kerr, R., Kerr, D., Tomlinson, I., Lothe, R. A., & Church, D. N.** (2019). Tumour-infiltrating CD8+ lymphocytes and colorectal cancer recurrence by tumour and nodal stage. *British Journal of Cancer*, March. <https://doi.org/10.1038/s41416-019-0540-4>
- Godbert, Y., Figueiredo, B. F. B., Chibon, F., Pe´rot, I. H. and G., Dupin, C., Daubech, A., Belleanne´e, G., & Italiano, A.** (2015). Remarkable Response to Crizotinib in Woman With Anaplastic Lymphoma. *Clinical Oncology*, 33, 84–88.
- Gopal, R. K., Kübler, K., Calvo, S. E., Polak, P., Livitz, D., Rosebrock, D., Sadow, P. M., Campbell, B., Donovan, S. E., Amin, S., & Gigliotti, B. J.** (2018). Widespread chromosomal losses and mitochondrial DNA alterations as genetic drivers in Hürthle cell Carcinoma HHS Public Access. *Cancer Cell*, 34, 242–255. <https://doi.org/10.1016/j.ccell.2018.06.013>
- Graceffa, G., Patrone, R., Vieni, S., Campanella, S., Calamia, S., Laise, I., Conzo, G., Latteri, M., & Cipolla, C.** (2019). Association between Hashimoto’s thyroiditis and papillary thyroid carcinoma: A retrospective analysis of 305 patients. *BMC Endocrine Disorders*, 19, 4–9. <https://doi.org/10.1186/s12902-019-0351-x>
- Guarino, V., Castellone, M. D., Avilla, E., & Melillo, R. M.** (2010). Thyroid cancer and inflammation. *Molecular and Cellular Endocrinology*, 321, 94–102. <https://doi.org/10.1016/j.mce.2009.10.003>
- Guerra, A., Sapio, M. R., Marotta, V., Campanile, E., Rossi, S., Forno, I., Fugazzola, L., Budillon, A., Moccia, T., Fenzi, G., & Vitale, M.** (2012). The primary occurrence of BRAFV600E is a rare clonal event in papillary thyroid carcinoma. *Journal of Clinical Endocrinology and Metabolism*, 97, 517–524. <https://doi.org/10.1210/jc.2011-0618>
- Hammes, S. R., & Davis, P. J.** (2015). Overlapping nongenomic and genomic actions of thyroid hormone and steroids. In *Best Practice and Research: Clinical Endocrinology and Metabolism*

(Vol. 29, Issue 4, pp. 581–593). Bailliere Tindall Ltd.  
<https://doi.org/10.1016/j.beem.2015.04.001>

- Hanly, E. K., Tuli, N. Y., Bednarczyk, R. B., Suriano, R., Geliebter, J., Moscatello, A. L., Darzynkiewicz, Z., & Tiwari, R. K.** (2016). Hyperactive ERK and persistent mTOR signaling characterize vemurafenib resistance in papillary thyroid cancer cells. *Oncotarget*, 7, 8676–8687. <https://doi.org/10.18632/oncotarget.6779>
- Harjunpää, H., & Guillerey, C.** (2019). TIGIT as an emerging immune checkpoint. *Clinical and Experimental Immunology*, 1–12. <https://doi.org/10.1111/cei.13407>
- Haugen, B. R., Alexander, E. K., Bible, K. C., Doherty, G. M., Mandel, S. J., Nikiforov, Y. E., Pacini, F., Randolph, G. W., Sawka, A. M., Schlumberger, M., Schuff, K. G., Sherman, S. I., Sosa, J. A., Steward, D. L., Tuttle, R. M., & Wartofsky, L.** (2016). 2015 American Thyroid Association Management Guidelines for Adult Patients with Thyroid Nodules and Differentiated Thyroid Cancer: The American Thyroid Association Guidelines Task Force on Thyroid Nodules and Differentiated Thyroid Cancer. *Thyroid*, 26, 1–133. <https://doi.org/10.1089/thy.2015.0020>
- Hayashi, H., Ichihara, M., Iwashita, T., Murakami, H., Shimono, Y., Kawai, K., Kurokawa, K., Murakumo, Y., Imai, T., Funahashi, H., Nakao, A., & Takahashi, M.** (2000). Characterization of intracellular signals via tyrosine 1062 in RET activated by glial cell line-derived neurotrophic factor. [www.nature.com/onc](http://www.nature.com/onc)
- Hazard, J. B.** (1977). The C Cells (Parafollicular Cells) of the Thyroid Gland and Medullary Thyroid Carcinoma A Review. *American Journal of Pathology*, 88, 213–250.
- Hemingway, F., Kashima, T. G., Knowles, H. J., & Athanasou, N. A.** (2013). Investigation of osteoclastogenic signalling of the RANKL substitute LIGHT. *Experimental and Molecular Pathology*, 94, 380–385. <https://doi.org/10.1016/j.yexmp.2013.01.003>
- Ho Ji, J., Lyun Oh, Y., Hong, M., Won Yun, J., Lee, H.-W., Kim, D., Ji, Y., Kim, D.-H., Park, W.-Y., Shin, H.-T., Kim, K.-M., Ahn, M.-J., Park, K., Sun, J.-M., H-w, L., & Nikiforov, Y. E.** (2015). Identification of Driving ALK Fusion Genes and Genomic Landscape of Medullary Thyroid Cancer. *PLoS Genet*, 11, 1005467. <https://doi.org/10.1371/journal.pgen.1005467>
- Hoang, J. K., Branstetter IV, B. F., Gafton, A. R., Lee, W. K., & Glastonbury, C. M.** (2013). Imaging of thyroid carcinoma with CT and MRI: Approaches to common scenarios. *Cancer Imaging*, 13, 128–139. <https://doi.org/10.1102/1470-7330.2013.0013>
- Hoermann, R., Midgley, J. E. M., Larisch, R., & Dietrich, J. W.** (2015). Homeostatic control of the thyroid-pituitary axis: Perspectives for diagnosis and treatment. In *Frontiers in Endocrinology* (Vol. 6, Issue NOV). Frontiers Research Foundation. <https://doi.org/10.3389/fendo.2015.00177>
- Hou, P., Ji, M., & Xing, M.** (2008). Association of PTEN gene methylation with genetic alterations in the phosphatidylinositol 3-kinase/AKT signaling pathway in thyroid tumors. *Cancer*, 113, 2440–2447. <https://doi.org/10.1002/cncr.23869>
- Hu, S., Liu, D., Tufano, R. P., Carson, K. A., Rosenbaum, E., Cohen, Y., Holt, E. H., Kiseljak-Vassiliades, K., Rhoden, K. J., Tolaney, S., Condouris, S., Tallini, G., Westra, W. H., Umbricht, C. B., Zeiger, M. A., Califano, J. A., Vasko, V., & Xing, M.** (2006). Association of aberrant methylation of tumor suppressor genes with tumor aggressiveness and BRAF mutation in papillary thyroid cancer. *International Journal of Cancer*, 119, 2322–2329.

<https://doi.org/10.1002/ijc.22110>

- Huang, M., Yan, C., Xiao, J., Wang, T., & Ling, R.** (n.d.). *Relevance and clinicopathologic relationship of BRAF V600E, TERT and NRAS mutations for papillary thyroid carcinoma patients in Northwest China*. <https://doi.org/10.1186/s13000-019-0849-6>
- Huang, N. S., Shi, X., Lei, B. W., Wei, W. J., Lu, Z. W., Yu, P. C., Wang, Y., Ji, Q. H., & Wang, Y. L.** (2019). An Update of the Appropriate Treatment Strategies in Anaplastic Thyroid Cancer: A Population-Based Study of 735 Patients. *International Journal of Endocrinology*, 2019. <https://doi.org/10.1155/2019/8428547>
- Hundahl, S. A., Fleming, I. D., Fremgen, A. M., & Menck, H. R.** (1998). A National Cancer Data Base report on 53,856 cases of thyroid carcinoma treated in the U.S., 1985-1995. *Cancer*, 83, 2638–2648. [https://doi.org/10.1002/\(SICI\)1097-0142\(19981215\)83:12<2638::AID-CNCR31>3.0.CO;2-1](https://doi.org/10.1002/(SICI)1097-0142(19981215)83:12<2638::AID-CNCR31>3.0.CO;2-1)
- Hyman, D. M., Puzanov, I., Subbiah, V., Faris, J. E., Chau, I., Blay, J.-Y., Wolf, J., Raje, N. S., Diamond, E. L., Hollebecque, A., Gervais, R., Elez-Fernandez, M. E., Italiano, A., Hofheinz, R.-D., Hidalgo, M., Chan, E., Schuler, M., Lasserre, S. F., Makrutzki, M., ... Baselga, J.** (2015). Vemurafenib in Multiple Nonmelanoma Cancers with BRAF V600 Mutations. *New England Journal of Medicine*, 373, 726–736. <https://doi.org/10.1056/NEJMoa1502309>
- Inoue, T., Sho, M., Yasuda, S., Nishiwada, S., Nakamura, S., Ueda, T., Nishigori, N., Kawasaki, K., Obara, S., Nakamoto, T., Koyama, F., Fujii, H., & Nakajima, Y.** (2015). HVEM expression contributes to tumor progression and prognosis in human colorectal cancer. *Anticancer Research*, 35, 1361–1368. <https://doi.org/35/3/1361> [pii]
- Iryani Abdullah, M., Mat Junit, S., Leong Ng, K., Jacqueline Jayapalan, J., Karikalan, B., Haji Hashim, O., & Onn Haji Hashim, P.** (2019). Papillary Thyroid Cancer: Genetic Alterations and Molecular Biomarker Investigations. *Int. J. Med. Sci*, 16, 450–460. <https://doi.org/10.7150/ijms.29935>
- Iwasaki, H., Toda, S., Suganuma, N., Murayama, D., Nakayama, H., & Masudo, K.** (2019). Lenvatinib vs. palliative therapy for stage IVC anaplastic thyroid cancer. *Molecular and Clinical Oncology*, 138–143. <https://doi.org/10.3892/mco.2019.1964>
- Iyer, P. C., Dadu, R., Gule-Monroe, M., Busaidy, N. L., Ferrarotto, R., Habra, M. A., Zafereo, M., Williams, M. D., Gunn, G. B., Grosu, H., Skinner, H. D., Sturgis, E. M., Gross, N., & Cabanillas, M. E.** (2018). Salvage pembrolizumab added to kinase inhibitor therapy for the treatment of anaplastic thyroid carcinoma. *Journal for ImmunoTherapy of Cancer*, 6, 1–10. <https://doi.org/10.1186/s40425-018-0378-y>
- Ji Jeon, M., Chun, S.-M., Kim, D., Kwon, H., Kyung Jang, E., Yong Kim, T., Bae Kim, W., Kee Shong, Y., Jin Jang, S., Eun Song, D., & Gu Kim, W.** (2016). Genomic Alterations of Anaplastic Thyroid Carcinoma Detected by Targeted Massive Parallel Sequencing in a BRAF V600E Mutation-Prevalent Area. *THYROID*, 26, 683–690. <https://doi.org/10.1089/thy.2015.0506>
- Jia, Y., Zhang, C., Hu, C., Yu, Y., Zheng, X., Li, Y., & Gao, M.** (2018). EGFR inhibition enhances the antitumor efficacy of a selective BRAF V600E inhibitor in thyroid cancer cell lines. *Oncology Letters*, 15, 6763–6769. <https://doi.org/10.3892/ol.2018.8093>
- Johnson, D. B., Balko, J. M., Compton, M. L., Chalkias, S., Gorham, J., Xu, Y., Hicks, M., Puzanov, I., Alexander, M. R., Bloomer, T. L., Becker, J. R., Slosky, D. A., Phillips, E. J., Pilkinton, M. A.,**

- Craig-Owens, L., Kola, N., Plautz, G., Reshef, D. S., Deutsch, J. S., ... Moslehi, J. J.** (2016). Fulminant myocarditis with combination immune checkpoint blockade. *New England Journal of Medicine*, 375, 1749–1755. <https://doi.org/10.1056/NEJMoa1609214>
- Joseph, M., & Enting, D.** (2019). Immune Responses in Bladder Cancer-Role of Immune Cell Populations, Prognostic Factors and Therapeutic Implications. *Frontiers in Oncology*, 9, 1–15. <https://doi.org/10.3389/fonc.2019.01270>
- Kelly, L. M., Barila, G., Liu, P., Evdokimova, V. N., Trivedi, S., Panebianco, F., Gandhi, M., Carty, S. E., Hodak, S. P., Luo, J., Dacic, S., Yu, Y. P., Nikiforova, M. N., Ferris, R. L., Altschuler, D. L., & Nikiforov, Y. E.** (2014). Identification of the transforming STRN-ALK fusion as a potential therapeutic target in the aggressive forms of thyroid cancer. *Proceedings of the National Academy of Sciences of the United States of America*, 111, 4233–4238. <https://doi.org/10.1073/pnas.1321937111>
- Kikushige, Y.** (2016). A TIM-3/galectin-9 autocrine stimulatory loop drives self-renewal of human myeloid leukemia stem cells and leukemia progression. [*Rinsho Ketsueki*] *The Japanese Journal of Clinical Hematology*, 57, 412–416. <https://doi.org/10.11406/rinketsu.57.412>
- Kim, J., Gosnell, J. E., & Roman, S. A.** (2020). Geographic influences in the global rise of thyroid cancer. *Nature Reviews Endocrinology*, 16, 17–29. <https://doi.org/10.1038/s41574-019-0263-x>
- Kim, S. K., Woo, J. W., Lee, J. H., Park, I., Choe, J. H., Kim, J. H., & Kim, J. S.** (2016). Chronic lymphocytic thyroiditis and braf v600e in papillary thyroid carcinoma. *Endocrine-Related Cancer*, 23, 27–34. <https://doi.org/10.1530/ERC-15-0408>
- Kim, Seunghwan, Cho, S. W., Min, H. S., Kim, K. M., Yeom, G. J., Kim, E. Y., Lee, K. E., Yun, Y. G., Park, D. J., & Park, Y. J.** (2013). The Expression of Tumor-Associated Macrophages in Papillary Thyroid Carcinoma. *Endocrinology and Metabolism*, 28, 192. <https://doi.org/10.3803/enm.2013.28.3.192>
- Kim, Seungwon, Yazici, Y. D., Calzada, G., Wang, Z. Y., Younes, M. N., Jasser, S. A., El-Naggar, A. K., & Myers, J. N.** (2007). Sorafenib inhibits the angiogenesis and growth of orthotopic anaplastic thyroid carcinoma xenografts in nude mice. *Molecular Cancer Therapeutics*, 6, 1785–1792. <https://doi.org/10.1158/1535-7163.MCT-06-0595>
- Kim, W. W., Ha, T. K., & Bae, S. K.** (2018). Clinical implications of the BRAF mutation in papillary thyroid carcinoma and chronic lymphocytic thyroiditis. *Journal of Otolaryngology - Head and Neck Surgery*, 47, 1–6. <https://doi.org/10.1186/s40463-017-0247-6>
- Kim, Y. W., Kim, S. K., Kim, C. S., Kim, I. Y., Cho, M. Y., & Kim, N. K.** (2014). Association of serum and intratumoral cytokine profiles with tumor stage and neutrophil lymphocyte ratio in colorectal cancer. *Anticancer Research*, 34, 3481–3487.
- Kitahara, C. M., Linet, M. S., Beane Freeman, L. E., Check, D. P., Church, T. R., Park, Y., Purdue, M. P., Schairer, C., & Berrington De González, A.** (2012). Cigarette smoking, alcohol intake, and thyroid cancer risk: A pooled analysis of five prospective studies in the United States. *Cancer Causes and Control*, 23, 1615–1624. <https://doi.org/10.1007/s10552-012-0039-2>
- Kitahara, C. M., Mccullough, M. L., Franceschi, S., Rinaldi, S., Wolk, A., Neta, G., Adami, H. O., Anderson, K., Andreotti, G., Freeman, L. E. B., Bernstein, L., Buring, J. E., Clavel-chapelon, F., Roo, L. A. De, Gao, Y., Michael, J., Giles, G. G., Håkansson, N., Horn-ross, P. L., ... González, B.**

- De.** (2015). Anthropometric factors and thyroid cancer risk by histological subtype : pooled analysis of 22 prospective studies Cari Meinhold Kitahara , PhD , MHS Division of Cancer Epidemiology and Genetics Financial disclosures : This work was supported in part by t. *National Cancer Institute*, 1–50. <https://doi.org/10.1089\thy.2015.0319>
- Knauf, J. A., Luckett, K. A., Chen, K. Y., Voza, F., Socci, N. D., Ghossein, R., & Fagin, J. A.** (2018a). Hgf/Met activation mediates resistance to BRAF inhibition in murine anaplastic thyroid cancers. *Journal of Clinical Investigation*, 128, 4086–4097. <https://doi.org/10.1172/JCI120966>
- Knauf, J. A., Luckett, K. A., Chen, K. Y., Voza, F., Socci, N. D., Ghossein, R., & Fagin, J. A.** (2018b). Hgf/Met activation mediates resistance to BRAF inhibition in murine anaplastic thyroid cancers. *Journal of Clinical Investigation*, 128, 4086–4097. <https://doi.org/10.1172/JCI120966>
- Kroll, T. G., Sarraf, P., Pecciarini, L., Chen, C. J., Mueller, E., Spiegelman, B. M., & Fletcher, J. A.** (2000). PAX8-PPAR $\gamma$ 1 fusion in oncogene human thyroid carcinoma. *Science*, 289, 1357–1360. <https://doi.org/10.1126/science.289.5483.1357>
- Kulbe, H., Thompson, R., Wilson, J. L., Robinson, S., Hagemann, T., Fatah, R., Gould, D., Ayhan, A., & Balkwill, F.** (2009). *The Inflammatory Cytokine Tumor Necrosis Factor- $\alpha$  Generates an Autocrine Tumor-Promoting Network in Epithelial Ovarian Cancer Cells Europe PMC Funders Group*. <https://doi.org/10.1158/0008-5472.CAN-06-2941>
- Kurzrock, R., Ball, D. W., Zahurak, M. L., Nelkin, B. D., Subbiah, V., Ahmed, S., O'Connor, A., Karunsena, E., Parkinson, R. M., Bishop, J. A., Ha, Y., Sharma, R., Gocke, C. D., Zinner, R., Rudek, M. A., Sherman, S. I., & Azad, N. S.** (2019). A phase i trial of the VEGF receptor tyrosine kinase inhibitor pazopanib in combination with the MEK inhibitor trametinib in advanced solid tumors and differentiated thyroid cancers. *Clinical Cancer Research*, 25, 5475–5484. <https://doi.org/10.1158/1078-0432.CCR-18-1881>
- La Vecchia, C., Franceschi, S., Negri, E., Talamini, R., & LB, M. D.** (1995). History of Thyroid Diseases and Subsequent Thyroid Cancer Risk. *Cancer Epidemiology, Biomarkers & Prevention*, 4, 193–199.
- Lan, X., Li, S., Quan, L., Yang, C., Ding, S., & Xue, Y.** (2017). Increased BTLA and HVEM in gastric cancer are associated with progression and poor prognosis. *OncoTargets and Therapy*, 10, 919–926. <https://doi.org/10.2147/OTT.S128825>
- Landa, I., Ibrahimpasic, T., Boucai, L., Sinha, R., Knauf, J. A., Shah, R. H., Dogan, S., Ricarte-Filho, J. C., Krishnamoorthy, G. P., Xu, B., Schultz, N., Berger, M. F., Sander, C., Taylor, B. S., Ghossein, R., Ganly, I., & Fagin, J. A.** (2016a). Genomic and Transcriptomic Hallmarks of Poorly-Differentiated and Anaplastic Thyroid Cancers Landa I, Ibrahimpasic T, Boucai L, Sinha R, Knauf JA, Shah RH, Dogan S, Ricarte-Filho JC, Krishnamoorthy GP, Xu B, Schultz N, Berger. *The Journal of Clinical Investigation*, 126. <https://doi.org/10.1172/JCI85271>
- Landa, I., Ibrahimpasic, T., Boucai, L., Sinha, R., Knauf, J. A., Shah, R. H., Dogan, S., Ricarte-Filho, J. C., Krishnamoorthy, G. P., Xu, B., Schultz, N., Berger, M. F., Sander, C., Taylor, B. S., Ghossein, R., Ganly, I., & Fagin, J. A.** (2016b). Genomic and transcriptomic hallmarks of poorly differentiated and anaplastic thyroid cancers. *Journal of Clinical Investigation*, 126, 1052–1066. <https://doi.org/10.1172/JCI85271>
- Lee, M. L., Chen, G. G., Vlantis, A. C., Tse, G. M. K., Leung, B. C. H., & Van Hasselt, C. A.** (2005). Induction of thyroid papillary carcinoma cell proliferation by estrogen is associated with an

altered expression of Bcl-xL. *Cancer Journal*, 11, 113–121. <https://doi.org/10.1097/00130404-200503000-00006>

- Li, J., Xu, J., Yan, X., Jin, K., Li, W., & Zhang, R.** (2018). Targeting interleukin-6 (IL-6) sensitizes anti-PD-L1 treatment in a colorectal cancer preclinical model. *Medical Science Monitor*, 24, 5501–5508. <https://doi.org/10.12659/MSM.907439>
- Liaw, D., Marsh, D. J., Li, J., Patricia, L. M., Steven, D., Wang, S. I., Zheng, Z., Bose, S., Call, K. M., Tsou, H. C., Peacock, M., Eng, C., & Parsons, R.** (1997). Germline mutations of the PTEN gene in Cowde disease, an inherited breast and thyroid cancer syndrome. *Nature Genetics*, 1, 64–67.
- Lim, S. M., Chang, H., Yoon, M. J., Hong, Y. K., Kim, H., Chung, W. Y., Park, C. S., Nam, K. H., Kang, S. W., Kim, M. K., Kim, B. S., Lee, S. H., Kim, H. G., Na, I. I., Kim, Y. S., Choi, M. Y., Kim, J. G., Park, K. U., Yun, H. J., ... Cho, B. C.** (2013). A multicenter, phase II trial of everolimus in locally advanced or metastatic thyroid cancer of all histologic subtypes. *Annals of Oncology*, 24, 3089–3093. <https://doi.org/10.1093/annonc/mdt379>
- Lin, L., Asthana, S., Chan, E., Bandyopadhyay, S., Martins, M. M., Olivas, V., Yan, J. J., Pham, L., Wang, M. M., Bollag, G., Solit, D. B., Collisson, E. A., Rudin, C. M., Taylor, B. S., & Bivon, T. G.** (2014). Mapping the molecular determinants of BRAF oncogene dependence in human lung cancer. *Proceedings of the National Academy of Sciences of the United States of America*, 111. <https://doi.org/10.1073/pnas.1320956111>
- Linsley, P. S., Brady, W., Urnes, M., Grosmaire, L. S., Damle, N. K., & Ledbetter, J. A.** (1991). CTLA4 is a Second Receptor for the B Cell Activation Antigen B7. *The Journal of Experimental Medicine*, 174, 561–569.
- Lipson, E. J., & Drake, C. G.** (2011). Ipilimumab: An anti-CTLA-4 antibody for metastatic melanoma. *Clinical Cancer Research*, 17, 6958–6962. <https://doi.org/10.1158/1078-0432.CCR-11-1595>
- Liu, Z., Hou, P., Ji, M., Guan, H., Studeman, K., Jensen, K., Vasko, V., El-Naggar, A. K., & Xing, M.** (2008). *Highly Prevalent Genetic Alterations in Receptor Tyrosine Kinases and Phosphatidylinositol 3-Kinase/Akt and Mitogen-Activated Protein Kinase Pathways in Anaplastic and Follicular Thyroid Cancers*. <https://doi.org/10.1210/jc.2008-0273>
- Long, X., Ye, Y., Zhang, L., Liu, P., Yu, W., Wei, F., Ren, X., & Yu, J.** (2016). IL-8, a novel messenger to cross-link inflammation and tumor EMT via autocrine and paracrine pathways (Review). *International Journal of Oncology*. <https://doi.org/10.3892/ijo.2015.3234>
- Luster, M., Clarke, S. E., Dietlein, M., Lassmann, M., Lind, P., Oyen, W. J. G., Tennvall, J., & Bombardieri, E.** (2008). Guidelines for radioiodine therapy of differentiated thyroid cancer. *European Journal of Nuclear Medicine and Molecular Imaging*, 35, 1941–1959. <https://doi.org/10.1007/s00259-008-0883-1>
- MA, H., LA, G., JE, V., B, A., RA, P., Y, C., AP, F., CY, P., JE, C., M, K., & JS, W.** (2016). Compact and highly active next-generation libraries for CRISPR-mediated gene repression and activation. *Elife*, 23. <https://doi.org/10.7554/eLife.19760>
- Malissen, N., Macagno, N., Granjeaud, S., Granier, C., Moutardier, V., Gaudy-Marqueste, C., Habel, N., Mandavit, M., Guillot, B., Pasero, C., Tartour, E., Ballotti, R., Grob, J. J., & Olive, D.** (2019). HVEM has a broader expression than PD-L1 and constitutes a negative prognostic marker and potential treatment target for melanoma. *OncolImmunology*, 8, 1–14.

<https://doi.org/10.1080/2162402X.2019.1665976>

- Manole, D., Schildknecht, B., Gosnell, B., Adams, E., & Derwahl, M.** (2001). Estrogen Promotes Growth of Human Thyroid Tumor Cells by Different Molecular Mechanisms<sup>1</sup>. *The Journal of Clinical Endocrinology & Metabolism*, 86, 1072–1077. <https://doi.org/10.1210/jcem.86.3.7283>
- Mansh, M.** (2011). Ipilimumab and cancer immunotherapy: A new hope for advanced stage melanoma. *Yale Journal of Biology and Medicine*, 84, 381–389.
- Marcucci, F., Rumio, C., & Corti, A.** (2017). Tumor cell-associated immune checkpoint molecules – Drivers of malignancy and stemness. *Biochimica et Biophysica Acta - Reviews on Cancer*, 1868, 571–583. <https://doi.org/10.1016/j.bbcan.2017.10.006>
- Massard, C., Gordon, M. S., Sharma, S., Rafii, S., Wainberg, Z. A., Luke, J., Curiel, T. J., Colon-Otero, G., Hamid, O., Sanborn, R. E., O'Donnell, P. H., Drakaki, A., Tan, W., Kurland, J. F., Rebelatto, M. C., Jin, X., Blake-Haskins, J. A., Gupta, A., & Segal, N. H.** (2016). Safety and efficacy of durvalumab (MEDI4736), an anti-programmed cell death ligand-1 immune checkpoint inhibitor, in patients with advanced urothelial bladder cancer. *Journal of Clinical Oncology*, 34, 3119–3125. <https://doi.org/10.1200/JCO.2016.67.9761>
- Mathews, J. D., Forsythe, A. V., Brady, Z., Butler, M. W., Goergen, S. K., Byrnes, G. B., Giles, G. G., Wallace, A. B., Anderson, P. R., Guiver, T. A., McGale, P., Cain, T. M., Dowty, J. G., Bickerstaffe, A. C., & Darby, S. C.** (2013). Cancer risk in 680 000 people exposed to computed tomography scans in childhood or adolescence: Data linkage study of 11 million Australians. *BMJ (Online)*, 346, 1–18. <https://doi.org/10.1136/bmj.f2360>
- Mendoza, M. C., Emrah Er, E., & Blenis, J.** (2011). *The Ras-ERK and PI3K-mTOR Pathways: Cross-talk and Compensation*. <https://doi.org/10.1016/j.tibs.2011.03.006>
- Meng, H., Yao, H., Hospital, R., JiaoTong, S., Dong, P., Watari, H., Sjb, H., Xiong, Y., Yue, J., & B Hanley, S. J.** (2018). Tumor-Intrinsic PD-L1 Signaling in Cancer Initiation, Development and Treatment: Beyond Immune Evasion. *Development and Treatment: Beyond Immune Evasion. Front. Oncol*, 8, 386. <https://doi.org/10.3389/fonc.2018.00386>
- Mimura, K., Liang Teh, J., Okayama, H., Shiraishi, K., Ley-Fang Kua, |, Koh, V., Smoot, D. T., Ashktorab, H., Shabbir, A., Yong, W.-P., So, J., Soong, | Richie, & Kono, K.** (2017). *PD-L1 expression is mainly regulated by interferon gamma associated with JAK-STAT pathway in gastric cancer*. <https://doi.org/10.1111/cas.13424>
- Minn, A. J., & Wherry, E. J.** (2016). Combination Cancer Therapies with Immune Checkpoint Blockade: Convergence on Interferon Signaling. *Cell*, 165, 272–275. <https://doi.org/10.1016/j.cell.2016.03.031>
- Mirabile, A., Brioschi, E., Ducceschi, M., Piva, S., Lazzari, C., Bulotta, A., Viganò, M. G., Petrella, G., Gianni, L., & Gregorc, V.** (2019). PD-1 inhibitors-related neurological toxicities in patients with non-small-cell lung cancer: A literature review. In *Cancers* (Vol. 11, Issue 3). MDPI AG. <https://doi.org/10.3390/cancers11030296>
- Mojic, M., Takeda, K., & Hayakawa, Y.** (2018). The dark side of IFN- $\gamma$ : Its role in promoting cancer immunoevasion. *International Journal of Molecular Sciences*, 19, 1–13. <https://doi.org/10.3390/ijms19010089>
- Moretti, S., Menicali, E., Voce, P., Morelli, S., Cantarelli, S., Sponziello, M., Colella, R., Fallarino, F.,**

- Orabona, C., Alunno, A., De Biase, D., Bini, V., Mameli, M. G., Filetti, S., Gerli, R., Macchiarulo, A., Melillo, R. M., Tallini, G., Santoro, M., ... Puxeddu, E.** (2014). Indoleamine 2,3-Dioxygenase 1 (IDO1) is up-regulated in thyroid carcinoma and drives the development of an immunosuppressant tumor microenvironment. *Journal of Clinical Endocrinology and Metabolism*, 99. <https://doi.org/10.1210/jc.2013-3351>
- Moss, M. L., & Minond, D.** (2017). Recent Advances in ADAM17 Research: A Promising Target for Cancer and Inflammation. *Mediators of Inflammation*, 2017. <https://doi.org/10.1155/2017/9673537>
- Munn, D. H., Sharma, M. D., & Mellor, A. L.** (2004). Ligation of B7-1/B7-2 by human CD4+ T cells triggers indoleamine 2,3-dioxygenase activity in dendritic cells. *Journal of Immunology (Baltimore, Md. : 1950)*, 172, 4100–4110. <https://doi.org/10.4049/JIMMUNOL.172.7.4100>
- Nagaiah, G., Hossain, A., Mooney, C. J., Parmentier, J., & Remick, S. C.** (2011). Anaplastic thyroid cancer: a review of epidemiology, pathogenesis, and treatment. *Journal of Oncology*, 2011, 542358. <https://doi.org/10.1155/2011/542358>
- Nakamura, Y.** (2019). Biomarkers for Immune Checkpoint Inhibitor-Mediated Tumor Response and Adverse Events. *Frontiers in Medicine*, 6. <https://doi.org/10.3389/fmed.2019.00119>
- NEL, C. J. C., van HEERDEN, J. A., GOELLNER, J. R., GHARIB, H., McCONAHEY, W. M., TAYLOR, W. F., & GRANT, C. S.** (1985). Anaplastic Carcinoma of the Thyroid: A Clinicopathologic Study of 82 Cases. *Mayo Clinic Proceedings*, 60, 51–58. [https://doi.org/10.1016/S0025-6196\(12\)65285-9](https://doi.org/10.1016/S0025-6196(12)65285-9)
- Nikiforov, Y., Biddinger, P. W., & Thompson, L. D. R.** (2012). *Diagnostic pathology and molecular genetics of the thyroid*. (2nd ed.). Wolters Kluwer Health/Lippincott Williams & Wilkins. <https://www.worldcat.org/title/diagnostic-pathology-and-molecular-genetics-of-the-thyroid/oclc/760270729>
- Nikiforov, Y. E., Biddinger, P. W., & Thomson, L. D. R.** (2009). *Diagnostic Pathology and Molecular Genetics of the Thyroid* (2nd ed.). Wolters Kluwer, Lippincott Williams & Wilkins.
- Nikiforova, M. N., Kimura, E. T., Gandhi, M., Biddinger, P. W., Knauf, J. A., Basolo, F., Zhu, Z., Gianni, R., Salvatore, G., Fusco, A., Santoro, M., Fagin, J. A., & Nikiforov, Y. E.** (2003). BRAF Mutations in Thyroid Tumors Are Restricted to Papillary Carcinomas and Anaplastic or Poorly Differentiated Carcinomas Arising from Papillary Carcinomas. *Z.Z., Y.E.N.) and Division of Endocrinology*, 88, 5399–5404. <https://doi.org/10.1210/jc.2003-030838>
- Nilsson, M., & Fagman, H.** (2017). Development of the thyroid gland. *Development (Cambridge)*, 144, 2123–2140. <https://doi.org/10.1242/dev.145615>
- Norris, D. O., & Carr, J. A.** (2013). The Hypothalamus–Pituitary–Thyroid (HPT) Axis of Mammals. In *Vertebrate Endocrinology* (pp. 207–230). Elsevier. <https://doi.org/10.1016/b978-0-12-394815-1.00006-9>
- Nosé, V.** (2011). Familial thyroid cancer: a review. *Modern Pathology*, 24, S19–S33. <https://doi.org/10.1038/modpathol.2010.147>
- O’Neill, C. J., Vaughan, L., Learoyd, D. L., Sidhu, S. B., Delbridge, L. W., & Sywak, M. S.** (2011). Management of follicular thyroid carcinoma should be individualised based on degree of capsular and vascular invasion. *European Journal of Surgical Oncology*, 37, 181–185. <https://doi.org/10.1016/j.ejso.2010.11.005>

- Oweida, A., Hararah, M. K., Phan, A., Binder, D., Bhatia, S., Lennon, S., Bukkapatnam, S., Van Court, B., Uyanga, N., Darragh, L., Kim, H. M., Raben, D., Tan, A. C., Heasley, L., Clambey, E., Nemenoff, R., & Karam, S. D. (2018). Resistance to radiotherapy and PD-L1 blockade is mediated by TIM-3 upregulation and regulatory T-cell infiltration. *Clinical Cancer Research*, 24, 5368–5380. <https://doi.org/10.1158/1078-0432.CCR-18-1038>
- Özdemir, B. C., Moehler, M., Syn, N. L. X., Tai, B. C., & Wagner, A. D. (2019). Immune checkpoint inhibitors plus chemotherapy versus chemotherapy or immune checkpoint inhibitors for first- or second-line treatment of advanced gastric and gastroesophageal junction cancer. *Cochrane Database of Systematic Reviews*, 2019. <https://doi.org/10.1002/14651858.CD013369>
- Park, A., Lee, Y., Kim, M. S., Kang, Y. J., Park, Y. J., Jung, H., Kim, T. D., Lee, H. G., Choi, I., & Yoon, S. R. (2018). Prostaglandin E2 secreted by thyroid cancer cells contributes to immune escape through the suppression of natural killer (NK) cell cytotoxicity and NK cell differentiation. *Frontiers in Immunology*, 9, 1–13. <https://doi.org/10.3389/fimmu.2018.01859>
- Park, A., Yang, Y., Lee, Y., Kim, M. S., Park, Y.-J., Jung, H., Kim, T.-D., Lee, H. G., Choi, I., & Yoon, S. R. (2019). Indoleamine-2,3-Dioxygenase in Thyroid Cancer Cells Suppresses Natural Killer Cell Function by Inhibiting NKG2D and NKp46 Expression via STAT Signaling Pathways. *Journal of Clinical Medicine*, 8, 842. <https://doi.org/10.3390/jcm8060842>
- Park, S., Zhu, J., Altan-Bonnet, G., & Cheng, S.-Y. (2019). Monocyte recruitment and activated inflammation are associated with thyroid carcinogenesis in a mouse model. In *Am J Cancer Res* (Vol. 9, Issue 7). [www.ajcr.us/](http://www.ajcr.us/)
- Paulos, C. M., & June, C. H. (2010). Putting the brakes on BTLA in T cell-mediated cancer immunotherapy. In *Journal of Clinical Investigation* (Vol. 120, Issue 1, pp. 76–80). <https://doi.org/10.1172/JCI41811>
- Pavlenko, E., Cabron, A. S., Arnold, P., Dobert, J. P., Rose-John, S., & Zunke, F. (2019). Functional characterization of colon cancer-associated mutations in ADAM17: Modifications in the pro-domain interfere with trafficking and maturation. *International Journal of Molecular Sciences*, 20, 1–18. <https://doi.org/10.3390/ijms20092198>
- Poulikakos, P. I., Persaud, Y., Janakiraman, M., Kong, X., Ng, C., Moriceau, G., Shi, H., Atefi, M., Titz, B., Gabay, M. T., Salton, M., Dahlman, K. B., Tadi, M., Wargo, J. A., Flaherty, K. T., Kelley, M. C., Misteli, T., Chapman, P. B., Sosman, J. A., ... Solit, D. B. (2011). RAF inhibitor resistance is mediated by dimerization of aberrantly spliced BRAF(V600E). *Nature*, 480, 387–390. <https://doi.org/10.1038/nature10662>
- Pylayeva-Gupta, Y., Lee, K. E., Hajdu, C. H., Miller, G., & Bar-Sagi, D. (2012). Oncogenic Kras-Induced GM-CSF Production Promotes the Development of Pancreatic Neoplasia. *Cancer Cell*, 21, 836–847. <https://doi.org/10.1016/j.ccr.2012.04.024>
- Pyo, J. S., Kang, G., Kim, D. H., Chae, S. W., Park, C., Kim, K., Do, S. I., Lee, H. J., Kim, J. H., & Sohn, J. H. (2013). Activation of nuclear factor- $\kappa$ B contributes to growth and aggressiveness of papillary thyroid carcinoma. *Pathology Research and Practice*, 209, 228–232. <https://doi.org/10.1016/j.prp.2013.02.004>
- Rajoria, S., Suriano, R., George, A., Shanmugam, A., Schantz, S. P., Geliebter, J., & Tiwari, R. K. (2011). Estrogen induced metastatic modulators MMP-2 and MMP-9 are targets of 3,3'-diindolylmethane in thyroid cancer. *PLoS ONE*, 6.

<https://doi.org/10.1371/journal.pone.0015879>

- Rajoria, S., Suriano, R., Shanmugam, A., Wilson, Y. L., Schantz, S. P., Geliebter, J., & Tiwari, R. K.** (2010). Metastatic Phenotype Is Regulated by Estrogen in Thyroid Cells. *Thyroid*, 20, 33–41. <https://doi.org/10.1089/thy.2009.0296>
- Ravi, N., Yang, M., Gretarsson, S., Jansson, C., Mylona, N., Sydow, S. R., Woodward, E. L., Ekblad, L., Wennerberg, J., & Paulsson, K.** (2019). Identification of targetable lesions in anaplastic thyroid cancer by genome profiling. *Cancers*, 11, 1–13. <https://doi.org/10.3390/cancers11030402>
- Reddi, H., Kumar, A., & Kulstad, R.** (2015). Anaplastic thyroid cancer &ndash; an overview of genetic variations and treatment modalities. *Advances in Genomics and Genetics*, 43. <https://doi.org/10.2147/agg.s53448>
- Ribas, A., & Wolchok, J. D.** (2018). Cancer immunotherapy using checkpoint blockade. In *Science* (Vol. 359, Issue 6382, pp. 1350–1355). American Association for the Advancement of Science. <https://doi.org/10.1126/science.aar4060>
- Rinaldi, S., Lise, M., Clavel-Chapelon, F., Boutron-Ruault, M. C., Guillas, G., Overvad, K., Tjønneland, A., Halkjær, J., Lukanova, A., Kaaks, R., Bergmann, M. M., Boeing, H., Trichopoulou, A., Zylis, D., Valanou, E., Palli, D., Agnoli, C., Tumino, R., Polidoro, S., ... Franceschi, S.** (2012). Body size and risk of differentiated thyroid carcinomas: Findings from the EPIC study. *International Journal of Cancer*, 131, 1004–1014. <https://doi.org/10.1002/ijc.27601>
- Rosenbaum, M. W., Gigliotti, B. J., Pai, S. I., Parangi, S., Wachtel, H., Mino-Kenudson, M., Gunda, V., & Faquin, W. C.** (2018). PD-L1 and IDO1 Are Expressed in Poorly Differentiated Thyroid Carcinoma. *Endocrine Pathology*, 29, 59–67. <https://doi.org/10.1007/s12022-018-9514-y>
- Rotondi, M., Coperchini, F., Latrofa, F., & Chiovato, L.** (2018). Role of chemokines in thyroid cancer microenvironment: Is CXCL8 the main player? *Frontiers in Endocrinology*, 9, 1–14. <https://doi.org/10.3389/fendo.2018.00314>
- Ryder, M., Ghossein, R. A., Ricarte-Filho, J. C. M., Knauf, J. A., & Fagin, J. A.** (2008). Increased density of tumor-associated macrophages is associated with decreased survival in advanced thyroid cancer. *Endocrine-Related Cancer*, 15, 1069–1074. <https://doi.org/10.1677/ERC-08-0036>
- Saad, M. I., Rose-John, S., & Jenkins, B. J.** (2019). ADAM17: An emerging therapeutic target for lung cancer. *Cancers*, 11. <https://doi.org/10.3390/cancers11091218>
- Salvatore, G., Giannini, R., Faviana, P., Caleo, A., Migliaccio, I., Fagin, J. A., Nikiforov, Y. E., Troncone, G., Palombini, L., Basolo, F., & Santoro, M.** (2004). Analysis of BRAF point mutation and RET/PTC rearrangement refines the fine-needle aspiration diagnosis of papillary thyroid carcinoma. *Journal of Clinical Endocrinology and Metabolism*, 89, 5175–5180. <https://doi.org/10.1210/jc.2003-032221>
- Salvatore, V., Silvia, F., Freddie, B., Christopher, P. W., Martyn, P., & Luigino, D. M.** (2016). Worldwide Thyroid-Cancer Epidemic? The Increasing Impact of Overdiagnosis. *New England Journal of Medicine*, 375, 612–614. <https://doi.org/10.1056/NEJMp1607866>
- Sato, E., Olson, S. H., Ahn, J., Bundy, B., Nishikawa, H., Qian, F., Jungbluth, A. A., Frosina, D., Gnjatic, S., Ambrosone, C., Kepner, J., Odunsi, T., Ritter, G., Lele, S., Chen, Y. T., Ohtani, H.,**

- Old, L. J., & Odunsi, K.** (2005). Intraepithelial CD8+ tumor-infiltrating lymphocytes and a high CD8+/regulatory T cell ratio are associated with favorable prognosis in ovarian cancer. *Proceedings of the National Academy of Sciences of the United States of America*, 102, 18538–18543. <https://doi.org/10.1073/pnas.0509182102>
- Savvides, P., Nagaiah, G., Lavertu, P., Fu, P., Wright, J. J., Chapman, R., Wasman, J., Dowlati, A., & Remick, S. C.** (2013). Phase II trial of sorafenib in patients with advanced anaplastic carcinoma of the thyroid. *Thyroid*, 23, 600–604. <https://doi.org/10.1089/thy.2012.0103>
- Shiraiwa, K., Matsuse, M., Nakazawa, Y., Ogi, T., Suzuki, K., Saenko, V., Xu, S., Umezawa, K., Yamashita, S., Tsukamoto, K., & Mitsutake, N.** (2019). JAK/STAT3 and NF-κB Signaling Pathways Regulate Cancer Stem-Cell Properties in Anaplastic Thyroid Cancer Cells. *Thyroid*, 29, 674–682. <https://doi.org/10.1089/thy.2018.0212>
- Shrestha, R., Bridle, K. R., Crawford, D. H. G., & Jayachandran, A.** (2019). Immune checkpoint blockade therapies for HCC: current status and future implications. *Hepatoma Research*, 5. <https://doi.org/10.20517/2394-5079.2019.24>
- Singer, M., Wang, C., Cong, L., Marjanovic, N. D., Kowalczyk, M. S., Zhang, H., Nyman, J., Sakuishi, K., Kurtulus, S., Gennert, D., Xia, J., Kwon, J. Y. H., Nevin, J., Herbst, R. H., Yanai, I., Rozenblatt-Rosen, O., Kuchroo, V. K., Regev, A., & Anderson, A. C.** (2016). A Distinct Gene Module for Dysfunction Uncoupled from Activation in Tumor-Infiltrating T Cells. *Cell*, 166, 1500-1511.e9. <https://doi.org/10.1016/j.cell.2016.08.052>
- Smallridge, R. C., Ain, K. B., Asa, S. L., Bible, K. C., Brierley, J. D., Burman, K. D., Kebebew, E., Lee, N. Y., Nikiforov, Y. E., Rosenthal, M. S., Shah, M. H., Shaha, A. R., & Tuttle for the American Thyroid Ass, R. M.** (2012). American Thyroid Association Guidelines for Management of Patients with Anaplastic Thyroid Cancer. *Thyroid*, 22, 1104–1139. <https://doi.org/10.1089/thy.2012.0302>
- Soldevilla, M. M., Villanueva, H., Meraviglia-Crivelli, D., Menon, A. P., Ruiz, M., Cebollero, J., Villalba, M., Moreno, B., Lozano, T., Llopiz, D., Pejenaute, Á., Sarobe, P., & Pastor, F.** (2019). ICOS Costimulation at the Tumor Site in Combination with CTLA-4 Blockade Therapy Elicits Strong Tumor Immunity. *Molecular Therapy*, 27, 1878–1891. <https://doi.org/10.1016/j.ymthe.2019.07.013>
- Solomon, B. L., & Garrido-Laguna, I.** (2018). TIGIT: a novel immunotherapy target moving from bench to bedside. *Cancer Immunology, Immunotherapy*, 67, 1659–1667. <https://doi.org/10.1007/s00262-018-2246-5>
- Soria, F., Beleni, A. I., David D'andrea, ·, Resch, I., Kilian, ·, Gust, M., Gontero, P., Shahrokh, ·, & Shariat, F.** (2018). Pseudoprogression and hyperprogression during immune checkpoint inhibitor therapy for urothelial and kidney cancer. *World Journal of Urology*, 36, 1703–1709. <https://doi.org/10.1007/s00345-018-2264-0>
- StatPearls.** (2019). *Doxorubicin*. NCBI Bookshelf. <https://www.ncbi.nlm.nih.gov/books/NBK459232/>
- Sumimoto, H., Imabayashi, F., Iwata, T., & Kawakami, Y.** (2006). The BRAF-MAPK signaling pathway is essential for cancer-immune evasion in human melanoma cells. *Journal of Experimental Medicine*, 203, 1651–1656. <https://doi.org/10.1084/jem.20051848>
- Sun, L., Wang, Q., Chen, B., Zhao, Y., Shen, B., Wang, H., Xu, J., Zhu, M., Zhao, X., Xu, C., Chen, Z.,**

- Wang, M., Xu, W., & Zhu, W.** (2018). Gastric cancer mesenchymal stem cells derived IL-8 induces PD-L1 expression in gastric cancer cells via STAT3/mTOR-c-Myc signal axis. *Cell Death and Disease*, 9. <https://doi.org/10.1038/s41419-018-0988-9>
- Sun, X. S., Sun, S. R., Guevara, N., Fakhry, N., Marcy, P. Y., Lassalle, S., Peyrottes, I., Bensadoun, R. J., Lacout, A., Santini, J., Cals, L., Bosset, J. F., Garden, A. S., & Thariat, J.** (2013). Chemoradiation in anaplastic thyroid carcinomas. In *Critical Reviews in Oncology/Hematology* (Vol. 86, Issue 3, pp. 290–301). <https://doi.org/10.1016/j.critrevonc.2012.10.006>
- SUZUKI, S., SHIBATA, M., GONDA, K., KANKE, Y., ASHIZAWA, M., UJIIE, D., SUZUSHINO, S., NAKANO, K., FUKUSHIMA, T., SAKURAI, K., TOMITA, R., KUMAMOTO, K., & TAKENOSHITA, S.** (2013). Immunosuppression involving increased myeloid-derived suppressor cell levels, systemic inflammation and hypoalbuminemia are present in patients with anaplastic thyroid cancer. *Molecular and Clinical Oncology*, 1, 959–964. <https://doi.org/10.3892/mco.2013.170>
- Tafuri, A., Shahinian, A., Bladt, F., Yoshinaga, S. K., Jordana, M., Wakeham, A., Boucher, L. M., Bouchard, D., Chan, V. S. F., Duncan, G., Odermatt, B., Ho, A., Itie, A., Horan, T., Whoriskey, J. S., Pawson, T., Penninger, J. M., Ohashi, P. S., & Mak, T. W.** (2001). ICOS is essential for effective T-helper-cell responses. *Nature*, 409, 105–109. <https://doi.org/10.1038/35051113>
- Tao, R., Wang, L., Murphy, K. M., Fraser, C. C., & Hancock, W. W.** (2008). Regulatory T Cell Expression of Herpesvirus Entry Mediator Suppresses the Function of B and T Lymphocyte Attenuator-Positive Effector T Cells. *The Journal of Immunology*, 180, 6649–6655. <https://doi.org/10.4049/jimmunol.180.10.6649>
- Tarhini, A.** (2013). Immune-Mediated Adverse Events Associated with Ipilimumab CTLA-4 Blockade Therapy: The Underlying Mechanisms and Clinical Management. *Scientifica*, 2013, 1–19. <https://doi.org/10.1155/2013/857519>
- Taube, J. H., Herschkowitz, J. I., Komurov, K., Zhou, A. Y., Gupta, S., Yang, J., Hartwell, K., Onder, T. T., Gupta, P. B., Evans, K. W., Hollier, B. G., Ram, P. T., Lander, E. S., Rosen, J. M., Weinberg, R. A., & Mani, S. A.** (2010). Core epithelial-to-mesenchymal transition interactome gene-expression signature is associated with claudin-low and metaplastic breast cancer subtypes. *Proceedings of the National Academy of Sciences of the United States of America*, 107, 15449–15454. <https://doi.org/10.1073/pnas.1004900107>
- Thyroid Cancer - Cancer Stat Facts.* (2019). <https://seer.cancer.gov/statfacts/html/thyro.html>
- Titz, B., Lomova, A., Le, A., Hugo, W., Kong, X., Ten Hoeve, J., Friedman, M., Shi, H., Moriceau, G., Song, C., Hong, A., Atefi, M., Li, R., Komisopoulou, E., Ribas, A., Lo, R. S., & Graeber, T. G.** (2016). JUN dependency in distinct early and late BRAF inhibition adaptation states of melanoma. *Cell Discovery*, 2. <https://doi.org/10.1038/celldisc.2016.28>
- Todaro, M., Zerilli, M., Ricci-Vitiani, L., Bini, M., Alea, M. P., Florena, A. M., Miceli, L., Condorelli, G., Bonventre, S., Di Gesù, G., De Maria, R., & Stassi, G.** (2006). Autocrine production of interleukin-4 and interleukin-10 is required for survival and growth of thyroid cancer cells. *Cancer Research*, 66, 1491–1499. <https://doi.org/10.1158/0008-5472.CAN-05-2514>
- Topalian, S. L., Drake, C. G., & Pardoll, D. M.** (2015). Immune checkpoint blockade: A common denominator approach to cancer therapy. *Cancer Cell*, 27, 450–461. <https://doi.org/10.1016/j.ccell.2015.03.001>

- Trovato, M., Frassetta, F., Villari, D., Batolo, D., Mackey, K., Trimarchi, F., & Benvenega, S.** (1999). Loss of heterozygosity of the long arm of chromosome 7 in follicular and anaplastic thyroid cancer, but not in papillary thyroid cancer. *Journal of Clinical Endocrinology and Metabolism*, 84, 3235–3240. <https://doi.org/10.1210/jcem.84.9.5986>
- Trovisco, V., Soares, P., Preto, A., De Castro, I. V., Lima, J., Castro, P., Máximo, V., Botelho, T., Moreira, S., Meireles, A. M., Magalhães, J., Abrosimov, A., Cameselle-Teijeiro, J., & Sobrinho-Simões, M.** (2005). Type and prevalence of BRAF mutations are closely associated with papillary thyroid carcinoma histotype and patients' age but not with tumour aggressiveness. *Virchows Archiv*, 446, 589–595. <https://doi.org/10.1007/s00428-005-1236-0>
- Tsuge, K., Takeda, H., Kawada, S., Maeda, K., & Yamakawa, M.** (2005). Characterization of dendritic cells in differentiated thyroid cancer. *Journal of Pathology*, 205, 565–576. <https://doi.org/10.1002/path.1731>
- Vaccarella, S., Silvia, F., Freddie, B., Wild, C. P., Plummer, M., & Dal Maso, L.** (2016). Worldwide Thyroid-Cancer Epidemic? The Increasing Impact of Overdiagnosis. *New England Journal of Medicine*, 375, 614–617. <https://doi.org/10.1056/NEJMp1607866>
- Varricchi, G., Loffredo, S., Marone, G., Modestino, L., Fallahi, P., Ferrari, S. M., De Paulis, A., Antonelli, A., & Galdiero, M. R.** (2019). The Immune Landscape of Thyroid Cancer in the Context of Immune Checkpoint Inhibition. *International Journal of Molecular Sciences*, 20. <https://doi.org/10.3390/ijms20163934>
- Wang, N., Liu, T., Sofiadis, A., Juhlin, C. C., Zedenius, J., Höög, A., Larsson, C., & Xu, D.** (2014). TERT promoter mutation as an early genetic event activating telomerase in follicular thyroid adenoma (FTA) and atypical FTA. *Cancer*, 120, 2965–2979. <https://doi.org/10.1002/cncr.28800>
- Wang, Y., Liu, D., Chen, P., Koeffler, H. P., Tong, X., & Xie, D.** (2008). Negative feedback regulation of IFN- $\gamma$  pathway by IFN regulatory factor 2 in esophageal cancers. *Cancer Research*, 68, 1136–1143. <https://doi.org/10.1158/0008-5472.CAN-07-5021>
- Ward-Kavanagh, L. K., Lin, W. W., Šedý, J. R., & Ware, C. F.** (2016). The TNF Receptor Superfamily in Co-stimulating and Co-inhibitory Responses. In *Immunity* (Vol. 44, Issue 5, pp. 1005–1019). <https://doi.org/10.1016/j.immuni.2016.04.019>
- Wei, C.-Y., Chou, Y.-H., Ho, F.-M., Hsieh, S.-L., & Lin, W.-W.** (2006). Signaling Pathways of LIGHT Induced Macrophage Migration and Vascular Smooth Muscle Cell Proliferation. *Journal Cellular Physiology*, 209, 735–743. <https://doi.org/10.1002/JCP>
- Welch, D. R., & Hurst, D. R.** (2019). Defining the Hallmarks of Metastasis. *Cancer Research*, 79, 3011–3027. <https://doi.org/10.1158/0008-5472.CAN-19-0458>
- Xing, M.** (2012). *BRAF V600E Mutation and Papillary Thyroid Cancer: Chicken or Egg?* <https://doi.org/10.1210/jc.2012-2201>
- Xing, M.** (2013). *Molecular pathogenesis and mechanisms of thyroid cancer.* <https://doi.org/10.1038/nrc3431>
- Xing, M. M.** (2007). Minireview: Gene methylation in thyroid tumorigenesis. *Endocrinology*, 148, 948–953. <https://doi.org/10.1210/en.2006-0927>
- Xiong, D., Wang, Y., & You, M.** (2019). Tumor intrinsic immunity related proteins may be novel

tumor suppressors in some types of cancer. *Scientific Reports*, 9, 1–16.  
<https://doi.org/10.1038/s41598-019-47382-3>

- Yadav, M., Agrawal, V., Pani, K. C., Verma, R., Jaiswal, S., Mishra, A., & Pandey, R.** (2018). C-cell hyperplasia in sporadic and familial medullary thyroid carcinoma. *Indian Journal of Pathology and Microbiology*, 61, 485–488. [https://doi.org/10.4103/IJPM.IJPM\\_478\\_17](https://doi.org/10.4103/IJPM.IJPM_478_17)
- Yan, H.-X., Pang, P., Wang, F.-L., Tian, W., Luo, Y.-K., Huang, W., Yang, G.-Q., Jin, N., Zang, L., Du, J., Ba, J.-M., Dou, J.-T., Mu, Y.-M., & Lyu, Z.-H.** (2017). Dynamic profile of differentiated thyroid cancer in male and female patients with thyroidectomy during 2000–2013 in China: a retrospective study. *Scientific Reports*, 7. <https://doi.org/10.1038/s41598-017-14963-z>
- Ye, S. L., Li, X. Y., Zhao, K., & Feng, T.** (2017). High expression of CD8 predicts favorable prognosis in patients with lung adenocarcinoma. *Medicine (United States)*, 96.  
<https://doi.org/10.1097/MD.00000000000006472>
- Yen, P. M.** (2001). *Physiological and Molecular Basis of Thyroid Hormone Action*.  
<http://physrev.physiology.org>
- Yin, M., Di, G., & Bian, M.** (2018). Dysfunction of natural killer cells mediated by PD-1 and Tim-3 pathway in anaplastic thyroid cancer. *International Immunopharmacology*, 64, 333–339.  
<https://doi.org/10.1016/j.intimp.2018.09.016>
- Zdanov, S., Mandapathil, M., Eid, R. A., Adamson-Fadeyi, S., Wilson, W., Qian, J., Carnie, A., Tarasova, N., Mkrtychyan, M., Berzofsky, J. A., Whiteside, T. L., & Khleif, S. N.** (2016). Mutant KRAS conversion of conventional T cells into regulatory T cells. *Cancer Immunology Research*, 4, 354–365. <https://doi.org/10.1158/2326-6066.CIR-15-0241>
- Zhang, J., Zhang, H., Wang, Z., Yang, H., Chen, H., Cheng, H., Zhou, J., Zheng, M., Tan, R., & Gu, M.** (2019). BtLA suppress acute rejection via regulating tCR downstream signals and cytokines production in kidney transplantation and prolonged allografts survival. *Scientific Reports*, 9.  
<https://doi.org/10.1038/s41598-019-48520-7>
- Zhao, H., Wang, J., Zhang, Y., Yuan, M., Yang, S., Li, L., & Yang, H.** (2018). Prognostic values of CCNE1 amplification and overexpression in cancer patients: A systematic review and meta-analysis. *Journal of Cancer*, 9, 2397–2407. <https://doi.org/10.7150/jca.24179>
- Zhao, Z. M., Yost, S. E., Hutchinson, K. E., Li, S. M., Yuan, Y. C., Noorbakhsh, J., Liu, Z., Warden, C., Johnson, R. M., Wu, X., Chuang, J. H., & Yuan, Y.** (2019). CCNE1 amplification is associated with poor prognosis in patients with triple negative breast cancer. *BMC Cancer*, 19, 1–11.  
<https://doi.org/10.1186/s12885-019-5290-4>
- Zheng, Y., Li, Y., Lian, J., Yang, H., Li, F., Zhao, S., Qi, Y., Zhang, Y., & Huang, L.** (2019a). TNF- $\alpha$ -induced Tim-3 expression marks the dysfunction of infiltrating natural killer cells in human esophageal cancer. *J Transl Med*, 17, 165. <https://doi.org/10.1186/s12967-019-1917-0>
- Zheng, Y., Li, Y., Lian, J., Yang, H., Li, F., Zhao, S., Qi, Y., Zhang, Y., & Huang, L.** (2019b). TNF- $\alpha$ -induced Tim-3 expression marks the dysfunction of infiltrating natural killer cells in human esophageal cancer. *Journal of Translational Medicine*, 17, 1–12.  
<https://doi.org/10.1186/s12967-019-1917-0>
- Zhou, X. M., Li, W. Q., Wu, Y. H., Han, L., Cao, X. G., Yang, X. M., Wang, H. F., Zhao, W. S., Zhai, W. J., Qi, Y. M., & Gao, Y. F.** (2018). Intrinsic expression of immune checkpoint molecule TIGIT

could help tumor growth in vivo by suppressing the function of NK and CD8+T Cells. *Frontiers in Immunology*, 9, 1–11. <https://doi.org/10.3389/fimmu.2018.02821>

**Zhu, X., Yao, J., & Tian, W.** (2015). Microarray technology to investigate genes associated with papillary thyroid carcinoma. *Molecular Medicine Reports*, 11, 3729–3733. <https://doi.org/10.3892/mmr.2015.3180>